University of Strathclyde

Department of Biomedical Engineering

DEVELOPMENT OF A DISPOSABLE SENSOR SYSTEM FOR MONITORING THE pH OF WOUNDS AND WOUND DRESSINGS

Stephen Milne, MEng

A thesis presented in the fulfilment of the requirements for the degree of Doctor of Engineering

2012

This thesis is the result of the author's original research. It has been composed by the author and has not been previously submitted for examination which has led to the award of a degree.

Signed:

Date:

Abstract

The pH of a wound can affect many different phases of the healing process such as oxygen levels, cell proliferation, protease enzyme activity and bacterial growth. If the pH level of a wound can be effectively monitored then it can act as a biological marker to aid in diagnostics and in establishing the optimum conditions for healing. However without an easy to use pH sensor for nurses and carers, this potentially important near-patient diagnostic parameter, will not enter clinical diagnostics. The standard glass pH electrode is still the only effective way to measure the pH of a wound. They are expensive and difficult to sterilise. The pH electrode has not been successfully adapted into smaller and alternate packaging because the membrane that forms the selective part of the electrode, being made of silicon glass, is fragile, thus limiting manufacture, sterilisation and practical application.

This thesis describes two defined areas of work. The first area reported details the development of a disposable hand-held measurement system for measuring wound pH. Four screen printed solid state sensor types are studied and evaluated. Three of the sensors are based on conducting polymers (Polypyrrole doped with Cl^- or PTS^- ions and PEDOT) with ion-selective membranes. The fourth sensor tested is the screen printed carbon electrode with an ion-selective membrane. The best performing sensor was the carbon coated with an ion-selective membrane which was operational in the pH range 3.5-10. The superior performance of the carbon substrate was investigated and attributed to the partial dissolving of the screen printed carbon layer during membrane deposition, enabling good sensor adhesion and stability between the membrane and conducting contact.

The second area for investigation that is reported here describes the use of the developed pH measurement system to observe the influence on pH of a number of wound dressings (Activon Tulle (Advancis Medical), Aquacel(Convatec), Tegaderm Matrix (3M) and Promogran(Systagenics)) in real time after application to a wound bed model. The wound dressings were first tested in a non-buffered (for pH) solution to observe the pH change. It was found that the dressings all had low pH values of below pH 4 in this environment. The second experiment used horse serum as a

wound exudate substitute to monitor the real time change in pH after application of wound dressing as it would mimic the buffering capacity of real wound exudate. The results showed that the Tegaderm dressing had the strongest acid concentration but that all the wound dressings would influence local pH in a wound to some extent. The variation in the pH measured on the wound bed model with the different dressings highlights the need to gain a further understanding of the role of pH, dressing influence on pH and the optimum pH conditions for wound healing.

Acknowledgements

Firstly I would like to thank my supervisor Professor Patricia Connolly for her valuable advice and support throughout my EngD project. I would also like to thank Dr Christopher McCormick and Brian Cartlidge for all their help, advice and good company in the lab. I would also like to acknowledge the EPSRC for providing funding that enabled me to conduct the project.

I would like to give thanks to Dr Tatyana Korochkina and her colleagues at the Welsh Centre for Printing and Coating at the University of Swansea who provided invaluable advice with screen printing and use of their facilities. I would also like to give thanks to Lynne Watret who gave me an interesting insight into the world of tissue viability nursing and for helping supply me with some of the dressings that were tested during the project.

Thanks to my fellow DTC students who always provided a constant source of entertainment for the duration of the EngD. Finally thanks to my family and friends for their encouragement and support over the years.

Symbol

a_i	Activity of the ion, i
C	Capacitance
C_{dl}	Capacitance of the double layer
C_i	Concentration of the species i
D_i	Diffusion coefficient of the species i
E	Electrical potential
E^0	Standard voltage potential
F	Faraday constant
f	Frequency
G	Differential change in free enthalpy
I	Current
i_0	Exchange current density
J_i	flux of species i
$K_{I,J}$	Selectivity coefficient
pK_a	Acid dissociation constant
q	Charge
R	General gas constant
R_{CT}	Differential charge transfer resistance
T	Temperature in Kelvin

V	Voltage
z	Charge of the ion
Z'	Real component of impedance
Z''	Imaginary component of impedance
α	Charge transfer coefficient
β	Buffer value
γ_b	Buffer capacity
ε	Dielectric constant of the solution
ε_0	Permittivity of free space
η	Over potential from equilibrium value
μ_i	Chemical potential
$\bar{\mu}_i$	Electrochemical potential
ϕ	Electrical potential of the phase
σ	Charge density
ω	Angular frequency

Abbreviations

ADC	Analogue to digital converter
Ag/AgCl	Silver/Silver Cholride
CPE	Constant phase element
EGF	Epidermal growth factor
EIS	Electrochemical impedance spectroscopy (EIS)
FGF	Fibroblast growth factor
ISFETS	Ion-selective field effect transistors
IHP	Inner Helmoltz plane
LCD	Liquid crystal display
LED	Light emitting diode
MMP	Matrix metalloproteinase
NHS	National Health Service
OHP	Outer Helmoltz plane
Op-amp	Operational amplifier
PCB	Printed circuit board
PEDOT	Poly(3,4-ethylenedioxythiophene)
PDGF	Platelet derived growth factor
PMMA	Polymethyl-methacrylate
PPY	Polypyrrole

PPYCl	Polypyrrole doped with Cl^- ions
PPYPTS	Polypyrrole doped with PTS^- ions
PTS	p-toluenesulfonate
PVC	Polyvinyl chloride
TGF alpha	Transforming growth factor alpha
TGF-ß	Transforming growth factor-beta
TIMPS	Tissue inhibitors of metalloproteinases
TNF-α	Tumor necrosis alpha

Contents

List of tables

1.

List of figures

Chapter 1 Introduction

Chronic wounds are a growing problem worldwide with the annual spend close to £190 million on wound dressings alone by the National Health Service, in England, during 2011 (NHS Authority Business Services, 2012). The high costs associated with chronic wounds are due to the complex healing patterns which do not follow the standard healing path of an acute wound and result in delayed healing. Currently there is a real lack of analytical tools available that assess the state of the wounds. At presents clinicians rely on observations to evaluate the healing of the wound and use treatments on a trial and error basis to achieve healing in chronic wounds. The use of analytical measurement tools for measuring healing parameters in wounds is still an emerging field in wound management and treatment. Analytical measurements such as wound pH, wound size and moisture balance would enable an objective measurement of healing to provide the clinician with the most efficient and effective techniques to heal the wound. By understanding the basic biological interactions and mechanisms that occur in the complex wound a marker such as wound pH could be used as a tool to assess the state of the wound and enable more effective treatment. Current methods of detecting pH in wounds are limited as they involve expensive glass electrodes that are large and difficult to sterilise for medical use. Due to the lack of a suitable solution to measure wound pH it is not a fully understood part of the wound healing process.

This thesis presents the development and testing of a solid state disposable potentiometric pH sensor that is capable of measuring the pH of wound fluid. It will provide a measurement tool that will enable the effect of pH on the wound healing process to be further studied. The thesis covers the design of a full disposable sensor system including battery operated measurement hardware. This system is then tested in a wound bed model to assess the real time effect of pH altering wound dressings on the pH of a physiological solution.

The layout of this thesis follows a traditional structure starting with a literature review Chapter 1, Chapter 2 covers the theory behind the operation of solid state sensors, Chapter 3 details the methods and materials used in the experimental

section, Chapter 4 and Chapter 5 cover the results of the experiments and Chapter 6 discusses the results of the experimental findings.

The following chapter is split into two sections, the first describing wound healing and the effect of pH on the process. The second section is a literature review of current pH sensing technology. The chapter starts by detailing the skin and the complex healing process that occurs in a wound of the skin. Next follows a description of the different wound types and current wound treatments/dressings. It then reviews the current knowledge of the effect of pH on various parts of the wound healing process this includes cells, enzymes and bacteria. Within this section the influence of pH modifying dressings and treatments is discussed. The second section starts with a review of the current pH sensing technology. Following this there is an in depth review of solid state pH sensors. Finally Chapter 1 closes with the objectives of the study.

1.1 Skin

Skin is the outer covering of the body which accounts for 16% of the total body weight (Martini, 2006). The skin organ is referred to as the integumentary system it performs many functions that are vital to survival.

The skin's main functions are:

- **Protection** of the internal organs and underling tissues by acting as an anatomical barrier between the body and the external environment.
- **Excretion** of salts, organic waste and water through the sweat glands.
- **Heat regulation** to help maintain the body's temperature in the normal range by insulation or cooling through sweating.
- **Synthesize** vitamin D through exposure to UV
- **Storage** of fats in adipocytes in the dermis and adipose tissue in the subcutaneous layer.
- **Sensing** of temperature, touch, pressure and pain.

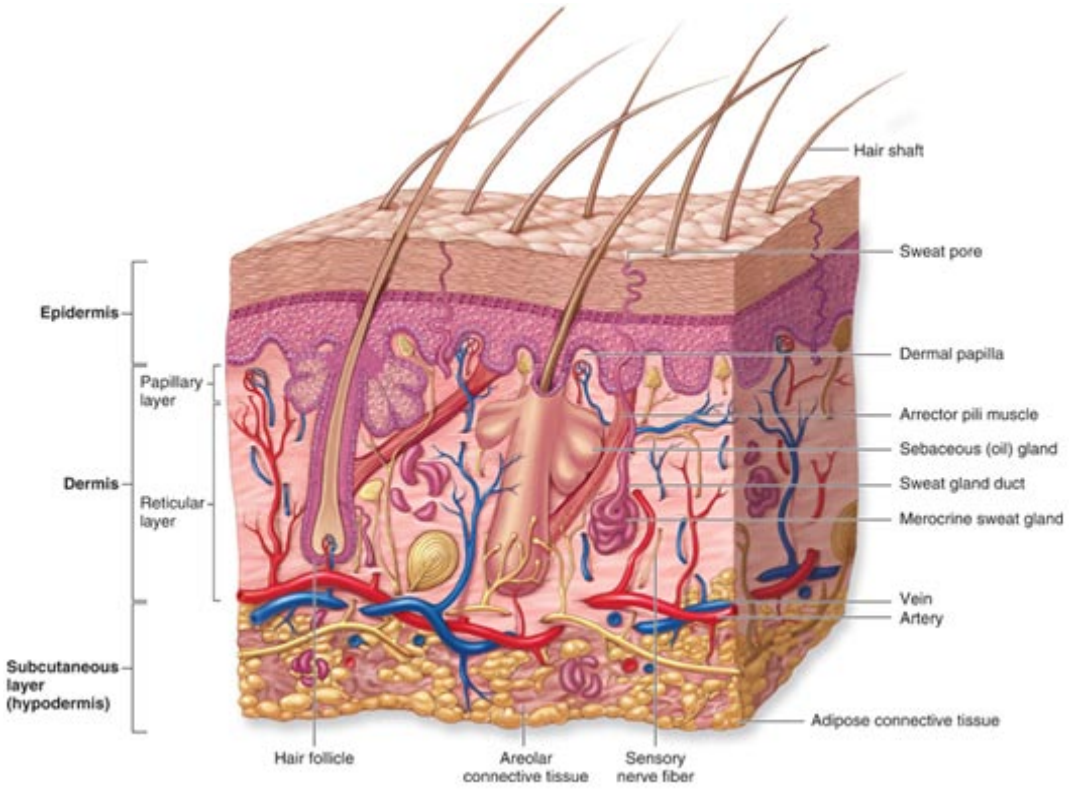

Figure 1.1 Cross section of skin showing different layers. (http://academic.kellogg.edu/herbrandsonc/bio201_mckinley/f5-1_layers_of_the_inte_c.jpg)

The cutaneous membrane (Skin) and the accessory structures are show in **Figure 1.1**. The cutaneous membrane has two components the epidermis and the dermis. Epidermis is the outer layers of the skin made up of epithelial cells. The dermis is the underlying area of connective tissue which provides elasticity to the skin. The epidermis and dermis will now be discussed in more detail.

1.1.1 Epidermis

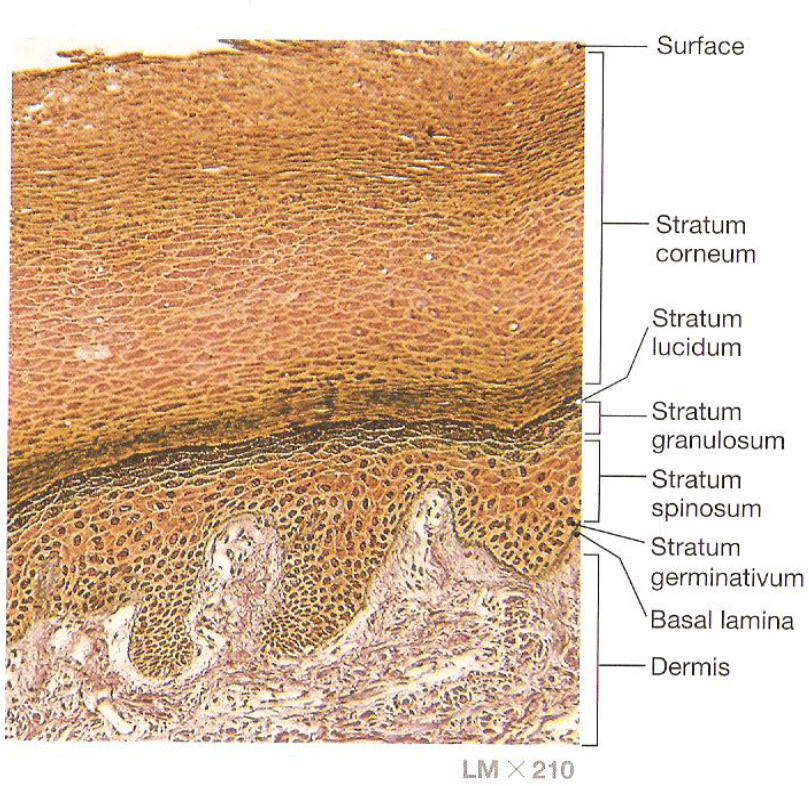

Figure 1.2 Layers of the epidermis in thick skin (Martini, 2006).

The epidermis provides mechanical protection and acts as a barrier against microbial infection. There are no blood vessels in the epidermis so it relies on diffusion of oxygen from the vessels in the dermis. Keratinocytes are the major cell in the epidermis and they contain the protein keratin. The epidermis has either 4 or 5 layers of keratinocytes if thin or thick skin shown in **Figure 1.2**. A cell can take from 15 to 30 days to move from the bottom layer to the skin surface where the dead cells can remain for around 2 weeks before they are shed. The different layers are listed below:

- **Stratum germinativum** is the bottom layer of the epidermis, basal cells dominate this layer of the skin. Basal cells are stem cells that divide to replace the keratinocytes that are lost at the skins surface.
- **Stratum spinosum** contains the product of the stem cell. The keratinocytes are pushed up into this layer from the stratum germinativum. This layer also

contains Langerhans cells which provide an immune response to skin cancers and microorganisms that penetrate the upper layers.

- **Stratum granulosum** the keratinocytes produce large volumes of keratin in this layer. In this section of the epidermis the keratinocyte cells start to grow flatter as the keratin fibers develop the cells are then dehydrated until all that is left is a tight layer of cells of keratin fibers surrounded by keratohyalin.
- **Stratum lucidum** is a layer only found in thick skin such as that found on the base of the feet and palms of the hand. The layers are densely packed flattened cells that are filled with keratin.
- **Stratum corneum** contains between 15 to 30 layers of superficial layers of cells filled with keratin. The dead cells are all interconnected this enables them to fall apart in large groups when the skin is shed.

1.1.2 Dermis

The dermis lies directly underneath the epidermis layer. The dermis layer is much thicker than the epidermis and consists of two separate layers, the papillary and the reticular, which lie on top of the subcutaneous layer. The papillary layer contains the capillaries, lymphatic and the sensory system which are located in branch networks throughout the dermis. The sensory system sends information to the central nervous system about touch, pressure, temperature and pain. The reticular layer is a dense layer that contains connective tissues such as collagen. The subcutaneous layer lies deep in the dermis and acts as a barrier between the skin and the other organs in the body. It is composed from connective tissues and lipid layers.

The dermis also contains the accessory structures of the skin which are composed of sweat glands, hair and nails. They are primarily located in the dermis and protrude through the epidermis to the skin surface. Skin glands are important in keeping the skin surface healthy and also maintaining the pH balance of the skin. There are two types of skin glands sebaceous and sweat glands. Sebaceous glands produce a lipid secretion called sebum this contains triacylglycerides, cholesterol, proteins and electrolytes. Sebum conditions the surrounding skin after its release and protects it from growth of bacteria.

1.2 Wound healing

Wound healing is a complex process that depends on many different factors. It starts with damage to the skin and can last for long periods of time depending on wound type and condition. An acute wound is a wound that heals in the expected fashion following a number of set healing stages. A chronic wound does not follow the normal set healing stages and is unpredictable in the healing time. In chronic wounds it is common that the balance of healing is lost and degradation occurs. Chronic wounds cost health services many millions of pounds in treatment every year**.** In the USA chronic wounds accounted for 31.4% of all direct treatment costs for dermatological diseases (Bickers et al., 2006). Chronic wounds mostly affect the over 60's and with an aging population this problem is set to rise year on year (Frost and Sullivan, 2003). The high costs associated with chronic wounds are due to the complex healing patterns which do not follow the standard healing path of an acute wound. There are many different forms of treatment for these chronic wounds and they are mostly based on a trial and error basis to find a suitable treatment. These various treatments can be very expensive hence finding the most appropriate course of action is critical to heal the wounds in the shortest time possible and to minimise costs.

Currently there is a real lack of analytical tools available that assess the state of the wounds (James et al., 2000). If these existed then the clinicians could use these to assess the stage of healing and condition of the wound and tailor the treatment to the specific patient. By understanding the basic biological interactions and mechanisms that occur in the complex wound a marker such as wound pH can be used as a tool to assess the state of the wound.

During wound healing damage to the dermis and epidermis is repaired through a series of four different stages: inflammatory, granulation, epithelialisation and maturation. This process of repair allows the skin to regenerate and regain tensile strength. This section will describe the main stages that occur during normal wound healing.

1.3 Normal wound healing

1.3.1 Inflammatory

The inflammatory response is the initial response by the body's defense mechanism. This initial stage is to protect the body and no healing occurs for around 12 hours after injury. When skin is damaged there is a complex series of events that starts with the release of platelets from the blood vessel which initiates the clotting cascade where coagulation of blood leaking from the blood vessel forms clots. The clots of interconnected fibrin cover the wound contracting it to bringing the wound edges together. White blood cells such as neutrophils and monocytes migrate in the wound initiating an inflammatory response. These cells help to increase blood supply to the wound site bringing extra oxygen and phagocytes (macrophages) which clear the wound of dead cells and toxins. Macrophages and neutrophils are the key components to ensure than the wound moves into the next stage of wound healing (White, 2002).

1.3.2 Granulation

This process occurs in deep dermal wounds. Macrophages send signals to the fibroblasts which produces reticulin across the wound which is later turned into collagen. Once this process is complete, new tissue is composed of a matrix of fibronectin, collagen, laminin, elastin, proteoglycan and hyaluronic acid. Once the granulation tissue is formed angiogenesis commences where new blood vessels are grown and the tissue is rapidly infiltrated by macrophages and fibroblasts. As the new tissue is formed the wound edges further contract reducing the wound size. Lack of oxygen in the wound reduces the mobility of the fibroblasts resulting is slower tissue formation.

1.3.3 Epithelialisation

In the epithelialisation stage the macrophages and fibroblasts continue to produce new dermis. Epithelial keratinocytes migrate from the edge of the wound and proliferate in the newly formed base tissue. When the keratinocytes are in contact with the extracellular network the cells express a number of adhesion molecules

which help bind the cells to the granulated tissue (O'Toole, 2001). These keratinocytes express a number of matrix metalloproteinase (MMP) which are a family of 20 proteases that act to degrade the components of the extracellular matrix once the new structures have been formed (Nagase and Woessner, 1999). Once the squamous cells have fully migrated across the wound epithelialisation is achieved. This is the final stage in wound healing above the dermis level of skin.

1.3.4 Maturation

Once tissue has been deposited across a wound it is fragile as it has a low tensile strength. The maturation stage consists of fibroblasts and macrophages migrating into the wound to strengthen the extracellular matrix and form more robust collagen (Martini, 2006).

1.4 Wound types

In an acute wound the inflammation process acts to recruit and activate fibroblasts as well as removing debris, bacterial contaminates and necrotic tissue. The inflammation response is very different in chronic non healing wounds as the inflammation is not controlled and further contributes to the breakdown of the wound (Menke et al., 2007). When the normal wound healing mechanisms cannot heal a wound a protracted inflammatory response occurs which further degrades the wound. In general the main features of a chronic wound are increased enzymatic activity of proteases, reduced response to growth factors and reduced cell proliferation (Shai, 2005). Chronic wounds are more likely to develop into malignant transformations; they are also susceptible to sepsis and bacterial infection.

Mentioned previously there are two main wound type categories acute and chronic. These categories can be further broken down into more specific wound types. There are three main categories of wound types in chronic wound healing that will be described: leg ulcers, diabetic ulcers and pressure ulcers (Mustoe, 2004). Some more complex wounds can have mixed healing properties in more than one of these categories. Two other types of wounds have been listed, burns and skin grafts, due to

their more complex healing properties. All five of these wound types would benefit from analytical measurements to test for wound healing.

1.4.1 Leg ulcers

Figure 1.3 Photograph of leg ulcer. Sourced from Wounds UK (www.wounds-uk.com).

Venous ulcers are caused by increased venous stasis in the leg. This results in fluid from the vessel leaking out causing an inflammatory response which leads to skin breakdown. They account for an estimated 70% to 90% of the cases of leg ulcers and are costly to treat due to their delayed healing properties (Snyder, 2005). An arterial ulcer is less common than a venous ulcer, they account for around 10% of chronic wounds (Romanelli et al., 2002). They are caused by damaged valves to the leg which results in less blood reaching the wound.

1.4.2 Diabetic foot ulcers

Figure 1.4 Photograph of diabetic foot ulcer. Sourced from Wounds UK (www.wounds-uk.com).

Diabetic foot ulcers are the second most common cause of chronic wounds although the percentage of these are growing (Menke et al., 2007). They occur in 15% of diabetes patients in their lifetime (Brem and Tomic-canic, 2007)**.** They become chronic wounds through a number of mechanisms, decreasing cell and growth factor response which leads to decreased angiogenesis. This lack of healing is the cause of 84% of amputations in diabetic patients in USA (Reiber, 1995). Another cause is loss of sensation in the lower limbs which can result in pressure on certain areas which eventually transform into ulcers**.**

1.4.3 Pressure ulcers

Figure 1.5 Photograph of stage III Pressure ulcer. Sourced from NHS Choices (www.NHS.uk).

Pressure ulcers, also known as bed sores, are formed as a result of pressure on the skin caused by bodyweight between the bone and a surface such as a bed or a wheelchair. Pressure ulcers can also be caused by a shearing force on the skin. The ulcer results from pressure causing lack of blood flow to the skin which eventually causes cell death and eventually skin breakdown. This commonly occurs in bed and wheelchair bound patients. Pressure sores are categorized by severity, from Stage I (earliest signs) to Stage IV (worst) (MedlinePlus, 2011a):

- **Stage I:** A reddened area on the skin that, when pressed, is "nonblanchable" (does not turn white). This indicates that a pressure ulcer is starting to develop.
- **Stage II:** The skin blisters or forms an open sore. The area around the sore may be red and irritated.
- **Stage III:** The skin breakdown now looks like a crater where there is damage to the tissue below the skin (see **figure 1.5**).

- **Stage IV:** The pressure ulcer has become so deep that there is damage to the muscle and bone, and sometimes tendons and joints.

1.4.4 Burns

When skin is exposed to excess heat a burn wound can occur. A burn wound can also be caused by chemicals destroying the skin layer. The injury is caused by rapid denaturation of proteins and cell damage. Any temperature over 60^{o}C can induce immediate cell death. The depth of injury is dependent on the heat or chemical penetration.

There are three types of burns classification (MedlinePlus, 2011b):

- First degree burns damage only the outer layer of skin
- Second degree burns damage the outer layer and the layer underneath
- Third degree burns damage or destroy the deepest layer of skin and tissues underneath

Burn wounds can display some of the characteristics of chronic wounds such as high protease activity which can affect the healing time and increase scar tissue (Ulrich et al., 2003).

1.4.5 Skin grafts

Figure 1.6 Photograph of leg skin graft receptor site. Sourced from Wounds UK (www.wounds-uk.com).

A skin graft is when healthy skin is taken from a location on the patient's own body and transplanted to an area of damaged skin (see **figure 1.6**). It is a commonly used method in burns as well as cutaneous ulcer treatment (Snyder, 2005). The depth of the skin graft can be either full or split thickness. A split thickness contains the epidermis and some of the dermis. The full graft contains the whole epidermis and dermis. The full thickness graft provides a more natural heal but needs a well vascularised site so in most ulcers the split thickness is used.

1.5 Wound repair

Healing in acute wounds is referred to as primary intention. An acute or surgical wound is closed by bring the skin edges close to each other and fixing them in place by suturing or stapling. This enables the wound to heal rapidly in the expected manner. Another method called delayed primary closure allows the wound to heal naturally for a few days before closing using the same technique as primary intention. The delayed method was used as it was thought to reduce infection but recent studies have shown that it has little benefit (Henry and Moss, 2005).

Chronic wounds and ulcers are called healing by secondary intention. This form of treatment is used for wounds that have a higher probability of infection. The wound is not closed but is left to close gradually through granulation tissue formation and re-epithelialisation (Shai, 2005). Due to the delayed and complex healing associated with secondary intention there are many different techniques used for promoting healing these will be documented below.

Currently used techniques

A suitable amount of moisture in a wound can provide optimum healing conditions for a chronic wound (McColl et al., 2007). It allows more efficient metabolic activity of cells in the wound healing process; a dry wound prevents growth factors acting. It is a fine balance because a wound that has excess fluid can become macerated which will prevent or delay further healing.

1.5.1 Hydrocolloid dressings

Hydrocolloids contain hydrophilic particles that form gels. A typical hydrocolloid dressing is composed of an inner sheet of the gel particles and an outer hydrophobic coating like the thin film dressings. They are the most commonly used type of dressing for mild to medium exudating wounds and burns, £6 million was spent in the by the NHS in England on hydrocolloids in 2011 (NHS Authority Business Services, 2012)**.** When applied, the fluid contained in the wound forms a gel with the hydrocolloid layer. The gel layer helps to maintain a moist wound environment and also acts to absorb material that prevents wound healing. Hydrocolloids have been found to have pH levels of 4.5 to 7 which can help to lower the pH of the wound (Thomas and Loveless, 1997).

1.5.2 Hydrogel dressings

Hydrogels are made up of a three dimensional matrix of hydrophilic polymers with a high water content. They can contain different additional molecules that can assist healing. They are used in wounds that are dry such as black necrotic ulcers. The hydrogel's purpose is to keep the wound hydrated although care has to be taken to ensure the wound does not become macerated. An estimated £4 million was spent by the NHS in England on hydrogels in 2011 (NHS Authority Business Services, 2012).

1.5.3 Alginate dressings

Alginate dressings are made from fibres of polysaccharides which contain alginic acids that are derived from seaweeds. The fibres absorb fluid in the wound by forming highly absorbent gels and they are capable of absorbing many times their mass in fluid. They are used to maintain the moisture balance in moderate to heavily exudating wounds. The alginate is thought to have some properties that contribute to healing although the exact mechanism is not fully understood (Thomas, 2000).

1.5.4 Film dressings

Film dressings are composed of thin sheets of polyurethane they act as a membrane that is permeable to moisture and gases but impermeable to fluid and bacteria. They are most commonly used in acute dry wounds.

1.5.5 Foam dressings

Foam dressings are composed of a polymeric material that is manufactured to contain air bubbles so that fluid can be absorbed. The absorbent capacity is dependent on the thickness of the foam and the manufacturer. They generally have a hydrophobic sheet such as a thin film to maintain a moist wound environment and act as a barrier to bacterial infection.

1.5.6 Honey based dressings

Honey based dressings are commonly used as they have antimicrobial and antibacterial qualities. It has been shown clinically to show a reduction in bacterial colonization of wounds (Gethin and Cowman, 2005). Other favorable qualities are that is can act to deodorized the wound and remove sough buildup. The honey is embedded in a fabric gauze so that when placed on a wound the honey can mix with the wound exudates and integrate with the wound. Manuka honey is the most commonly used honey and it is commonly sterilized with gamma radiation before integration with wound dressings (Kwakman and Zaat, 2012). Honey does act to modify pH in the wound as it has a natural low pH and this has been proposed as one of its main methods of operation (Gethin et al., 2008). The pH of honey is further discussed in **Section 3.11.3**.

1.5.7 Protease (MMP) modulating dressings

These dressings claim to reduce the enzyme activity associated with matrix metalloproteinase's (MMPs). The MMPs have been associated with delayed wound healing (Schultz et al., 2005). MMPs and their effect on wound healing is discussed in **Section 1.9.5**. There are a number of wound dressings that claim to modulate MMP activity some of the commonly used types are Cadesorb (Smith and Nephew),

Tegaderm (3M) and Promogran (Systagenix). These dressings embed the active components in a gauze (Tegaderm), ointment (Cadesorb) or collagen cellulose matrix (Promogran). Their active components are not disclosed, however all these dressings act to lower the pH of the wound which in turn has been shown to lower MMP levels (Greener et al., 2005). An estimated £20 million was spent by the NHS in England on protease modulating dressings in 2011 (NHS Authority Business Services, 2012). The pH influence of these dressings is further discussed in **Section 1.11**.

1.5.8 Anti microbial dressings

There are a number of different antimicrobial dressings that include silver, iodine or charcoal which act to prevent bacterial growth in the wound. Iodine penetrates cell walls of microorganisms. Its antibacterial effect is attributed to its disruption of proteins and nucleic acids. Although there is also evidence that the antimicrobial effect also acts on cells which in turn could disrupt the healing process (Hidalgo and Domínguez, 1998). Silver antimicrobial dressings were estimated to account for around £20 million in 2011 by the NHS in England(NHS Authority Business Services, 2012). The bacterial action depends on the amount of silver and its rate of release (Percival et al., 2007). Charcoal dressings are used to adsorb exudates and bacteria from the wound bed. These are also used to treat malodors that are released from the wound (CarboFlex, Convatec).

1.5.9 Wound debridement

Debridement methods are aimed at decreasing the necrotic (dead) tissue and protease burden in the wound. It acts to reset the wound so that only healthy tissue is left resulting in the wound healing as an acute wound (Menke et al., 2007). There are a number of different methods for debriding a wound. Surgical debridement removes necrotic tissue by cutting it away with scalpels or forceps - it is a difficult technique as care needs to be taken to only remove necrotic tissue. Mechanical debridement is used to soften or remove necrotic tissue - this can be achieved by soaking the wound in water or saline solution. Maggot therapy is used to break down dead tissue by using a specific type of maggots (Green bottle blowfly) that only eat the dead tissue. Chemical debridement is used when an ulcer is fully covered by necrotic material - it

involves using mild acid preparations (Aserbine) or enzymatic chemicals (Santyl, Abbott lab). The mild acid acts to change the pH of the wound so that the surface proteins swell resulting in easy removal. Enzyme debridement targets and breaks down fibrin, collagen or DNA/RNA in the wound.

1.5.10 Biological dressings

Biological dressings are skin substitutes that are originally derived from or contain living cells. The main type used in treatments is a collagen dressing. They are sheets of cultured and processed collagen that provides a scaffold on which new tissue is formed (Adhirajan et al., 2009). These tissue scaffolds are becoming more complex as they now contain active ingredients to limit enzyme activity and alter pH level (Promogran, J&J). Living substitutes are derived from samples of the patient's own keratinocytes skin cells where they are cultured outside then integrated into a dressing (Epicel, Genzyme). Apligraf and Orcel both use a collagen matrix implanted with donor epidermal keratinocytes and dermal fibroblasts to stimulate faster healing (Orcel, Forticell Bioscience)(Apligraf, Apligraf). These living biologically active skins can achieve faster healing rates but their price is prohibitive for wide spread use (Shai, 2005).

1.5.11 Growth factors

Growth factors are a specific group of cytokines that are secreted by a wide range of cells involved in the healing process (macrophages, fibroblasts, platelets and endothelial cells) (Shai, 2005). They act at the cellular level to stimulate and enhance proliferation of certain key cells related to wound healing. Wound treatments have been investigated that increase growth factor within the wound with the aim of stimulating healing. The growth factor therapies used are fibroblast growth factor (FGF), transforming growth factor alpha (TGF alpha), epidermal growth factor (EGF) and platelet derived growth factor (PDGF). The pH level of the wound is important in the response of all of these cells as if the pH balance is outwith a certain range then it will affect the overall effectiveness of the growth factor treatment (Mercier et al., 2002). The only one of these growth factors that has shown any clinical significance is PDGF. It is thought that growth factor treatments in chronic

wounds are only effective once the inflammatory and protease response levels are reduced towards acute wound healing levels (Menke et al., 2007) (Trengove et al., 1999).

1.5.12 Emerging Technologies

There are a number of emerging technologies that are used in wound care to enhance wound healing. These include advanced wound imaging, wound moisture monitors, electrical stimulation, hyperbaric oxygen therapy, negative wound pressure therapy and ultrasound. Advanced wound imaging used image processing software to map wound size change (Silhouette ,Aranz Medical Limited). Wound moisture monitoring enables clinicians to see the moisture balance in the wound without removing dressings enabling optimum healing conditions to be achieved with minimal disruption to the wound bed (WoundSense, Ohmedics). Electrical stimulation of healing works by passing a current through a chronic wound to promote wound healing factors (LifeWave Bed Sore Treatment, LifeWave). Hyperbaric oxygen therapy uses pure oxygen to speed up and improve the body's natural ability to heal (Hyper Ox Inc). Negative wound pressure therapy encourages the formation of granulation tissue by helping to close the wound using an airtight seal (Venturi NPWT, Talley Group). Ultrasound is used as a method of debridement and also to stimulate healing in the wound (Qoustic Wound Therapy System, Arobella Medical).

1.6 Wound fluid

Wound fluid or wound exudate is the medium in which repair occurs. It contains various components shown in **Table 1.1** which vary depending on the stage of healing (White, 2006). The constituents are different depending on whether the wound is acute or chronic. These will discussed further in the following section.

Component	Function
Fibrin	Clotting.
Platelets	Clotting.
Polymorphonuclearcytes (PMNs)	Immune defense, production of growth factors.
Lymphocytes	Immune defense.
Macrophages	Immune defense, production of growth factors.
Micro-organisms	Exogenous factor.
Plasma proteins, albumin, globulin, fibrinogen	Maintain osmotic pressure, immunity, transport of macromolecules.
Lactic acid	Product of cellular metabolism and indicates biochemical hypoxia.
Glucose	Cellular energy source.
Inorganic salts	Buffering, pH hydrogen ion concentration in a solution.
Growth factors	Proteins controlling factor-specific healing activities.
Wound debris/dead cells	No function.
Proteolytic enzymes	Enzymes that degrade protein, including serine, cysteine, aspartic proteases and matrix metalloproteinases (MMPs)
Tissue inhibitors of metalloproteinases (TIMPS)	Controlled inhibition of metalloproteinases.

Table 1.1 Components in wound exudates (White, 2006).

The constituents of wound fluid can give further information about the state of a chronic wound. Analysis of these components would help clinicians identify molecules and biological markers that indicate the stage of healing or health of the wound (James et al., 2000). The collection of wound fluid is a non invasive procedure so if a component of this fluid was to be a predictor of healing or overall

health of the wound it would be a useful analytical tool in wound analysis. This thesis will focus on the measurement of pH and its relation to wound healing. Its aim is to show that pH can be used as a simple measurement to assess the overall health of a wound. The following section will focus on pH and how it applies to wound healing.

1.7 pH and skin

1.7.1 pH scale

The measurement of pH is one of the most important variables in science as it can have a large effect on biological mechanisms and chemical reactions. It stands for power of hydrogen and is a used as a measuring scale for the acidity or alkalinity of a solution. It is a measure of the amount of hydrogen ions H^+ that are dissolved in a solution. The pH scale itself is the negative logarithm of the concentration of H^+ ions in a solution defined as $pH = - \log_{10} [H^+]$(Myers, 2009). The pH range is from 0 to 14 with 7 being neutral above 7 is alkaline and below 7 is acidic. This range has H^+ ion concentrations from 10^0-10^{-14}mol/l. The pH scale in a balance between H^+ and OH^- ions in the solution; when H^+ ions dominate the solution is acidic and when OH^- ions exceed the concentration of H^+ the solution is alkaline. The theory behind pH scale and acid base relationship is detailed in **Section 2.14**.

1.7.2 pH of healthy skin

Healthy skin has a pH level of around 4-6 depending on the place that the reading is taken and the age of the skin (Greener et al., 2005). The pH of healthy skin is influenced by secretions of amino and fatty acids from the keratin layer of the skin. The weakly acidic nature of the skin acts as a natural barrier to the external environment by inhibiting the activity of bacterial growth and digestive enzymes on the skins surface (Schultz et al., 2005). Most human pathogenic bacteria need a pH above 6 and are inhibited by pH levels below this. *Candida albicans* yeast is a common pathogen, it needs a lower pH level to control it or an overgrowth is found on the skin (Schmid-Wendtner and Korting, 2006).

1.7.3 Body pH regulation

The internal pH of the body is maintained by the acid base balance. The protein buffering system is the most plentiful buffering system in the blood and tissue cells - it depends on amino acids to release or accept H^+ ions when changes in pH occur. The extracellular fluid in the body has a pH of between 7.35-7.45 (Martini, 2006). When this balance is upset it is extremely dangerous as it alters the structure of proteins, disrupts the cell membranes and changes the activities of the enzymes in the whole body. A more detailed explanation of pH buffering in physiological solution can be found in **Section 2.14.1**.

1.8 Wound pH

When the skin is broken the internal pH of the body is exposed moving the pH from the acidic skin towards the alkali pH of the internal body. Chronic wounds have been reported to be in the range from 5.45-8.9 (Dissemond et al., 2003; Greener et al., 2005; Gethin, 2007). There is a large range of reported data on pH level of wounds. The large range is interesting as the level of pH directly and indirectly affects all of the processes that take place in the wound. It has been reported that the mean values of chronic wounds are in the same range as the body's extracellular pH of between 7.35-7.45(Dissemond et al., 2003). The pH level in the wound is influenced by many different factors. The mean level of pH in a chronic wound shows that the pH level is mostly influenced by the body's physiological pH level. The pH in a wound can also be directly influenced by oxygen levels, bacterial load and healing stage of the wound (Schneider et al., 2007). The pH of healthy skin around a wound is also affected by a wound as the pH was found to rise to between 6.2-6.6 (Schneider et al., 2007). The pH of a wound varies as it heals moving from an alkaline pH towards an acidic pH during re-epithelialisation as the skin layer reforms (Romanelli et al., 2002). Research has shown that non healing wounds and those with a high bacterial load generally have a pH level above 7.6 (Gethin et al., 2008). There is currently no data to suggest the most effective pH level for wound healing. The lack of data on this subject is somewhat related to the difficulties in measuring wounds. The next

section will focus on how the pH of a wound alters the healing process at a cellular level.

1.8.1 Oxygen, Temperature and pH

One requirement of all healing tissues is an available supply of oxygen. Oxygen at a molecular level is involved with the synthesis of collagen and the growth of fibroblasts. The body uses haemoglobin as a buffer to pH it is called the oxygen–haemoglobin dissociation curve. The pH, temperature and the concentration of 2,3-diphosphoglycerate affect the position of the curve (Barrett and Ganong, 2010). When the wound is alkaline the oxygen is needed to stabilise oxyhemoglobin hence reducing the level of oxygen in the wound. It is thought that wounds will not heal if the oxygen level is below 20 mmHg; chronic wounds have been shown to have oxygen levels of 5–20 mmHg (Hunt and Hopt, 1997). A small change in wound pH could induce wide changes in the available wound oxygen a shift down of pH by only 0.6 releases almost 50% more oxygen thus improving healing within the wound (Leveen et al., 1973).

1.8.2 Skin Grafts

Another area of skin healing that requires control of the pH levels is in the skin graft procedure. In the ex vivo model it was found that the skin grafts were most effective at a pH of 8.43 (Sharpe et al., 2009). This is an interesting result as the levels of pH needed for successful grafts are different from healing conditions in chronic wounds. This could be due to the skin grafts showing acute healing where all the enzyme activity is balanced. This area of wound healing wound benefit from regular pH measurements to determine the health of the graft and treat it accordingly.

1.9 Skin molecules and pH level

An understanding needs to be achieved on the overall complex processes that occur in a complex wound, **Figure 1.7** shows the relationships between the healing components. It has been suggested that if the cell and enzyme activity throughout the complex wound cycle was known it would indicate the stage of healing (Menke et al., 2007). The knowledge of how pH relates to the enzymes to control their activity

could be related to the stage of healing this could be a very important breakthrough in wound management and could lead to new techniques and treatments.

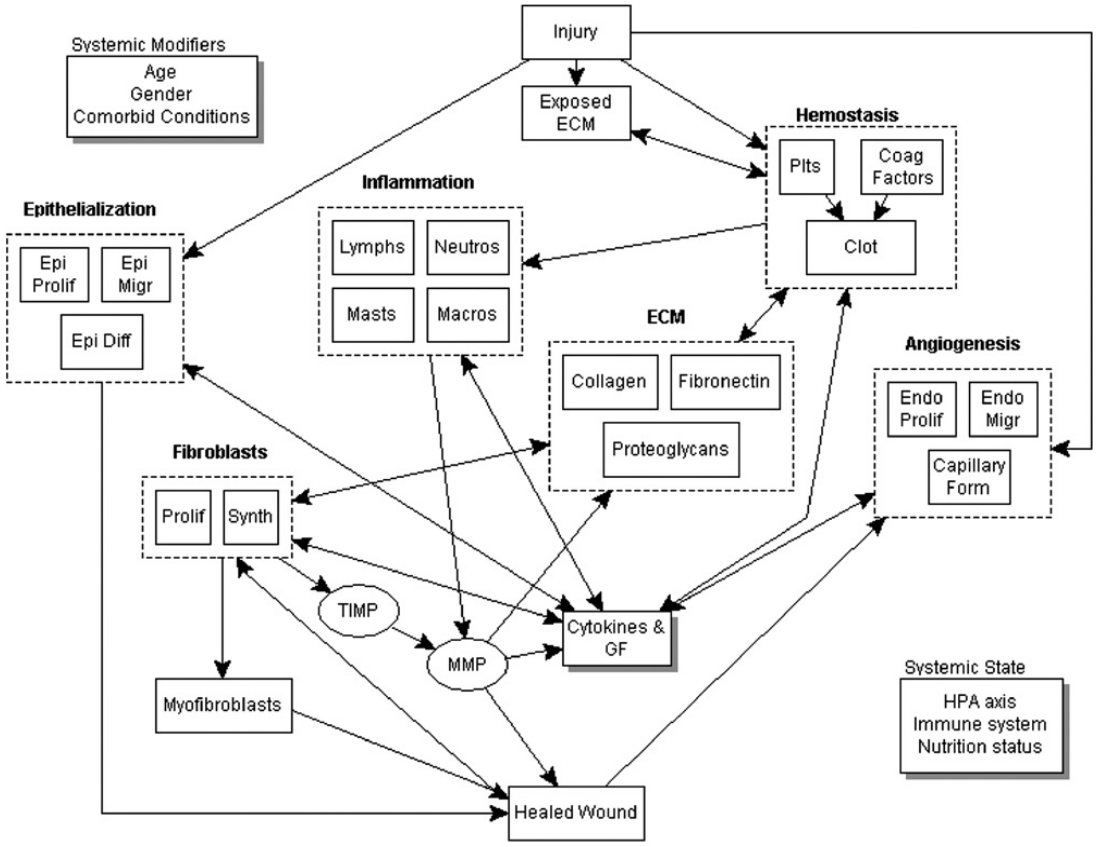

Figure 1.7 Flow and processes to achieve healing in a wound (Menke et al., 2007).

During the wound healing many cells and enzymes have high activity levels. The cells listed in this section are vital to the wound healing process, they include neutrophils, platelets, fibroblasts, keratinocytes and the matrix metalloproteinase (MMP) enzymes. The function of each cell/enzyme and the influence of pH on it within the wound healing cycle is discussed. They are listed in their order of activation during the wound healing process.

1.9.1 Neutrophils

Neutrophils are one of the first cells to migrate into the wound following injury. They are normally found in the blood and migrate through tissues to reach the site of

inflammation. The neutrophil plays an important part in the secretion of the enzymes MMP-9 and storage of MMP-8 (Kaehaeri, 1997). When a large amount of neutrophils are activated the MMPs that are secreted upset the balance of the wound due to their derivative properties (Menke et al., 2007). Excessive infiltration of these chronic wounds by neutrophils appears to be a significant biological marker for delayed healing (Diegelmann and Evans, 2004). Neutrophils also produce elastases which contribute to the proteolytic activity in chronic wounds by destroying important healing factors such as platelet derived growth factors and transforming growth factor-beta (TGF-ß) (Kainulainen et al., 1998). It was reported that elastases proliferation was sensitive to pH changes in the wound with maximum activity being found at a pH level of 8.3 (Greener et al., 2005). This indicates that lower pH levels will reduce the proliferation of elastases hence improving wound healing conditions.

1.9.2 Platelets

Platelets cause the blood to clot in the wound. They also produce growth factors which are vital to the chemical progression of wound healing. The two most important healing factors are platelet derived growth factors (PDGF) and transforming growth factor-beta (TGF-ß) (Diegelmann and Evans, 2004). Platelet derived growth factors start the cell proliferation of fibroblasts and helps promote angiogenesis. TGF-ß attracts macrophages and stimulates them to produce additional cytokines including FGF (fibroblast growth factor), TNF-α (tumor necrosis alpha) which is important to the healing cascade. In chronic wounds inflammatory cytokines such as TNF-α dominate - this leads to a reduction in PDGF and matrix deposition such as TGF-ß (Menke et al., 2007). An increase in platelet derived growth factor was found at lower pH levels with the optimum occurring at a pH of 5 (Liu et al., 2002). In the same study it found that synthesis of TGF-ß was highest at a pH of 7.1. The control of pH in the early stages of wounds could have an effect on the overall progress of healing in the wound.

1.9.3 Fibroblasts

Fibroblasts are one of the key cells in the wound healing process. They are abundant in connective tissue and are one of the first cells to enter the wound area after the

initial inflammatory response. Their proliferation in the initial wound combined with their production of components of the extracellular matrix and their differentiation into myofibroblasts combine to heal the wound and reform a new stable skin layer. Fibroblasts produce many of the components vital for formation of the extracellular matrix they include collagens, glycosaminoglycans, reticular and elastic fibers, and glycoprotein's. Fibroblasts contribute to raised levels of MMP1 and MMP3 within chronic wound fluid (Subramaniam et al., 2008). Myofibroblasts enhance wound healing by contracting the wounds edges in granulated tissue.

The rate of fibroblast proliferation is one of the main constituents of fast and effective wound closure. It was found that the rate of fibroblast proliferation is dependent on the level of pH in the wound (Lengheden and Jansson, 1995). The study found that at a pH of 7.2 the rate of migration and DNA synthesis was greater than at higher pH levels. When the pH was above 7.8 the cells started to show deformations. In contrast to these results it was reported that fibroblasts have their optimum proliferation rates at a pH values between 7.3-8.3 as shown in **Figure 1.8** (Sharpe et al., 2009).

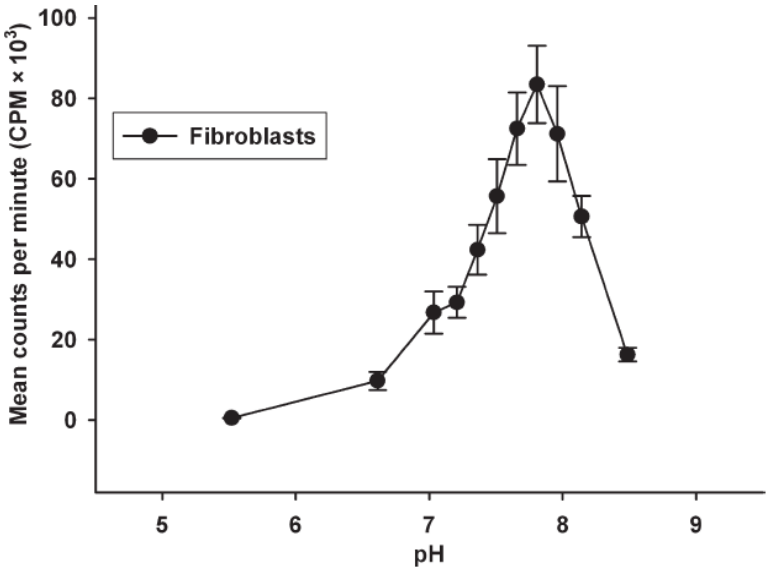

Figure 1.8 Proliferation of fibroblasts at various pH levels (Sharpe et al., 2009).

As the new skin layer is reformed the pH of the skin drops from an alkali level to an acidic one. Myofibroblasts are also affected by this shift in pH with the most acidic medium tested of 5.5 producing the greatest contraction (Pipelzadeh and Naylor, 1998). These results suggest that lowering of the pH in the final stages of wound repair will help to enhance wound contraction caused by myofibroblasts.

1.9.4 Keratinocytes

Keratinocytes are the cells that form the epidermis layer of the skin. When they migrate into the wound they produce and secrete MMP-2 and MMP-9 (Schultz et al., 2005). The optimum range of pH for the proliferation of keratinocytes was between 7.2 and 8.3 (Sharpe et al., 2009). The pH level was found to have an effect on the differentiation of the keratinocytes with lower pH producing more of the K1 cytokeratins.

1.9.5 Matrix Metalloproteinases

Matrix metalloproteinases (MMPs) are involved in every phase of wound healing (Muller et al., 2008). MMPs are produced by several different types of cells in that are crucial in the wound healing process these include fibroblasts, keratinocytes, macrophages, endothelial cells, mast cells, and eosinophils (Kaehaeri, 1997). There are 20 known MMPs which collectively are able to degrade the extracellular matrix. In acute wound healing they act to remove necrotic tissue, promote migrations of fibroblasts and keratinocytes, regulate the activity of some growth factors, contract the wound matrix and promote angiogenesis. During the final stages of re-epithelialisation they are active in remodeling the newly formed granulation tissue (Lobmann et al., 2002). If the balance of the MMPs is upset within a wound it can upset the cellular processes preventing healing and eventually causing further damage to the wound. In chronic wounds the amount of MMP activity has been found to be 30 times more than in acute wounds (Trengove et al., 1999). As a chronic venous ulcer wound moves towards healing the activity of MMPs decreases. MMPs are partially regulated by tissue inhibitors of metalloproteinases (TIMPs) of which 4 are known (Nagase and Woessner, 1999). Healthy wounds have a balance of MMPs to TIMPs. A reduction in TIMPs results in an increase in MMP activity which

contributes to the non healing nature of the wound (Lobmann et al., 2002). In chronic wounds a reduction in MMPs and increase in TIMPs is desirable for healing.

MMP-2 is expressed by a number of cells including keratinocytes and fibroblasts; it degrades type 1 collagen. MMP 9 is produced by keratinocytes and stored on neutrophils; it can degrade type I, II and V collagens. MMP 1 degrades type III collagen, MMP 8 degrades type 1 most effectively. MMP 12 degrades elastin and is expressed by macrophages (Kaehaeri, 1997). It has been suggested that MMP2, MMP8 and MMP9, as they degrade type 1 fibrin collagen, have the biggest role in degrading the extracellular matrix and have been found at high levels in chronic wound fluid (Schultz et al., 2005). Another study has shown that MMP 9 is a key enzyme in delayed wound healing as it directly delays wound healing through interference with re-epithelialization by impeding keratinocyte migration (Reiss et al., 2010).

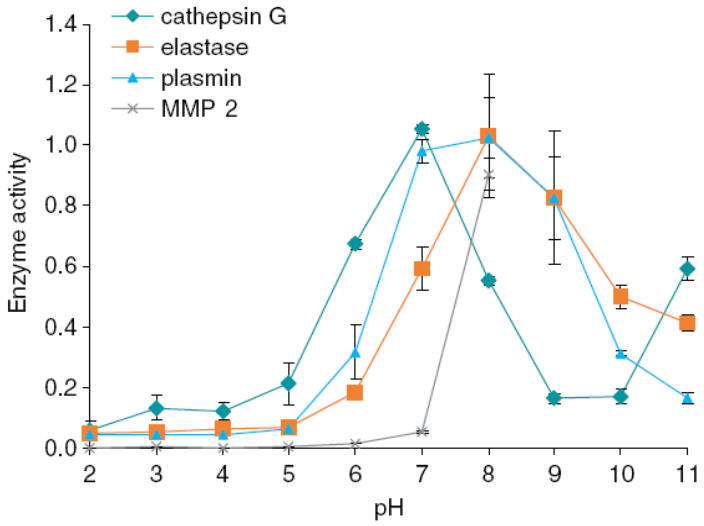

Figure 1.9 MMP levels and variation with pH level (Greener et al., 2005).

The pH level of the wound affects the enzyme activity of the MMPs (Schreml et al., 2010). Proteins are broken down more rapidly when the enzyme activity is high. If the enzyme activity can be reduced then the wound healing would accelerate. The adjustment of the pH level in the wound has been suggested as a method of reducing the activity (Schultz et al., 2005). MMP activity increases as the pH of the wound moves towards more acidic levels in burns wounds (Prager et al., 1994). A pH of

below 4 stops MMP activity whereas a pH above 7 can degrade a chronic wound further (Greener et al., 2005). **Figure 1.9** shows the key wound healing enzyme activity found at different pH levels. If a wound pH is reduced from pH 8 to a pH of 4 then the MMP enzyme activity would drop by 80% (Greener et al., 2005). A high level of MMP activity is known to prevent healing and even contribute to further damage. In chronic wounds the MMP activity is elevated, so by a process of reducing, controlling and monitoring the pH the wound may heal at a faster rate. This evidence suggests that control of the MMP proliferation in the wound is key to reducing wound healing times. The link of pH level to enzyme activity is interesting as if the pH can be monitored and controlled then successful healing of a chronic wound may be achieved.

1.10 Bacteria and pH

There are many common bacterial infections that can colonise a chronic wound and cause further disruption and complications to healing. The UK has one of the highest rates of bacterial infection in Europe and this is estimated to cost the NHS around 1 billion pounds a year to treat (Frost and Sullivan, 2003). Wounds are very susceptible to bacterial infection which has resulted in a trend of using antimicrobial dressings to stop infection. There are some strains of wound bacteria such as *Pseudomonas aeruginosa* which infect many wounds and show resistance to treatment. Bacteria are very sensitive to pH levels with higher values of wound pH lead to higher rates of infections. The minimum pH values for growth of some common wound-infecting species are: *Escherichia coli*, 4.3; *Pseudomonas aeruginosa*, 4.4; and *Streptococcus pyogenes* 4.5 (Gethin et al., 2008). Acidification of the wound could prevent and slow the rate of bacterial colonisation for these wound infections many of which are resistant to other forms of antibacterial therapies. However, lowering the pH to low levels would also prevent the wound healing cells proliferating. In a study a 97% eradication of *Pseudomonas aeruginosa* was achieved by applying white wine vinegar (pH 3) to the wound site combined with oral antibiotics (Leung et al., 2001). The antibiotic effectiveness was influenced by pH in a study as the lower the pH the less effective the antibiotic was although some antibiotics were shown not to be affected (Mercier et al., 2002).

Other studies have shown that bacterial colonisation of specific bacteria changes the pH level of the skin (Schreml et al., 2010). If the most common bacterial infections were studied with regards to pH of the wound, pH could be used as an indication of bacterial infection. Certain bacteria produce ammonia which can prevent the wound healing by elevating the pH and reducing oxygen (Leveen et al., 1973). An alkaline wound encourages wound bed slough to form which in turn prevents the wound healing and provides a good environment for bacteria to proliferate (Gethin et al., 2008).

1.11 Wound healing technology

This section will review the wound healing technologies that utilise pH in the treatment techniques.

1.11.1 Therapeutic modulation of pH

There have been a number of studies into the modification of pH in the wound which show that mild acidification of the wound produces healing in chronic wounds. In a study on burn wounds the wounds treated with a solution of pH 3.5 showed significantly better rate of re-epithelialisation (Kaufman et al., 1985). When wound pH was chemically altered it was proven that the tissues received more oxygen (Leveen et al., 1973).

There is a trend towards new dressings that induce pH change in the wound. One popular treatment using manuka honey (Comvita) to promote healing has shown that its pH of 3.5-4 aids healing by lowering the wound bed pH. The study found that wounds with a pH of above 7.8 did not achieve healing or increased in size. The wounds that had a pH of under 7.6 achieved a 30% reduction in size and that the reduction of pH in the wound correlated with this (Gethin et al., 2008). Other natural wound treatments such as aloe vera with a pH of 3.5 may also improve healing by reducing the wound pH level. In a study to look at pH level of popular wound dressings, the dressings were immersed in NaCl solution and the pH of the solution was then measured. It was found that the dressing pH values ranged from a pH of 2.44 to 7.5 (Dissemond et al., 2003). The most acidic of these dressings are

Promogran (Systagenix) with a pH of 2.44 and Skinoren (Schering Plough) with a pH of 3.48. Skinoren cream (Schering Plough) contains the active ingredient azelaic acid, which is a medicine used to treat acne. It reduces the growth of the keratin surface skin cells and kills bacteria associated with acne. Promogran (Johnson & Johnson Advanced Wound Care) is used by the NHS as a protease-modulating matrix that aims to balance the wound environment. It targets neutrophil-derived elastase, plasmin, and matrix metalloproteinase in the wound. The dressing is composed of processed bovine collagen with oxidized regenerated cellulose then it is embedded with 0.05M acetic acid (Cullen et al., 2002). Cadesorb (Smith and Nephew) is a starch based sterile ointment that lowers wound pH and thereby modulates MMP activity. It has been shown to have a pH value of 4.35 (Dissemond et al., 2003). In a study using Cadesorb (Smith and Nephew), the wound pH before application had a mean value of 7.7; after 24 hours the wound pH values had dropped to 6.69 (Dissemond et al., 2004). Another Smith and Nephew product is BIOSTEP (Smith and Nephew) it uses ethylenediaminetetracetic acid in a collagen matrix to limit MMP enzyme activity. Tegaderm (3M) uses pH change to lower MMP levels this is achieved through embedding citric acid in the wound dressing. Using one of these dressings it was found that the MMP 9 level was significantly reduced and the patients exhibited a more rapid healing rate (Cullen et al., 2002). The low pH of these dressings suggests that these dressings use the modification in pH to control and reduce the MMP activity in the wound.

New forms of wound dressings are in development that react to pH change in the wound and release active ingredients accordingly. They use alginate hydrogel beads that are pH and temperature sensitive and can release drugs when changes occur (Shi et al., 2006). This technological advance could result in smart dressings that can react and modify the constituents of the wound when different wound healing conditions occur. For this to be achieved the relationship of how pH controls processes in wounds such as MMP activity and cell proliferation would have to be extensively studied.

1.11.2 Enzyme wound debridement

Wound debridement which involves removing the top layer of cells to stimulate healing can be achieved by using proteolytic enzymes. The proteolytic enzymes need to be in a specific pH range to be effective (Mercier et al., 2002). The optimum pH range for wound enzymes is shown in **Table 1.2**.

Debridement enzyme	pH operation range
DNAse	Activity pH 4.5–5.5 (Fibrinolysis) Activity pH 7.0–8.0 (DNA lysis)
Fibrinolysin	Activity pH 7.0–8.0
Collagenase	pH optimum 6.0–8.0
Krill-enzyme	pH optimum above 7.5
Papain	Activity pH 3.0–12.9 pH optimum 7.0
Plasmin	pH optimum 7.0
Streptodornase	pH optimum pH 7.5
Streptokinase	Activity pH 7.3–7.6
Sutilain	pH optimum 6.0–6.8
Trypsin	pH optimum 7.0

Table 1.2 Optimum pH for specific enzymes used for debridement (Dissemond et al., 2003)(Schneider et al., 2007).

If the pH of the wound is not monitored before application of enzymes then they may fail to work effectively if outside their optimum pH range. This is one example when the measurement of pH could be used to select the most appropriate enzyme for debriding the wound (Schneider et al., 2007).

1.12 Summary of pH and wound healing

The previous sections detail how pH has a large influence on many of the vital wound healing processes. The pH level recorded for wounds in various studies shows that the pH of a wound will have a large effect on the healing process. At a cellular level the cells that are most active in the early stages of wound healing neutrophils and platelets are at their most effective when at lower pH values below 7. The fibroblasts and keratinocytes are more active at later stage of wound healing have higher activities at pH levels between pH 7-8. Myofibroblasts are most active at the end stage of healing; they have an optimum effect on wound closing at a pH of 5.5.

The cell which is most active at the end stage of healing myofibroblasts has an optimum wound closing at a pH of 5.5. Although these findings are based on in vitro cell experiments it suggests that the optimum pH for cell proliferation will change over the healing stages. At a cell based level the pH may need to change dependent on the healing stage to kick start the healing process. With further studies it could relate the stage of wound healing to an optimum pH level which could lead to faster wound healing.

The trend in recent advanced wound dressings in reducing pH suggests that a lower wound pH helps start the healing process of chronic wounds. A lower wound pH would increase the wound oxygen, reduce MMP levels and reduce the proliferation of bacteria. While this trend toward lower pH may help with some aspects of the healing process the overall role of pH in a wound is not fully understood and further research needs to be conducted. A tool to measure pH level in an easy, cost effective and reliable way will enable the pH of a wound to be studied further to find its overall influence on the healing process. The measurement of pH as an analytical tool would be useful for measuring the wound pH of skin grafts and for measuring wound pH for the optimum application of enzymes for debridement procedures. The following section will discuss the measurement of pH in wound care and look at new technologies to help achieve cheaper easier methods of testing the wound pH.

1.13 pH sensing technology

This section will start with a description of the current pH sensing techniques used in wound care. Following this there is a review of current pH sensing techniques and research into alternative pH sensing methods such as optical, metal oxide and ISFET. The review will then focus on the sensing method used in this thesis which is a solid state potentiometric sensor. The solid state sensors are composed of 3 different layers; conducting contact, conducting polymer ion to electrode conductor and a PVC based ion-selective membrane. This review will introduce the current research into each of these solid state sensor components. From this literature review the best reported elements that are suitable for medical use were chosen as the components of the sensors evaluated in the experimental sections of this thesis.

1.14 Current pH sensors

1.14.1 Glass/ Ion-selective membrane

The design of the most commonly used glass pH electrodes has not changed significantly since it was first invented in 1908 by Fritz Haber (Galster, 1991). It was not until 1934 that the first complete pH meter was available commercially. The measurement works by having a glass membrane between the solution to be measured and a saturated electrolyte contained within the glass with a half cell for measuring which is most commonly an Ag/AgCl or a calomel system. The glass acts as an ion-selective barrier that produces a potential difference when immersed in different concentrations of the primary sensing ion. The potential difference of the sensing half cell is measured against a reference electrode which should provide a constant voltage potential in the different primary ion concentrations. The full theory behind the operation of the ion-selective electrode can be found in **Section 2.9**.

Figure 1.10 Photograph of glass membrane pH electrode.

Glass electrodes are the most common pH electrodes in use today due to good sensitivity, stable potentials and good selectivity to the primary ion (Galster, 1991). In a combination electrode both the reference and the sensor are contained within the one device. An example of a pH combined electrode is shown in **Figure 1.10**. The glass electrode needs to be calibrated before use. This calibration is common throughout all pH sensors before use to ensure accurate pH measurement values. The response of the glass electrode sensors follows an equation known as the Nernst equation which gives a limit of 59.16mV/decade change in primary ion concentration. The Nernst response is described in detail in **Section 2.7**.

1.14.2 Current methods for testing wound pH

For measuring the pH of skin the glass membrane has been adapted into a flat surface. The skin electrode is a planer flat membrane glass electrode which is placed on the skin or wound. It has a large surface area and combines both the reference and active electrode into a single electrode. There are two glass electrodes specifically used for measuring the pH of skin currently commercially available. The two meters are the pH900 from Courage & Khazaka and 1140 pH from Mettler and Toledo. The accuracy of these sensors has been compared by Ehlers et al (2001). They found, that for accurate measurements, a seven second stabilisation time is needed after contact on the wound bed. To gain an accurate pH measurement they found that the test site should not to be washed within 24 hours before the test commences.

The glass electrode is the only commercially available measurement tool for clinicians to measure wound pH accurately. Previous studies that have looked at pH and healing rates have had to rely on glass pH probes with flat bottoms to measure the pH of the wound. The pH electrode has not been successfully adapted into smaller and alternate packaging because the membrane that forms the selective part of the electrode being made of silicon glass that is fragile, thus limiting the way that it can be manufactured. It is not a widely used technique due to the discomfort to the patient when measuring, the time to take each measurement and the problems sterilising the probe after use. A quick, simple and non invasive system is needed to measure pH level in the wound. A new system will enable more insight into role of

pH level in the wound healing process and enable the therapeutic modulation of pH to be monitored (Schreml et al., 2010).

1.15 pH sensor research

Although the standard glass electrode is still the most common pH sensor type due to excellent performance characteristics it is not suitable for small and disposable sensors because of its cost, brittleness, need for internal liquid junction and difficult manufacturing techniques that require high temperatures. Another commonly used method is the use of litmus paper although inexpensive this method does not provide a precise pH value and cannot be sterilised. There are a number of different techniques and methods that can be used to find the pH of a solution these include:

- Sol glass which enables glass ion-selective membranes to be made with a simpler manufacturing process
- Optical sensors that use pH sensitive dyes or gels
- ISFETS which are ion sensitive semiconductors
- pH sensitive metal oxides
- Solid state potentiometric pH sensors based on plastic ion-selective membranes and conducting polymers

The aim of the majority of the research focuses on the miniaturisation of the electrodes and search for suitable replacements for the internal filling solutions in standard glass electrodes. This section will briefly document the main areas of research for alternative pH sensors and how they could to relate to the measurement of wound pH.

1.15.1 Sol glass/gel

Sol glass or gel is a form of glass which is cheap and can be processed at low temperatures which makes the manufacturing process simpler. With suitable dopants this glass can be used as a pH sensor much the same way as the traditional glass electrode. It is used in optical pH sensors to form the glass membrane that encases pH sensitive dyes (Grant and Glass, 1997). In a study by Li et al (2002) a sol glass

membrane was used to produce a screen printable pH sensor. A carbon zeolite was used as a receptor molecule for detecting the amount of hydrogen ions. The results shown in this paper show a close to a Nernst response of 60mV/decade H^+ ion concentration response rates over a pH range of 2-12. Sol gel pH sensors have also been shown to give responses of 55mV/decade H^+ ion concentration when the receptor molecule is covalently bound to the sol gel (Marxer and Schoenfisch, 2005). The problem with this technique is the processing of the sol gel membrane as it is still susceptible to cracking which would not be suitable if the sensor was to be used in wound care.

1.15.2 Fibre optic

Figure 1.11 Ocean optic coloured dye fibre optic pH sensor (sourced from www.oceanoptics.com).

The fibre optic pH sensor operates by having a pH sensitive dye or gel, whose colour is dependent on the concentration of H^+ ions encased in an ion-selective membrane that allows movement of H^+ ions from the solution to the dye (Grant and Glass, 1997). The probe is small and can be designed to be used in-vitro or in-vivo. When the probe is in use the H^+ ions in the solution alter the colour of the dye inside the probe then the change in colour is measured by the fibre optic cable and the pH is determined by the colour change in the solution. The dyes change colour reversibly depending on the pH of the solution. A company called Ocean Optics manufacture

optical pH sensors for use in industrial settings an example of this is shown in **Figure 1.11**. The cost of the probes is expensive with the need for spectrometer equipment to analyse the light sample. The dye specific pH indicators allow constant measurement of pH although they take a few minutes to adjust to new pH levels. A study of pH sensitive dyes found that Thymol blue could measure in the pH range 1-9 which would make it suitable for pH measurements in wound care (Aizawa et al., 2007). The dyes have a high sensitivity to changes in pH which is needed in the monitoring of wound pH because of the small fluctuations that occur. Another positive characteristic of these sensors is that they are not directly influenced by electricity. This would be an advantage in the wound as it would make it electrically isolated from any other sensors or interference in the surrounding area.

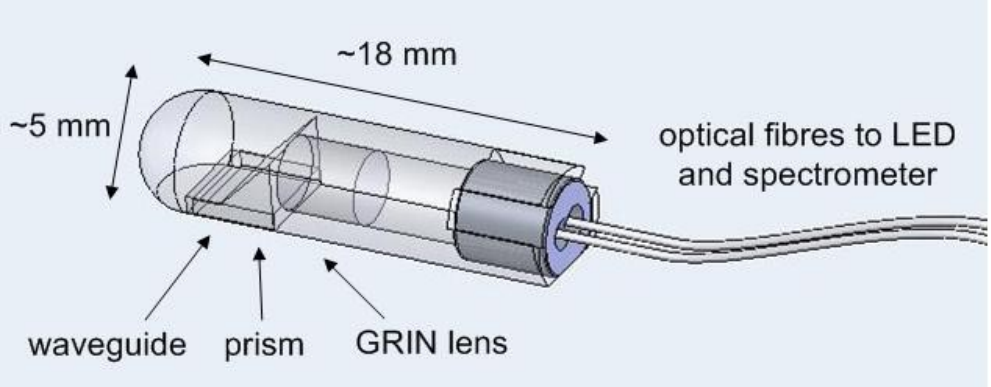

Figure 1.12 Biotex optical sensor for wound pH measurement (Pasche et al., 2008).

The fibre optic pH sensors are biologically safe and have chemical stability so they are useful in a number of situations such as gastric pH sensors and cell biology monitoring (Lin, 2000). A problem with using this in wound monitoring is how to ensure that correct contact is being made between the sensor and the wound fluid. This problem applies to both wound measurements as well as gastric stomach acid sensors. This has been solved for gastric sensors as the sensor can be vacuum sealed onto the patient's throat. The difficulty for this technique in wound measurement would be that any fixing to the wound would disturb any healing in that area.

A research group called Biotex based in Switzerland produce wearable sensors with the final aim of integration into textiles so that they can be worn by the patient (Pasche et al., 2008). They have produced a wound healing sensor prototype that

incorporates an optical pH sensor, **Figure 1.12**. The sensor is based on the osmotic reaction of a polyvinyl alcohol which is cross linked with polyacrylic acid to produce a reversible swelling effect when pH is increased. The pH is measured by optically measuring the change in the refractive index from light from a white LED. The devices works well for a short period of time but it does not work effectively for longer term monitoring due to the polymer that absorbs the ions being unable to return to its original size. The same group has produced a bandage that integrates coated fibre optic wires into a wound bandage that allows the monitoring of pH within a wound as shown in **Figure 1.13**. This was used to show pH changes within a human serum solution, however, the work has not been published so the accuracy of the system is unknown.

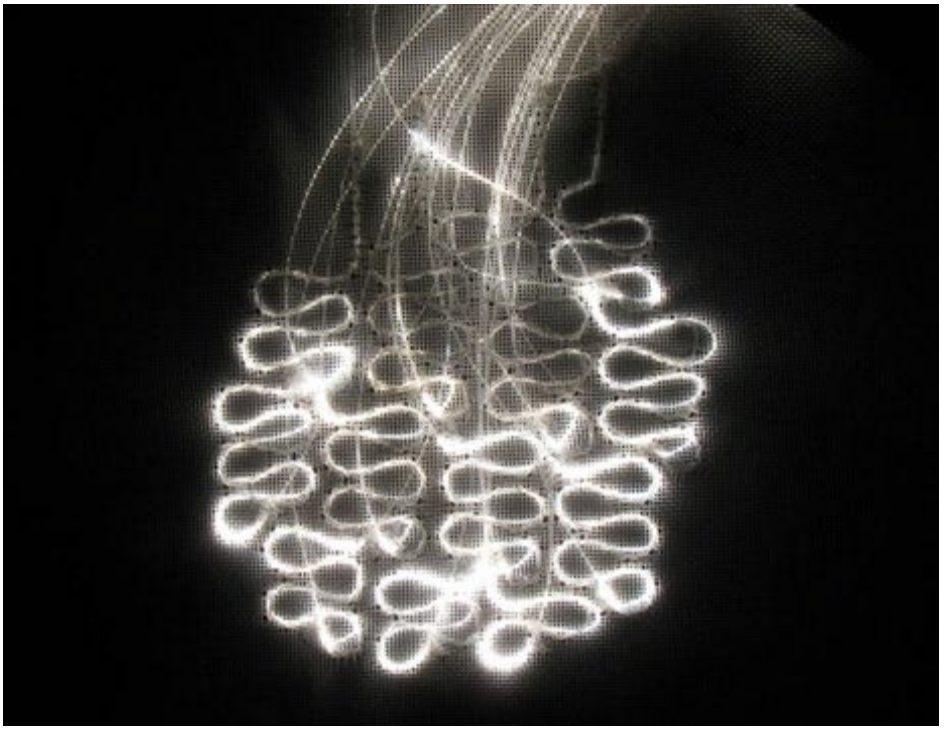

Figure 1.13 pH sensitive fibre optic wires integrated in wound bandage (Sourced from http://spectrum.ieee.org/biomedical/diagnostics/optical-fiber-watches-wounds).

Overall the cost of the sensors both for the sensor itself and the optical measuring equipment would be the main negative factor for the use of these sensors. They have been shown to work effectively so in a different form such as the more cost effective

coated fibre optic cables (Laursen, 2011) the sensor may have future possibilities for use in wound pH sensing.

1.15.3 ISFETS

Ion-selective field effect transistors (ISFETS) have been developed to measure a number of biological parameters. The sensor is based on semiconductor technology where a current is produced depending on the surface adsorption of charges at the ISFET sensor (Korostynska et al., 2008). The ISFET sensors are available commercially but they are expensive and not suitable for disposable operation. Their main operation is in industrial settings where glass electrodes are unsuitable, **Figure 1.14** shows a commercially available ISFET sensor.

Figure 1.14 Commercially available Mettler-Toledo Inpro3300 ISFET pH electrode (Sourced from www.mt.com).

ISFET pH sensors have been used on lab on a chip applications due to the small sensor size (Hammond et al., 2002). The pH sensitivity of these sensors has been reported at 46mV/decade H^+ ion concentration (Milgrew and Cumming, 2008). Pourciel-Gouzy et al (2008) demonstrate the use of pH sensitive ISFETS to monitor bacterial activity this technique could be further researched and developed so that they can detect certain bacterial forms relevant to wounds. ISFETS could be used for measuring pH on the skin as a low level moisture is needed for a pH measurement to

be made. If the ISFET pH sensor was adapted into a more suitable/cost effective package it would have potential to be used in wound pH measurement.

1.15.4 Metal-metal oxide

Metal oxides were one of the first disposable pH sensors investigated due to their ease of manufacture and low cost. The sensors are robust and can be used in harsh environments where a glass electrode would not be suitable. The pH sensitive nature is due to the formation of an oxide layer on the surface for the metal. The materials that are used for the pH sensitive sensors are metals that are easily oxidised.

The choice of metal is important as many of the most sensitive and lowest firing temperature metal oxides would be toxic and hence unsuitable for wound measurements (Koncki and Mascini, 1997). The most commonly used metal oxide sensor used in medical pH measurements due to their cheaper cost and solid state nature is made from an antimony/antimony oxide electrode. Antimony sensor is used in gastric pH sensors such as BRAVO developed by Medtronic (Korostynska et al., 2008). It has been approved for medical use and transmits the signal through wireless transmission. The antimony electrode requires high temperatures during manufacture to produce the oxide layer (Jones et al., 1982). Gill et al (2007) investigated the use of metal oxides using titanium oxide and tin oxides which are used in dental implants and should be safe to use in wound care monitoring. The sensors were found to have pH sensitivity but were temperature dependant and the electrode was not stable over long measurement periods. The surface of the metal electrodes becomes covered in an oxide layer when in contact with air which causes a hysteresis effect for measurements. The outcome of these experiments with biologically safe metals showed a drift in the measurements over time due to the continuous corrosion of the metals.

1.16 Solid state potentiometric pH sensors

This section will discuss the research that has previously been conducted into solid state potentiometric pH sensors. Solid state sensors replace the need for the internal filling solution associated with traditional glass ion-selective electrodes making the device more robust and easier to manufacture. The ideal solid state pH sensor would have the following attributes:

- Low cost
- Disposable
- No liquid phase
- Potentiometric
- Biocompatible materials
- Good contact with skin/wound
- Accurate in the pH range 4-9
- Good voltage stability
- No calibration
- Screen printed

This project uses the screen printing method to produce pH sensors. This method was chosen because of the ease of manufacture for large numbers of sensors, the low cost of sensor production and the consistency of screen printing. These parameters will allow the printed sensor to achieve a number of the ideal qualities that are stated above. The electronic measurement circuitry for potentiometric measurements can be made with cheap electrical components and when combined with the cheap disposable sensors it makes for a cost effective solution to pH sensing.

Disposable sensors have a huge commercial market. The most successful of these is the glucose sensor for monitoring blood sugar levels. The blood glucose sensors use an amperometric detection technique that senses change in glucose with change in current. The most successful commercial potentiometric sensors are produced by Abbot and are part of a multi sensor system called ISTAT. ISTAT is a point of care analytical device for measuring many different biological markers in blood including pH. The technology uses disposable cartridges onto which blood is deposited. The technology for sensing uses a range of solid state sensors an example is shown in **Figure 1.15**. The ISTAT would not be suitable for measuring wound pH as it is optimised for blood pH measurements which would mean the measurement range is small between 6.50 – 8.20 (Abbott, 2011). The design of the disposable sensors reported in this thesis will take elements from both the blood glucose sensors and the Abbott ISTAT system.

Figure 1.15 ISTAT machine (Left) and sensor based cartridges (Right).

The potential market for a disposable pH sensor is large because of the need for this measurement in many different fields including wound care pH monitoring. Other potential uses for this sensor are in the biological testing market where they test for molecules that contaminate traditional glass sensors. It would also have applications in the food testing market and point of care devices. The following section will discuss the research developments of solid state potentiometric pH sensors.

1.16.1 History of solid state sensors

The first research into solid state sensors occurred in the early 1970's where wires were coated with an ion-selective membrane by Cattrall (Cattrall and Freiser, 1971). This showed that it was possible to detect ion concentration through a solid state sensor. The issue with the coated wire electrode is that it experiences voltage measurement drift due to a blocked interface between the ionic conducting ion-selective membrane and the electron conducting wire. This voltage drift results in inaccurate ion sensing. The theory behind this is fully explained in **Section 2.9.2**. This problem has been addressed with the introduction of a middle layer between the metal contact and the ion-selective membrane. This middle layer works to exchange the electrical signal carried by charged ions in the solution to electrons in the metal through a redox reaction. The full theory of this can be found in **Section 2.10.4**. The middle layer acts to replace the liquid phase of the glass electrodes and function to maintain a stable voltage response of the sensing electrode.

The sensors that will be studied in this thesis consist of three distinct layers. The top layer is the ion-selective membrane which acts as a barrier between the solution and sensor allowing specific ions to flow across it. The middle layer is the ion to electron transducer layer which allows the ions that flow through to be exchanged into an electronic signal and vice versa to maintain a stable electrode voltage. The final layer is the metal contact which acts as the conductor to allow flow of electrons to and from the measurement circuitry. The three layer sensor is shown in **Figure 1.16**. This section will detail the different research into these different types of sensors and how the different layers affect results.

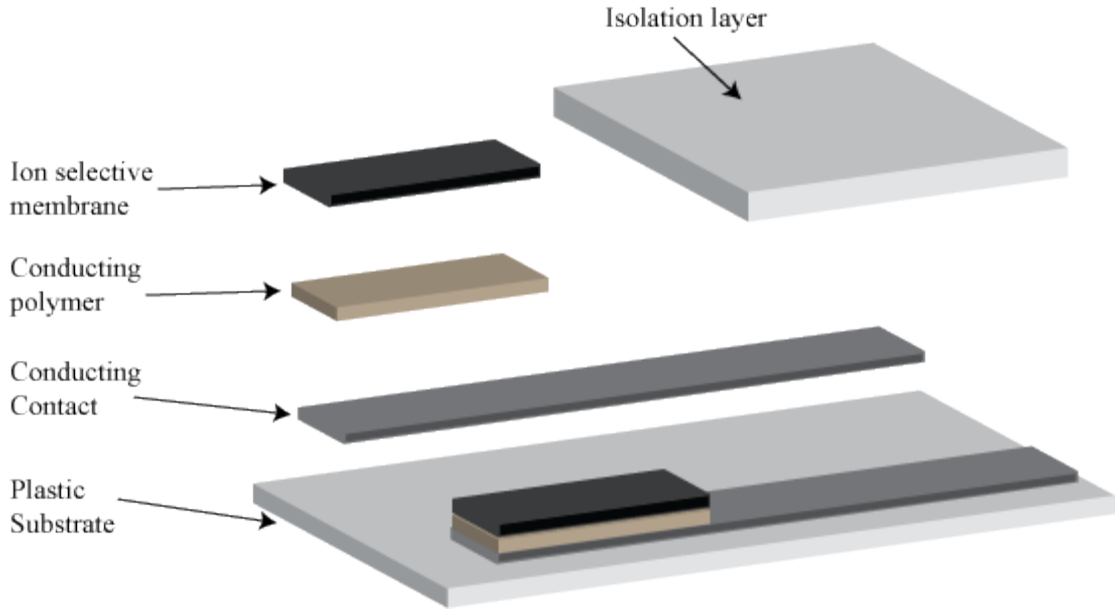

Figure 1.16 Three layer solid state sensor showing substrate, conducting contact, conducting polymer, ion-selective membrane and isolation layer.

The majority of solid state research documented in the following section is based on platinum wires or glassy carbon rods as electrical conducting contacts for the electrodes. These would not be suitable for disposable sensors due to their cost although their findings can be applied to cheaper conducting contacts such as screen printed electrodes. The research in this thesis focuses on screen printed carbon conducting contacts as these are inexpensive and the manufacturing process is simple. The following sections will discuss the current research and developments in the area of solid state sensing. Specific research on screen printed electrodes follows in a later section. Each part of the solid state sensor will be broken down into ion-selective membrane and ion to electron transducers and is discussed in their component parts.

1.17 Ion-selective membranes

The ion-selective membrane's main function in a pH sensor is to enable flow of hydrogen ions through the membrane of the sensor as well as preventing unwanted ions moving through which would affect the membrane sensing potential. The ions are transported through the membrane by ionophores which are ion transport carriers. Ionophores are lipid soluble molecules that allow ion transport across the membrane by binding the primary ion. The operation of the ion-selective membrane is discussed in detail in **Section 2.8.1**. This section will summarize the current research of ion-selective membranes.

1.17.1 Ionophores

Ionophores can be used to produce ion-selective membranes by increasing their permeability to the primary ion of interest. Different ionophores have been shown to be ion-selective to a wide variety of biologically relevant ions such as potassium, calcium, sodium and chloride as well as many others such as metal ions (Buhlmann et al., 1998). There are a number of ionophores suitable for use in a hydrogen ion-selective electrode. The choice of ionophore depends on the range of pH sensing and selectivity. From the literature it is difficult to compare different types of sensors in various papers due to differences in the sensor materials, production methods and experimental setups.

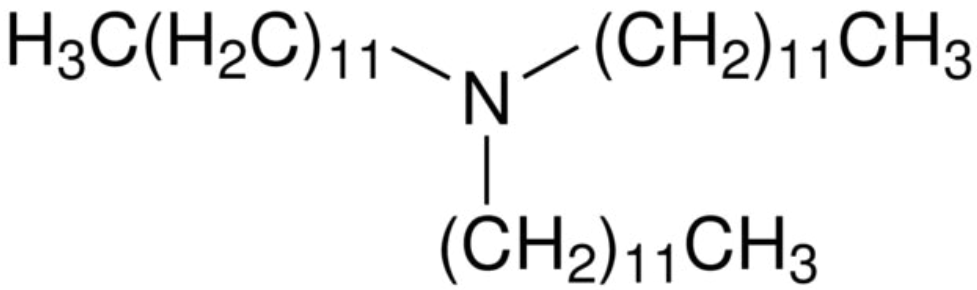

Figure 1.17 Tridodecylamine hydrogen selective ionophore structure.

The Ionophore is the most varied part of the sensor membrane within the literature as it is the key component of the membrane to allow transportation of the hydrogen ions across the membrane. Within the literature there are many different types of ionophore used the choice depends on what range of pH is needed for detection and the ability of the ionophore to select the primary ion of interest. The range of an ionophore for sensitivity of its primary ion is limited by cation interference at high pH and anion interference at low pH (Bakker et al., 1994). The majority of alkaline sensing ionophores are from the amine family tend to stop transporting ions effectively at high acidity levels, the typical stable range of these is 4-10 on the pH scale (Samsonova et al., 2008). The ionophore tridodecylamine was the first successful highly selective neutral carrier ionophore found. It showed good selectivity similar to glass pH electrodes and a linear pH response range of 4.5-10, its structure is shown in **Figure 1.17** (Lindner et al., 1995). Microelectrodes formed with this ionophore were found to be successful (Buhlmann et al., 1998). Tridodecylamine has been used successfully to measure the pH of blood and blood serum (Anker et al., 1983). The tridodecylamine ionophore is the most commonly used and cheapest commercially available H^+ ionophore. Other ionophores with good performance for hydrogen ion selectivity are Tribenzylamine which has a large linear pH range of 2.8-10.6 (Han et al., 2003b). An ionophore from the amine group dibenzylpyrenemethylamine has shown good acidic sensitivity in pH range 0.5-10.2 which is unusually low pH sensitivity for an ionophore in the amine ionophore family (Han et al., 2004). Other non amine based ionophores are more commonly used for strong acid sensing. These include the ionophores octadecyl isonicotinate and hexabutyltriamodophosphate which were used to produce effective sensors in the pH range 0-6 (Lutov and Mikhelson, 1994).

The ionophore to be used in a specific sensor must be chosen by the range of pH levels being tested. For the purpose of wound sensing any sensor that is stable in the range 5-10 would be ideal. As previously stated the amine family of ionophores with their stable range generally in the 4-10pH range would be suitable for the biological wound pH sensing. An important factor in the membrane operation is the other membrane components such as ionic additives, plastic and plasticiser the next section

will discuss the other membrane components and how they affect membrane performance.

1.17.2 PVC based ion-selective membranes

PVC is the most common type of membrane for solid state sensors. It is chosen because of its ease of manufacture and fast diffusion rates when compared to other membrane material types (Heng et al., 2004). The membranes are composed of a number of different components which can all have an effect on the outcome of the sensitivity of the sensor. The main components of an ion-selective membrane are:

- PVC
- Plasticizer
- Ionophore
- Ionic salt.

The operation of a membrane is discussed in detail in **Section 2.8.1**.

The optimum membrane characteristics are achieved when the stabilizing interactions between the primary and interfering ions are minimised (Bakker et al., 1994). This can be achieved by ensuring the ionophore and plasticizer should have no functional groups with which interfering cations can interact. The plasticisers can have a large effect on the sensitivity of the membrane as they can contain coordination sites such as amide, ester, or ether groups that can react with the cations (Oesch et al., 1986). The plasticizers DOP, DOA or 2-Nitrophenyl octyl ether are the most commonly used types. An ionic salt is used in the membrane to ensure that no significant counter ions are extracted into the membrane when the primary ion enters the membrane phase (Ammann et al., 1985). Typically the ionic salt such as potassium tetrakis(4-chlorophenyl)borate (KTpClPB) is used due to it having weak ion pair formation capabilities. The most effective membrane measurement range has been found to occur when the ionic salt additive is at 50% molecular weight of the ionophore (Bakker et al., 1994).

PVC membranes have been shown to suffer in long term use from poor adhesion to conducting contact and plasticizer and ionophores leeching out of the membrane (Kuruoğlu et al., 2003). The PVC membrane has problems with adhesion over a longer time period as the voltage response of the sensor becomes unstable. This instability is due to liquid pockets forming between the membrane and the sensor contact (Fibbioli et al., 2000). The membrane adhesion is important to the operation of the sensor to prevent a water layer forming between the membrane and sensor contact. To address the problems with adhesion lipophilic layers were shown to improve membrane adhesion and prevent formation of a water layer (Fibbioli et al., 2002). Using screen printed electrodes Musa et al (2011) used a pretreatment to increase surface roughness which they credit as giving better adhesion to the membrane. Another technique used to improve membrane adhesion is the introduction of RVT silicon rubber into a PVC (Piao et al., 2003) (Cha et al., 1991).

1.17.3 Non PVC Membranes

Due to problems with adhesion and leaching of ionophores and plasticisers in PVC membranes there has been some research into different membranes that are more stable and do not contain plasticizer. The most popular type of non PVC membrane is polymethyl-methacrylate/polydecyl-methacrylate (PMMA/PDMA) copolymer. The ionic diffusion in a PMMA/PDMA ion-selective membrane was found to be 1000 times slower that a PVC membrane (Heng et al., 2004). The slower diffusion times will lead to slower response times.These membranes have good adhesion properties so they are accurate for long periods of time (Peng et al., 2007). PMMA/PDMA copolymer is 20 times more hydrophobic than the PVC which would lead to further advantages for the stability of the sensor as less water would penetrate the layers (Crespo et al., 2008).

1.18 Ion to electron Transducers

The purpose of the ion to electron transducer is to enable the conversion of an ionically carried charge in the solution to an electronic one carried by electrons. The reason for the poor reported voltage stability of coated wire electrodes is due to there being a blocked interface between these two different phases which allows charge to build up changing the electrode voltage potential. The theory behind the operation of ion to electron conductors can be found in **Section 2.10.4**. In a traditional electrode the most commonly found redox couple is the Ag/AgCl couple in a saturated KCl solution; the theory behind this is discussed in **Section 2.11**. The purpose of solid state sensors it to replace the liquid junction used in conventional glass electrodes and allow stable voltage potential. In a solid state sensor this takes the form of a middle layer between the ion-selective membrane and the conducting contact. Replacing the liquid junction enables smaller, cheaper sensors to be produced. There are a number of research areas such as conducting polymers, hydrogels and carbon nanotubes that have been used to replace the liquid junction. This section will discuss the research conducted in these areas.

1.18.1 Conducting polymers

Conducting polymers have a number of properties that make them suitable for ion to electron transduction in solid state pH sensors. They are electrically conducting, they can tranduce an electronic signal to an electronic one through redox reactions and can be easily formed on metal and carbon electrodes. The conducting polymers have many promising characteristics that are good for ion to electron transduction such as high redox capacitance which relates to the voltage stability of the electrode (Bobacka, 1999). The theory behind the operation of conducting polymers in a solid state sensor system can be found in S**ection 2.10.4**. There are a number of different techniques that can be used to deposit different kinds of the conducting polymer, namely, electropolymerization, screen printing and solution casting.

There are many different types of conducting polymers the most commonly used for pH sensing is polypyrrole. The use of conducting polymers as ion to electron transducers is common in many ion sensing electrodes, polypyrrole and PEDOT are

frequently used. There are a number of factors which can influence the operation of conducting polymers the most important of which is the dopant ion used in the formation of the polymer this can affect the conductivity, stability and ion exchange properties of the polymer (Crespo et al., 2008). The theory behind the dopant ion can be found in **Section 2.10.2**. The following section will document the key research into conducting polymers that relates to pH sensors.

1.18.2 Polypyrrole

Polypyrrole is one of the most commonly used conducting polymers due to its ease of formation and its non toxic qualities (Bobacka, 2006). The deposition technique of the polypyrrole is also important as it can be chemically synthesized or electro deposited onto a conducting material with a high material work function. Almost all the papers that study polypyrrole use platinum or glassy carbon discs as the conducting contact. The most common deposition technique is electropolymerisation where the polymer is formed through a charge transfer reaction. Further details are given in **Section 2.10.1**. There are two types of polymerization commonly used:- fixed voltage and cyclic voltage sweeps. Early studies into polypyrrole used a fixed voltage technique for depositing the conducting polymer. This involved placing a constant voltage across a solution containing pyrrole and a counter doping ion. This technique was found not be effective for sensing as the layer formed in uneven growth patterns (Cosiner and Karyakin, 2010). The most commonly used technique is a cyclic voltammetry which involves the buildup of layers of conducting polymer at each voltage sweep allowing an even polymer film growth on the electrode.

Polypyrrole with no ion-selective membrane has been shown to have a linear response to hydrogen ion concentration. It achieves this with immobilized recognition sites within the conducting polymer. The dopant ion of the conducting polymer can affect the results of the sensitivity of the conducting polymer. There are many papers which research this to find the most effective doping ion for a sensor. Different dopant ion sizes affect the overall response of the sensor; smaller ions are easily exchangeable with the solution and give similar pH responses but larger ions do not transfer as readily (Michalska and Maksymiuk, 2003). Using this technique, the best reported polypyrrole only sensor has been reported as having pH sensitivity

in the range 3-10 with a response of up to Nernstian response values of 59mV/decade H^+ ion concentration using a large molecule tetrabutylammonium p-toluenesulfonate (PTS) as the dopant ion (Pandey and Singh, 2008). Other research in conducting polymer sensors have studied how the different amounts of the conducting polymer deposit influences the sensitivity of its pH response. Within the literature the pH response of the conducting polymer did not depend on the electropolymerization conditions such as concentration of pyrrole, solvent used, type of electropolymerization technique (potentiometric or cyclic voltammetry)or step size used for cyclic voltammetry. The study found that the main variable that affected the response to pH was the thickness of the deposited layer. They found that a layer less than 2microns of polypyrrole showed a linear response to pH from 2-12(Shiu et al., 1999). Another report found that the optimum coating thickness for the deposition of polypyrrole on a platinum wire was using cyclic voltammetry between 0 to 3 volts with a 100mV/s scan rate. Three cycles of this produced the optimum sensitivity of 51mV/decade H^+ ion concentration(Lakard et al., 2007). The polypyrrole coated onto metal electrodes has shown poor long term stability. This has been improved when a more adhesive L-PEI coating was used to coat the metal contact before deposition of polypyrrole (Segut et al., 2007). These sensors while being shown to be sensitive to changes in pH are not very ion-selective and could only be used in tightly controlled experimental setups (Michalska, 2000). Other issues such as slow equilibrium of the sensing mechanism lead to long sensor settling times and inconsistent sensor response over long time periods (Michalska and Maksymiuk, 2003).

The redox functionality of the conducting polymer has been used as an ion to electron transducer in between the ion-selective membrane and the conducting contact of the solid state electrode. The ion to electron transducer enables sensors with greater voltage stability than coated wire electrodes. It has been shown that the conducting polymer acting as an ion to electron transducer gives a faster response time and a larger voltage drop per decade than the same sensor without the conducting polymer layer (Masalles et al., 2002). In a study by Han et al (2003) they used a consistent membrane and the conducting polymer mid layer was varied. The study found that with a platinum wire coated with the membrane the response time was slow and there was a 42mV/decade H^+ ion concentration response. When a

polypyrrole ion exchanger was added the response time was 9 seconds with a response slope of 57.7mV/decade H^+ ion concentration. This study also gave evidence that without the conducting polymer a blocked interface occurred between the metal contact and the membrane (Han et al, 2003). The doped conducting polymer is used to prevent this electron blocking occurring aiding exchange of ions and electrons through a redox reaction. The theory behind blocked interfaces can be found in **Section 2.9.2**.

The ion to electron transducer should enable the sensor to be stable over a longer time period and have consistent performance. The best performing dopant ion reported is the hexacyanoferrate redox molecule. It has been shown by Han et al (2003) and Zielinska et al (2002) to have long term voltage stability but it would be unsuitable for its use within a medical device due to it being a toxic substance. Other promising polypyrrole transducers were doped with Cl^- ions the sensors doped with this recorded slightly slower response times but with stable voltage response (Michalska and Maksymiuk, 2005) (Momma et al., 1996). Polypyrrole conducting polymer has also been used as an ion to electron transducer in many other sensor types as once the ion-selective membrane has been applied to the sensor the operation of the conducting polymer is independent from the primary ion sensing. The theory behind this can be found in **Section 2.10.4**. The use of polypyrrole as an ion to electron transducer has been shown to also produce effective sensors for K^+ (Gyurcsányi et al., 2004), Ca^{2+}(Konopka et al., 2006), Cu^{2+}(Marquesdeoliveira et al., 2006) and carbonate Sensors (Kim et al., 2004). Of these sensors polypyrrole doped with larger dopant ions were found to produce stable voltage response which indicates effective ion to electron transduction (Pandey et al., 2002) (Marquesdeoliveira et al., 2006).

1.18.3 PEDOT

PEDOT comes from the polythiophenes family of conducting polymers the operation is similar to that of polypyrrole when used as a ion to electron transducer; this method of operation can be found in **Section 2.10.4**. This family of conducting polymers are useful as they have hydrophobic properties which will help to prevent the formation of a water layer between the membrane and conducting polymer which

can enhance voltage stability (Sutter, Radu, et al., 2004). During the polymerization of PEDOT it can be doped with poly(styrenesulfonate) (PSS). PEDOT doped with PSS is stable and has low sensitivity to O_2 and CO_2 and therefore makes it a popular material for ion to electron transducers (Vázquez et al., 2004). The PEDOT is known to have a high redox capacitance which makes the sensor have high voltage stability (Bobacka, 1999). PEDOT (PSS) has been used effectively in a number of potassium ion sensors as the ion to electron transducer (Mousavi et al., 2009). There were no examples of PEDOT being used as an ion to electron transducer for pH electrodes in the literature. PEDOT doped with PSS is available commercially from Agfa as a readymade ink which can be used for screen printing conducting polymer layers. The availability of the PEDOT (PSS) ink introduces many different possibilities for manufacturing the sensor in a more controlled way than electropolymerization which should lead to more constant and easier to produce sensors.

1.18.4 Nanoscale carbon

Nanoscale carbon is a relatively new development in material science. It is composed of structured formations of carbon which increases the surface area of an electrode (Yáñez-Sedeño et al., 2010). They have some useful qualities such as electrical conductivity, high surface capacitance and they are hydrophobic. They are toxic due to their small particle size but once processed into a safer form such as an ink they can be easily and safely used (Wang and Musameh, 2004). Their method of operation is similar to the coated wire electrodes as discussed in **Section 2.9.2**. Although not an ion to electron transducer there is some debate as to their method of operation as their stable voltage sensing performance is due to high surface capacitance but it has been proposed by Crespo, Macho, et al (2009) that more complex ion interactions occur at the carbon nanotube surface.

The majority of research into carbon nanotubes sensors has been into enzyme sensors such as hydrogen peroxide (Sánchez et al., 2007), glucose (Wang and Musameh, 2004) and ion sensors for silver and potassium (Lai et al., 2007, 2009). The manufacture of a potassium sensor is similar to that of a pH sensor but with different ionophores in the ion-selective membrane so this arrangement could be used to produce an effective pH sensor. A pH sensor has been reported using an acrylate ion-

selective membrane with the conducting contact being carbon nanotubes (Crespo, Macho, et al., 2009).

1.18.5 Hydrogels

Hydrogels have been used as a method of reducing the size of the traditional liquid phase of an ion sensor. They operate in the same manner as the traditional glass electrode by having a liquid and an Ag/AgCl electrode to ensure a stable voltage phase between the ion and electron conducting phases. The method of this operation can be read in **Section 2.9**. The hydrogel is placed between the Ag/AgCl electrode and the ion-selective membrane which is made from a non glass material such as PVC to enable the sensor to be made in smaller packaging. The sensors do not operate well when compared to conducting polymer based sensors as they suffer from long term voltage drift (Gyurcsányi et al., 2004). This could be due to extended equilibrium times and ion leaching from the hydrogel. For pH electrodes there is a problem with CO_2 changing the pH of the hydrogel over time resulting in an incorrect pH measurement (Lindner and Gyurcsányi, 2008).

1.19 Disposable solid state sensors

The majority of the research discussed in the previous sections involving conducting polymers as ion to electron transducers use platinum and glassy carbon rods as the conducting contact. For disposable sensors these conducting contacts are expensive and would price the sensor out of the disposable market. A number of alternative methods such as screen printing (Tymecki et al., 2006) and micro fabrication (Lakard, 2004) techniques have been used to produce cheaper potentiometric ion sensors.

Screen printing is a one of the most cost effective methods of producing sensors. Conducting inks such as carbon, platinum and Ag/AgCl can be printed on plastic substrates to form the basis of a solid state ion-selective electrode (Renedo et al., 2007). The manufacturing technique is simple and large numbers of sensors can be produced at low cost. An example of a screen printing machine and a screen printed sensor is shown in **Figure 1.18**. Coated wire type ion-selective sensors have been demonstrated using screen printed electrodes. Musa et al (2011) produced screen printed carbon electrodes coated with a PVC ion-selective membrane. With pre-treatment of the screen printed carbon to increase membrane adhesion the pH sensors showed a Nernstian response of 51.7mV/ decade H^+ ion concentration response in the pH range 7.0-7.6. The voltage stability of these sensors was not tested so it is unknown how these sensors responded without an ion to electron transducer.

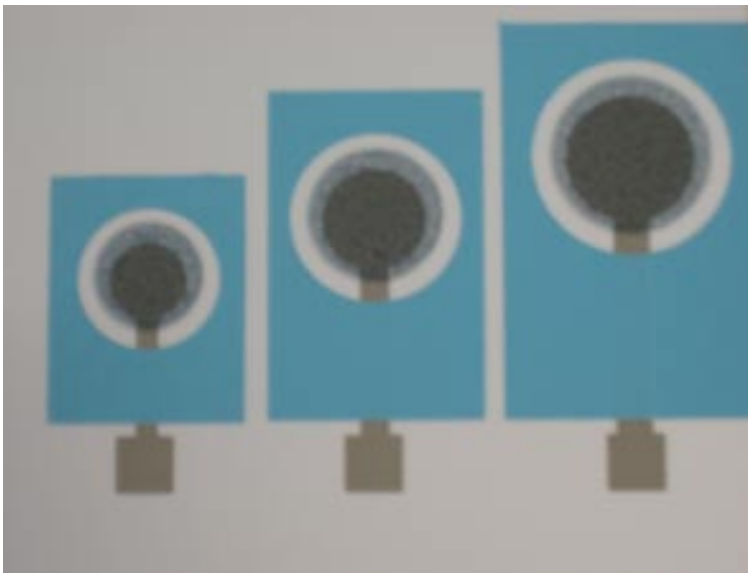

Figure 1.18 DEK 248 screen printing machine (Top) Screen printed sensors with silver conducting contact, screen printed PEDOT layer and blue electrical insulator (bottom).

Other more complex sensors using conducting polymers have been manufactured using screen printed electrodes. Most of these sensors have used PEDOT as it is a commercially available ink for screen printing. This enables both the conducting contact and conducting polymer to be screen printed and an example of this is shown in **Figure 1.18** (bottom picture). PEDOT screen printed sensors have been used for potassium ion sensors (Vázquez et al., 2004). The PEDOT used in this sensor was

modified by cross linking the PEDOT with redox active $Ru(NH_3)_6^{2+/3+}$ which increased the redox capacitance of the electrode and lead to better voltage stability of the sensor. Another research group found Nernstian responses for screen printed PEDOT sensors coated with potassium selective ion-selective membranes although the sensor had low ion selectivity (Xu et al., 2010). Screen printed electrodes have also been shown to be effective chloride ion sensors. A screen printed chloride ion-selective membrane was shown to have better voltage stability when an adhesive was applied between ion to electron transducer and membrane to prevent water layer formation (Paciorek and Zurawska, 2005). In another screen printed chloride sensor it was found that hydrolysis of the screen printed carbon ink resulted in reduced sensor stability due to the organic compounds contained in the conducting ink (Zielinska et al., 2002). It is possible to electropolymerise polypyrrole on a screen printed carbon electrode as this was reported by Li and Wang (2007) for a hydrogen peroxide sensor. Electropolymerised conducting polymers on screen printed electrodes is an area that has not been researched in any depth. It has potential to produce cost effective voltage stable sensors for use as ion-selective sensors.

1.20 pH sensors summary

The pH of a wound has been shown to have an influence over many different factors within the wound healing process. The amount of different cells and enzymes that pH can affect makes it an important marker to study in wound healing so that its influence on the wound healing process can be fully understood. With the increased use of pH modifying dressings to control the proliferation of MMP's there is a requirement for a pH sensor that can easily and effectively monitor the influence these dressings are having on wound pH so that further wound dressings can be chosen depending on the current state of the wound. The current technology available for wound pH measurement is expensive, difficult to sterilise and not disposable so there is a real need for an alternative sensing technology.

Research has been conduced into a broad range of alternative pH sensing technology such as optical pH sensors, metal oxide, ISFETS and disposable solid state potentiometric sensors. The most promising of these for cheap disposable sensing is

the solid state potentiometric sensors as the current research into ion-selective membranes and conducting polymers can be adapted into inexpensive screen printed sensors.

In solid state sensing the use of conducting polymers as ion to electron transducers enables the sensor to have better long term voltage stability. The membrane components such as the ionophore determine the primary ion selectivity and the sensor range. Other membrane components such as choice of membrane material determine the ion diffusion and also have an influence on the selectivity to interfering ions. Every component within the ion-selective membrane can have an influence on the overall sensing ability for this reason all components need to be chosen carefully to achieve the desired sensing requirements for the membrane.

The use of solid state sensors based on screen printing technology and utilizing conducting polymers as ion to electron transducers could provide an alternative to the expensive glass electrodes that are currently used to monitor pH in wound care. It would enable clinicians to gain further insight into the complex healing patterns associated with chronic wound healing.

1.21 Objectives of Study

This study will investigate disposable solid state sensors for measuring the pH of a wound. The pH of a wound can affect many different areas of the healing process such as oxygen levels, cell proliferation, protease enzyme activity and bacterial growth. A tool to measure pH level in an easy, cost effective and reliable way will enable the pH of a wound to be studied further to find its overall influence on the healing process.

The sensors will be based on screen printed carbon electrodes with conducting polymers as an ion to electron transducers and a PVC based hydrogen ion-selective membrane. The membrane composition will use a proven membrane formulation with a tridodecylamine ionophore (Schulthess et al., 1981) and will remain constant throughout the experiments to enable the operation of the conducting polymer to be assessed. Three different conducting polymer types will be tested and characterised. Two electropolymerised polypyrrole the first doped with small Cl^- ions and the second with larger PTS^- ions; this will enable the effect of different sized dopant ions to be assessed. The third conducting polymer tested is a commercially available PEDOT (PSS) ink. These sensors will be tested against a screen printed carbon sensor with ion-selective membrane that has no additional layer.

The sensor has a number of key aims that have to be achieved. They are:

- **Linear primary ion voltage response** - needs to provide correct pH measurements.

- **Sensing range** – The sensor will have a linear voltage response in the pH range 4-10.

- **Selectivity** - The device needs to be ion specific so that other small ions such as K^+, Na^+ and Ca^{2+} don't interfere with the measurement of H^+ molecules.

- **Voltage stability** - One of the major reasons that the glass electrode is still universally used is because of its voltage stability over time. A single use sensor to test the current pH of a wound would not have issues as the sensor

would not be in use over long time periods. If the sensor was to be embedded in a wound dressing to test the pH levels continuously the sensor would need to show no voltage drift during measurement after calibration for up to 7 days.

- **Cost**- Due to the disposable nature of the sensor it will have to be cost effective.

- **Manufacturing**- The design needs to be simple to manufacture so that consistent sensors can be produced and also to keep costs down.

- **Biocompatibility**- As the device will be used in a wound environment is vital that it does not cause any adverse effects to the patient.

Once a suitable sensor has been developed the electronic measurement circuitry will be designed. The aims are:

- Design a hand held battery operated measurement device to measure the voltage potential of the pH sensor when combined with a reference electrode.
- Enhance the voltage stability of the sensor.
- The device will calibrate the sensor system.
- Display a pH of a sample to the user.

The full sensing system will then be used to assess the real time change in pH that occurs in a wound bed model when various pH modifying dressings are applied. This has never previously been studied as it has not previously been possible to measure the pH effect of these dressings in real time. The aim of these experiments is:

- Measure the pH of modern advanced wound dressings using the designed sensors.
- Monitor the real time pH effect of applying wound dressings to a wound bed model.
- Observe the acidic strength of the dressings.

The theory behind the operation of the solid state ion-selective electrode, materials and methods, results from the experimental findings and the analysis and discussion of the results will now be presented.

Chapter 2 - Theory

This chapter provides an overview of the theory behind the operation of solid state pH sensors. The chapter begins by describing the movement of ions within a solution and how an electrochemical cell potential is made and measured. The theory of operation of the individual components of the solid state pH sensor is discussed this includes operation of ion-selective membranes, conducting polymers, reference electrodes and the influence of measurement circuitry on the electrochemical cell. The theory behind the analysis technique electrochemical impedance spectroscopy that is the basis for the analysis conducted in **Chapter 5** is discussed briefly. The chapter closes with discussions on the theory of pH and how this relates to the pH change in a physiological solution.

2.1 Ionics

Ionics governs how ions interact within a solution. An ion-selective sensor system will measure the activity of the ions from within the solution. The movement of ions across the cell through various phases will have an influence on the overall potential that the cell generates (Bard and Faulkner, 2001). In an electrochemical cell charge is carried by ions within the solution. Mass transfer is the movement of one material from one location to another in a solution. The three modes of mass transfer are:

Diffusion – The movement of a species caused by the influence of a chemical potential.

Migration – The movement of charged ions under the influence of an electrical field.

Convection – The movement of ions that occurs through stirring or hydrodynamic transport.

2.1.1 Mass transfer

Mass transfer is determined by three different forces within a solution; diffusion, migration and convection. A concentration gradient will cause ions to diffuse and migrate into areas with lower concentrations. The movement of this is driven by

electrochemical potential of the ions, $\bar{\mu}_i$. Migration is movement of charged ions driven by an electrical potential. Convection is produced from an imbalance of forces in a solution. Mass transfer at an electrode is governed by the Nernst-Planck equation and is written as 1 dimensional mass transfer along the X axis as detailed in **Equation 2.1**.

$$J_i(x) = -D_i \frac{dC_i(x)}{dx} - \frac{nF}{RT} D_i C_i \frac{d\phi(x)}{dx} + C_i v(x) \qquad \textbf{Equation 2.1}$$

$J_i(x)$ is the flux of species i at a distance x from the electrode, D_i is the diffusion coefficient of the species i, $\frac{dC_i(x)}{dx}$ is the concentration gradient at distance x from the electrode, C_i is the concentration of the species i, $\frac{d\phi(x)}{dx}$ is the potential gradient and $v(x)$ is the the velocity with which a volume element moves along the X axis.

The first term of **equation 2.1** is known as Fick's first law of diffusion it states that the flux of an ion is proportional to the concentration gradient (Bard and Faulkner, 2001). Fick's second law of diffusion models the change in concentration of a species, C_i with time and distance in one dimension as shown in **Equation 2.2**. D_i is the diffusion coefficient of the species i.

$$\frac{dC_i(x,t)}{dt} = D_i \left(\frac{d^2 C_i(x,t)}{dx^2} \right) \qquad \textbf{Equation 2.2}$$

The ion movement within a sensor membrane follows Fick's laws so it is an important parameter to consider when considering the function of an ion-selective membrane.

In most electrochemical cells the mass transfer can be simplified to negate the effects of the migration and convection. Migration effects can be reduced by adding a supporting electrolyte at larger concentrations than the electro active species. Convection can be negated by preventing stirring and vibrations in the electrochemical cell (Bockris and Reddy, 2000).

2.2 Cell potential

When a metal or a conductor such as carbon is immersed in an ionic solution a potential difference is formed between the material phases. This is due to an accumulation of charge between the metal and the ionic solution. This charge barrier is known as the electronic double layer which will be discussed in more detail in a later section. Potential differences occur not only at solution/conductor interfaces but at any change in material between conducting phases such as platinum/carbon. This change in phase is due to the difference in charge between the two phases.

2.2.1 Measuring electrochemical cell potential

An electrochemical cell has to have at least two electrodes so that an electrical potential can be established in the system. This is due to direct measurement being impossible as the electrode would have to be in simultaneous contact with both phases of the reaction (Bockris and Reddy, 2000). For this reason the individual phase potentials cannot be measured and a series of potentials has to be measured to find the overall potential. The potential between different phases is known as the Galvani potential. In an electrochemical system the different phase potentials combine to give the overall potential of a cell.

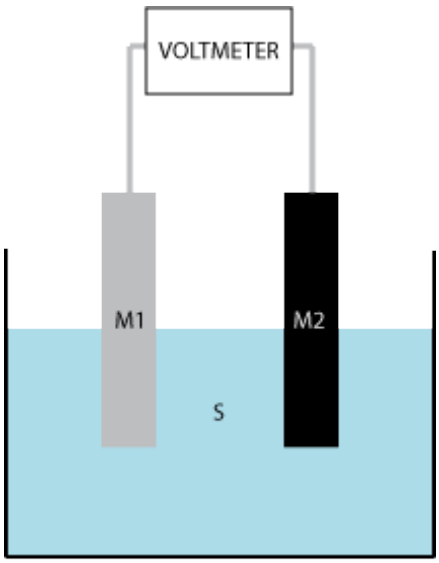

Figure 2.1 Simple electrochemical cell with two electrodes of different metals.

Figure 2.1 illustrates a simple cell with two metal electrodes in an ionic solution the overall potential will be a sum of the individual phase potentials across the cell. When measuring the overall cell potential, E of **Figure 2.1** there are three phase potentials (M1 electrode and solution, $PD_{M1/S}$, Solution and M2 electrode, $PD_{S/M2}$ and M2 electrode and M1 electrode, $PD_{M2/M1}$) the sum of the potentials is given by **Equation 2.3**.

$$E = PD_{M1/S} + PD_{S/M2} + PD_{M2/M1} \qquad \textbf{Equation 2.3}$$

The example given in **Figure 2.1** is a simple cell with few potential differences across the cell. In reality a system will have more potential differences across a cell to consider. A cell can be designed so that the interface of interest can be isolated this is the aim for design for a sensor system. If the M1 electrode is replaced by a reference electrode then the potential between reference and solution, $PD_{REF/S}$ will be constant and not depend on the solution that the electrode is immersed in. The interface between the metals ($PD_{M2/M1}$) is determined by the metal composition so this is also a constant value and is not dependent on the ionic solution. This leaves the interface between the solution and the M2 electrode ($PD_{M2/S}$) which if changed

to a sensor the interface can be studied. This technique is the basis of sensor operation. The **Equation 2.3** would become:

$$E = PD_{REF/S} - PD_{M2/S} \qquad \textbf{Equation 2.4}$$

If the M2 electrode is changed to a sensor that can detect changes in the pH of a solution ($\delta PD_{pH\ sensor/S}$) then the cell will change potential with a change in pH as shown in **Equation 2.5**.

$$\delta E = \delta PD_{REF/S} - \delta PD_{pH\ sensor/S} \qquad \textbf{Equation 2.5}$$

Using this system all potential changes will be relative to the constant potential of the reference electrode. As the change in solution will not change the potential of the reference half cell any change in potential will be due to the pH sensor solution interface.

$$\delta E = \delta PD_{pH\ sensor/S} \qquad \textbf{Equation 2.6}$$

For this example the interfaces in both the reference electrode and sensor have been simplified and they will be discussed in detail in **Section 2.9** and **Section 2.11**. The next section will discuss how the potential differences are determined in the various phases.

2.3 Double layer

An electrical double layer occurs at the interface between the electrode and the solution. It is composed of charged ions at a solution interface and behaves as a capacitor of charged negative and positive ions. This occurs due to different potentials between the metal and solution phase. In the solution phase the double layer is made up of an inner layer of charged ions which is closest to the electrode. This example will describe the double layer for a negatively charge electrode. It consists of solvent molecules (water molecules in aqueous solutions) that are aligned

with their positive charge towards the negatively charged electrode. The layer also contains specifically absorbed anions. This layer of charged ions is known as the inner Helmoltz plane (IHP) which is positioned at the centre of the specifically absorbed anions as shown in **Figure 2.2**. Total charge density of this layer is σ^i $\mu C/cm^2$.

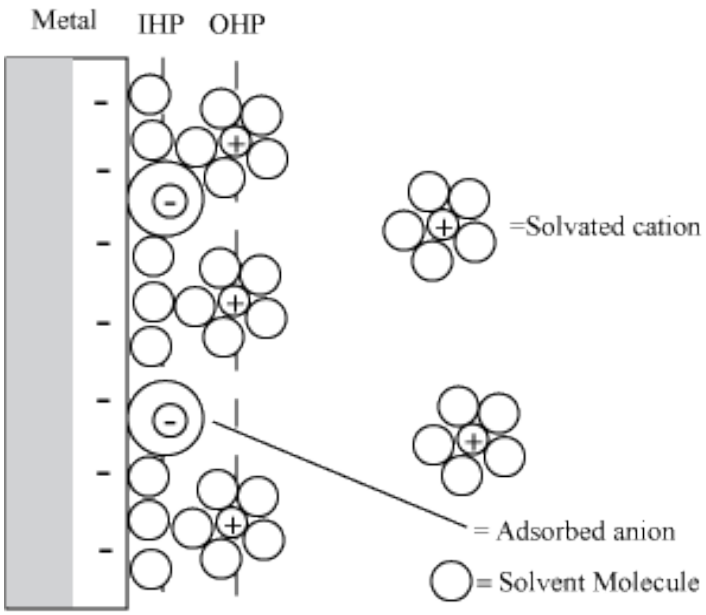

Figure 2.2 Diagram of double layer at metal electrode. Showing inner Helmoltz plane (IHP) and outer Helmoltz plane (OHP).

In the immediate vicinity of the IHP the charge is negative which attracts solvated cations (cations surrounded by water molecules). The Solvated cations can only approach the electrode at a distance known as the outer Helmoltz plane (OHP). These ions are known as non-specifically absorbed. The non-specifically absorbed ions are distributed in an area from the OHP to the bulk solution called the diffuse layer it has a charge density of σ^d $\mu C/cm^2$. The thickness of this layer depends on the ionic concentration of the solution. For an ionic solution with concentration of 10^{-2}M the double layer is less than 100Å thick. The charge density of the bulk solution, σ^S is a sum (**Equation 2.7**) of the diffuse layer charge density, $\sigma^{Diffuse}$ and the IHP charge density, σ^{IHP}. The solution charge density is equal to the negative charge density of the metal, σ^M.

$$\sigma^{S} = \sigma^{IHP} + \sigma^{Diffuse} = -\sigma^{M} \qquad \textbf{Equation 2.7}$$

The cations of the OHP and diffuse layer compensate for the negative charge of the electrode. The potential close to the electrode is lower than the potential of the bulk solution. **Figure 2.3** shows how the electrochemical potential is affected by both the inner and outer Helmholtz planes. The electrical potential between the OHP and the bulk solution is known as the zeta potential.

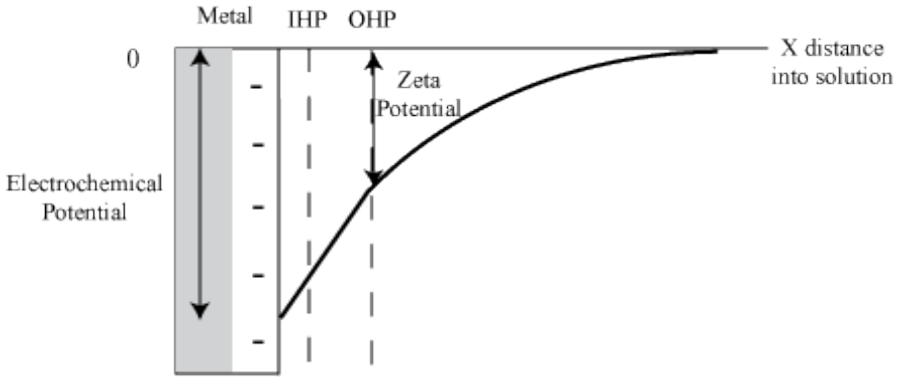

Figure 2.3 The electrochemical potential of the double layer Gouy-Chapman-Stern model.

The Helmholtz model is the simplest model for describing the double layer structure. It is composed of two charged parallel plates that that have a structure equivalent to a parallel plate capacitor. Where the charge density, σ μC/cm^{2}of the double layer is given by:

$$\sigma = \frac{\varepsilon\varepsilon_0}{d}V \qquad \textbf{Equation 2.8}$$

Where V is the voltage drop between the plates of the double layer, ε is the dielectric constant of the solution, ε_0 is the permittivity of free space and d the distance between the plates. From **Equation 2.8** the capacitance of the double layer (C_{dl}) can be derived as:

$$\frac{d\sigma}{dV} = C_{dl} = \frac{\varepsilon\varepsilon_0}{\mathrm{d}} \qquad \textbf{Equation 2.9}$$

2.4 Electrochemical Potential

The chemical potential, μ_i of a cell is defined (**Equation 2.10**) as the differential change in free enthalpy, G with the change in the amount of a substance, i. Temperature, pressure and concentration are all constant.

$$\left(\frac{\delta G}{\delta n_i}\right)_{T,p,n} \equiv \mu_i \qquad \textbf{Equation 2.10}$$

The term also applies to chemical reactions. If two phases of different chemical potentials are in contact then chemical reactions involving changes in the substances and the amount of free enthalpy can take place. The absolute values of chemical potentials and free enthalpies are not known so the calculations for these have to be with respect to a starting state.

The change in free enthalpy depends on the ideal gas law which can be applied to solutions of ions as they behave like an ideal gas. In a system with change in concentration of substance, a_1 in contact with substance, a_2 the free energy, G increases with changes in the concentrations of the solutions:

$$\Delta G = nRT \ln \frac{a_2}{a_1} \qquad \textbf{Equation 2.11}$$

R is the general gas constant and T is the temperature in Kelvin. To transform 1 mole of substance i **Equation 2.11** becomes the chemical potential, μ_i:

$$\mu_i = RTln\ \frac{a_i}{a_i^0} = \mu_i^0 + \ln a_i \qquad \textbf{Equation 2.12}$$

Where μ_i^0 is the standard chemical potential of the substance i (this is a fixed value). a_i^0 is the standard activity and a_i the activity of substance i.

The electrochemical potential, $\bar{\mu}_i$ is different to the chemical potential as it requires additional electrical work for the ions to leave their phase. The electrochemical potential of a substance, i with a charge is given by:

$$\bar{\mu}_i = \mu_i + z_i F \phi \qquad \textbf{Equation 2.13}$$

Where z_i is the charge of the ion, F is the Faraday constant and ϕ is the electrical potential of the phase. When the electrochemical potential **Equation 2.13** is combined with **Equation 2.12** it gives the electrochemical potential of two contacting phases:

$$\bar{\mu}_i = \mu_i^0 + \ln a_i + z_i F \phi \qquad \textbf{Equation 2.14}$$

2.5 Charge transfer

There are two types of charge transfer reactions that occur at an electrode. The first is the reduction/oxidation of an ion in the solution the charge transfer for this reaction is dominated by the electrons transferring from electrode to ions or vice versa. The ions in the solution layer hardly move as electrons transfer from the electrode.

The second charge transfer reaction is an ion transfer between solution and electrode in an adsorption process, an example of this is the deposition of a metal ion onto an electrode. An ion near the electrode in the solution layer will experience an electron transfer where the ion is also transferred onto the electrode. The reverse of this reaction involves the metal atoms leaving the electrode and becoming metal ions in the solution.

Charge transfer can occur between ions and an electrode at the outer Helmholtz plane. When an electrode is at equilibrium the net electron transfer must be balanced so that no current flows in one direction of the reaction. Charge transfer at the electrode implies that a chemical reaction is taking place (Bockris and Reddy, 2000). The charge transfer between an electronic and ionic conductor occurs through a quantum mechanical tunnelling effect.

If an electrical potential is applied to the electrochemical cell then the overall current at the electrodes will be a sum of the two electrode reactions. The polarisation or over potential, η is defined as the amount of voltage applied above the equilibrium potential, $\Delta\phi_e$. This can occur by applying a voltage across the electrodes or produced by changing the composition of the electrolyte solution.

$$\Delta\phi - \Delta\phi_e = \eta \qquad \textbf{Equation 2.15}$$

Where $\Delta\phi$ is the electrochemical potential at current i. When η is negative, electrons will flow into the electrode producing a net flow of ions into the solution, this is known as a cathodic current. When η is positive, there will be a flow of electrons into the electrode, this is knows as a anodic current.

When the electrode is in equilibrium and there is no net current flow the current at the anode (i_a) and cathode (i_c) electrodes are equal to each other. The electrochemical equilibrium occurs when there is no net current transfer so $i_a=i_c=i_o$, the value i_o is the exchange current density. The exchange current density is a measure of the rate of exchange of ions and charge when the electrode is at equilibrium, the larger the value the faster the exchange.

For a cathodic current:

$$i_{cath} = \vec{\imath} - \overleftarrow{\imath} \ (\Delta\phi < \Delta\phi_e) \qquad \textbf{Equation 2.16}$$

The values of i can be derived by finding the rate of ions crossing the interface from their jump frequency. The current density for a net cathodic current is given by:

$$i_{cath} = F\vec{k}c_i e^{-\alpha\Delta\emptyset F/RT} - F\overleftarrow{k}c_A e^{(1-\alpha)\Delta\emptyset F/RT} \qquad \textbf{Equation 2.17}$$

Where c_i is the concentration of ionic species i and A is atoms forming on the electrode. R is the general gas constant and T is the temperature in Kelvin and F is the Faraday constant. α is the charge transfer coefficient. When $\Delta\phi = \Delta\phi_e$ the cathode current is zero so the exchange current density, i_o equals:

$$F\vec{k}c_i e^{-\alpha\Delta\emptyset F/RT} = i_o = F\overleftarrow{k}c_i e^{(1-\alpha)\Delta\emptyset F/RT} \qquad \textbf{Equation 2.18}$$

From $\Delta\phi = \eta + \Delta\phi_e$ and the **equation 2.17** the equation below can be derived:

$$i_{cath} = i_o(e^{-\alpha\eta\frac{F}{RT}} - e^{(1-\alpha)\eta\frac{F}{RT}}) \qquad \textbf{Equation 2.19}$$

This equation is known as the Butler-Volmer equation. It describes the electrode kinetics of ion transfer. It is valid when there is a plentiful supply of reactants within easy diffusion range of the electrode.

2.6 Polarisable and non-polarisable interfaces

The ideal polarisable interface is one when a potential is applied across an electrode there will be a change in potential but no flow of current. The ideal polarisable electrode can be thought of as a capacitor (double layer) as charge will pass into the plates resulting in a change of voltage.

$$dV = \frac{dq}{C} \qquad \textbf{Equation 2.20}$$

Where V is the voltage change induced by the amount of charge (q) that flows into the capacitance (C) of the double layer.

The ideal non-polarisable electrode will experience a current flow across the interface when a potential is applied across it. The current flow will result in a constant voltage across the interface due to no build up of charge between the electrode and the double layer.

In reality no electrode is fully polarisable or non-polarisable but they tend to have properties closer to one or other (Bockris and Reddy, 2000). The polarisability of an electrode can be described from the exchange current density, i_0. The Butler-Volmer equation (**Equation 2.19**) has a limiting case where the over potential (η) is less that the RT/F expression (R is the general gas constant and T is the temperature in Kelvin and F is the Faraday constant) which at room temperature is around 50mV. When this condition occurs the Butler-Volmer equation becomes a linear relationship between current density and overpotential.

$$i = i_o \frac{\eta F}{RT} \qquad \textbf{Equation 2.21}$$

Then:

$$\frac{d\eta}{di} = \frac{RT}{i_o F} \qquad \textbf{Equation 2.22}$$

Using ohms law E=IR this equation becomes:

$$\frac{d\mathrm{E}}{di} = \frac{RT}{i_o F} = R_{CT} \qquad \textbf{Equation 2.23}$$

Where R_{CT} is the differential charge transfer resistance. From this equation a large i_o value will have a small charge transfer resistance, this would give the electrode non-

polarisable qualities. A small i_o value will lead to a high charge transfer resistance and an electrode with polarisable qualities.

The polar nature of the electrodes used in sensor systems plays an important part in the overall electrochemical cell as interfaces that are not of interest to a study such as reference electrodes will want to be non-polarisable so that any external change in voltage will not affect the potential of the interface. This will be discussed further in the sensor and reference electrode descriptions.

2.7 Nernst equation

The mass transfer to an electrode is governed by the Nernst-plank equation. It represents the flux from all three types of mass transfer (Bockris and Reddy, 2000). If a system follows the Nernst equation in its response the electrode reaction is thermodynamically or electrochemically reversible. A Nernstian reaction is one that the principal ions obey thermodynamic relationships at the electrodes surface. The Nernst equation is important in determining response from an ion-selective electrode. This section will show how it is derived from the electrochemical potential of an electron transfer reaction.

When a charge is transferred between two phases for example a metal/ion electron exchange reaction.

$$M^{z+} + ze^- \rightleftarrows M \qquad \textbf{Equation 2.24}$$

The thermodynamic condition for equilibrium in a reaction involving electrons and charged particles is shown in equation 2.25 where the chemical potential, μ_M is equal to the electrochemical potential of the metal ions, $\overline{\mu_{M^{z+}}}$ and z number of electrons, $z\overline{\mu_e}$.

$$\mu_M = \overline{\mu_{M^{z+}}} + z\overline{\mu_e} \qquad \textbf{Equation 2.25}$$

The electrochemical potential of the metal ion, $\overline{\mu_{M^{z+}}}$ and electron, $\overline{\mu_e}$ is given by **Equation 2.26** and **Equation 2.27.** F is the Faraday constant and $\emptyset$ the electrochemical potential difference of the solution, $\emptyset_s$ and metal, $\emptyset_M$ phase.

$$\overline{\mu_{M^{z+}}} = \mu_{M^{z+}} + zF\emptyset_s \qquad \textbf{Equation 2.26}$$

$$\overline{\mu_e} = \mu_e + zF\emptyset_M \qquad \textbf{Equation 2.27}$$

The electrochemical potential, $\overline{\mu_M}$ for the non charged metal atom is equal to the chemical potential, μ_M. Inserting the electrochemical potentials into **Equation 2.25** it gives us the electrochemical potential difference, $\Delta\emptyset_e$ between the metal, $\emptyset_M$ and solution phase, $\emptyset_s$.

$$\Delta\emptyset_e = \emptyset_M - \emptyset_s = \frac{1}{zF}(\mu_{M^{z+}} + \mu_e - \mu_M) \qquad \textbf{Equation 2.28}$$

The chemical potentials in this phase are equal to $\mu_i = \mu_i^0 + \ln a_i$. The activity of metal ions, a_M and electrons, a_e are both equal to 1 as they are in pure form in their standard state and the second part of the chemical potential is equal to zero. Substituting in these values into **Equation 2.28** gives:

$$\Delta\emptyset_e = \frac{1}{zF}\left(\mu^0_{M^{z+}} + \mu^0_e - \mu^0_M\right) + \frac{RT}{zF} ln a_{M^{z+}} \qquad \textbf{Equation 2.29}$$

The first term of this equation is a constant as it is not dependent on concentration it is called the standard potential of the electrode, $\Delta\emptyset_e^0$ when the activity of a_i is equal to 1. The $\frac{RT}{zF}$ term is the Nernst potential where R is the general gas constant, T is the temperature in Kelvin, z the charge of the ion and F is the Faraday constant. **Equation 2.29** can then simplify to:

$$\Delta\emptyset_e = \Delta\emptyset_e^0 + \frac{RT}{zF} lna_{M^{z+}}$$ **Equation 2.30**

Equation 2.30 can be linked to voltage across the interface due to the fact that the electrochemical potential and the voltage are not concentration dependent so the electrochemical potential difference, $\Delta\emptyset_e$ and standard potential, $\Delta\emptyset_e^0$ terms can be changed to voltage potential, E and standard voltage potential, E^0 respectively as shown in **Equation 2.31**.

$$E = E^0 + \frac{RT}{zF} lna_{M^{z+}}$$ **Equation 2.31**

The term $\frac{RT}{zF}$ is known as the Nernst potential and at 25^{o}C it has a value of 59.16mV. This value limits the response of a sensor to the Nernst value per decade change in ion concentration. The Nernst equation forms the fundamental principle behind the response of an ion-selective electrode. The next section will describe how this applies to ion-selective membranes.

2.8 Membrane

2.8.1 Membrane potential

A sensor for detecting concentrations in a solution depends on a form of the Nernst equation. The ion-selective sensors investigated in this study use an ion-selective membrane that enables a potential difference to form which relates to concentration of the ion of interest. The ion-selective membrane is made of PVC with an ionophore based carrier which acts to transport the primary ions through the membrane.

If a PVC membrane is to conduct ions it needs to be plasticised so that its glass transition temperature is below room temperature. The ionophore based membranes have a 2:1 plasticiser ratio to PVC so they are essentially very viscous liquids (Johnson and Bachas, 2003). The ionophore is the most important constituent of the membrane. It is neutral in charge and acts to bind the primary ion and transport it through the membrane as shown in **Figure 2.4**. The final ingredient in the PVC ion-selective membranes are the ionic salts to provide anionic sites in the membrane. They are used in the membrane to ensure that no significant counter ions are extracted into the membrane when the primary ion enters. They also reduce the electrical resistance of the membranes and allow further mobility of ions (Ammann et al., 1985).

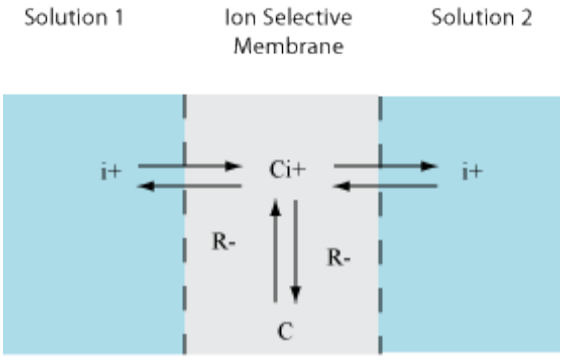

Figure 2.4 Ionophore membrane operation showing neutral charge ionophore, C binding the target molecule, i^+ to form, Ci^+. The anionic salts, R^- are also shown.

The membrane potential is the based on the same Nernst principle as the ion transport discussed in the previous section. The potential of the membrane can be

determined from the ratio of ion activity in the solution over the ion activity in the membrane (Bobacka et al., 2008). At equilibrium the electrochemical potential of both phases (solution and membrane) are equal. The potential, E can be derived in a similar way to as the Nernst equation in **Section 2.7** to get **Equation 2.32**.

$$E = E^0 + \frac{RT}{zF} ln \frac{a_i(aq)}{\bar{a}_i(mem)} \qquad \textbf{Equation 2.32}$$

Where $a_i(aq)$ is the activity of the primary ion in the solution and $\bar{a}_i(mem)$ the activity in the membrane phase of the electrode, $\frac{RT}{zF}$ is the Nernst potential and E^0 the standard voltage potential. The number of ionophore transport sites is constant in the membrane so the activity can be set to 1, the potential is determined by the activity of cation i in the solution. The a_i term is the activity coefficient that can be related to solution concentration by the Debye-Hückel equation. In aqueous solutions the ionic strengths are normally at values that mean the activity coefficients are constant. If the activity coefficients are constant then the activity values can be replaced by ion concentration, c_i and the membrane potential can be simplified to:

$$E = E^0 + \frac{RT}{zF} ln\, c_i(aq) \qquad \textbf{Equation 2.33}$$

This model does not take into account the influence of interfering ions and the influence of their ion mobility on the response of the sensor. To model the time response of a sensor a more complicated model is required to detail the effect of time on response of the sensor. Diffusion is an important factor in the design of the solid state sensor as this will be one of the rate limiting factors for the sensor response time after immersion in an initial solution. When a membrane comes contact with the primary selective ion for the first time it will take time for the primary ion to diffuse into the membrane. The ion mobility is slower in PVC than in an aqueous solution so the thicker the membrane the longer the stabilisation times until the membrane reaches equilibrium with the solution (Bakker et al., 1997). Once the membrane potential has stabilised is it said to be conditioned. A conditioned electrode will have

a concentration of primary ions within the membrane and when immersed in a new solution the diffusion within the membrane is negligible and will hence settle faster.

2.8.2 Membrane selectivity

The potential of the membrane is dependent on the selectivity of the ion-selective membrane. An interfering ion will change the membrane potential if it is allowed to travel through the membrane. **Equation 2.33** can be expanded to include the effect of interfering ions on the membrane potential. The membrane exchange of primary ion, i and interfering ion, j is shown in **Equation 2.34** where the lined symbols ($\bar{\imath}^+, \bar{\jmath}^+$) indicate that they are in the membrane phase.

$$\bar{\imath}^+ + j^+ \rightleftarrows \bar{\jmath}^+ + i^+ \qquad \textbf{Equation 2.34}$$

The potentiometric selectivity coefficient, $K_{i,j}$ is derived from **Equation 2.34** so that:

$$K_{i,j} = \frac{c_i \bar{c}_j}{c_j \bar{c}_i} \qquad \textbf{Equation 2.35}$$

This equation determines the effect of the interfering ion depending on the concentration of the primary ion, c_i and interfering ion c_j in the solution and membrane phase ($\bar{c}_j$, $\bar{c}_i$). The potentiometric selectivity coefficient gives a measure of the ability of the membrane to distinguish between primary and interfering ions. This coefficient can be introduced into **Equation 2.33** to form an equation known as the Nikolskii-Eisenman (**Equation 2.36**) that determines the membrane potential, E with respect to primary and interfering ions and their charges, z. $\frac{RT}{zF}$ is the Nernst potential and E^0 the standard voltage potential.

$$E = E^0 + \frac{RT}{zF} \ln \left(c_i + K_{i,j} c_j^{\frac{z_i}{z_j}}\right) \qquad \textbf{Equation 2.36}$$

2.9 Ion-selective electrode operation

The ion-selective electrode produces a potential depending on the concentration of the solution it is immersed in. The phases of a standard ion-selective electrode with internal filling solution are shown in **Figure 2.5**.

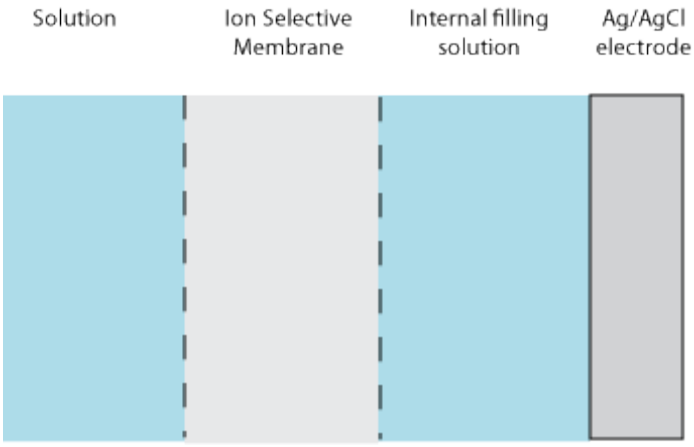

Figure 2.5 Different phases of standard ion-selective electrode with ion-selective membrane, internal filling solution and Ag/AgCl electrode.

The cell potential for this system is given by the sum of potential difference across the various phases. The ion-selective electrode is designed so that the potentials of the interfaces that are not of interest are of constant potential and will resist change with the application of external influences such as voltage, light and oxygen. The phase potentials that make up the sensor half cell potential in **Figure 2.5** are given by the sum of the phase potential between the different interfaces of the electrode as shown in **Equation 2.37**.

$$E = E_{Solution/Membrane} + E_{Membrane} + E_{Membrane/Solution} + E_{Solution/Conductor}$$

Equation 2.37

The conducting contact in the system is normally an Ag/AgCl electrode as this has a high current exchange density and has characteristics of a non polarisable electrode. The high exchange current density means that the potential will remain constant and not be affected by small voltage fluctuations from the external circuitry. The internal filling solution that the Ag/AgCl electrode is immersed in is most commonly a saturated KCl solution. The potential of the internal filling solution/conductor interface is determined by the chloride concentration of the solution as determined by the Nernst equation (**Equation 2.38**) the derivation for this is shown in **Section 2.11**:

$$E = E^0 + \frac{RT}{nF} lnc_{Cl-} \qquad \textbf{Equation 2.38}$$

The potential will remain constant across this interface due to the constant solution concentration and the resistance to electrical change at the non polar electrode interface. The $E_{Membrane/Solution}$interface is also at constant potential due to the constant saturation solution activity. $E_{Membrane}$ is constant as this is due to diffusion effects which are constant throughout the ion-selective membrane. This leaves the $E_{Solution/Membrane}$ interface that will vary with concentration of primary ion with the potential response determined by the Nernst equation as discussed in the ion-selective membrane operation, **Section 2.8.1**. When this system is measured against a stable reference half cell the potential of the $E_{Solution/Membrane}$ will be the only interface that will change potential with change in the solution concentration enabling the interface to be studied. The variation of membrane response can be described by **Equation 2.36** in **Section 2.8.1**.

2.9.1 Solid state sensor electrode

A solid state sensor is one that replaces the liquid phase internal filling solution with a solid contact. This section will discuss the operation of coated wire electrodes and conducting polymer based sensors.

2.9.2 Coated wire electrode

As described previously the ideal sensor operation will have a conducting electrode that has non polarisable charge transfer characteristics so that the potential is determined by the ion concentration in the solution coming into contact with an ion-selective membrane as dictated by the Nernst equation.

The potential across the different phases in the coated wire configuration is given by:

$$E = E_{Solution/Membrane} + E_{Membrane} + E_{Membrane/Conductor} \quad \textbf{Equation 2.39}$$

The main response of the electrode will be determined by the $E_{Solution/Membrane}$ potential again following the Nernst equation. The $E_{Membrane}$ will be a constant value so can be ignored as it will not alter during measurement. The third potential determining step is the interface between the membrane and the conducting contact electrode. There is no charge transfer reaction at the conduction contact so the potential will be determined from the double layer interface of membrane to conductor as discussed in **Section 2.3**. The problem with the coated wire electrodes is in the interface between the membrane and electrical conductor, which will act as a polarised interface that will change potential as the double layer charges due to small currents induced by the measuring hardware. This will affect the accuracy of the sensor and introduce an unwanted changeable interface potential into the sensor system.

2.9.3 Ion to electron conduction

A solid state ion-selective electrode replaces a liquid junction after the ion-selective membrane with a solid phase that acts as an ion to electron transducer. The ion to electron transducer exists to act as a redox couple to convert the charge transported by ions into electronically conducting charges. The most common couple as found in glass electrodes is the Ag/AgCl couple. The redox couple enables the solid state transducer to have a large current density which stops the interface between the ionic charge carriers and electronic conductor becoming polarised and changing potential.

Bobacka (1999) identified three conditions that are required to have an effective solid state sensor:

- A reversible and stable conduction from ionic to electronic states
- Larger exchange current than current produced from measuring devices
- No side reaction caused by interfering gases and ions

Conducting polymers have been found to have promising properties that make them suitable as ion to electron converters in solid state sensors. They are used in the mid layer of a sensor between the ion-selective membrane and the conducting contact. They can be used as ion to electron conductors as they have a number of properties that make them useful for sensors: (Bobacka, 2006)

- They are electrically conducting
- Conducting polymers can transduce an ionic signal to a electronic one using redox reactions
- Conducting polymers can be formed on surfaces that have a large high function such as platinum and carbon.
- They can be deposited on a conducting surface using electrochemical polymerisation.
- They produce a sensor with large redox capacitances which increases the stability of the sensor (Michalska et al., 2006).

These properties enable the conducting polymer to be an effective ion to electron conductor that enables a stable and responsive sensor. There are some negatives associated with the use of conducting polymers and solid state sensors that can cause the performance of the sensor to change over time (Yáñez-Sedeño et al., 2010). These are:

- Membrane can result in a water layer
- Conducting polymers have been known to degrade
- They can suffer from side reactions (O_2, CO_2) that can influence the reaction.

- Conducting polymers can be sensitive to light
- Leaching of ionophore into solution

The following sections will discuss the theory of conducting polymer operation in sensors.

2.10 Conducting polymer

2.10.1 Polymerisation

The formation of a conducting polymer known as pyrrole black is formed through the oxidation of pyrrole. The oxidation occurs by driving a potential across an electrochemical cell in a pyrrole solution containing an ionic salt.

A three electrode system is used where the current flows between the counter and working electrodes as detailed in **Section 3.1.2**. The voltage can then be measured between the working electrode and reference without being affected by the current flow and reactions taking place within the electrochemical cell. The electrode material needs to have a high work function to ensure that the current passed does not alter the surface of the working electrode.

The first stage of polymerisation is the oxidation of the pyrrole molecule to form a radical cation of the monomer. This occurs at a voltage of $E_{polymerisation}$ and corresponds to the oxidation potential of the monomer. The polymerisation voltage, $E_{polymerisation}$ and deposition rate of the conducting polymers will depend on the concentration of the pyrrole monomer in the solution. The radical cation reacts with another radical cation to then form a dimer by expelling two protons (hydrogen ions). The dimer molecule is more easily oxidised at the initial oxidation voltage. The dimer increases size by adding further radical cation molecules to form polymer chains. The growth of the chain stops when the chain gets blocked from further reaction or when the radical cation of the polymer chain becomes less reactive. The formed polymer chains have a positive charge for every 2 to 4 pyrrole rings (Vork, 1988). The positive charge is balanced by the incorporation of dopant anions from the electrolyte solution as shown in **Figure 2.6**. The formation of chains and

chemical bonds between neighbouring chains results in the insolubility of the polymer film (Sabouraud et al., 2000).

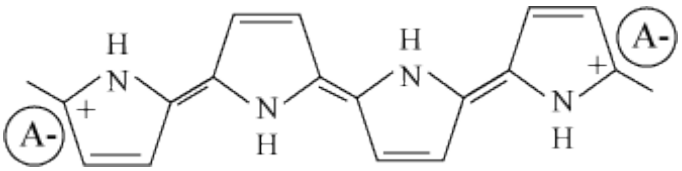

Figure 2.6 Oxidised PPY with dopant anions after polymerization.

There are two commonly used methods for electrochemical deposition of polymers on an electrode. The polymer can be formed on an electrode using a potentiometric technique where a set voltage above the polymerisation voltage is applied across the cell. The second method uses cyclic voltammetry which cycles the voltage potential of the electrode from a voltage before polymerisation occurs to a set voltage above the polymerisation charge. Cyclic voltammetry produces uniform and stable films due to the build up of films during each cycle rather than continuous growth at a set voltage.

2.10.2 Dopant ions

The dopant ion plays a part in the response of a conducting polymer as the polymer can be doped with both large and small molecules. The conducting polymer can be doped with anions. Polypyrrole doped with Cl^- and PTS^- molecules were chosen to be investigated as ion to electron tranducers as they had displayed promising attributes in the literature. PEDOT PSS and PPY are examples of p-doped polymers that are stable in aqueous solutions and in their aqueous state (Vázquez et al., 2004). The PTS had also been shown to be sensitive to pH changes (Pandey and Singh, 2008). The PPY doped with Cl^- ions was shown to be sensitive to pH and has fast exchange properties while the ions of the solution are incorporated into the polypyrrole chain to compensate for the oxidation of the polymer chain (Michalska and Maksymiuk, 2003).The following sections will discuss the operation of conducting polymers and how they are useful in solid state sensors.

2.10.3 Oxidation/reduction conducting polymer

After electropolymerisation of the conducting polymer onto a substrate the polymer chains are fully oxidised as shown in the bottom diagram of **Figure 2.7** (Pei and Qian, 1991). In this state the conducting polymer carries a positive charge that is compensated by the dopant ion to maintain electroneutrality of the polymer. In this fully oxidised state the polypyrrole undergoes spontaneous discharge/reduction which involves dopant ion loss under open circuit conditions when immersed in aqueous solutions (Dumanska, 2001). The discharge reaction results in a release of dopant ions due to the loss of positive charge within the polymer. **Figure 2.7** shows the structure of a neutral charge polypyrrole ($Poly^0$) and its oxidation to charged polypyrrole ($Poly^+$).

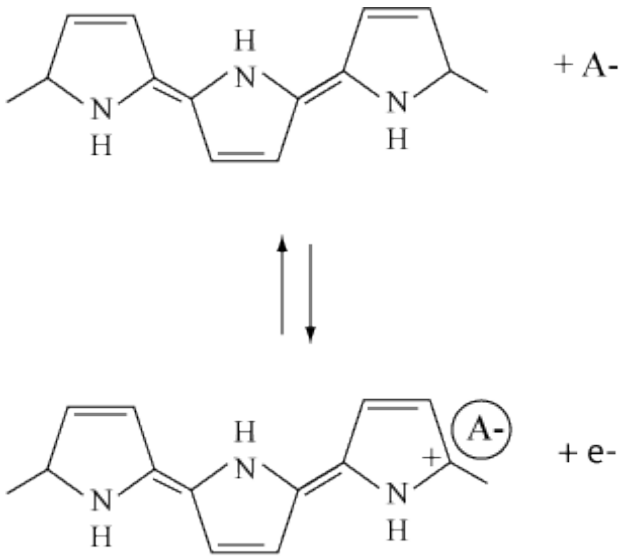

Figure 2.7 Process of redox reaction of polypyrrole conducting polymer showing reduced, $Poly^0$ (top) to oxidised, $Poly^+$ (bottom) (Inzelt, 2008)

The potentiometric potential, $E_{polymer}$ due to the oxidised state of the polymer is given by:

$$E_{polymer} = \frac{RT}{zF} ln \frac{poly^+}{Poly} \qquad \textbf{Equation 2.43}$$

The polymer can be reduced or oxidised by applying a voltage across the electrode. A negative voltage puts it in a reduced state that is electronically insulating and applying a positive puts it in an oxidised state that is its conductive state (Doblhofer, 1992). If an electron enters the polymer an anion is expelled to maintain electro neutrality as shown in **Figure 2.8** (Cosiner and Karyakin, 2010). This reaction results in an exchange of dopant ion and the polymer will form in its non conducting state poly^0. Only small ions are able to be exchanged freely with the solution. Larger dopant ions that are unable to move from the conducting polymer will make the polymer response as a cationic ion sensor as a cation will be attracted to the dopant ion to neutralise the charge on the conducting polymer.

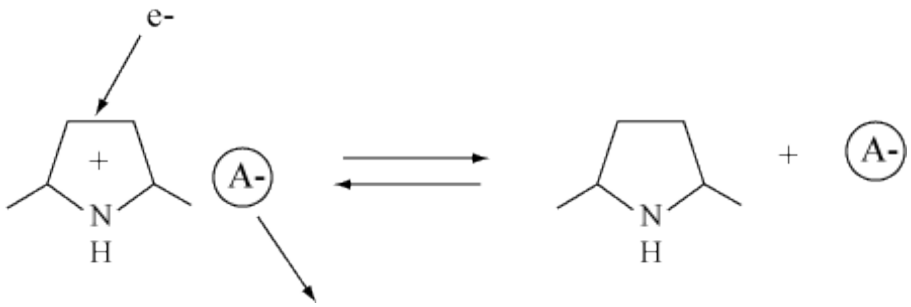

Figure 2.8 Dopant ion oxidation/reduction reaction of PPY for mobile dopant ions.

These reactions can be related to the interfacial current flow so at equilibrium the current exchange is equal in both directions. In these ion exchange reactions the exchange current density, i_o will be larger which results in a non-polarisable interface between polymer and solution (Cosiner and Karyakin, 2010).

2.10.4 Conducting polymer ion to electron transducer operation

The mixed ionic and electronic nature of the conducting polymers enables it to be a suitable replacement for the inner liquid electrode configuration as discussed in **Section 2.9**. The conducting polymer operates in a similar way to the Ag/AgCl electrode in a conventional electrode (Bobacka, 2006). The oxidation/reduction of the polymer enables electrons to move from the electrode into the conducting polymer reducing charge build up and a change of potential of the interface. The reversible charge transfer reaction results in stable sensors (Maksymiuk, 2006). The operation of the different phases of a solid state ion-selective electrode is shown in **Figure 2.9**.

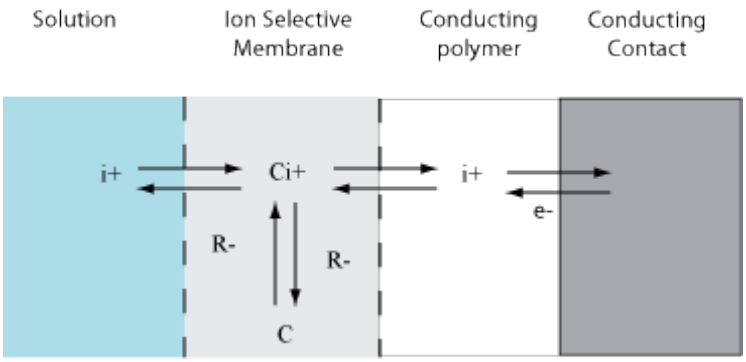

Figure 2.9 Operation of conducting polymer membrane solid state sensor. The ion interactions in the membrane, conducting polymer phase and conducting contact are illustrated.

The membrane that is applied for a pH sensor is known as a cation sensing membrane. It allows the H^+ ions to move freely between the solution and the solid contact. The influence of other ions within the solution is reduced when they are coated with an ion-selective membrane which acts as a barrier to these potential interfering ions and molecules. The membrane selectivity will determine how many of these interfering ions can penetrate the membrane and cause changes in the sensor potential. The higher capacitance of the ion to electron transducer does not protect against drift from interfering ions. Side reactions with O_2, H_2O and CO_2 can occur in conducting polymers as the ion-selective membranes are permeable to these interfering molecules (Michalska and Maksymiuk, 2005).

The conducting polymer after electropolymerisation will be in its oxidised state (poly+) with dopant Cl^- ions attracted to the polymer chain. When an ion-selective membrane is applied over the conducting polymer it will prevent the Cl^- ions from moving from the conducting polymer chain (Michalska and Maksymiuk, 2005). The ion-selective membrane will allow the H^+ ions to move freely through it. As the amount of ion recognition sites are constant within the membrane once conditioned, the conduction polymer will have a stable potential due to the activity of hydrogen ions being constant at the membrane polymer interface.

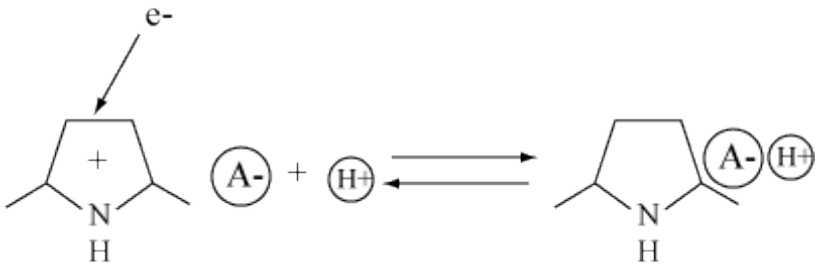

Figure 2.10 The oxidation/reduction process for polypyrrole when the dopant ions are immobile.

The conducting polymer layer does not freely exchange the dopant ions as membrane blocks movement. This changes the operation of the conducting polymer to become a cation exchanger to maintain electro neutrality (Michalska and Maksymiuk, 2005). The anion dopant ions are unable to move through the membrane. They will act as a site for the cation recognition by forming a soluble salt in the conducting polymer membrane (Gyurcsányi et al., 2004). The cation is attracted to the chain to balance any charge from electron entering the conducting polymer (Cosiner and Karyakin, 2010). To maintain the electro neutrality of the conducting polymer it charges by expelling cations and to discharge it takes cations into the membrane as shown in **Figure 2.10**. If there was no ion to compensate the charge then the electrode would become polarisable.

2.11 Reference electrode

The reference electrode role is to provide a stable half cell that produces a constant voltage response across a range of solution concentrations and constituents. This constant voltage enables the change in response of a sensing half cell to be measured against the potential of the reference electrode. The standard reference electrode used in electrochemistry is the Standard Hydrogen Electrode (SHE). Generally standard potentials are referred to against the SHE electrode as it produces a stable and reproducible potential. It generates a potential from the H_2/H^+ couple against a platinum electrode. It is not practical for many measurements due to the need for hydrogen gas to be bubbled over the electrode, an accurate value of H_3O^+ activity and the need for the platinum electrode to be re-platinised due to impurities forming on the electrode. Due to the difficulties associated with the SHE electrode other reference electrodes have been found that produce stable potentials with simpler methods. The most commonly used reference electrodes are the calomel and the Ag/AgCl electrode. When measured against the SHE they have potentials of 241mV for saturated KCl calomel electrode and 197mV for the saturated KCl Ag/AgCl electrode. These values enable the standard potentials to be adjusted for the different reference electrodes.

The Ag/AgCl reference produces a stable potential through the equilibrium value of the Ag/AgCl couple (Janz and Ives, 1968):

$$Ag\ (s) \rightleftarrows Ag^+\ (aq) + e^- \qquad \textbf{Equation 2.44}$$

$$AgCl\ (s) \rightleftarrows Ag^+\ (aq) + Cl^-(aq) \qquad \textbf{Equation 2.45}$$

Deriving from the silver, silver ion **equation 2.44** the potential, E_{Ag} is determined from the Nernst equation:

$$E_{Ag} = E^0_{Ag,Ag+} + \frac{RT}{F}\ln a_{ag+} \qquad \textbf{Equation 2.46}$$

Where $E^0_{Ag,Ag+}$ is the standard electrode potential of the silver/silver ion, $\frac{RT}{F}$ is the Nernst term (R is the general gas constant and T is the temperature in Kelvin and F is the Faraday constant) and a_{ag+} the activity of the silver ions.

The presence of the AgCl salt causes the special condition for solubility, K_S from the law of mass action of the activities of chloride, a_{cl-} and silver ions, a_{ag+}.

$$K_S = a_{cl-}a_{ag+} \qquad \textbf{Equation 2.47}$$

The solubility of the salt is constant so **Equation 2.47** can be substituted into **Equation 2.46** to show the potential of the electrode, $E_{Ag/AgCl}$ is determined by the equation:

$$E_{Ag/AgCl} = E^0_{Ag/AgCl} - \frac{RT}{F}\ln a_{Cl-} \qquad \textbf{Equation 2.48}$$

And,

$$E^0_{Ag/AgCl} = E^0_{Ag,Ag+} + \frac{RT}{F}\ln K_s \qquad \textbf{Equation 2.49}$$

From the above equation it can be observed that the potential of the Ag/AgCl reference electrode is determined by the standard potential and the activity of the Cl^- ions in the solution. When the Ag^+ ion concentration in the solution is in excess of the Cl^- concentration the potential will be determined by **Equation 2.46**. If a solution has a constant Cl^- concentration then an Ag/AgCl wire can be used alone as a reference. This system can be used in blood measurements as the concentration of Cl^- is within a tightly controlled range of 98 - 108 mmol/L (Martini, 2006).

2.11.1 Operation of glass Ag/AgCl reference electrode

The standard glass Ag/AgCl reference electrode operates by having an Ag/AgCl electrode in a saturated KCl solution. KCl is used for two reasons, the first is that it contains Cl^- ions which influence potential of electrode and provides a steady voltage potential. The second is that when dissolved the salts ions both have similar ionic mobilities so the diffusion potential of the liquid/liquid junction will be reduced. It is connected to the external solution by an ion porous frit that allows movement of ions between the two solutions. The porous junction is normally made of a ceramic plug that allows ion flow (Galster, 1991). As the liquid junction potential will be small it will not influence the overall cell potential and the potential of the reference electrode will be determined by **Equation 2.48**. Due to the high concentration of KCl the flow of ions out will mean that there will be no significant flow of ions into the internal reference solution unless the solution being measured is of very high ionic concentration.

2.12 Circuit design

To measure the potential across an electrochemical cell a voltmeter needs to be placed across the two cell electrodes to form a complete electrical circuit. The sensors response is recorded by a potentiometric measurement which is a measure of cell potential when there is no current flow across the sensing and reference electrode. The potential of the cell is determined as a function of capacitance (Bard and Faulkner, 2001). The aim of the measurement circuitry is to enable an accurate measurement of the open circuit voltage response of the electrochemical cell without influencing the performance of the sensor. The design of the measurement circuitry plays an important role in accuracy of voltage measurement and sensor stability. The detailed design of the measurement circuitry is covered in **Section 3.5**. This section will discuss the theory behind the factors of the measurement circuitry that can affect the performance of the solid state sensor.

The cell potential voltage is measured through the input of an operational amplifier with the pH sensor connected to the positive input terminal and the reference electrode attached to ground. The input resistance of the operational amplifier is an important factor as by connecting the two electrodes it will cause a circuit to form across the electrochemical cell as shown in **Figure 2.11**. When the measurement operational amplifier is connected to the electrochemical cell the input impedance of the operational amplifier is in parallel with the electrochemical cell resistance. The operational amplifier input impedance needs to be high so that only a small as possible current flows through the operational amplifier and there is no voltage drop across the input resistor of the operational amplifier. A current flow through the operational amplifier input impedance would affect the measurement and lead to inaccurate measurement values. This is a particular problem for potentiometric sensor systems as the load resistance of the electrochemical cell can be high, e.g glass pH electrodes can have resistances of up to 100MΩ (Galster, 1991). For a voltmeter to have a less than 0.1% voltage drop the operational amplifier input impedance in parallel with the electrochemical cell must be 100 times greater than the electrochemical cell impedance.

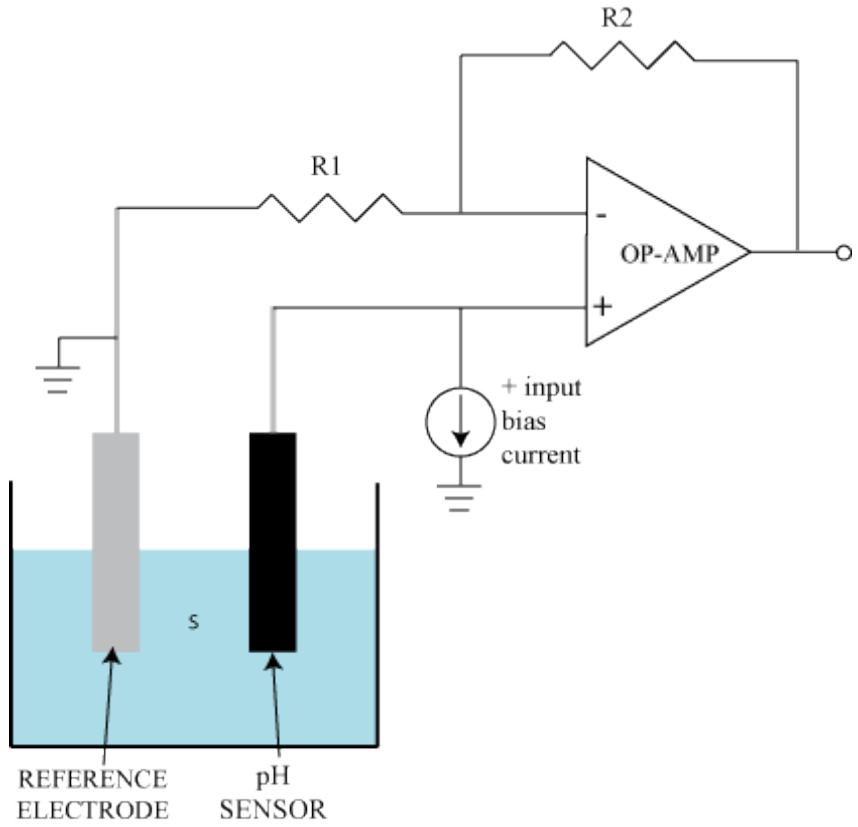

Figure 2.11 Operational amplifier setup for measuring voltage in the electrochemical cell. The input bias current on the positive input flows through the electrochemical cell to ground.

The second factor that can affect the stability of the electrochemical cell is the operational amplifier bias current. The offset current from the positive input terminal to the operational amplifier drives a small current through the electrochemical cell to the ground which is attached to the reference electrode. This small bias current can charge the double layer capacitance causing unwanted drift in the sensor voltage. The bias current on the negative input terminal does not flow into the electrochemical cell. The current induced by the measurement circuitry must be less than the exchange current density of the electrode otherwise the double layer capacitance of the electrode will start to charge changing the voltage potential which leads to inaccurate voltage measurements (Bockris and Reddy, 2000). The influence of circuit current, i on change of potential from equilibrium value, η with regards to the

exchange current density, i_0 is given in **Equation 2.50**. R is the general gas constant and T is the temperature in Kelvin and F is the Faraday constant.

$$i = i_0 \frac{F}{RT} \eta \qquad \textbf{Equation 2.50}$$

2.13 Electrochemical impedance spectroscopy

Electrochemical impedance spectroscopy (EIS) uses an AC wave of varying frequencies to study the charge transfer and charge transport of an electrode (MacDonald, 1987). EIS uses an AC voltage wave with small amplitude so as not to affect the equilibrium condition of the electrode in the solution.

An alternating voltage, $E(t)$ is used for EIS:

$$E(t) = Esin(\omega t) \qquad \textbf{Equation 2.51}$$

The angular frequency $\omega = 2\pi f$ where f is the wave frequency at voltage amplitude, E. This is applied to an electrode where the current response, $I(t)$ is:

$$I(t) = Isin(\omega t + \vartheta) \qquad \textbf{Equation 2.52}$$

Where ϑ is the phase difference between the voltage and current, I. The impedance is defined by:

$$\frac{E(t)}{I(t)} = |Z|\exp(i\vartheta) = Z' + iZ'' \qquad \textbf{Equation 2.53}$$

Where $Z'$and Z'' are the real and imaginary components of Z. The impedance in its real and imaginary values can be plotted against log ω to give a Bode plot. The shape of each of these graphs will define the processes happening at the electrode. The Z' values plotted against Z'' give the plot named Cole-Cole or complex impedance plot.

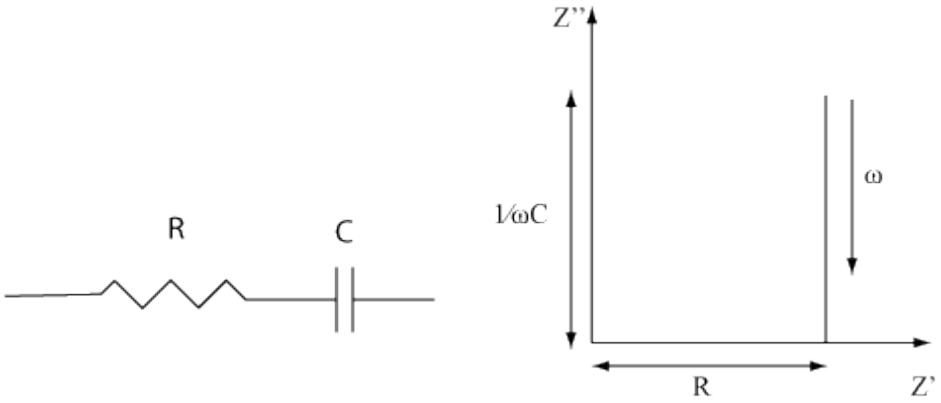

Figure 2.12 Complex impedance response of RC circuit.

For a circuit containing resistive and capacitive components as illustrated in **Figure 2.12** the resistance is not affected by frequency so $Z' = R_s$. Capacitance is affected by frequency as $Z'' = -1/\omega C$ as frequency changes the imaginary component of Z'' will change as shown in the complex impedance plot **Figure 2.12**. The impedance response measured as a function of frequency is characteristic of the electrical circuit being measured. In an electrochemical cell this technique can be used to measure the properties of the working electrode. The response can be modelled by a combination of resistive and capacitive components.

The simplest model of an electrode interface is given by a resistor and capacitor in parallel **Figure 2.13** (Bard and Faulkner, 2001). In this, the resistor models the resistance to charge transfer across the interface and the capacitor models the double layer capacitance of the interface. Every electrode in a solution has a capacitance with a resistance in parallel to it (MacDonald, 1987). For an electron transfer system the charge transfer resistance is low and the output will be a circle and respond as a non-polarisable interface **Figure 2.13** (bottom). When there is no redox electrode reaction the charge transfer resistance is very high and the EIS plot will respond like a capacitor as in a polarisable interface **Figure 2.13** (top).

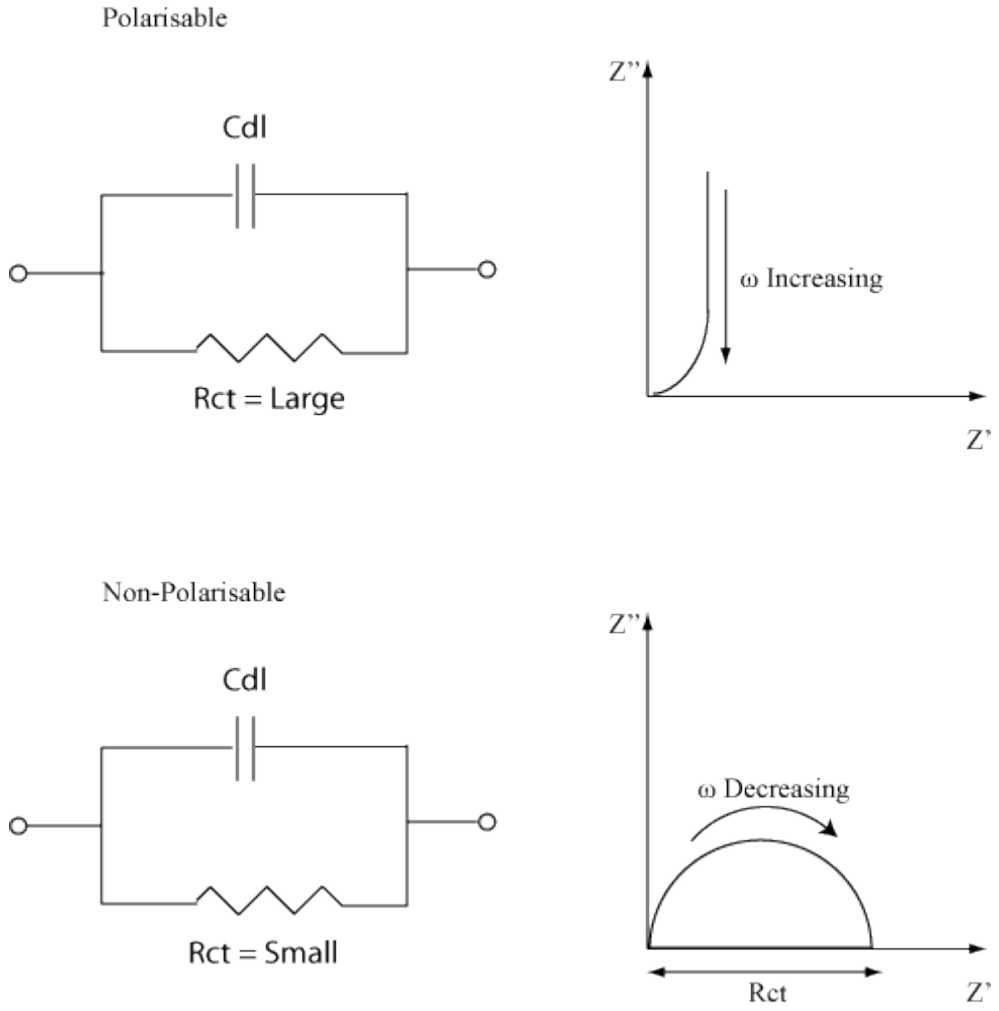

Figure 2.13 Polarisable (top) and non-polarisable (bottom) impedance plot and circuit diagram for same frequency scan.

Figure 2.13 does not take into account the solution resistance of an electrochemical cell. At high frequencies the capacitor is effectively a short circuit and the current will flow through the capacitor leaving the only resistance in the system being the solution resistance. As the frequency decreases the flow of current through the capacitor reduces allowing the response due to the charge transfer resistance to increase.

In a real system the reactions at a charge transfer electrode are limited by the diffusion of ionic species at the electrode interface. The effect of diffusion is observed at low frequencies (Bard and Faulkner, 2001). This response is known as the Warburg impedance which resists mass transfer at the electrode. The Randles

equivalent circuit (**Figure 2.14**) is commonly used to model the interface of an electrochemical cell.

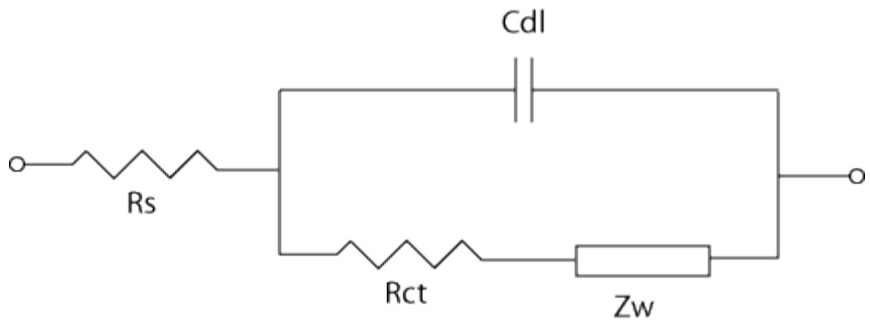

Figure 2.14 Randles equivalent circuit: Rs, solution resistance; Rct charge transfer resistance; Zw, Warburg impedance; Cdl, double layer capacitance.

The effects of the Warburg impedance in a cell with high transfer resistance are negligible due to low current exchange at the electrode and can be removed from the equivalent circuit. The Randles equivalent circuit can be used to model the complex frequency response from an EIS experiment. The data from the model will enable values for the double layer capacitance and charge transfer resistance to be calculated.

2.14 pH

The Brønsted theory defines acids and bases as substances that are capable of either donating or accepting hydrogen ions as shown by **Equation 2.54** (Galster, 1991).

$$Acid \leftrightarrow Base + Proton \qquad \textbf{Equation 2.54}$$

The definition of an acid states that the hydrogen ion plays a role in all acid base reactions and can be used to define the pH scale. In an aqueous solution the hydrogen ion concentration can vary between 10^{0} to 10^{-14} mol/litre. The pH of a solution is approximately the negative logarithm of hydrogen ion concentration, c_{H^+} it is given by:

$$pH = -\log_{10} c_{H^+}$$ **Equation 2.55**

A buffer solution is a solution that acts to maintain its pH when small quantities of acids or bases are added. The buffer capacity is the amount which a buffer solution can resist a pH change when an acid or base is added to the system. The buffer capacity, γ_b of a solution is given by:

$$\gamma_b = \frac{1}{b}\frac{db}{dpH}$$ **Equation 2.56**

Where b is quantity of substance added to the solution. The buffer value, β is the gram equivalent of the buffer capacity given in mol/L-pH:

$$\beta = \frac{1}{V_0}\left|\frac{dn}{dpH}\right|$$ **Equation 2.57**

Where n is the amount of strong acid or base added and $V_0$the volume in litres of the buffer solution.

From the law of mass action the acid activity, a_{HA} and base, a_B gives the constant:

$$pK_a = -log_{10}\frac{a_B a_{H^+}}{a_{HA}}$$ **Equation 2.58**

Where pK_a is the acid dissociation constant which is a measure of the strength of an acid in a solution. A strong acid is almost completely disassociated in a solution. A weak acid is only partially disassociated. From the acid dissociation constant **Equation 2.58** the Henderson–Hasselbalch equation of pH can be derived it gives the change in pH of a chemical or biological solution as a measure of acidity. The Henderson–Hasselbalch equation is given by:

$$pH = pK_a + log_{10}\frac{a_B a_{H^+}}{a_{HA}} \qquad \textbf{Equation 2.59}$$

The pKa values indicate the point where the acid is half neutralised and the acid concentration equals the base concentration of the solution when the second term of **Equation 2.59** equals 0 so that:

$$pH = pK_a \qquad \textbf{Equation 2.60}$$

Around the pKa point the acid has a buffering capacity that extends ±1pH level (Shriver, D.F; Atkins, 1999).

The pH of a solution varies with temperature as if a solution temperature increases the acid has greater disassociation. Strong acids are not affected by temperature due to their full disassociation in solutions. The equation for temperature, T dependence of pH of weak acids is given by:

$$\frac{dpK_a}{dT} = \frac{0.9 - pK_a}{T} \qquad \textbf{Equation 2.61}$$

2.14.1 pH buffering of biological fluids

The body has a number of systems that maintain a constant pH of blood within the body. These different systems are split into three major categories (Martini, 2006):

- Protein buffer systems
- Carbonic acid-buffer system
- Phosphate buffer system

These systems operate in conjunction with the respiratory and renal systems of the body to maintain the body's pH between 7.35-7.45. Of these systems the protein buffer systems are the only ones that will act to buffer pH when blood, blood serum and wound fluids which have similar properties to blood serum are removed from the

body (White, 2002). This is an important factor for wound healing as the wound fluid is only buffered by the buffering capacity of the proteins contained within the wound fluid. This investigation uses horse blood serum as a substitute for wound fluid. Horse serum can be used as a substitute for human blood serum and wound fluid in experiments due to the similarity of the components.

Blood serum is produced from blood by removing red and white blood cells as well as clotting factors. The serum components are made up of salts (Na^+, Ca^{2+}, HCO_3^-, Cl^-), proteins (Albumin, globulins), lipids (cholesterol) and water. Of these components the proteins, bicarbonate ions and phosphate ions play a role in buffering the pH of the serum solution (Martini, 2006). The buffer with the largest capacity in serum is from the amino acid chains that form the blood proteins albumin and globulin (Nelson and Lehninger, 2008). The carbonic acid bicarbonate buffer plays the second biggest role in buffering pH within the serum. The buffering value β in human serum is 8 mmol /L-pH. When this value is broken down bicarbonate contributes 2.6 mol /L-pH for the proteins it is given as 5 mmol /L-pH and phosphate ions contribute 0.4 mmol /L-pH (Gilbert, 1960). The buffering capacity will be most active around the pK_a value and it extends ±1pH level from the pK_a point. The pK_avalues of carbonic acid and albumin are 6.37 and 6.75 respectively. The pK_a values of the two strongest buffers in horse serum and human serum will have buffering properties in the region from approximately pH 7.75 – pH 5.37.

Overview

The theory discussed in this section covers the important theoretical aspects behind the operation of ion-selective electrodes. The chapter covers the main components of solid state ion-selective sensors such as ion-selective membranes and conducting polymers and these individual components will be tested to find a suitable disposable pH selective electrode that can be used to test the pH of wounds. The chapter also details the theoretical background to the experiments conducted in this thesis. The following chapter will detail the materials and methods used to investigate the solid state pH sensor.

Chapter 3 Materials and Methods

This chapter details the materials and methods used to produce and test the disposable pH electrodes. The methods and material section is split into three sections. The first details the methods used to produce and test the disposable pH sensors and reference electrodes. The second section discusses the design of the measurement hardware and software used and the methods used to test the system. The third and final section details the methods for the testing of the pH modifying wound dressings.

The first section of the methods and materials is split into two parts the first part will detail the materials and manufacturing methods used to produce both the pH sensor and reference electrode, the second part details the testing methods used to assess the sensor system. Four different sensor types were produced using a combination of conducting polymers. The sensor types are all produced using the same techniques with only the conducting polymer component varied. One of the sensors does not have any conducting polymer mid-layer. Two of the sensors are produced with electropolymerised polypyrrole conducting polymers doped with different doping ions. The final sensor type made from PEDOT is produced with the only commercially available conducting polymer ink.

3.1 Sensor manufacturing

3.1.1 Screen printing

A screen printing method was used to produce the conducting layers for the disposable pH sensors - all four types of sensors tested use this method. The 4 types of sensors being produced had a carbon contact and an isolation layer printed (**Figure 3.1**) and one type of sensor has an additional PEDOT conducting polymer layer printed.

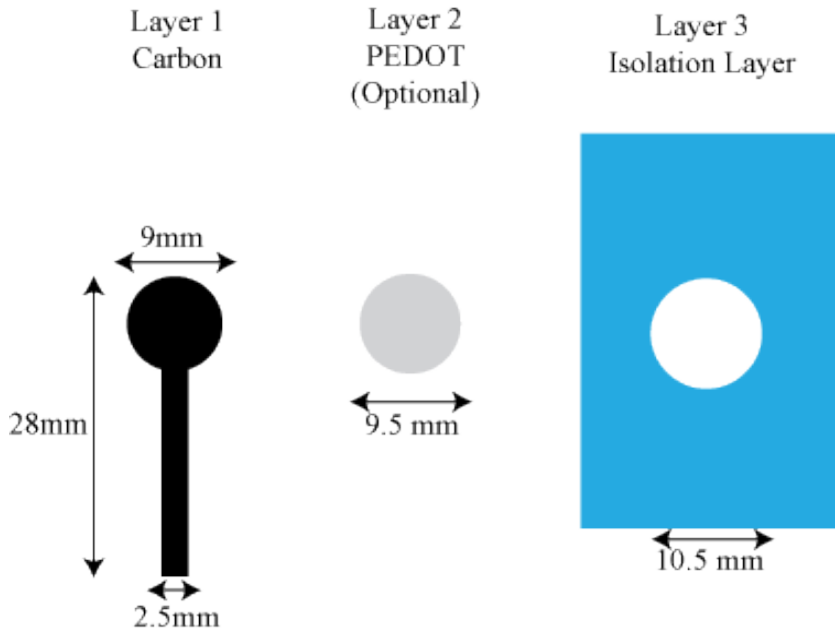

Figure 3.1 Screen printed electrode showing conducting carbon (left), optional PEDOT layer (Middle) and isolation layer (right). The dimensions of the different layers are shown.

The screen printing process was conducted using a DEK 248 (DEK) screen printing machine. The screens were produced by DEK and have a 90/230 poly(ethylene terephthalate) (PET) with a 35µm mesh size configuration. The screen printing process was used to screen print various layers onto the sensor substrate. The substrate used for the printing was a 250 µm thick polyester sheet (Hifi films, PMX749 250 micron). The carbon ink used was a carbon/graphite paste (Gwent Electronic Materials, Carbon/Graphite Paste C2000802P2). The isolation layer used was a polymer dielectric paste (Gwent Electronic Materials, Polymer Dielectric Paste D2020823D2) this layer prevents the solution contacting non-sensing areas of the sensor. Only the PEDOT:PSS conducting polymer was available as an ink for screen printing (Agfa, ORGACON^{TM} EL-P3040). The DEK screen printing machine was adjusted for each ink type due to different ink viscosities to ensure sufficient pressure was used to produce a complete print. Each printed electrode was given two coats of each ink before drying this involved two cycles of the squeegee (forward and back) across the printing masks. The printed electrode sheets were then put in an air dryer conveyer belt oven (SC technical services dryer) at 80^{o}C to dry the ink. Each sheet

was run through the dryer five times before being left overnight to fully dry. The electrode has a 9mm diameter of the sensing area which results in a sensor with a 6.36cm^2 surface area. A photograph of the screen printed sensor is shown in **Figure 3.2**.

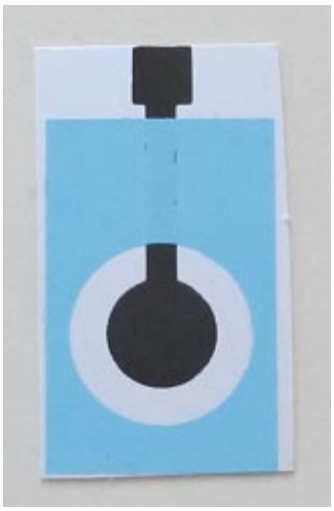

Figure 3.2 Photograph of screen printed electrode showing conducting carbon (black) and isolation layer (Blue).

3.1.2 Electropolymerisation

Electropolymerisation from a polymer solution was used to coat two of the screen printed electrodes with deposits of polypyrrole conducting polymer, doped with different ions. The electropolymerization was conducted using a 1286 Electrochemical Interface (Solartron). The electropolymerization was conducted using a traditional 3 electrode electrochemical configuration comprising working, counter and reference electrode. The electrode to be coated was the working electrode, a platinum wire was the counter electrode and a double junction calomel electrode (Fisher scientific, CR11) was the reference electrode. A diagram of this arrangement is shown in **Figure 3.3**. The sensors doped with chloride ions were made from an aqueous solution of 50ml deionised water (ELGA, Purelab Ultra), 346.2µL pyrrole (C_4H_5N) (Aldrich 131709) to make 0.1M and 372.7mg of potassium chloride (KCl)(Sigma Aldrich P9333) to make 0.1M. The Sensors doped with tetrabutylammonium p-toluenesulfonate (PTS) (Aldrich 358681) were made from an aqueous solution of deionised water (ELGA, Purelab Ultra) 346.2µL pyrrole

(C_4H_5N) (Aldrich 131709) to make 0.1M and 2.06g PTS (Aldrich 358681) to make 0.1M concentration.

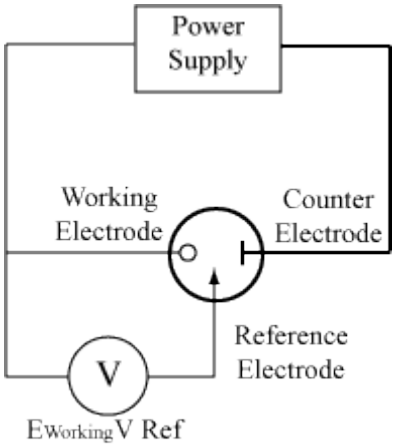

Figure 3.3 Three electrode system used for electrochemical polymerisation.

Cyclic voltammetry was used to coat the electrodes to ensure an even coating of polypyrrole on the electrode. The electrodes were cycled from 0 to 3 volts with a 100mV/s scan rate it was reported to produce a smooth coating of polypyrrole (Segut et al., 2007). The amount of polypyrrole that is deposited on the electrode is dependent on the number of cycles performed as this relates to oxidation current passed - this is discussed in **Section 2.10.1**. Therefore, in order to determine the effect of coating thickness the electrode was cycled a number of times (1,3,5 times) to determine the most effective deposition of PPY as detailed in **Section 4.2**. After electropolymerization the sensor was washed with distilled water and air dried before use. For the full sensors with ion-selective membranes the PPYCl and the PPYPTS were cycled three times as this was found to give the most effective coatings in the experiments detailed in **Section 3.3**. The PEDOT sensor was produced through screen printing as discussed in **Section 3.1.1**.

3.1.3 Ion-selective membrane

The ion-selective membrane was used to coat the screen printed electrodes the formulation being that taken from a paper by Schulthess et al (1981). The membrane was produced from a mixture of Tridodecylamine (Sigma 95292) 1%wt, KTpClPB (Sigma 60591) 0.5%wt, DOS plasticiser (Sigma 84818) 65.5%wt, PVC (Sigma

81392) 33%wt and THF solvent (Sigma 186562). The solution was prepared under a fume hood in 10ml glass bottles with screw tops that are resistant to THF. The membrane solution was made in batches with 5ml THF, 5mg Tridodecylamine, 2.5mg KTpClPB, 358µL DOS and 165mg PVC. Once dissolved in the solvent the membrane solution was ready to deposit. The same membrane was used for all 4 sensor types.

3.1.4 Membrane deposition

The ion-selective membrane as detailed in **Section 3.1.3** was deposited onto the screen printed electrodes using two methods. The first method is the drop coating method this uses a pipette (Eppendorf) to deposit the membrane solution over the sensor surface as shown in **Figure 3.4**. The drop coating method uses around 180µL to cover the carbon sensor surface. The pipette is used to ensure that the surface of the electrode (carbon contact/conducting polymer) is covered in the ion-selective membrane solution. This process is conducted in a fume hood. After coating, the electrodes were left for 2 hours to allow the solvent in the membrane solution to evaporate creating a solid polymer ion-selective membrane.

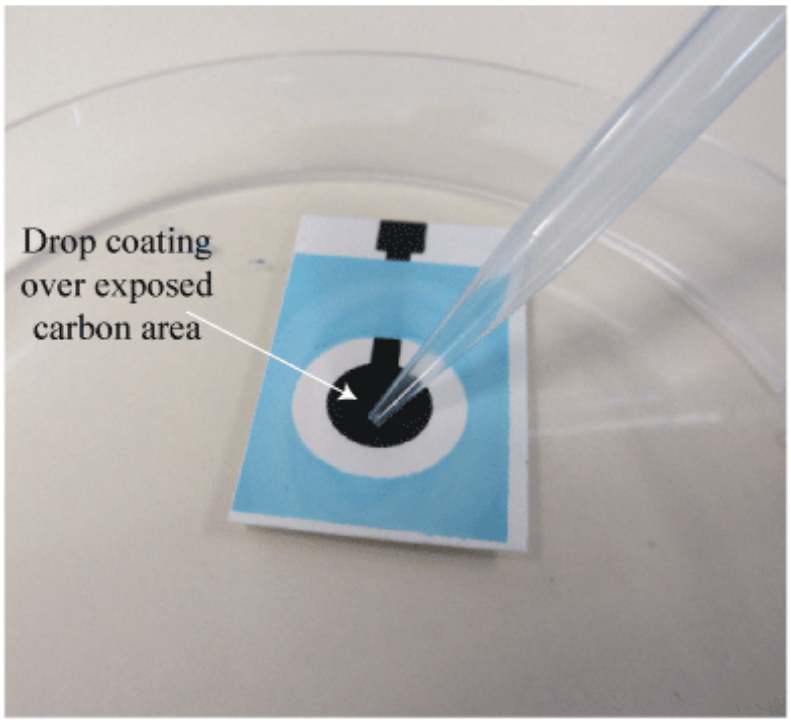

Figure 3.4 Drop coating of membrane onto sensor with pipette.

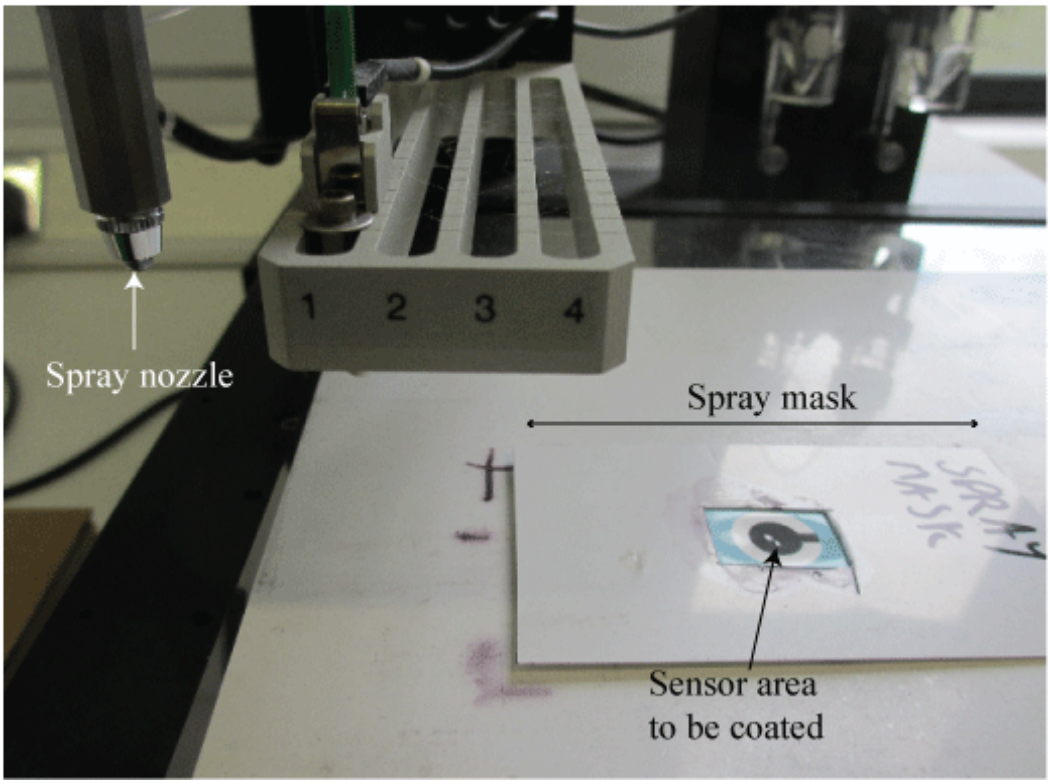

Figure 3.5 Biodot machine with spray mask and dispensing nozzle labeled.

The second method uses the Biodot Airjet automatic dispensing machine (Biodot). The machine was set to nozzle travel speed 25mm/s, at a height of 20cm and pressure of 10psi. Each sensor was sprayed with membrane for 1.5cm of dispensing nozzle travel at the different dispensing amounts to cover the sensing area. The dispensing rate was varied from 12.5-100µl/cm travelled depending on the amount of membrane being deposited. 100µl/cm travelled, 75µl/cm travelled, 50µl/cm travelled, 25µl/cm travelled and 12.5µl/cm travelled settings for membrane deposits amounts. Each sensor is sprayed over 1.5cm of nozzle travel which results in deposition of 150µl, 112.5µl, 75µl, 37.5µl and 18.75µl respectively of membrane solution deposited. A spray mask is used to ensure the membrane is deposited in the correct area this is shown in **Figure 3.5**.

3.1.5 Sensor isolation

To fully isolate the sensor so that it can be fully immersed in a moist environment the conducting contact has to be isolated from any potential liquid contact. This full isolation is only needed when using larger samples of fluid or where the testing

liquid may come into contact with other parts of the sensor other than the ion-selective membrane. To achieve this, a disposable isolated wire was attached to the sensor using a conducting epoxy glue (Conductive epoxy, Chemtronics) then coated in the isolation polymer dielectric paste (Gwent Electronic Materials, Polymer Dielectric Paste D2020823D2). The sensor was then baked at 80^{o}C to allow the isolation paint to set. **Figure 3.6** shows the full isolated sensor.

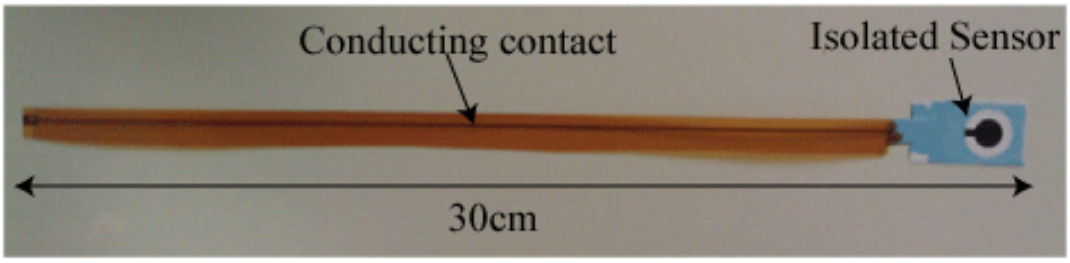

Figure 3.6 Fully isolated sensor with covered conducting contact and dielectric isolation ink.

3.2 Solutions

3.2.1 pH buffer solution

For testing of the response of pH alone a universal solution had to be found that would be easy to titrate and involve a constant ionic content. A version of the Britton-Robinson buffer (McGraw-Hill, 2002) was chosen as it contains three separate buffer solutions so that it has a stable titration gradient across the pH range 4-10. The buffer solution is composed of 0.04M of acetic acid (CH_3CO_2H)(Sigma-Aldrich, 04102320099), 0.04M boric acid (H_3BO_3)(Sigma, B6768) and 0.04M Phosphoric acid (H_3PO_4)(Sigma-Aldrich, 04102) in deionised water (ELGA, Purelab Ultra) this is then titrated with 0.2M sodium hydroxide (NaOH)(Sigma-Aldrich, S5881) in deionised water (ELGA, Purelab Ultra) to get the required pH values. To make 200ml solutions of pH buffer solution at pH levels 4-10 the following amounts were used for the acidic solution to be titrated 2.3ml acetic acid, 2.74ml phosphoric acid and 2.4732g of boric acid are measured into a glass bottle then to get the required strength the solution is made up to 1litre with deionised water. For the second titration solution 7g of sodium hydroxide is dissolved in 875ml deionised

water. Once both solutions have been made the acidic solution is titrated with the sodium hydroxide solution until the correct pH level has been reached. Once a pH has been reached the solution is decanted into a 200ml glass bottle before further titration to reach higher pH levels. During the titration the pH of the solution is constantly monitored with a glass pH electrode. Each solution is then tested for its pH value before use.

3.2.2 Solution A

British Pharmacopoeia Solution A was used in a number of experiments to mimic salt levels in physiological fluids. Solution A is an ionic solution containing 0.142M sodium chloride (NaCl) (Sigma-Aldrich, S7653) and 0.0025M calcium chloride dihydrate ($CaCl_2 \cdot 2H_2O$) (Sigma-Aldrich, 223506) giving the solution a similar ionic concentration to serum and wound exudates (British Pharmacopoeia Addendum, 1995). It is the recommended standard solution for testing moisture capacity in wound dressings and has been used to emulate ionic conductivity of wound fluid in model systems (McColl et al., 2007). One litre of Solution A requires 8.298g sodium chloride and 0.368g calcium chloride dihydrate dissolved in deionised water (ELGA, Purelab Ultra) to a volume of one litre.

3.2.3 Modified pH buffer solution

To mimic wound exudate more closely a combination of the physiological salts used in Solution A were combined with the pH buffer solution to produce a modified buffer that contained physiological levels of salts. pH buffer solutions at pH levels 4-10pH were produced following the procedure detailed in **Section 3.2.1**. The solution A salts (0.142M sodium chloride (NaCl) (Sigma-Aldrich, S7653) and 0.0025M calcium chloride dihydrate ($CaCl_2H_2O$) (Sigma-Aldrich, 223506)) were then added to the individual pH solutions. To modify the 200ml pH solutions described in **Section 3.2.1** the following amounts of salts were added to the pH solutions to produce similar salt levels as Solution A 1.66g sodium chloride and 0.074g calcium chloride dehydrate. The pH of the solutions was then retested and adjusted accordingly with 0.2M sodium hydroxide (NaOH)(Sigma-Aldrich, S5881) in deionised water(described in **Section 3.2.1)**.

3.2.3 Horse serum

Horse serum (donor horse serum, Harlan Seralab S-0004A) is used as a biological solution that acts as a substitute for wound fluid with similar acid buffering capabilities and constituents (White, 2002) (Eming et al., 2008). The horse serum was used to test the pH response of wound dressings as described in **Section 3.11**. Horse serum was obtained in bulk volumes 500ml and it is frozen for long-term storage. Serum was only defrosted once before use. Dilute horse serum was also used to produce a less viscous mixture - this was made by mixing 50% solution A (**Section 3.2.2**) with 50% horse serum.

3.3 Sensor characterisation

This section discusses the methods and materials used to characterise the four sensor types and their component parts.

3.3.1 Membrane thickness – Micrometer

The ion-selective membrane thickness was estimated using two different methods using a digital micrometer and a white light interferometer.

The ion-selective membrane thickness was determined using a digital micrometer (RS electronics) with a 0.001mm resolution. The micrometer has a 3mm diameter measurement area. The measurement was taken in the middle of the sensor circle as shown in **Figure 3.7**. The thickness of the screen printed carbon electrode with no membrane was measured in the same position as **figure 3.5** to find the average thickness of substrate and carbon layer. This value can then be subtracted from the full sensor thickness measurement to give an estimate of membrane thickness.

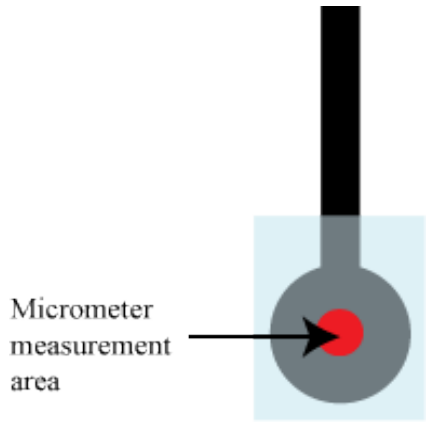

Figure 3.7 Measurement position on sensor surface for micrometer membrane thickness measurement.

3.3.2 Membrane thickness - White light interferometer

The Veeco Wyco NT9300 interferometer was used to image the membrane surface to get data concerning membrane depth. The sensors were brushed with fine aluminium powder applied with a paint brush to provide a reflective surface on the electrode. The particle size is very small so it is insignificant thickness compared to the thickness of the membranes. A scan across the centre of the electrode was taken as shown in **Figure 3.8**. To ensure an accurate measurement an edge is needed between the plastic substrate and the membrane so that a depth reference point can be found.

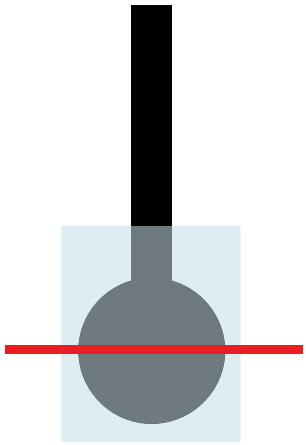

Figure 3.8 Red line shows track of white light interferometer scan across centre of electrode.

3.3.3 Potentiometric measurement experimental arrangement

All potentiometric measurements detailed in this thesis used the two electrode arrangement shown in **Figure 3.9**. Only two electrodes are required due to no current flow being induced during the measurement. The two electrodes are the working electrode and reference electrode. The sensor type and reference was changed for the different experiments these will be discussed in the following sections. The experiments that use this experimental arrangement are:

- pH Voltage response of full sensors (**Section 3.3.4**)
- Sensor settling (**Section 3.3.5**)
- Selectivity (**Section 3.3.6**)
- Hysteresis (**Section 3.3.7**)
- Water layer (**Section 3.3.8**)
- Sensor heat stress (**Section 3.3.9**)
- Sensor range (**Section 3.3.10**)
- Sensor long term drift (**Section 3.3.12**)

The experiments used the Solartron 1286 electrochemical interface or the designed handheld measurement hardware as voltmeters to measure the electrochemical cell potential. The Solartron 1286 electrochemical interface was operated and data recorded through CORRWARE (Scribner Associates Inc) software on a PC.

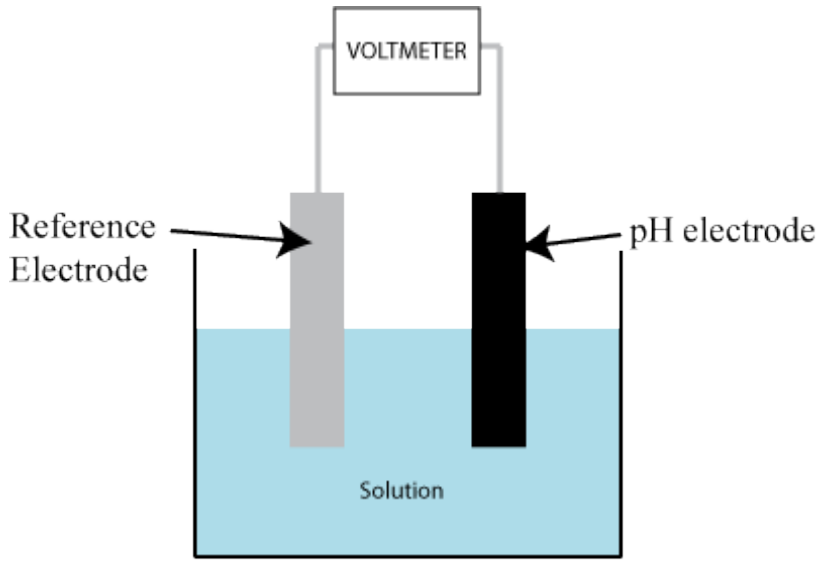

Figure 3.9 Potentiometric cell showing two electrode configuration with pH electrode and reference electrode with voltage measured with a voltmeter.

3.3.4 pH Voltage response of full sensors

The full membrane coated sensors manufactured using the technique in **Sections 3.1.1, 3.1.2 and 3.1.3** were tested for voltage response to change in pH. The pH voltage response tests were conducted using the Solartron 1286 electrochemical interface to measure voltage response of the various sensors controlled through the computer software Corrware. For measuring the voltage response a potentiometric voltage was measured between the working electrode and the reference electrode, a saturated calomel electrode, as detailed in the potentiometric arrangement **Section 3.3.3**. The electrodes were tested at seven pH points from pH 4 to pH 10 in buffer solution (**Section 3.2.1**). Each test had a duration of 5 minutes to give the sensor time to settle to a stable voltage potential. For the long life testing the electrodes were tested then stored for 60 days in a dark dry environment then retested for pH response. The slope per decade of response to H^+ ion concentration was calculated using the best fit line through the voltage points recorded at each pH level. This test was repeated on 7 sensors of each electrode type (Carbon membrane, PEDOT, PPYCL and PPYPTS) with the results detailed in **Section 4.5.1**.

3.3.5 Sensor settling

To observe the time the sensors took to reach equilibrium and achieve stable voltage potential the sensors produced using the method in **Sections 3.1.1, 3.1.2 and 3.1.3** were tested for voltage settling times. The new sensors that have not been immersed in liquid were immersed in a Britton-Robinson buffer (S**ection 3.2.1**) of pH 4 against a double junction calomel reference electrode. The sensor and reference electrode were configured in the potentiometric arrangement shown in **Section 3.3.3**. The potentiometric voltage was measured using a Solartron 1286 electrochemical interface for a 30 minute period to observe the drift in voltage potential over this initial immersion period while the sensor reached equilibrium with the solution. This test was repeated on 7 sensors of each electrode type (Carbon membrane, PEDOT, PPYCL and PPYPTS) with the results detailed in **Section 4.5.3**.

3.3.6 Selectivity

The Separate Solution Method (SSM) was used to determine the selectivity of the sensor electrodes (Bakker et al., 2000). The SSM method was chosen as it is one of the IUPAC's recommended techniques for assessing selectivity of potentiometric sensors (Buck and Lindneri, 1994). The potential was measured against a double junction calomel electrode using the Solartron 1286 electrochemical interface with the potentiometric arrangement detailed in **Section 3.3.3**. First the sensor voltage response to hydrogen ion was found by testing the sensors from pH 4 to pH 10 in the pH buffer solutions described in **Section 3.2.1**. Potassium chloride (KCl)(Sigma-Aldrich, P9333), sodium chloride (NaCl)(Sigma-Aldrich, S7653), calcium chloride ($CaCl_2$)(Aldrich, 499609) and lithium chloride (LiCl)(Sigma-Aldrich, L4408) solutions at 5 different molar concentrations 10^{-5}-10^{-1}M were used to determine the potential of the sensors to interfering ions. To produce 100ml samples of the four interfering ions at 5 different concentrations the following amounts were measured 0.745g Potassium chloride, 0.584g sodium chloride, 1.11g calcium chloride and 0.424g lithium chloride and placed in separate 200ml glass beakers. The beakers were then made up to 100ml with deionised water (ELGA, Purelab Ultra) this produced 0.1M solutions of the respective interfering ions. The lower concentration solutions were made by decanting 10ml in a new beaker and making it up to 100ml

using deionised water. This procedure was repeated to produce the required concentrations.

The selectivity coefficient of each sensor was then calculated by taking the extrapolated pH response to 1M concentration and calculating the estimated voltage. The extrapolated value is found by calculating the line gradient and intercept from the voltage response of the sensor as shown in **Figure 3.10**.

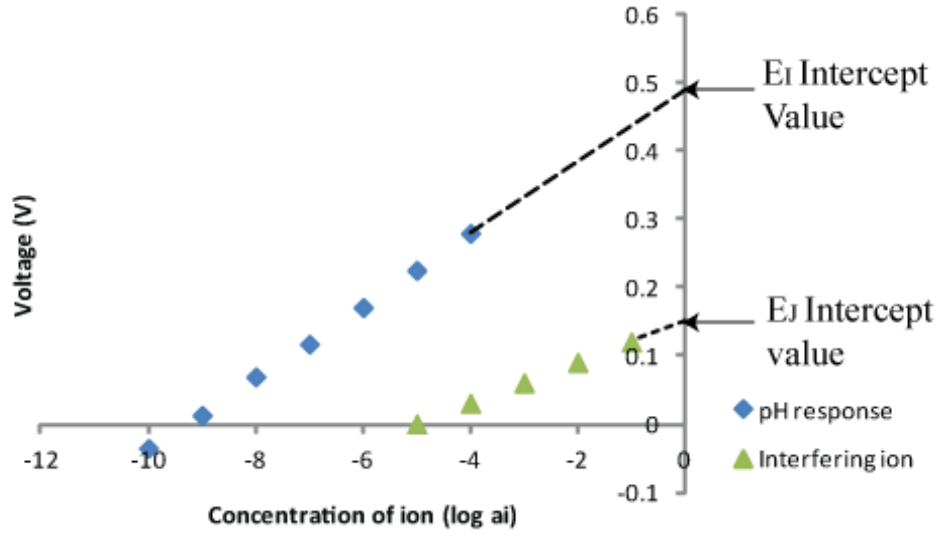

Figure 3.10 Graph of example sensor response to primary and interfering ion. The calculated extrapolated lines are shown by the dotted lines with the axis intercept at 1M ion concentration. Voltage values labeled for primary $\boldsymbol{E_I}$and interfering ion, $\boldsymbol{E_J}$are used with **Equation 3.1** to calculate the selectivity coefficient.

The extrapolated voltage response and the maximum voltage response of the interfering ion were used with **Equation 3.1** to give the maximum selectivity coefficient. If no Nernstian response to any of the interfering ions is observed the maximum activity level voltage was used to calculate the selectivity coefficient against the extrapolated primary ion value as recommended by Bakker et al (2000). **Equation 3.1** is used to find the selectivity coefficient, $K_{I,J}$ using the extrapolated or maximum activity values of primary, E_I and interfering ion, E_J. a_I is the activity of the primary ion that the potential was taken at this is normally 1M so that this term is equal to zero. z_I and z_J is the charge of the primary and interfering ion respectively.

F is the Faraday constant, R the universal gas constant and T the absolute temperature.

$$\log K_{I,J} = \frac{(E_j - E_I)z_i F}{2.303RT} + \left(1 - \frac{z_I}{z_j}\right) lga_I \qquad \textbf{Equation 3.1}$$

This test was repeated on 7 sensors of each electrode type (Carbon membrane, PEDOT, PPYCL and PPYPTS) with the results detailed in **Section 4.5.4**.

3.3.7 Hysteresis

The hysteresis testing would measure if the sensor display any change in voltage potential when immersed in solutions of low pH (pH 4) to high pH (pH 10) then back down to low pH (pH 4) again. This experiment used the pH buffer solution documented in **Section 3.2.1**. The potential was measured against a double junction calomel electrode using the Solartron 1286 electrochemical interface using the potentiometric arrangement detailed in **Section 3.3.3**. The sensor was immersed in each solution and the voltage was recorded once voltage stability was achieved. The pH of the solutions started at pH4 up to pH 10 then from pH 10 down to pH 4. The sensors were washed in distilled water before being immersed in different solutions. This test was repeated on 7 sensors of each electrode type (Carbon membrane, PEDOT, PPYCL and PPYPTS) with the results detailed in **Section 4.5.5**.

3.3.8 Water layer

Formation of a liquid layer between the layers of the solid state sensor can cause additional potential determining reactions that can cause inaccurate voltage potential measurements (Fibbioli et al., 2000). To test for the formation of a water layer the sensors were immersed in a pH4 solution for 1 hour then immersed in pH10 for 1 hour then again in pH4 for 2 hours. The sensors were washed in distilled water before being immersed in different solutions. The solutions were the pH buffer solution detailed in **Section 3.2.1**. The potential was measured against a double junction calomel electrode using the Solartron 1286 electrochemical interface using the potentiometric arrangement detailed in **Section 3.3.3**. If a liquid layer forms the

sensor will experience voltage drift after a change in solution due to the constituents of the liquid layer changing. The results of this are described in **Section 4.5.6** each test was conducted on 3 sensors of each type (Carbon membrane, PEDOT, PPYCL and PPYPTS).

3.3.9 Sensor heat stress

The sensors were subjected to heat stress to assess if this affected performance. The fully isolated sensors described in **Section 3.1.5** were used for this experiment. The potential was measured against a double junction calomel electrode using the Solartron 1286 electrochemical interface using the potentiometric arrangement detailed in **Section 3.3.3**. The carbon membrane sensors were placed on metal oven tray and baked in an 80^{o}C oven (WTB Binder). The sensors are retested after 15, 30 150 hours to determine if there is any change in the pH-dependent, voltage response slope performance characteristics. The results are detailed in **Section 4.6.2** each test was repeated 5 times on different sensors.

3.3.10 Sensor range

To assess the range of linear response the carbon membrane sensor (described in **Section 3.1.1 and 3.1.3**) was tested to the extremities of its lower range. Only the lower range was tested as the pH of some wound dressings was lower than the initial designed range of pH 4 to pH 10. The potential was measured against a double junction calomel electrode using the Solartron 1286 electrochemical interface using the potentiometric arrangement detailed in **Section 3.3.3**. The pH solutions were made as in **Section 3.2.1** but samples were taken from pH 2 to pH 7, six pH levels were tested in total. The sensor was immersed in the pH 7 solution first then transferred down the pH solutions to the pH 2 solution. The voltage was recorded at each level once the sensors reached a stable potential. The sensors were washed with deionised water before being immersed in each new solution. The results for this experiment can be found in **Section 4.6.3**. Each test was performed on 4 different sensors.

3.3.11 Sensor long term drift

Long term voltage stability of the carbon membrane sensors was tested to assess how stable the sensor voltage response is over a 12 hour time period. The carbon membrane sensors (**Section 3.1.1 and 3.1.3**) were tested over a 12 hour period in a pH 7 buffer solution to find the long term voltage drift of the sensor in a pH solution. The buffer solution is described in **Section 3.2.1**. The fully isolated sensors described in **Section 3.1.3** were used. The solution was immersed in a 32^{o}C water bath (Grant GD120) to ensure constant temperature during test period. The potential was measured against a double junction calomel electrode using the Solartron 1286 electrochemical interface using the potentiometric arrangement detailed in **Section 3.3.3**. This test was repeated on 3 sensors with the results detailed in **Section 4.6.3**.

3.3.12 Electrochemical impedance spectroscopy

Electrochemical impedance spectroscopy (EIS) is used to determine the characteristics of the screen printed carbon electrode. This testing was conducted on the carbon membrane electrode to gain an understanding of the double layer capacitance of the electrode using equivalent circuit modelling this is further discussed in **Section 2.13**. The double layer capacitance of the carbon electrode is important as it is one of the important factors in ensuring sensor voltage stability during measurement in the carbon membrane sensor. The sensors with conducting polymer have a different mechanism of stability so were not tested using this method this is further detailed in **Section 2.10**. A Solartron 1286 electrochemical interface and a Solartron 1260 impedance/gain-phase analyzer (Solartron) were used to perform the tests. The test was conducted using a 3 electrode configuration (**Figure 3.3**) which consisted of the screen printed electrode, a platinum wire counter electrode and a double junction calomel reference electrode. The sweep was from 10kHz to 0.1Hz using a 100mV voltage. The tests were conducted in a 0.1M potassium chloride (KCl)(Sigma-Aldrich, P9333) solution made from 0.745g Potassium chloride made up to 100ml volume with deionised water (ELGA, Purelab Ultra). The data was recorded on a computer using the ZPLOT (Scribner Associates Inc.) software.

The EIS data was analysed using ZView software (Scribner Associates Inc.). Equivalent circuit modelling was performed on the screen printed carbon electrode to gain further information of the materials properties. The electrode response was modelled on the Randles equivalent circuit which is described in **Section 2.13**. The ZView software was used to model the response of the EIS experiment based on electrical components of the Randles equivalent circuit. From the modelled response the double layer capacitance, charge transfer resistance and solution resistance could be found. The best fit model was chosen as it had the lowest component errors and could be used to describe the response of the sensor. This test was repeated on 3 screen printed electrodes with the results detailed in **Section 4.6.1**.

3.4 Reference electrode characterisation

3.4.1 Reference electrode pH sensitivity

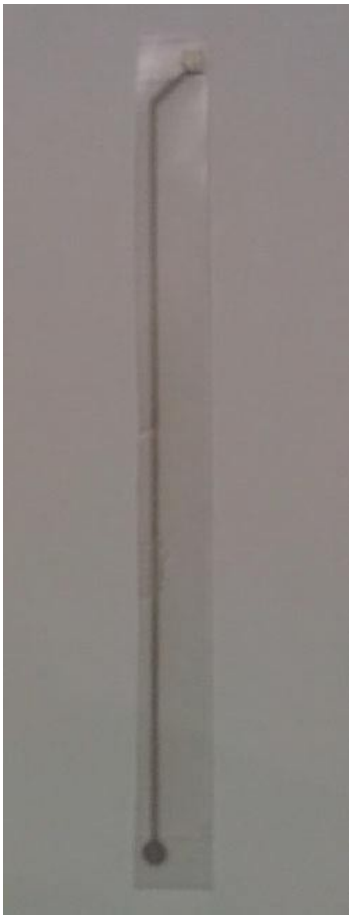

Figure 3.11 Screen printed Ag/AgCl of reference electrode.

The screen printed Ag/AgCl reference electrode (Ohmmedics) was assessed in pH solutions to assess if the voltage potential was stable across a range of pH levels. The operation of the Ag/AgCl reference electrode is described in **Section 2.11**. To test if the pH screen printed Ag/AgCl reference electrode (**Figure 3.11**) was stable and did not respond electrically to pH, the potential was measured from pH4 to pH10 in a chloride adjusted pH solution to mimic the physiological chloride concentration as detailed in **Section 3.2.3**. The reference electrode was tested against a glass calomel reference electrode using the Solartron 1286 electrochemical interface in the potentiometric arrangement detailed in **Section 3.3.3**. Both electrodes were washed in distilled water before each test. This test was repeated on 5 sensors with the results detailed in **Section 4.7.1**.

3.4.2 Reference chloride concentration

The theory of the screen printed Ag/AgCl reference electrode states that the chloride levels in a solution determine the potential of the electrode - this is detailed in **Section 2.11**. The screen printed Ag/AgCl reference electrode was tested in different chloride concentrations solutions to observe the potential response. Separate solutions were made of sodium chloride (NaCl)(Sigma-Aldrich, S7653) and potassium chloride (KCl) (Sigma-Aldrich, P9333) with molar values of 10^{-4}M to 10^{-0}M of Cl^- ions. To produce 100ml samples of the two chloride solutions 5 different concentrations the following amounts were measured 7.45g Potassium chloride and 5.84g sodium chloride and placed in separate 200ml glass beakers. The beakers were then made up to 100ml with deionised water (ELGA, Purelab Ultra) this produced 10^{-0}M solutions of the chloride ion solutions. The lower concentration solutions were made by decanting 10ml in a new beaker and making it up to 100ml using deionised water. This procedure was repeated to produce the required concentrations. The potential of the screen printed Ag/AgCl reference electrode was measured against a glass calomel reference electrode using a Solartron 1286 electrochemical interface in the potentiometric arrangement detailed in **Section 3.3.3**. This test was repeated on 5 sensors with the results detailed in **section 4.7.2**.

3.4.3 Reference electrode long term voltage drift

The screen printed Ag/AgCl reference electrodes were tested over a 12 hour period in a pH 7 buffer solution to find the long term drift of the sensor in a pH solution. The chloride adjusted buffer solution is described in **Section 3.2.3**. The solution contained in a glass beaker, was immersed in a 32^{o}C water bath (Grant GD120) to ensure constant temperature during the test period. The potential was measured against a double junction calomel electrode using the Solartron 1286 electrochemical interface using the potentiometric arrangement detailed in **Section 3.3.3**. This test was repeated on 5 sensors with the results detailed in **Section 4.7.3**.

3.5 Measurement hardware design

The purpose of the hardware that was designed specifically for this study is to measure the voltage between the reference and sensor electrode then display the result on a Liquid Crystal Display (LCD) screen. From the voltage the pH can be calculated from a stored calibration curve and displayed. This section details the design of the hardware and software to achieve the design aims.

3.6 Hardware

The Hardware consists of a number of different modules to create a hand held measurement device for both voltage and pH. A simplified block diagram of the main components of the measurement hardware is shown in **Figure 3.12**.

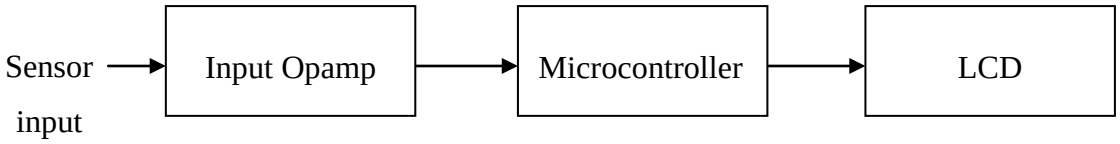

Figure 3.12 Simplified block diagram of sensor hardware.

3.6.1 Operational Amplifier

The operational amplifier is critical to the operation of the measurement hardware. The first stage of the operational amplifier function is to first amplify the signal by 2. The second amplifier stage is to provide an offset voltage so that the input into the Analogue to Digital Converter (ADC) is a positive voltage. The operational amplifier needs to have a large input impedance as the screen printed electrodes have a resistance of around 500kΩ. Due to the high resistance of the printed reference and sensor the input impedance must be many times larger than the electrode impedances so that ideally no current is drawn through the input of the operational amplifier.

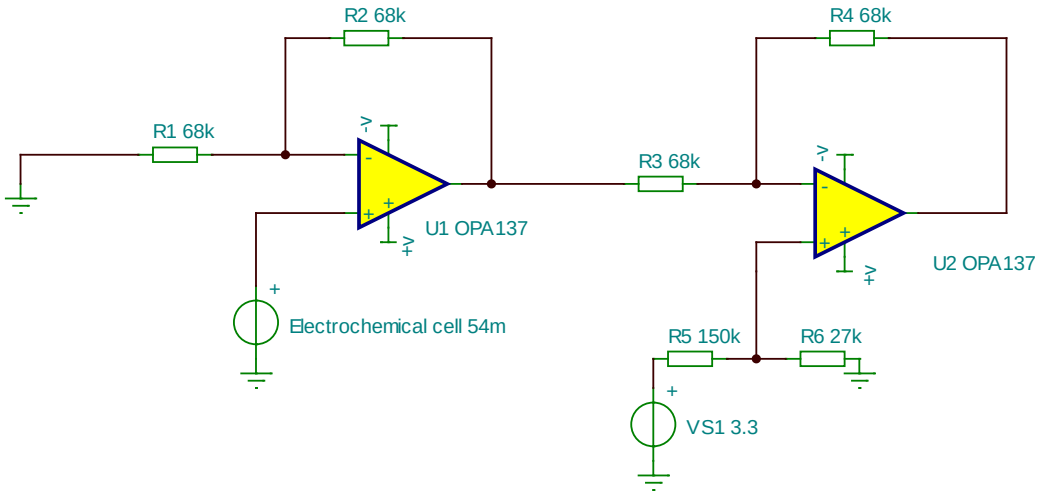

Figure 3.13 Schematic of input operational amplifier circuit showing input (First) and offset (Second) amplifier.

The operational amplifier chip used is the OPA137 (Farnell 1097425) the package has 2 operational amplifiers on the one packaging meaning that this can be used for both the input and offset amplifiers. The power input to the operational amplifiers is a dual supply as the inputs to the operational amplifier have the potential to be negative voltages. The operational amplifiers are powered by a ±2.5V supply from the voltage converter. **Figure 3.13** shows the input operational amplifier schematic diagram.

3.6.2 Microcontroller

The microcontroller chosen was the s08LL16 from Freescale Semiconductor. This was chosen as it is designed for battery operated operation and has a 12 bit analogue to digital converter. The microcontroller operates at a voltage of 1.8V to 3.6V. The microcontroller's function is to convert the output voltage from the second stage of the operational amplifier into a digital value. This is then processed by the microcontroller and the resultant voltage and pH values can be displayed on the LCD screen. The microcontroller program is detailed in **Section 3.7**.

3.6.3 Power supply

The device is powered off a standard 9 volt battery. The 9V source is regulated down to 5V using a voltage regulator L7805ABV (STMICROELECTRONICS). From this regulated supply the voltage supply to the microcontroller is further regulated down to 3.3V using a 3.3V zener diode. The LCD is powered directly from the 5V source. A ICL7660 CPAZ voltage converter (Farnell 1018170) is used to provide a dual ±2.5V supply to the operational amplifiers this enables the operational amplifiers to amplify both positive and negative voltage inputs.

3.6.4 Liquid Crystal Display (LCD) Module

The LCD module is a 2x8 character screen it is manufactured by Powertip (Farnell 1671493). It is powered off the 5V voltage rectifier rail. The LCD screen contrast is set by using a voltage divider circuit.

3.7 Software

The program's function is to control the inputs and outputs to the microcontroller so that the voltage and the pH can be displayed to the user on the LCD screen. The program is written in the software language C and the full program can be found in **Appendix A**.

Simplified Program flow diagram

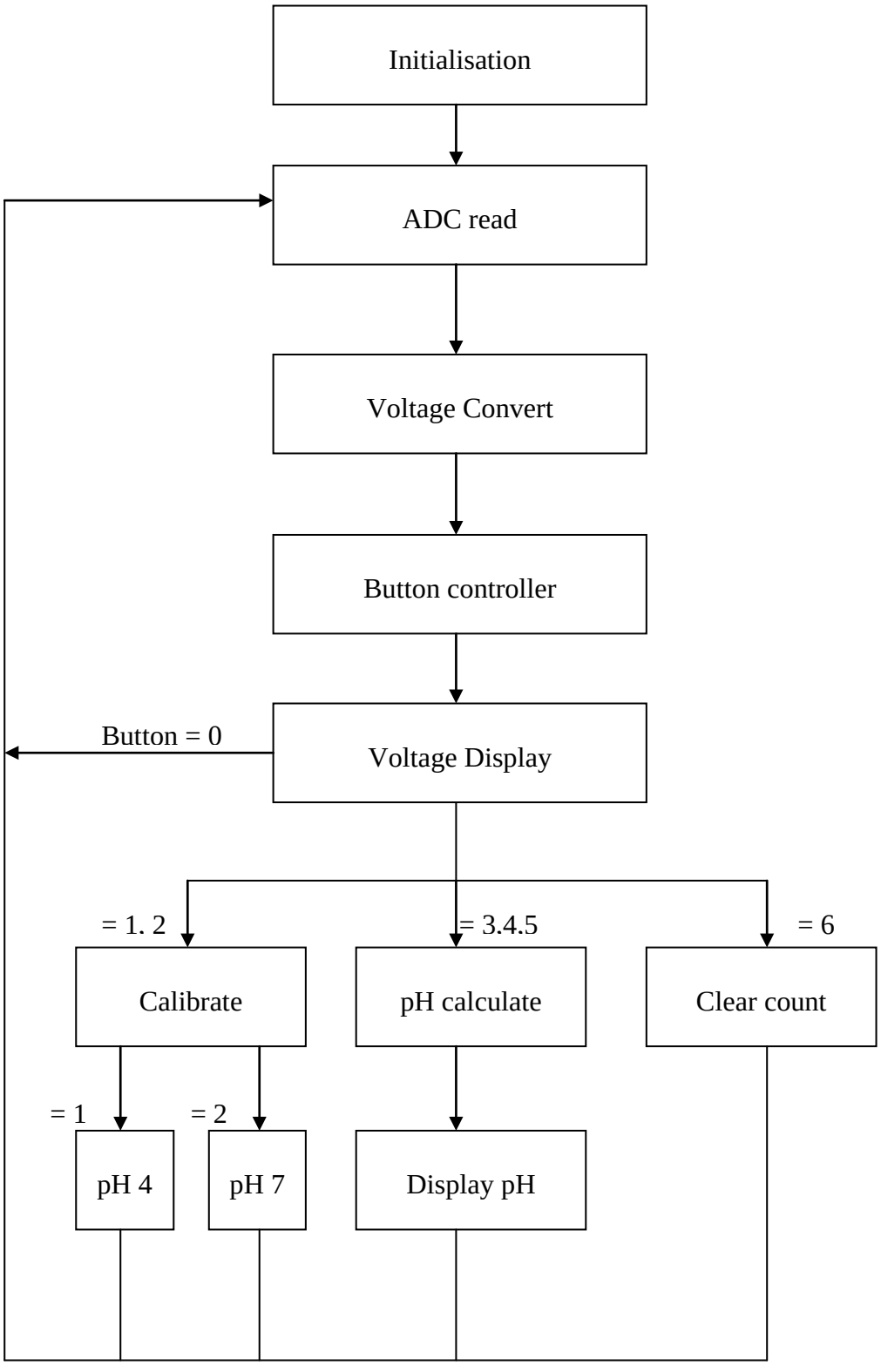

Figure 3.14 Simplified flow diagram of full program operation.

The simplified flow diagram is displayed in **Figure 3.14**. This details the main flow and modules of the microcontroller program each of the main modules are detailed below.

3.7.1 Initialisation

The initialisation of the device is only performed once on device start/restart. This configures the microcontroller peripheral such as the ADC and bus clock speeds. The initialisation enables interrupts and executes the LCD setup function.

3.7.2 Analogue to Digital Converter (ADC)

The ADC function of the program reads the output from the 12bit ADC which corresponds to the analogue input voltage from the input operational amplifiers. The program waits for the conversion to complete before continuing to read the values. The values are stored in 2 registers (high, low values) which are read and recorded. These upper and lower register values are then combined by shifting the bits so that the ADC value can be stored and processed as float.

3.7.3 Voltage convert

The voltage is calculated from **Equation 3.2** it uses the ADC value (ADCcountvalue) and multiplies this by the ADC reference voltage/number of ADC steps to give the digital voltage value. The ADC reference voltage (reference voltage) is set externally by a voltage diode so that it is a fixed value. The ADC in the S08LL16 is a 12bit ADC which means it has 4096 different voltage values and has a voltage resolution of the reference voltage/4096.

$$Voltage = ADCcountvalue * (\frac{reference\ voltage}{4096}) \qquad \textbf{Equation 3.2}$$

After conversion the voltage value is saved in a global variable as a float number. This value can then be converted to be sent to the LCD or used to calculate the pH value of the solution it is immersed in.

3.7.4 Data conversion

The s08LL16 microcontroller does not have enough memory to implement library conversion of floating point of integer numbers to a string. The data needs to be converted to string for it to be sent to the LCD as the string binary code corresponds to the ASCII characters needed for the LCD display module.

To convert the float numbers for voltage reading and pH each character has to be individually matched to its corresponding letter in string using a switch statement that can convert any number from 0-9 to a string character. This is achieved by sending one character at a time to be converted into a string. Once converted the individual characters are saved to a string array which can then be transmitted to the LDC module.

3.7.5 Display

The output for the display is controlled through the LCD.C string. This function controls the data being sent to the LCD module by sensing one ASCII character at a time with a time delay sequence as the microcontroller clock speed needs to be slowed down to ensure correct data transmission to the LCD module. The LCD function acts to initialise the LCD module so that it is ready to accept data being sent.

3.7.6 Button interrupt

The button press in controlled through an interrupt routine which when pressed the program jumps to the interrupt function where the number of button presses is incremented. The interrupt routine other function is to save the voltage values for the calibration of the device. This button counter acts as the control mechanism for the button controller in the main program. Once the program has performed the interrupt routine it returns to the point before the interrupt break.

3.7.7 Button controller

This is the main control switch of the program that controls what is on the display at the correct time. It is initiated through a switch statement that is controlled by a counter that records the number of button press events. The program continuously loops through this control statement where depending on the button counter value the program executes calculations and sends information to the LCD. The loop nature of this ensures that the voltage and pH being recorded can be continuously refreshed and displayed to the user.

3.7.8 Calibration

For the sensors to operate accurately each sensor and reference couple needs to be calibrated so that its response to pH change can be recorded and used to calculate and display the pH value. The program achieves calibration through the push button control which will prompt the user to immerse the sensor couple in calibration solutions - this is further discussed in **Section 3.9**. Once the user is satisfied that the sensor has stabilised in the calibration solution (voltage level stable) they press the control button which will cause an interrupt route. The interrupt routing saves the calibrated voltage values to a global variable so that they can be called upon when needed by the pH converting function.

3.7.9 pH convert

The pH of the Solution is calculated by using the equations shown below:

$$Voltage\ per\ pH\ level = \frac{(pH7voltage - pH4voltage)}{3} \qquad \textbf{Equation 3.3}$$

$$intercept = pH4voltage - (Voltage\ per\ pH\ level * 4) \qquad \textbf{Equation 3.4}$$

$$pH = \frac{(Current\ Voltage - Intercept)}{Slope}$$ **Equation 3.5**

Equations 3.3 and 3.4 are calculated after calibration to find the sensor calibration slope and intercept. **Equation 3.3** calculates the sensor calibration slope to pH change (Voltage per pH level) it is calculated by subtracting the sensor voltage response in a pH 7 solution (pH7voltage) from the sensor voltage response in a pH 4 solution (pH4voltage) and dividing the result by 3 which is the number of pH levels to gain voltage response per change in pH level. **Equation 3.4** calculates the axis intercept of the sensor calibration slope (intercept) this is calculated by multiplying the sensor voltage response (Voltage per pH level) that was calculated in equation 3.3 by 4 then subtracting this value from the sensor voltage response in a pH 4 solution (pH4voltage).

Equation 3.5 calculates the pH value of a solution (pH) by subtracting the current voltage reading from the sensor (CurrentVoltage) from the calibration intercept value (Intercept) found in **Equation 3.4**. This value is then divided by the voltage per pH level (slope) found in equation 3.3 to give a pH value.

3.8 Hardware testing

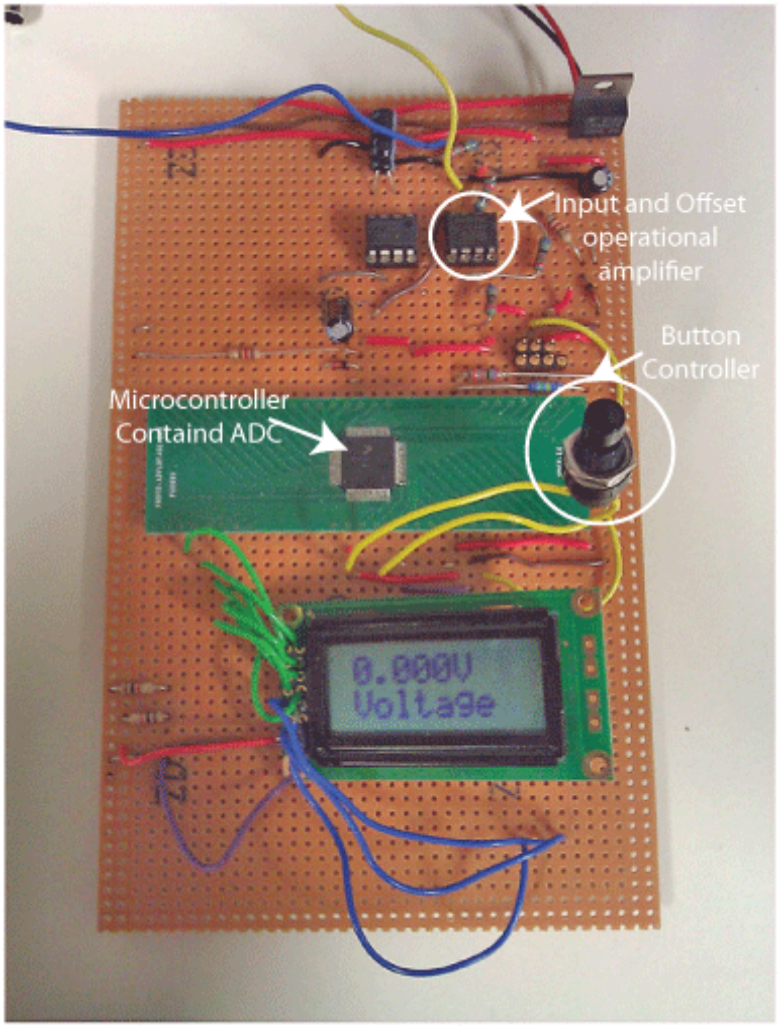

Figure 3.15 Measurement circuitry on prototype board the major components of the system are highlighted.

3.8.1 Operational amplifier testing

The hardware was tested by simulating the input from the sensors by using a voltage source (TTi EL3025). Both stages of the operational amplifier circuitry shown in **Figure 3.15** were tested. The voltage input from the voltage source was applied to the input operational amplifier stage and connected with voltage input to working electrode connection and ground to the reference electrode connection. The voltage was varied from 350mV and -350mV in 50mV steps. The voltage was measured and

recorded at the output of both the first and second stages using a digital voltmeter (TENMA 72-7720).

3.8.2 Analogue to Digital Converter (ADC) testing

To test the accuracy of the ADC and voltage converter algorithm, the voltage difference between the voltage displayed on the LCD screen and the voltage input to the analogue to digital converter was compared. The voltage input from the voltage source (TTi EL3025) was applied to the input operational amplifier stage and connected with voltage input to working electrode connection and ground to the reference electrode connection. The voltage was varied from 350mV and -350mV in 50mV steps. At each 50mV step the voltage input to the ADC and the voltage output displayed on the LCD screen were recorded and compared. The input voltage to the ADC was measured using a digital voltmeter (TENMA 72-7720).

3.9 Hardware method of operation

For voltage only measurement the device is ready to use as soon as voltage is supplied to the device. Once the sensor and reference electrodes are attached and immersed in the solution being measured the voltage output will be displayed on the screen as shown in stage one of **Figure 3.16**.

3.9.1 User Interface

The control of the hardware device is controlled through a single push button (Farnell 1634682). The software operations are controlled by the push button as shown in **Figure 3.16**.

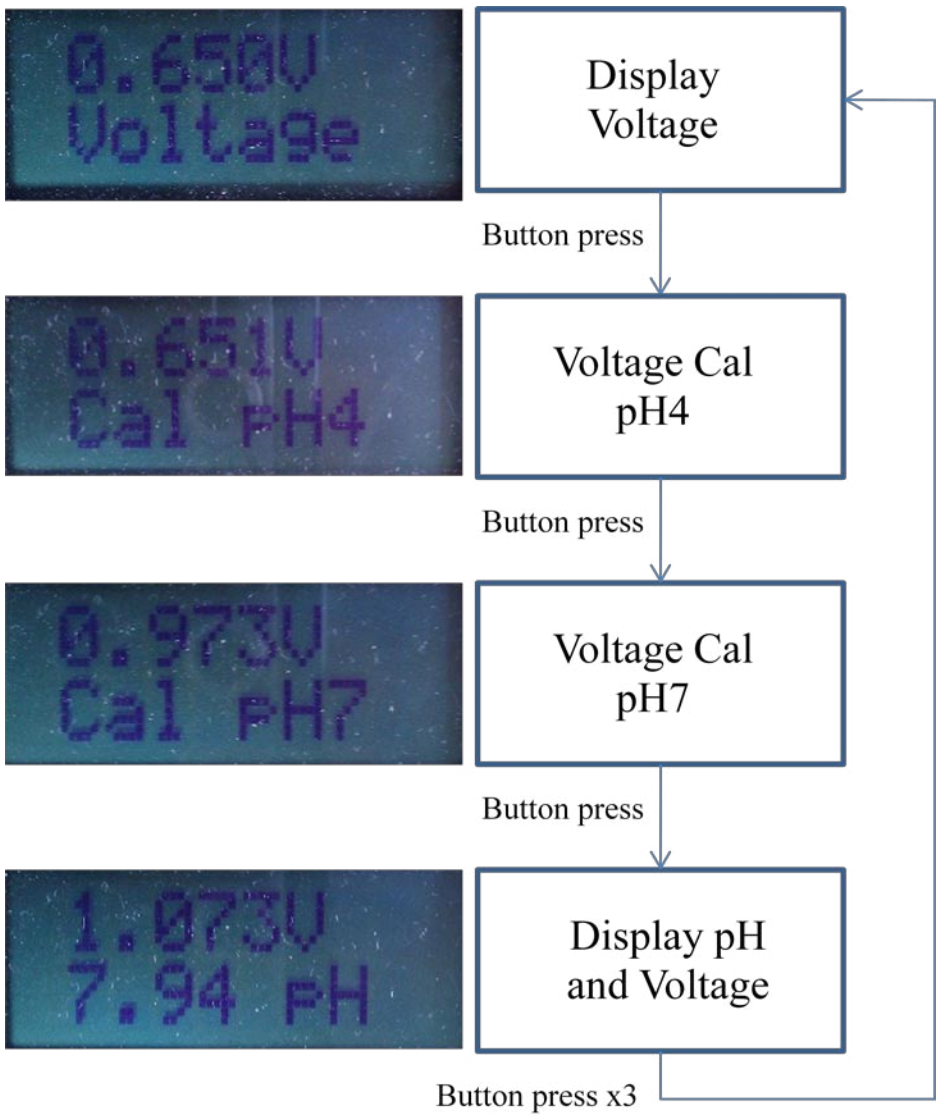

Figure 3.16 Showing display of program and user control of program.

Figure 3.16 shows the user interface which is controlled by the user pressing the single control button. The LCD screen displays the current stage of button cycle if the user makes a mistake when calibrating the device they can cycle through the other instructions to get back to the first stage of calibration. Once calibrated and the screen is displaying both the pH and voltage the button has to be pressed three times; this is so that the user does not accidently reset the sensor after one press of the button.

3.9.2 Sensor calibration designed measurement hardware

Figure 3.17 Disposable sensor couple pH sensor (left) and screen printed reference (right).

For pH measurement the device first needs to be calibrated. The pH calibration is detailed in **Figure 3.16**. The reference electrode was supplied by Ohmedics (Ohmmedics). The screen printed pH and reference electrodes are connected to the device using crocodile clips as shown in **Figure 3.17**. The sensor couple is calibrated in pH4 and pH7 buffer solutions which have been pH tested with a pH meter (Fisher brand Hydrus 300) and had their pH adjusted to ensure they are at pH 4 and pH7. The pH buffer solution used is the chloride adjusted pH solution detailed in **Section 3.2.3**. The sensor couple is first immersed in the pH 4then the pH 7 buffer solution and allowed to settle before pressing the calibration button. After each immersion the sensor is dipped in distilled water to avoid any contamination of samples. Once the sensor has been calibrated in the pH test solutions by following the flow on the user interface (**Section 3.9.1**) the sensor is ready for operation. When testing for pH the

sensor and reference electrode are immersed in the solution of interest the sensors are left to settle before recording the result. The electrodes are washed in distilled water before each immersion.

3.9.3 pH calculation from voltage measurements

The pH measurements calculated using the voltage potential recorded on the Solartron 1286 electrochemical interface have to be calculated manually from the voltage measurements. The potentiometric measurement arrangement used is detailed in **Section 3.3.3**. A two point calibration method is used which is similar to the method for the designed hardware. Chloride adjusted pH buffer solutions were made following the method detailed in **Section 3.2.3**. The sensor couple is calibrated in pH4 and pH7 buffer solutions which have been pH tested with a pH meter (Fisher brand Hydrus 300) before calibration. The voltage potential of the sensor couple is recorded in the pH 4 and pH 7 solutions. The electrodes are washed in distilled water before each immersion.

The pH values for the voltage measurements taken on the Solartron electrochemical interface were calculated in EXCEL (Microsoft) using the same formulae as detailed in **Section 3.7.9**. The formula calculates the sensor response voltage response slope and intercept from the recorded calibration voltages at pH 4 and pH 7. After the sensor response slope (**Equation 3.3**) and intercept (**Equation 3.4**) are found the pH of the other solutions can be found by recording the voltage response and using this data in **Equation 3.5**.

3.10 Combined pH testing

The hardware and screen printed sensor and reference electrode were tested by immersing the sensors in a different pH solutions and comparing the result The pH solutions used are the chloride adjusted buffer solution described in **Section 3.2.3**. The pH of these was adjusted further by adding 0.2M sodium hydroxide (NaOH) (Sigma-Aldrich, S5881) in deionised water (described in **Section 3.2.1**) to the buffer solutions so that pH values of 3.5, 4.5, 5.5, 6.5 and 7.5. The pH of these solutions was measured with the glass pH meter (Fisher Scientific). The electrodes and

hardware were first calibrated see **Section 3.9.2**. The test involved the calibrated sensors being immersed in the individual pH solutions and their voltage recorded once the sensor and reference couple had stabilised. After each test the sensors were recalibrated.

	pH Glass electrode	**Sensor V ref**	**Sensor V printed ref**	**Device**
Sensor	Glass pH	Carbon membrane	Carbon membrane	Carbon membrane
Reference	Ag/AgCl combined	Glass calomel reference	screen printed Ag/AgCl reference	screen printed Ag/AgCl reference
Measurement hardware	Mettle Toledo (Fisher brand Hydrus 300)	Solartron 1286 electrochemical interface	Solartron 1286 electrochemical interface	Designed measurement hardware

Table 3.1 Components of different pH testing configurations.

The technique used was the same for the three configurations tested which were printed sensor versus calomel reference electrode, printed pH sensor versus printed Ag/AgCl reference electrode and the printed sensor and reference with the hardware. The printed sensors were first tested with the calomel reference electrode (Fisher Scientific) and the voltage was measured with the 1286 Solarton electrochemical interface using the potentiometric arrangement detailed in **Section 3.3.3**. The second configuration tested had the printed pH sensors and the screen printed Ag/AgCl reference electrode the voltage was measured with the 1286 Solarton electrochemical interface. The third configuration tested the full designed system with printed sensor and Ag/AgCl reference couple with the pH value of the electrode recorded from the LCD screen. The testing configurations are summarised in **Table 3.1**. For the voltage

measurements conducted on the Solarton 1286 electrochemical interface the pH was calculated using the calibration voltages and the voltages recorded using the method in **Section 3.9.3**. For each configuration the sensors 5 different sensors were tested the results can be found in **Section 4.9.2**.

3.11 Wound dressing testing

3.11.1 Wound dressing pH dressing tested

All dressings tested are used by the National Health Service in the UK. The products are primary dressings which means they are in contact with the wound and they are generally used with a secondary dressing which covers the wound area. The following section gives the information about the various dressings used in the wound dressing pH testing.

3.11.2 Promogran/Promogran Prisma

Figure 3.18 Promogran dressing.

Promogran (Systagenix) is made with 55% collagen and 45% oxidised regenerated cellulose shown in **Figure 3.18**. It is marketed as a protease (MMP) modifying dressing, MMP's were discussed in **Section 1.5.7**. The Promogran alters pH by combining acetic acid within the wound dressing (Cullen et al., 2002). Systagenix do not state that the dressing modifies pH and the marketing material concentrates on the enhanced healing effect of the oxidised regenerated cellulose when compared to 100% collagen dressings (Systagenix, 2011). A second Systagenix dressing was tested called Promogran Prisma which contains the same constituents but has 1% oxidised regenerated cellulose/Ag compound which acts to prevent infection through the integration of silver particles which act to prevent bacterial growth (Systagenix, 2011).

3.11.3 Activon Tulle/ Activon

Figure 3.19 Activon tulle honey dressing.

Activon Tulle (Advancis Medical) is a honey dressing used by the NHS. It uses pure Manuka honey, with no additives, integrated within a fabric gauze dressing shown in **Figure 3.19**. The honey stimulates the healing process, has antibacterial and

antimicrobial properties that reduce infection and that it helps maintain a moist wound environment (Gethin and Cowman, 2005). Honey is known to have a low pH and it contains many different acids depending on the honey types (Kwakman and Zaat, 2012) (Stefan and Bogdanov, 1997). The marketing material does not make any claim about honey modifying the pH of a wound although the pH of gluconic acid is given as the reason for reduced microbial growth (AdvancisMedical, 2011).

Figure 3.20 Activon medical grade honey.

The second honey dressing tested is the Activon honey contained in a tube as shown in **Figure 3.20**. This is a sterilised manuka honey ointment of the same type used in the Activon Tulle dressing but used for direct application to a wound to be covered by a secondary dressing.

3.11.4 Aquacel/Aquacel Ag

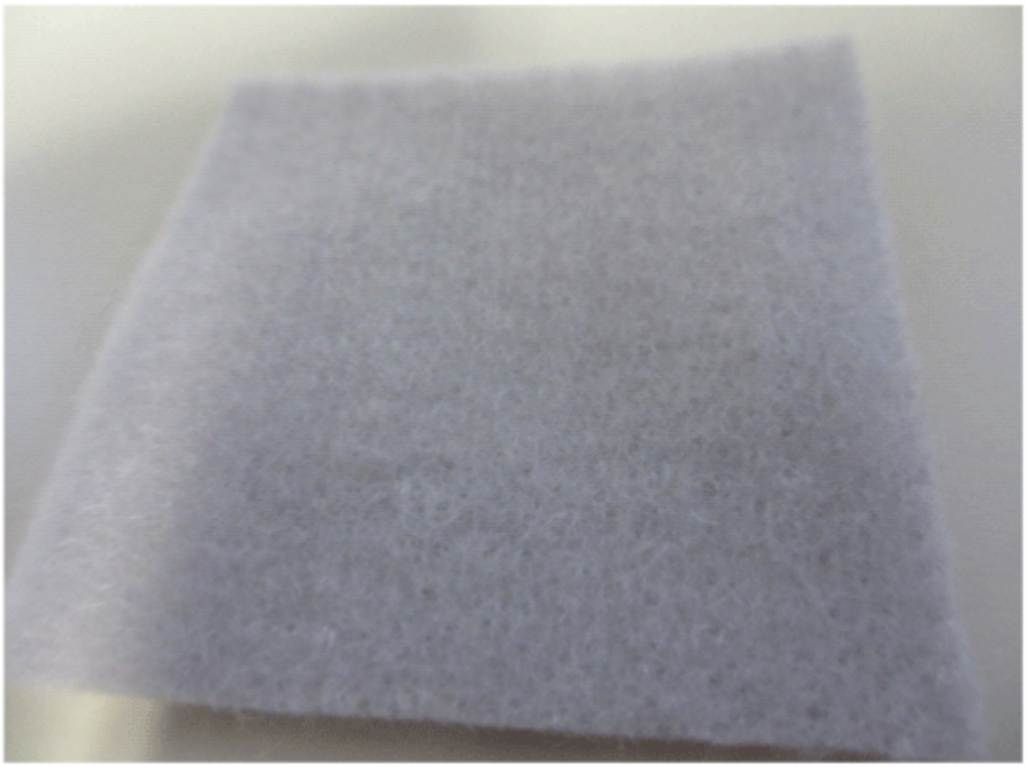

Figure 3.21 Aquacel wound dressing.

Aquacel (Convatec) is a hydrofiber based dressing made from sodium carboxymethylcellulose (shown in **Figure 3.21**) this turns to a gel like substance when it comes into contact with liquid. The gel helps to maintain a moist wound environment which results in an improved healing rate (Schultz et al., 2005). The dressing does not claim to alter pH (Convatec, 2011).

A second Convatec dressing was tested Aquacel Ag (Convatec) it has the same constituents as the Aquacel dressings but with silver ions added to provide some antibacterial protection when in contact with wound exudate (Convatec, 2011).

3.11.5 Tegaderm Matrix

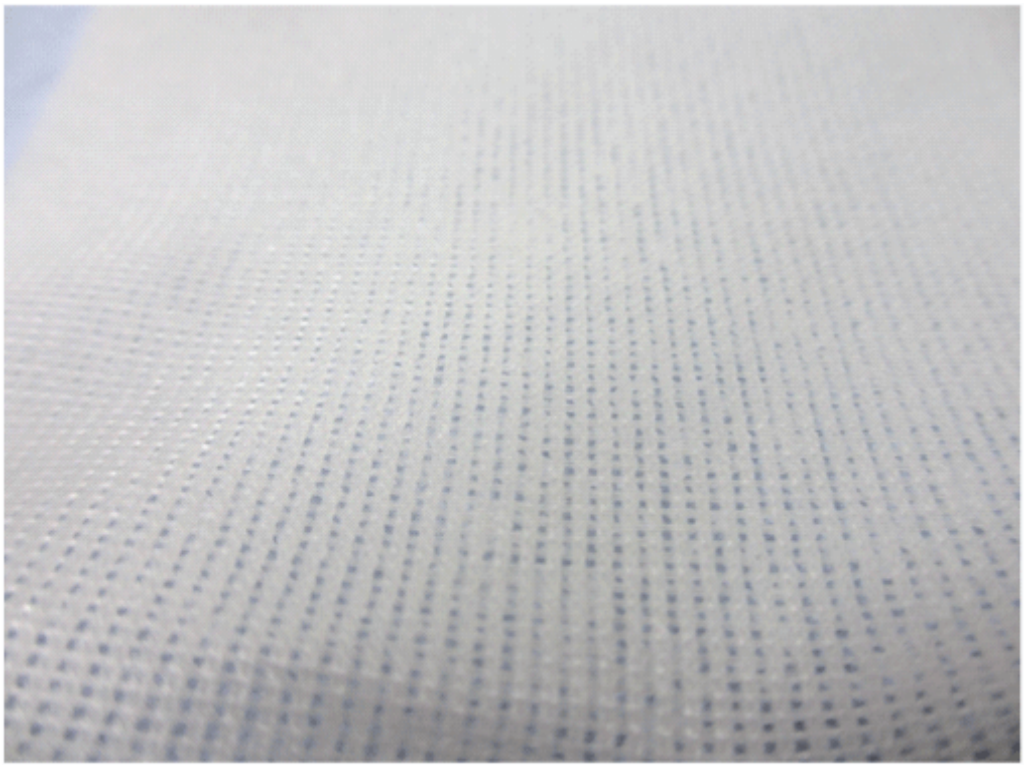

Figure 3.22 Tegaderm Matrix wound dressing.

Tegaderm Matrix (3M) is a polymer mesh that is coated in Poly Hydrated Ionogen (PHI) (shown in **Figure 3.22**) this contains metal ions (rubidium, calcium, zinc and potassium) and citric acid to inhibit the proteases within the wound and thus help the healing process (3M, 2011). The marketing material states that the citric acid lowers the wounds pH which in turn helps to provide the optimum healing environment - this is further detailed in **section 1.11.2** (3M, 2011).

3.11.6 Cadesorb

Figure 3.23 Cadesorb wound ointment.

The Cadesorb (Smith & Nephew) dressing specifically says that it controls the pH of a wound hence lowering the protease (MMP) activity (shown in **Figure 3.23)**. Its is an ointment which is directly applied onto the wound area with a secondary dressing applied to cover the wound. It is made of a starch based ointment that controls the pH of a wound although Smith & Nephew do not disclose the acid used for reducing pH but state it has a pKa value of 4.75 (Smith&Nephew, 2011). The ointment is stated by Smith & Nephew that it will reduce the acidity within the wound to around pH 5 (Smith&Nephew, 2011).

3.12 Wound dressing pH

The pH of the dressings in the previous section was tested to determine their pH level. The wound dressings were hydrated in 20ml of Solution A. Solution A is an aqueous salt solution that mimics the physiological concentrations of salts in human serum (the detailed method for Solution A is given in **Section 3.2.2)**. For all pH testing the dressings were cut into 5cmx5cm squares. For the pH testing of the ointments 2g was weighed out and mixed into 20ml of solution A. The dressings were hydrated as shown in **Figure 3.24** and mixed then left for 20 minutes to ensure mixing of dressing constituents with measurement solution. The pH of the wound dressing solution was then tested with a glass pH electrode (Fisher Scientific) and meter (Fisher brand Hydrus 300) the pH electrode was placed in the solution containing the wound dressing (**Figure 3.24**). Each dressing type was tested 3 times with new dressings and solutions. The results can be found in **Section 5.2.1**.

Figure 3.24 Wound dressing hydrated in 20ml of Solution A.

3.12.1 Dressing pH testing with carbon membrane pH electrode

This test was conducted to ensure that the carbon membrane pH electrode and reference combinations could effectively measure the pH of the wound dressings. Four different measurement configurations were used as described previously in **Table 3.1**. The experimental configurations are a glass pH electrode and three configurations using the screen printed pH sensors. The three screen printed pH

sensor arrangements are printed sensor versus calomel reference electrode, printed pH sensor versus printed Ag/AgCl reference electrode and the printed sensor and reference with the hardware. The arrangement of the printed pH sensor versus printed Ag/AgCl reference electrode in the measurement solution is shown in **Figure 3.25**.

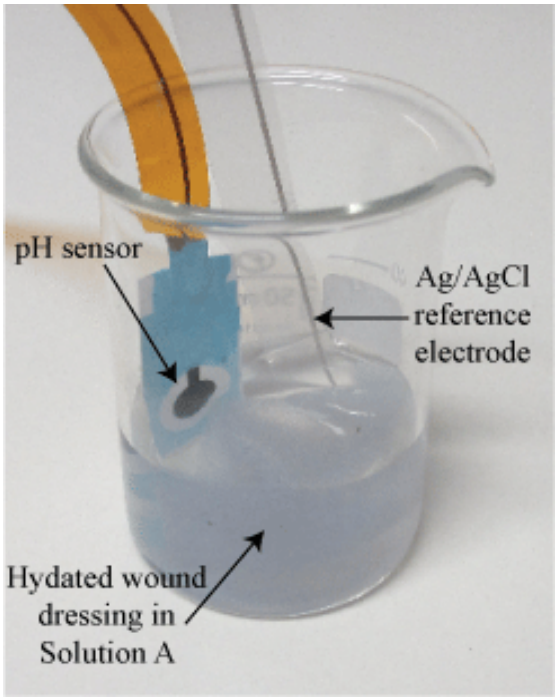

Figure 3.25 Disposable pH sensor and Ag/AgCl electrodes in solution of Solution A and wound dressing.

The dressing types tested were Aquacel (Convatec), Aquacel Ag (Convatec), Activon Tulle (Advancis medical), Activon Tube (Advancis medical) and Tegaderm (3M). The Promogran (Systagenix) and Cadesorb (Smith & Nephew) were not tested due to their pH being outwith the sensor range. The samples were prepared using the same method as given in **Section 3.12**. The printed sensors were first tested with the calomel reference electrode (Fisher scientific) and the voltage was measured with the 1286 Solarton electrochemical interface using the potentiometric arrangement detailed in **Section 3.3.3**. The second configuration tested had the printed pH sensors and the screen printed Ag/AgCl reference electrode; the voltage was measured with the 1286 Solarton electrochemical interface using the potentiometric arrangement detailed in **Section 3.3.3**. The third configuration tested the full designed system with

printed sensor and Ag/AgCl reference couple with the pH value of the electrode recorded from the LCD screen as described in **Section 3.9.2**. For the voltage measurements conducted on the Solarton 1286 electrochemical interface the pH was calculated using the calibration voltages and the voltages recorded using the method in **Section 3.9.3**. Each dressing type was tested 3 times with new sensors, dressings and solutions the results can be found in **Section 5.3.1**.

3.12.2 Horse serum testing

The purpose of this test was to assess the performance of the pH sensor when immersed in horse serum or a diluted horse serum mixture to observe if a correct pH reading could be recorded in a biological solution. Diluted horse serum was used to reduce the viscosity of the horse serum mixture. This is composed of 50% solution A described in **Section 3.2.2** and 50% horse serum as described in **Section 3.2.3**. Four different measurement configurations were used as described previously in **Table 3.1**. The configurations are a glass pH electrode and three arrangements using the screen printed pH sensors. The three screen printed pH sensor arrangements are printed sensor versus calomel reference electrode, printed pH sensor versus printed Ag/AgCl reference electrode and the printed sensor and reference with the hardware. During each test the voltage (or pH) was allowed to stabilise before values were recorded. The printed sensors were first tested with the calomel reference electrode (Fisher scientific) and the voltage was measured with the 1286 Solarton electrochemical interface using the potentiometric arrangement detailed in **Section 3.3.3**. The second configuration tested had the printed pH sensors and the screen printed Ag/AgCl reference electrode; the voltage was measured with the 1286 Solarton electrochemical interface using the potentiometric arrangement detailed in **Section 3.3.3**. The third configuration tested the full designed system with printed sensor and Ag/AgCl reference couple with the pH value of the electrode recorded from the LCD screen as described in **Section 3.9.2**. For the voltage measurements conducted on the Solarton 1286 electrochemical interface the pH was calculated using the calibration voltages and the voltages recorded using the method in **Section 3.9.3**. Each test was run 3 times with new sensors and solutions; the results can be found in **Section 5.3.2**.

3.13 Dressing simulation testing

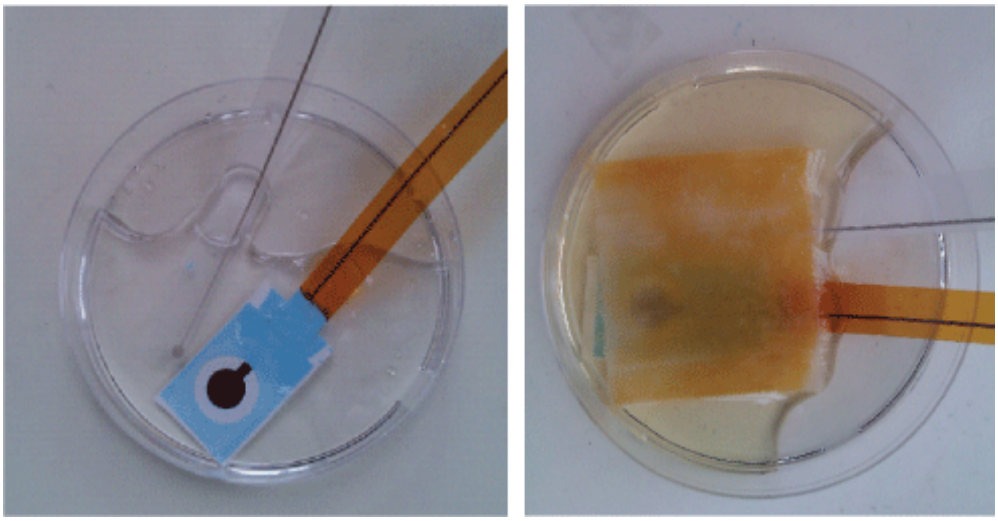

Figure 3.26 Wound bed model showing screen printed pH sensor and screen printed Ag/AgCl reference electrode immersed in Solution A in petri dish before application of wound dressing (Left). Wound bed model after application of an Activon honey dressing (Right).

The wound dressings are tested in a simulated wound bed model to replicate the application of wound dressings to demonstrate how they affect pH in real time after application. The investigation is designed to show the change in pH once a wound dressing has been applied to a simulated wound bed as shown in **Figure 3.26**. The testing uses four different dressing types that were shown to have an influence on pH. The dressings tested for both types of solution are the Activon Tulle (Advancis medical), Aquacel (Convatec), Tegaderm Matrix (3M) and Promogran(Systagenics) more information on the dressing types can be found in **Section 3.11.1**. The dressings were cut into 5cmx5cm squares before application. Two different solutions were used for the experiment: Solution A and a diluted horse serum mixture that will have acid buffering qualities as discussed in **Section 2.3.3**. The Solution A formulation is discussed in **Section 3.2.2**, it does not contain any acid or buffering qualities so it will enable the pH of the dressings to be recorded with no buffer resistance. Diluted horse serum was used to reduce the viscosity of the horse serum mixture this is composed of 50% solution A described in **Section 3.2.2** and 50% horse serum as described in **Section 3.2.3**.

The sensors used are the isolated carbon membrane sensor as detailed in **Section 3.1.5**. The reference electrode used was the screen printed Ag/AgCl electrode supplied by Ohmedics. The voltage was recorded on a Solartron 1286 electrochemical interface using the potentiometric arrangement detailed in **Section 3.3.3**.

The printed carbon membrane pH sensor and the screen printed Ag/AgCl reference electrode are used to measure the voltage response from which the pH is calculated. The sensors were given a two point calibration in chloride adjusted pH 4 and pH 7 solutions as described in **Section 3.9.2**. The voltage was recorded on a Solartron 1286 electrochemical interface. The potentiometric method can be found in **Section 3.3.3** and the formula for pH conversion in **Section 3.7.9**. Before operation the electrode couple was calibrated using the two point calibration method detailed in **section 3.9.3**. The sensor and reference couple were then placed beside each other in a standard petri dish (as shown **Figure 3.26)**. A pipette was used to deposit 10ml of the test solution (Solution A or horse serum mixture) over the sensor and reference couple as shown in **Figure 3.26**. The voltage was recorded on the Solartron 1286 electrochemical interface for 120 seconds before application of the dressing. The 5cmx5cm dressing square was placed onto the sensors and liquid solution and was left until the voltage had stabilised. The pH was calculated using the method in **Section 3.9.3**. All dressings were tested 3 times with new dressings and sensors for solution A pH response and 3 times for horse serum mixture pH response. The results can be found in **Section 5.4**.

Chapter 4 – Results sensor development

4.1 Sensor development

This section details the results of the experiments that were described in C**hapter 3**. The results have been split into two chapters detailing the different experimental stages. Chapter 4 describes the important experimental results from preliminary testing of ion-selective membrane deposition, conducting polymer formation on screen printed electrodes through to the full pH sensor development and hardware testing. Chapter 5 details the results from tests of the full combined sensor and electronics system embedded within a wound bed model and includes real time pH monitoring of wound dressings with simulated wound fluid to mimic buffering effects.

The experiments in this chapter demonstrate the stages investigated to find the optimum sensor configuration for pH sensing. The first experiment reports details of an investigation into the optimum coating deposit of conducting polymers onto a screen printed carbon electrode. The second section investigated the most effective ion-selective membrane deposition method so as to achieve the most consistent pH sensor. The third section details the full characterisation of four different pH sensor types for comparison in sensitivity, stability and repeatability. The final section details the results of the testing of the hardware with the sensors, illustrating the combined performance when testing in solutions of different pH.

4.2 Conducting polymer experiments

The deposition of conducting polymers was investigated to assess if polypyrrole could be electrochemically deposited on the screen printed carbon electrodes. Conducting polymers are being investigated for use in a sensor due to their promising ion exchange attributes that can enable them to replace the liquid junction in traditional sensing electrodes. The redox mechanism of the conducting polymers is important to the operation of the conducting polymers as ion to electron transducers within a solid state sensor; this is discussed in detail in **Section 2.10**

4.2.1 Cyclic voltammetry deposition of conducting polymer

The screen printed carbon electrodes were coated in a polypyrrole conducting polymer doped with two different ions Cl^- and PTS^-. The printed carbon electrodes were coated using cyclic voltammetry from 0V to 3V in 100mV/s scan rate the full method is detailed in **Section 3.1.2**. The sensors were subjected to this voltage range to ensure that the full oxidation peak was included in the sweep. The images shown below in **Figures 4.2 to 4.7** show the deposits of the deposited polypyrrole on the surface of the screen printed carbon electrode. The images shown are screen printed carbon electrodes coated separately with 1, 3 and 5 cycles of the conducting polymer. The aim was to find a smooth and consistent coating of the conducting polymer so that it would be suitable for subsequent application of the ion-selective membrane.

4.2.2 Carbon SEM

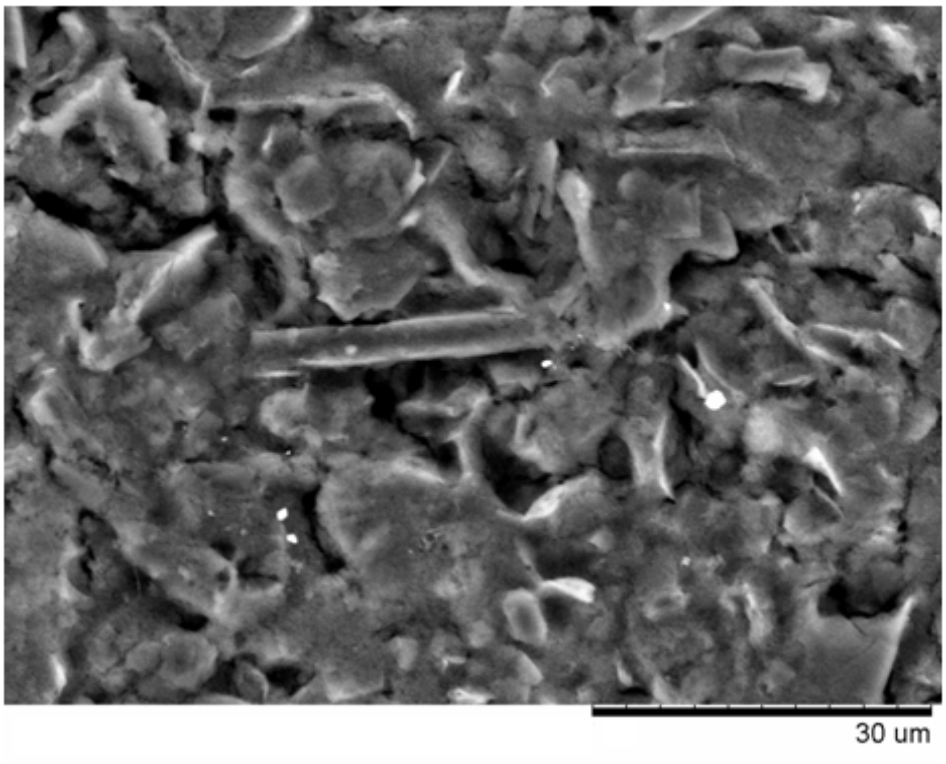

Figure 4.1 Screen printed carbon with no polypyrrole coating SEM image, 2000x magnification.

The SEM image of the screen printed carbon electrode in **Figure 4.1** shows the structure of the carbon electrode. The printing produces a rough surface which increases the surface area of the electrode. The individual structures of the carbon graphite can be seen in flake like structures.

4.2.3 PPYCl- SEM

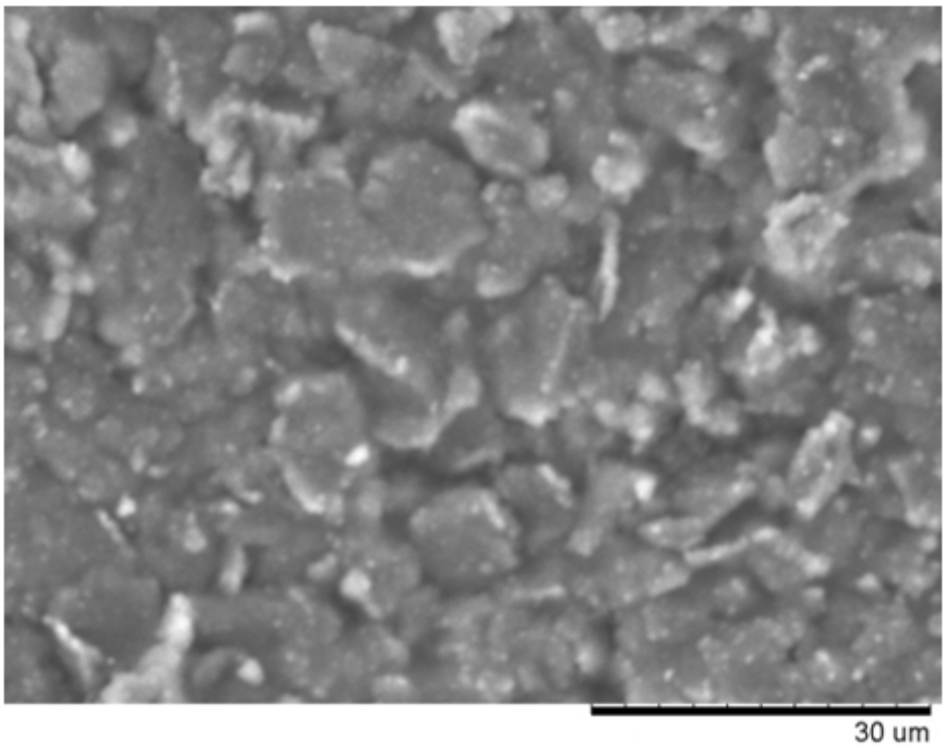

Figure 4.2 Screen printed carbon coated with 1 cycle PPYCl 0 to 3V with a 100mV/s scan rate, 2000x magnification.

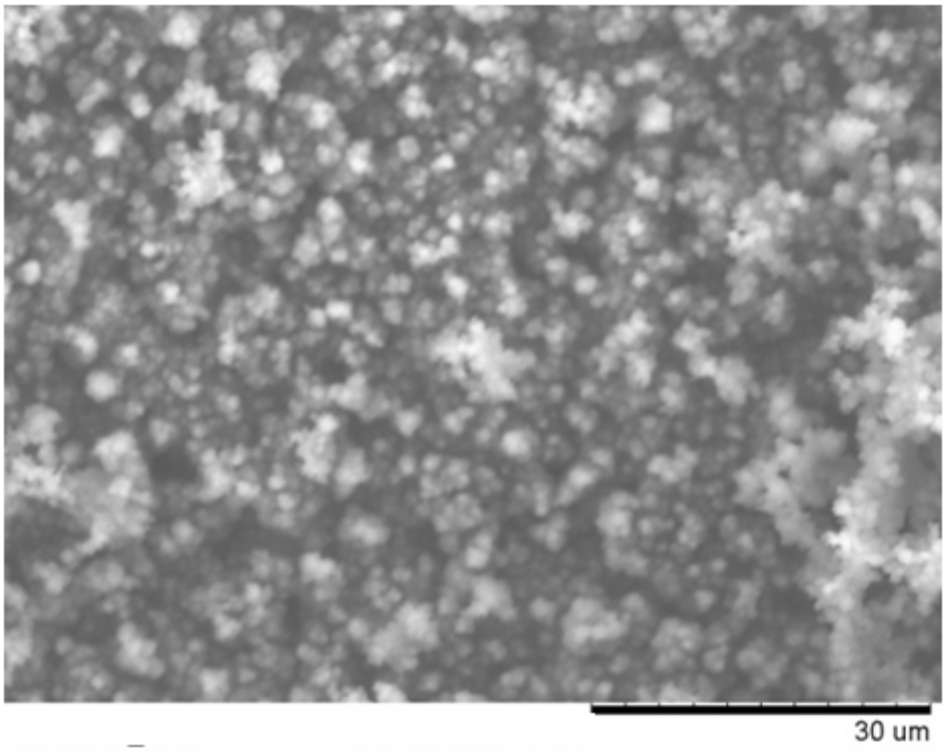

Figure 4.3 Screen printed carbon coated with 3 cycles PPYCl 0 to 3V with a 100mV/s scan rate, 2000x magnification.

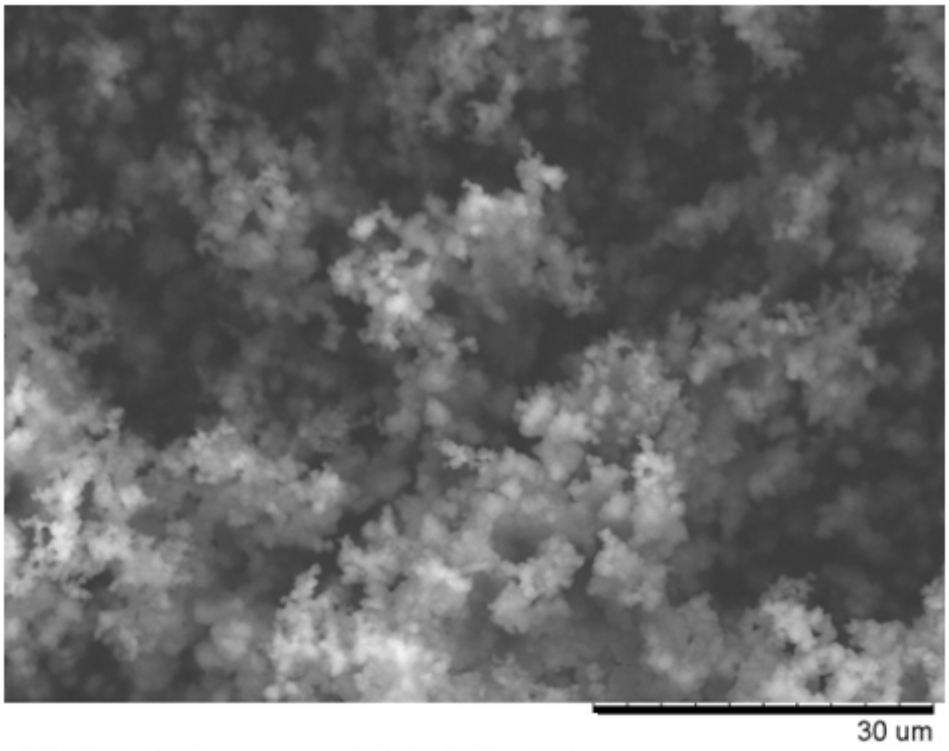

Figure 4.4 Screen printed carbon coated with 5 cycles PPYCl 0 to 3V with a 100mV/s scan rate, 2000x magnification.

The SEM images in **Figures 4.2-4.4** show the growth of the deposits of PPYCl on the screen printed electrode. It can be observed that as the number of cycles of deposition increases structural changes occur to the deposited polypyrrole. The amount of deposit in **Figure 4.2** shows that after 1 cycle the deposit covers the carbon in a very thin film as the structure of the carbon is still visible. **Figure 4.3** shows that after 3 cycles the structure of the printed carbon is no longer visible as the surface is covered in small spherical dome like structures. In **Figure 4.4** the structure of the PPYCl after 5 cycles is growing out from the surface of the carbon electrodes, this growth is not uniform as the deposits seem to grow in branch like structures out from the surface of the printed carbon electrode. These branch like structures will increase the surface area but will produce a much greater surface roughness that could result in uneven ion-selective membrane coverage.

4.2.4 PPYPTS SEM

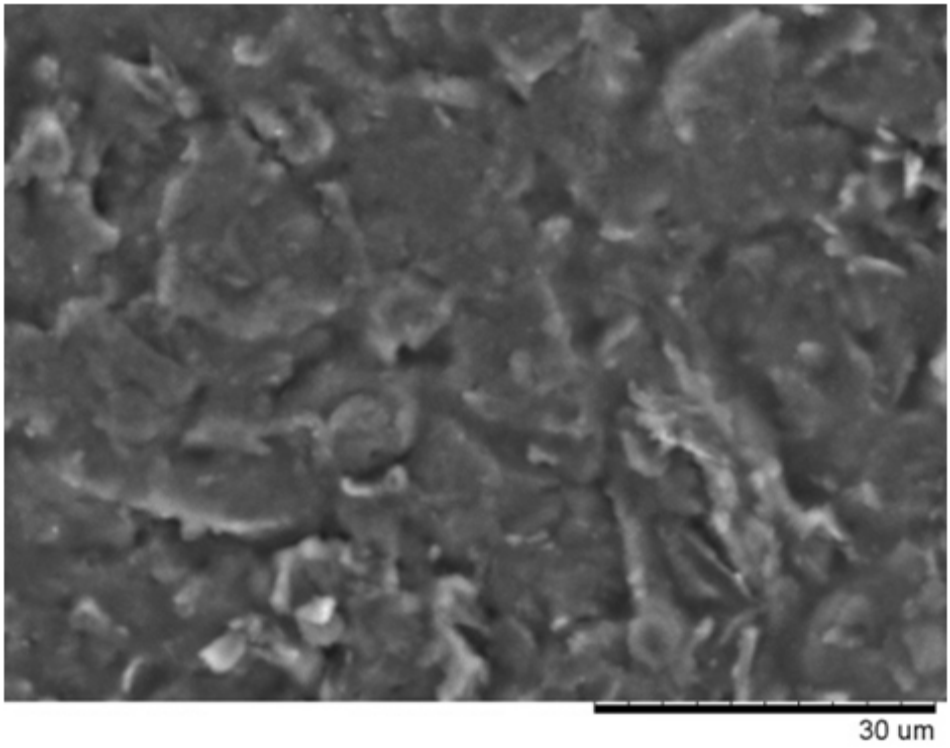

Figure 4.5 Screen printed carbon coated with 1 cycle PPYPTS 0 to 3V with a 100mV/s scan rate, 2000x magnification.

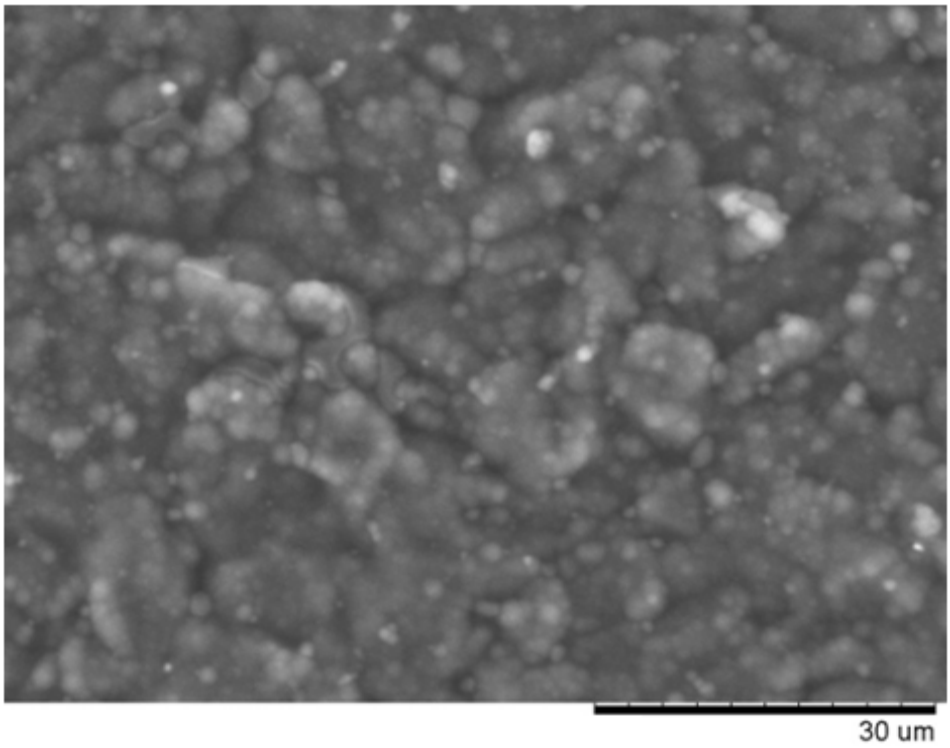

Figure 4.6 Screen printed carbon coated with 3 cycles PPYPTS 0 to 3V with a 100mV/s scan rate, 2000x magnification.

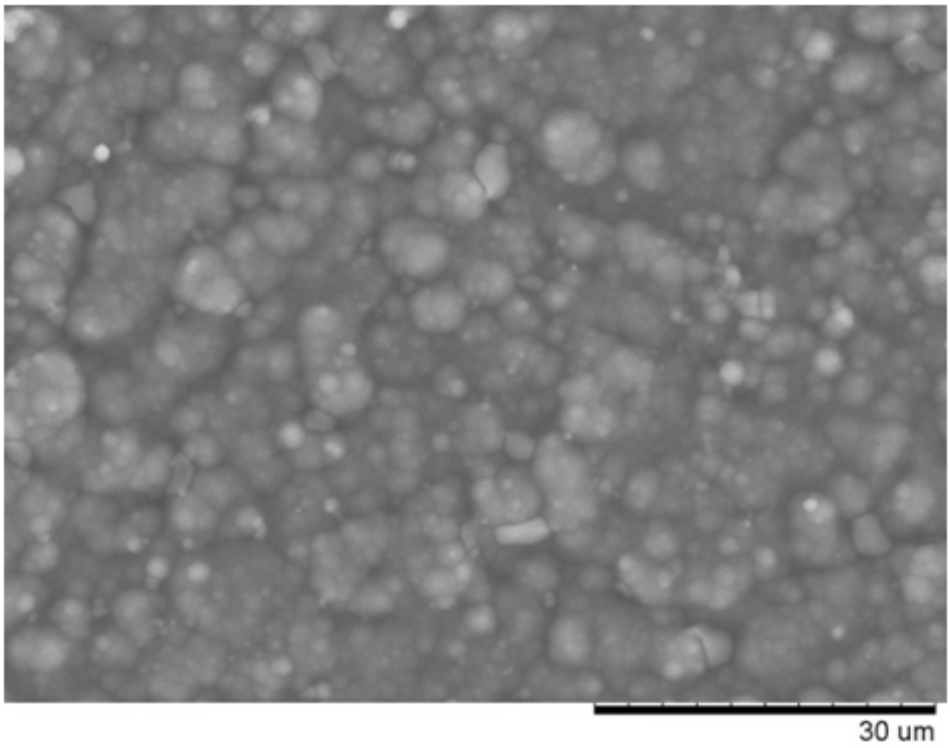

Figure 4.7 Screen printed carbon coated with 5 cycles PPYPTS 0 to 3V with a 100mv step/s 2000x magnification.

The SEM images from **Figures 4.5 to 4.7** show the different coatings of a printed carbon electrode with polypyrrole doped with PTS^- ions. **Figures 4.5 to 4.7** show the growth of the conducting polymer from 1, 3 and 5 cycles. **Figure 4.5** shows the growth after 1 cycle. A thin film of polymer is deposited as the structure of the screen printed carbon electrode is still visible although the contours are less visible than on the PPYCl after 1 cycle, **Figure 4.2**. The electrode with 3 cycles is shown in **Figure 4.6** it shows that deposits of the conducting polymer have started to form on the printed carbon surface; the carbon surface is now barely visible. **Figure 4.7** shows that the surface of the electrode after 5 cycles is completely covered by deposits of the conducting polymer as the carbon is no longer visible. The deposits have continued to form in circular formations and these have continued to grow in size.

4.3 Ion-selective membrane investigation

The pH membrane deposition method was investigated in this section to find the optimum coating conditions for the sensor. The drop coating method is compared to the machine spray technique from the Biodot deposition machine. The Biodot machine deposits solution by spraying a preset amount per centimetre travelled. To assess the Biodot deposition method the sensors were tested with different deposition amounts of membrane. The screen printed carbon electrodes have been coated with 100µl/cm, 75µl/cm, 50µl/cm, 25µl/cm and 12.5µl/cm of membrane deposits. The length of spray over the electrode was 1.5cm so this results in membrane deposits of 150µl, 112.5µl, 75µl, 37.5µl and 18.75µl on the sensors. The screen printed carbon substrate was used as the conducting contact as this will enable the assessment of the membrane deposition before any conducting polymer mid layer for ion to electron transduction is introduced into the sensor system. The full method for the coating techniques can be found in **Section 3.1.4**.

Preliminary testing showed the hand drop coating method provides membranes that are not consistent in thickness. The surface of the sensor after membrane deposition was imaged using a white light interferometer the full method for this can be found in **Section 3.3.2**.

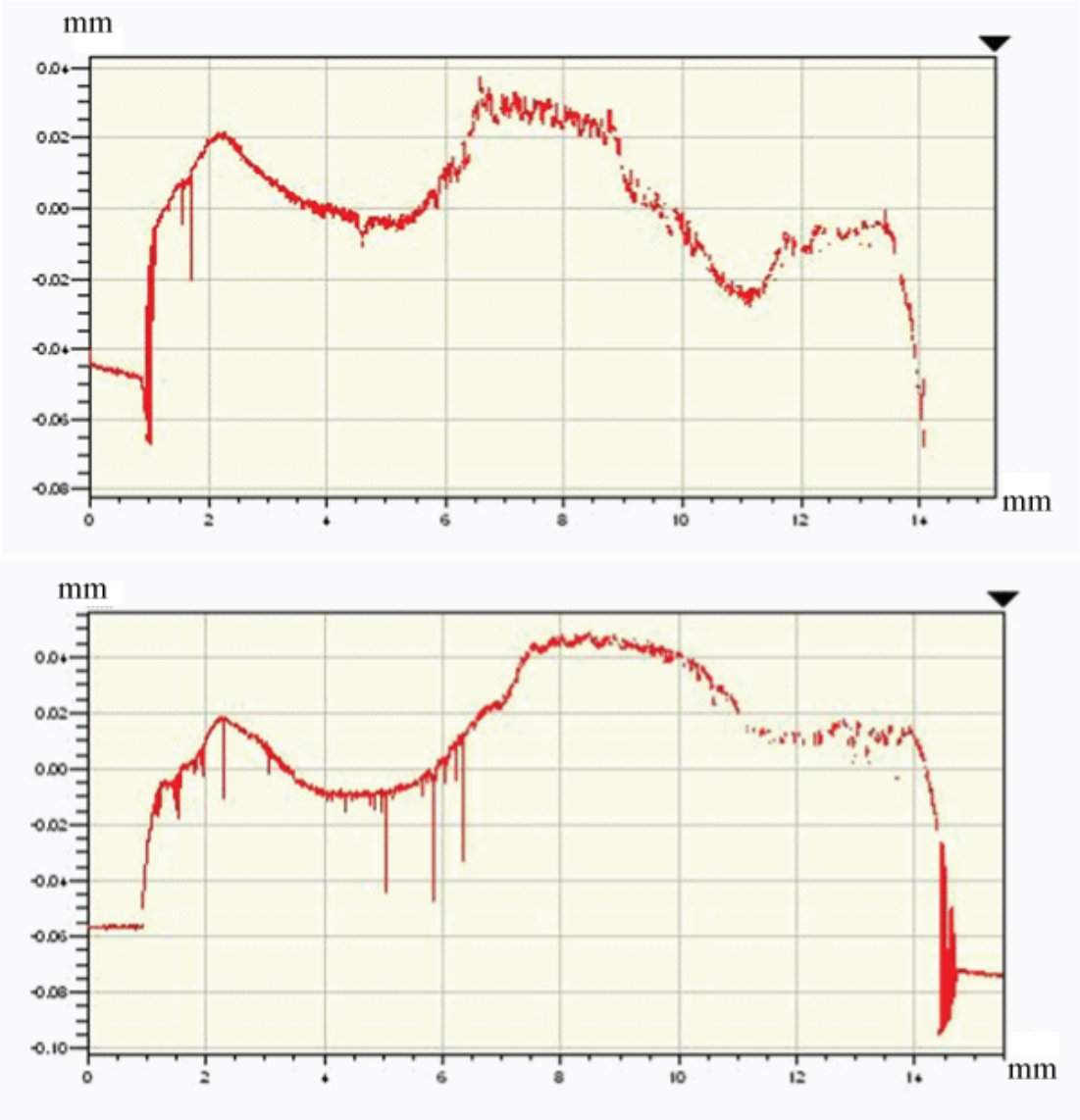

Figure 4.8 Cross sectional white light interferometer image of different hand deposited sensors showing variation in membrane thickness across sensor (Image 1 – top, Image 2 – bottom).

Figure 4.8 shows the scan across the surface of the electrode taken using a white light interferometer the area of the scan is detailed in **Section 3.3.2**. The sensors were coated with a thin layer of aluminum powder so that the light would have a reflective surface off the transparent membrane. **Figure 4.8** shows how the coatings are uneven and inconsistent when analysed. Image 1 and 2 both show peaks and troughs of the sensor coating that demonstrate differing membrane thicknesses.

The use of the Biodot spray deposition method should enable more consistent and repeatable membranes. Another advantage of using a spray deposition technique is that less membrane solution will be required which results in thinner membrane deposits. A thinner membrane should allow the sensor to settle faster due to shorter diffusion distances within the ion-selective membrane. This section of the results investigates the response of the hand drop coating method against various deposition amounts from the Biodot spray deposit machine to find the membrane deposit with the best membrane thickness, sensitivity and drift.

4.3.1 Membrane thickness

The ion-selective membrane deposits of the coatings applied by the Biodot spray dispensing machine and hand drop coating method were tested for thickness using a micrometer and a white light interferometer. The detailed method can be found in **Section 3.3.1**.

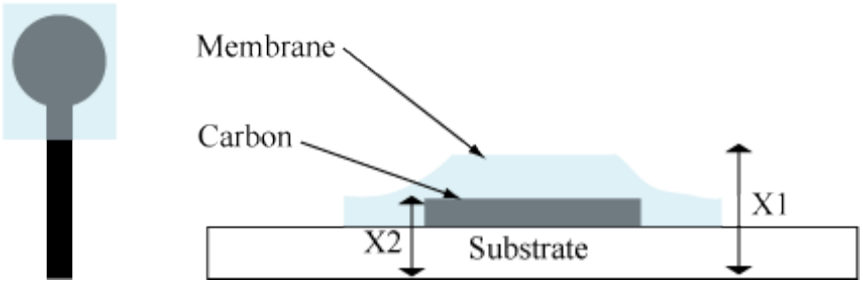

Figure 4.9 Top down view of sensor and membrane (left).Thickness of membrane deposits (right) the measurements are taken at the centre of the carbon circle electrode. X1 the full substrate, carbon and membrane measurement. X2 thickness of substrate and carbon layer.

Figure 4.9 shows the cross section of the sensor. The thickness measurement with a micrometer takes the thickness of the whole electrode as shown by X1 in **Figure 4.9**. The carbon ink layer is around 30 microns thick. The carbon and substrate has a thickness of 0.381±0.003mm as shown by X2 in **Figure 4.9**. The membrane thickness is calculated by subtracting the micrometer measurement X1 values from the substrate and carbon ink value X2.

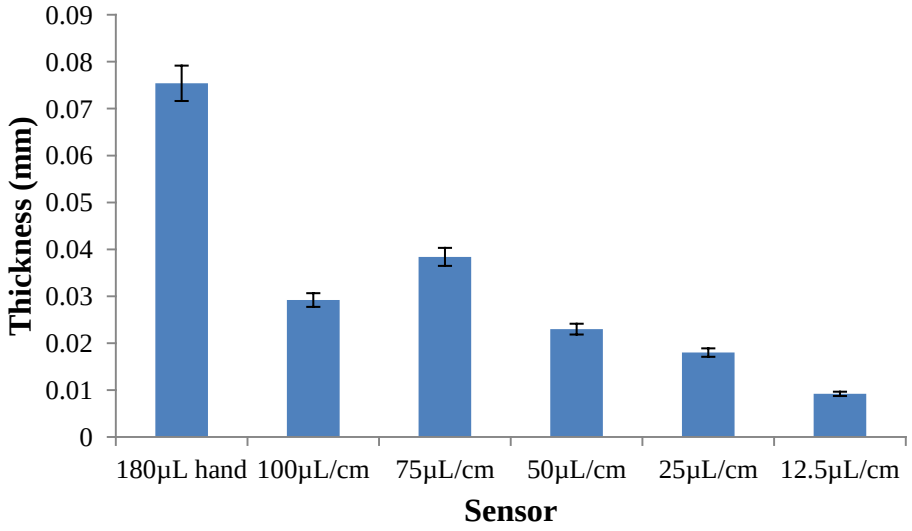

Figure 4.10 Membrane layer thicknesses measured with micrometer (n=5).

The membrane thicknesses are shown in **Figure 4.10**. The deposition technique shows that the drop coated deposit is by far the thickest membrane deposit with a mean value of 0.0754mm. The results show that all the Biodot machine deposited membranes are much thinner than the hand drop coated membrane. The largest volume 100µl/cm spray had a thickness of 0.0292mm which was thinner than the 75µl/cm deposit of 0.0384mm this could be due to the large spread of the membrane solution which covered a greater area of the substrate than any of the other deposits. From the 75 µl/cm spray towards lower values the membrane thickness reduced with the amount of membrane deposited. The thicknesses were 0.023mm for 50µl/cm membrane, 0.018mm for 25µl/cm membrane and for the 0.0092mm for 12.5ul/cm membrane.

The membranes were also tested using a white light interferometer but unfortunately this technique was difficult to get results as the membrane coatings were too thin on the 12.5µl/cm and 25µl/cm samples. The 100µl/cm coating depth values could not be found by this technique due to the spread of the membrane across the substrate which resulted in no suitable edge to get the correct membrane depth. The technique was able to get results for the hand, 75µl/cm and 50µl/cm membrane deposits. The hand

deposit was 0.0701±0.017mm the 75µl/cm 0.0362±0.003mm and the 50µl/cm 0.0297±0.001mm. These measurements are for the screen printed carbon and deposited membrane. The measurement is the averaged height across a line at the centre of the sensor circle. The results for the white light interferometer are similar to the values recorded from the micrometer. The results show that the machine deposited membranes are at least half as thick as the drop coated hand deposited membrane.

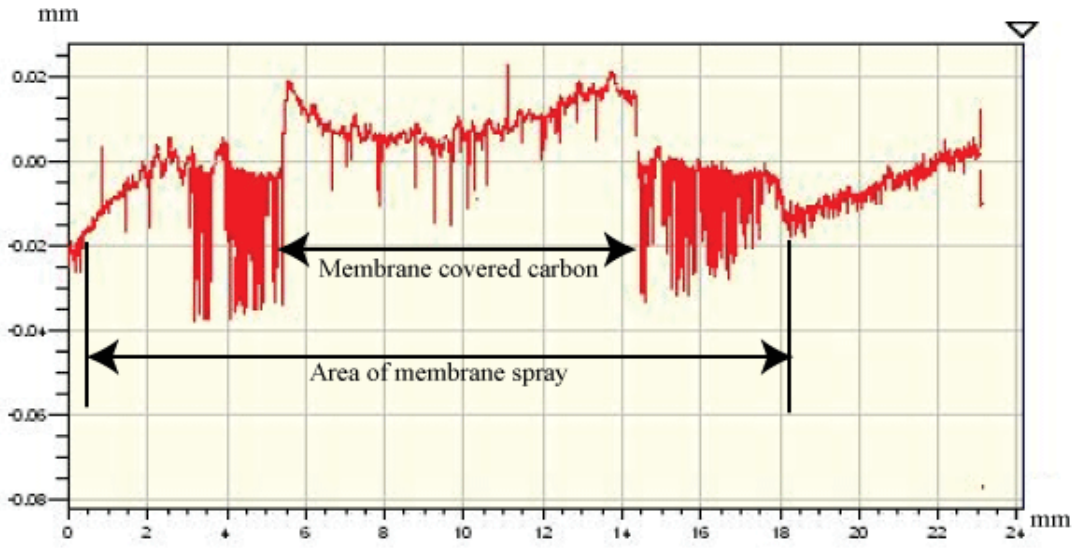

Figure 4.11 Biodot deposited membrane surface showing surface over sensor using 50µl/cm deposition image taken with white light interferometer. Due to the thin membrane interference is shown at the fringes of the figure.

Figure 4.11 shows the membrane surface of a 50µl/cm membrane spray deposited by the Biodot machine. When this is compared to the cross sectional topographies of the hand sensor in **Figures 4.8** it demonstrates that the spray deposition method produces smoother membranes.

4.3.2 Sensor voltage response

Sensor voltage response to pH of the different coated electrodes was assessed by immersing the sensors in universal buffer solution of varying pH levels from pH4 to

pH10 and recording the result verses a glass calomel reference electrode. The full method for the experiment can be found in **Section 3.3.4**.

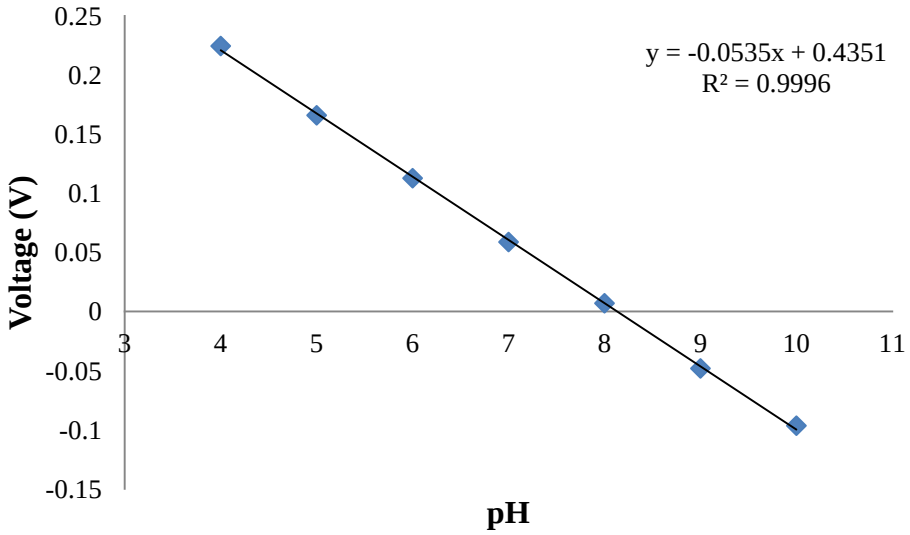

Figure 4.12 Example of sensor response to pH the sensor shown is a Biodot 50µl/cm coated screen printed carbon electrode (n=1).

Figure 4.12 shows the response of the 50µl/cm coated sensor. Shown is the linear response to the pH solutions in the range 4 to 10. The best fit line drawn on the graph gives a high R^2 value of 0.9996. This indicates a good linear response across the pH range for the 50µl/cm sensor. The response of the other sensors in **Table 4.1** give similar correlation values near R^2 =1. This indicates all sensors tested have a near linear response to pH change.

Sensor	pH decade response (mV) + standard deviation (n=5)
180µL drop coated hand deposit	53.87±0.142
100µl/cm Biodot	53.49±0.122
75µl/cm Biodot	54.00±0.242
50µl/cm Biodot	53.50±0.120
25µl/cm Biodot	52.79±0.523
12.5µl/cm Biodot	51.37±0.836

Table 4.1 Voltage response of pH sensor membrane depositions voltage per decade change in H^+ concentration (n=5).

Table 4.1 shows that the 75µl/cm sensor coating had the largest slope with a voltage response of 54mV/decade H^+ ion concentration in pH concentration. The hand deposit has a 53.87mV/decade H^+ ion concentration and the 50µl/cm with a 53.5mV/decade H^+ ion concentration. This data shows that all sensors are able to sense the change in pH level with the membrane thickness or deposition technique only having a small effect on the voltage response.

4.3.3 Sensor voltage settling

When a new sensor is immersed in a solution an initial drift will occur until the membrane reaches equilibrium with the solution. Once equilibrium has been reached the sensor is known as being conditioned and subsequent immersions in new solutions will result in fast equilibrium times. The membrane thickness should determine the speed with which the electrode reaches equilibrium due to less distance for the primary ion to diffuse across the membrane. This experiment would determine which of the Biodot coated sensors would settle the fastest when placed into a pH 4 solution by measuring the drift for 1800 seconds after the sensor was immersed. The full method for this test can be found in **Section 3.3.5**.

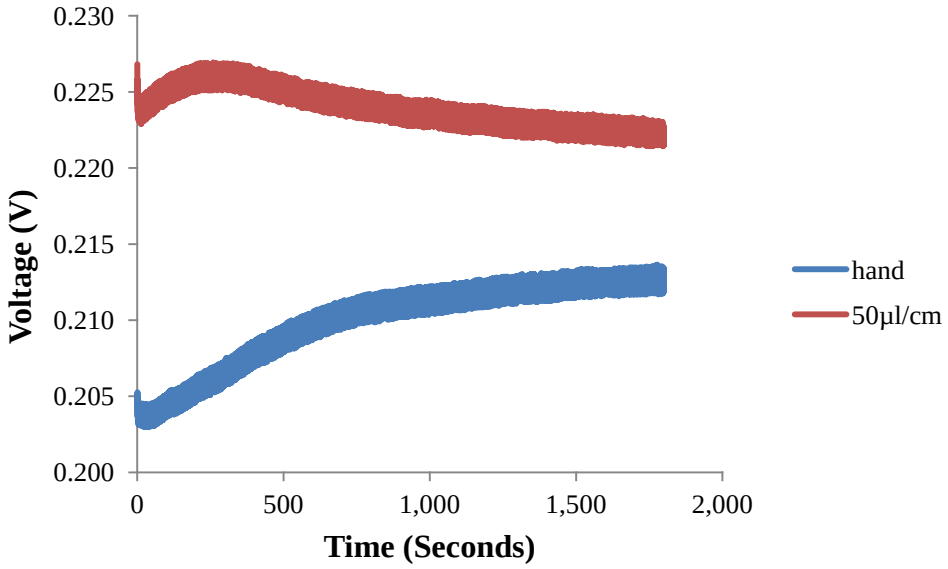

Figure 4.13 Showing potentiometric voltage measurement of drop coated and 50µl/cm Biodot membrane coated sensors after initial immersion in pH 4 solution for 1800 seconds.

Figure 4.13 shows an example of the initial drift once the electrodes are immersed in a pH 4 solution for the first time. The drift is due to the membrane reaching equilibrium with the solution. The graph shows that the 50µl/cm Biodot coated sensor experiences less drift than the hand deposited membrane sensor.

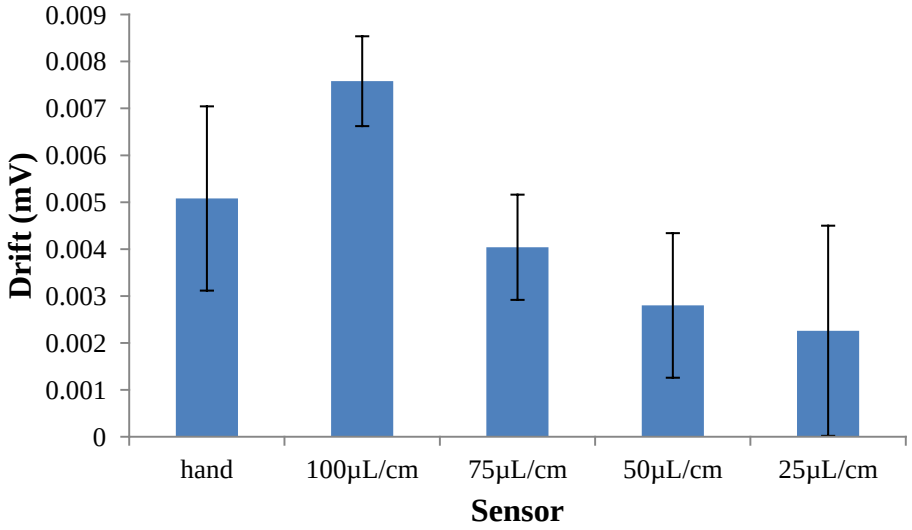

Figure 4.14 First immersion voltage drift in pH4 solution for 30 minutes. The voltage shown is the difference between the initial voltage to the voltage at 30 minutes. Error bars show standard deviation. (n=5)

Figure 4.14 shows the drift in settling from the initial immersion in solution. The 25µL/cm shows the lowest drift of 2.26±2.24mV but the standard deviation is large which indicates the sensors are inconsistent in their response. The 50µL/cm and the 75µL/cm are the best performing at 2.8±1.54mV and 4.04±1.12mV respectively over the 30 minute period. The 12.5µl/cm is not included on the graph due to a large deviation in results 3.76±5.68mV which indicates the sensor performance is very inconsistent. The 100µl/cm Biodot produces the largest drift over the 30 minute period this is unexpected as the membrane layer is thinner that both the hand and 75µl/cm membrane. This large initial drift could point to ineffective coating of the sensor.

Excluding the 100µl/cm result the sensors respond as expected with less drift on average occurring as the membrane thickness decreases. The thinnest membranes gave inconsistent responses this may be due to incomplete coverage of the carbon sensor for the 12.5µl/cm and 25µl/cm sensor. Overall the 50µl/cm Biodot sensor was the best performing with good pH sensitivity and one of the lowest values of drift. This membrane coverage technique was chosen to cover the optimum coating of conducting polymers as discussed in **Section 4.2**. The next section of results will

discuss the combined performance of the sensor membrane when combined with conducting polymers.

4.4 Manufacture

The previous sections investigated the optimum coatings of electropolymerised conducting polymer for PPY doped with Cl^- and PTS^- ions. The optimum machine deposited membrane was also found to ensure that the sensors could be compared with a consistent ion-selective membrane deposit. This section of results describes the pH sensor testing and characterisation with respect to the different conducting polymer middle layers of the sensor. The conducting polymer layer was expected to improve the sensor's voltage stability. Four different types of sensors are tested each with a different ion to electron mid layer. The sensor cross sections are shown in **Figure 4.15**.

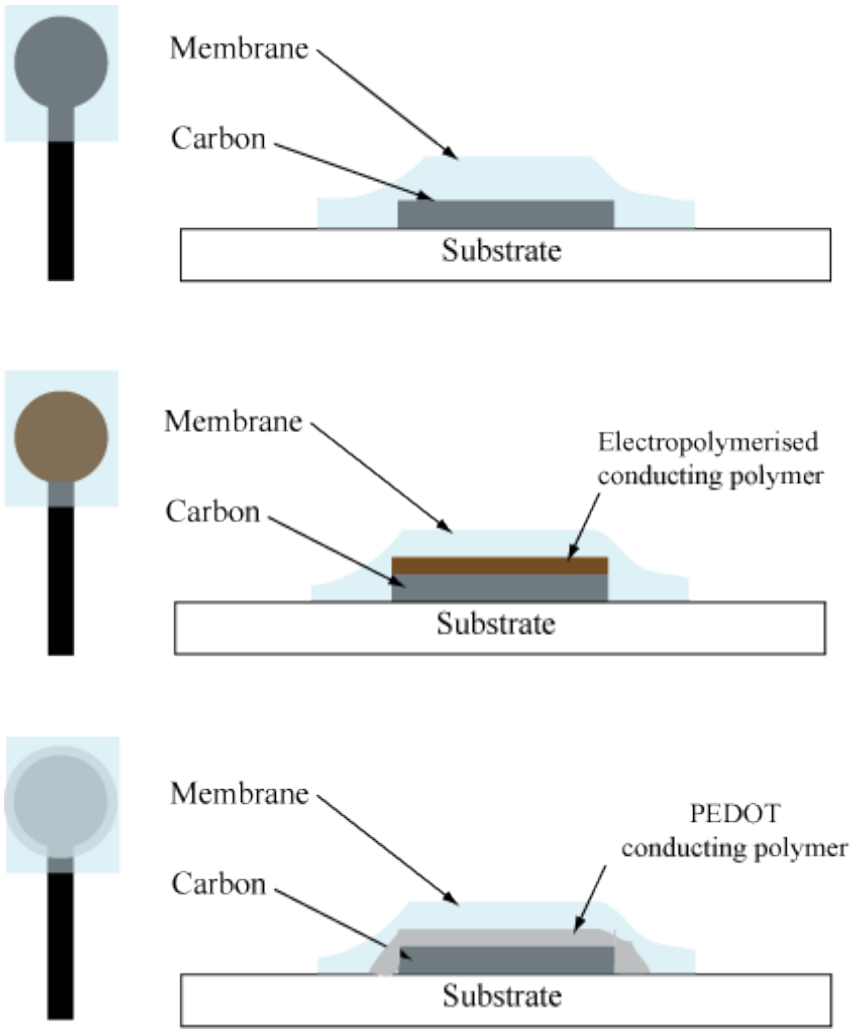

Figure 4.15 Diagram showing cross section of sensor types. Screen printed carbon coated with membrane (top). Cross section for the two electropolymerised conducting polymer based sensors (middle). Screen printed PEDOT conducting polymer with membrane (bottom).

All sensors have a carbon conducting contact on a polyester substrate. Two of the sensors are coated with the optimum 3 cycle 0 to 3 volt coating of conducting polymer found in **Section 4.2**. These sensors are the PPYCl and PPYPTS sensors both of these showed promising redox reactions during cyclic voltammetry. The cross section of these electropolymerised conducting polymers is shown in **Figure 4.15** (middle). The screen printed PEDOT sensor will also be tested due to its ease of manufacturing as shown in **Figure 4.15** (bottom). The fourth sensor is the screen

printed carbon with no mid layer as shown in **Figure 4.15 (top image)**. These four sensor types were coated with the optimum membrane coating of 50µl/cm from the Biodot spray deposit machine. The protocol for manufacturing of the sensors is described in full in **Section 3.1**.

The membrane coating was applied to the carbon only electrode and also to the two types of electropolymerised conducting polymer sensors successfully. An example of the successful membrane coating of a PPYPTS conducting polymer can be observed in the surface contour map shown in **Figure 4.16**. The image shows a smooth surface over the conducting polymer. The coating of the carbon membrane has been previously discussed in **Section 4.3**. The membrane surface images shown below were taken on a white light interferometer the method of this is described in **Section 3.3.2**.

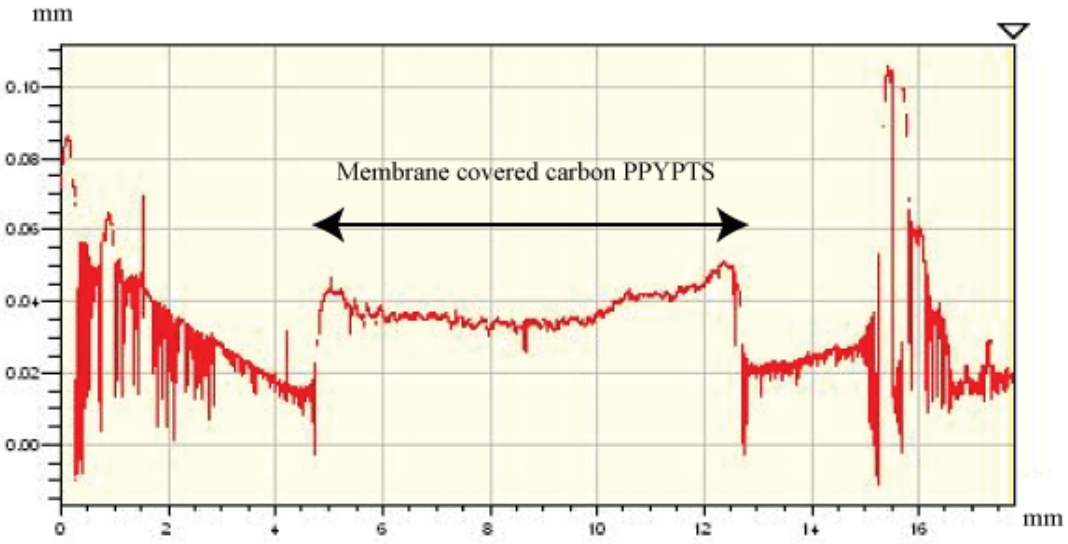

Figure 4.16 White light interferometer image of the membrane surface of a coated PPYPTS. Due to the thin membrane interference is shown at the fringes of the figure.

The coating caused some problems with the PEDOT sensor membrane with formation of bubbles within the membrane as shown in **Figure 4.17**. Many PEDOT sensors were produced using the Biodot spray deposition method but every sensor formed bubbles in the ion-selective membrane. The bubbles caused the surface of the sensor to form peaks around the bubbles as shown by the red surrounding area in

Figure 4.17. The bubble formation will lead to inconsistent membrane coatings using this membrane deposition method. The bubbles are likely caused by the hydrophobic nature of the PEDOT this is discussed further in **Section 6.3**.

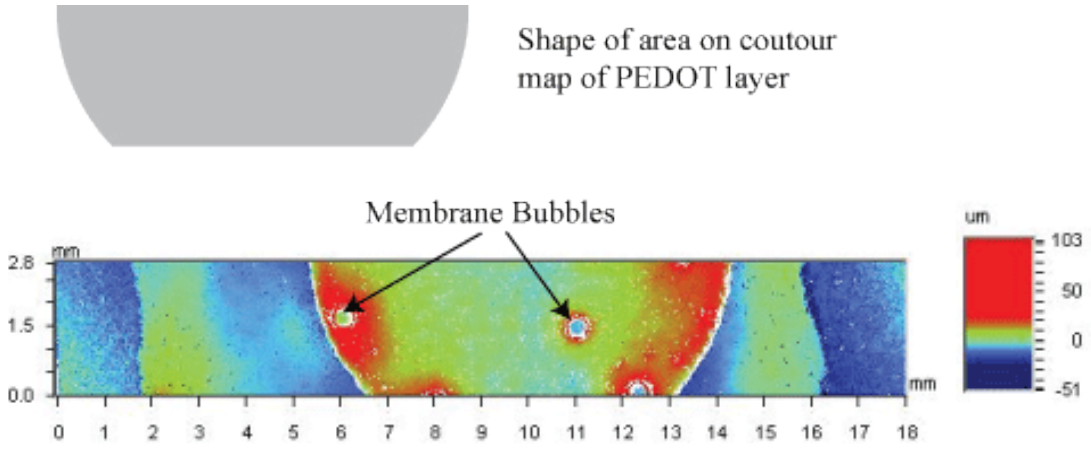

Figure 4.17 White light interferometer contour image of the membrane surface of a coated PEDOT sensor showing bubbles in membrane. The area of PEDOT coverage is shown by the grey circle shape. The scale of the contours is to the right hand side.

4.5 Results of full sensor testing

This section details the results from the testing and characterisation of the 4 different types of sensor. The 4 sensor types are manufactured using the techniques detailed in methods **Section 3.1**. The investigation assesses the properties of the different conducting polymer ion to electron transducers layers when covered in a hydrogen ion-selective membrane. The 3 redox active conducting polymers are electropolymerised PPYCl, PPYPTS and screen printed PEDOT. These will be compared against the screen printed carbon membrane sensor that has no ion to electron transducing mid layer.

4.5.1 Voltage response of sensor to pH

The potentiometric voltage response of the pH sensor was found using the method detailed in **Section 3.3.4**. The tests were used to determine how the different mid layer influences the voltage response of the sensor over the range pH4-pH10.

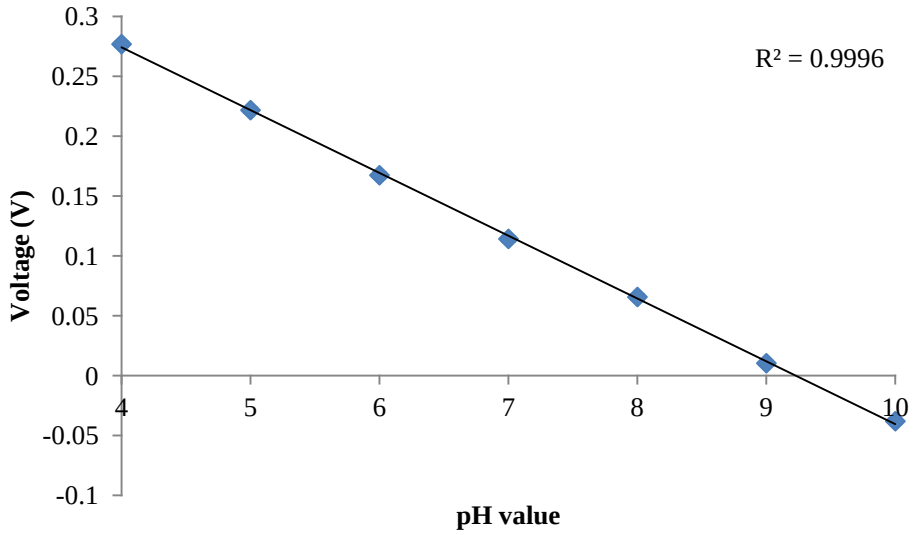

Figure 4.18 Potentiometric voltage response of carbon membrane sensor to change in pH (n=7). Error bars not visible due to scale.

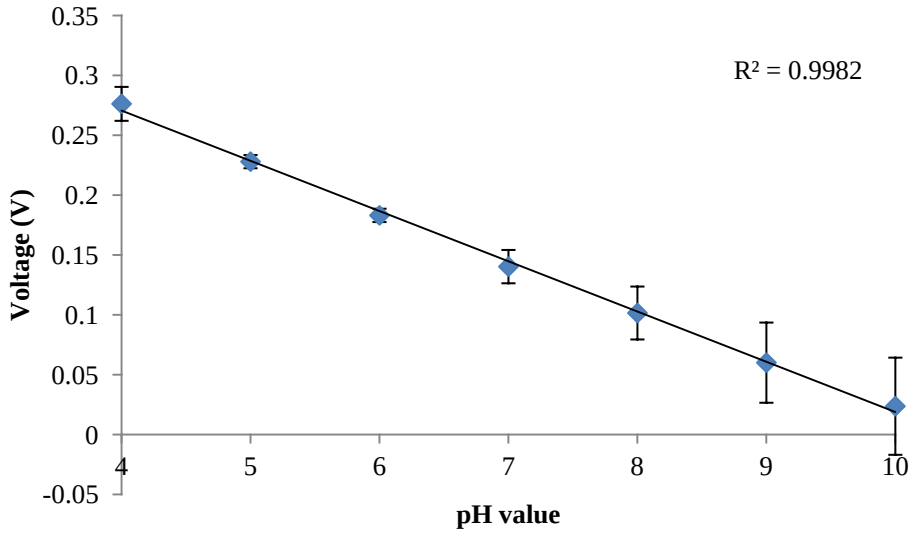

Figure 4.19 Potentiometric voltage response of PEDOT membrane sensor to change in pH (n=7).

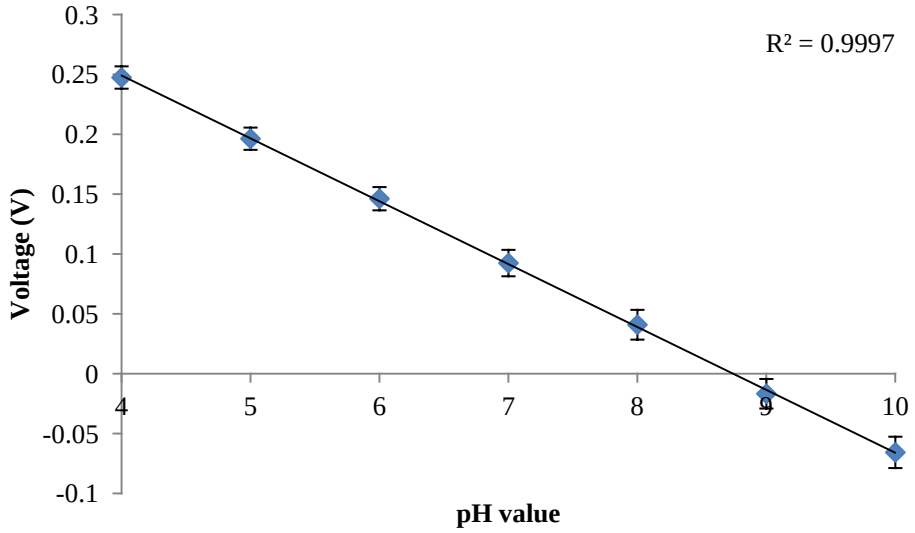

Figure 4.20 Potentiometric voltage response of PPYCl membrane sensor to change in pH (n=7).

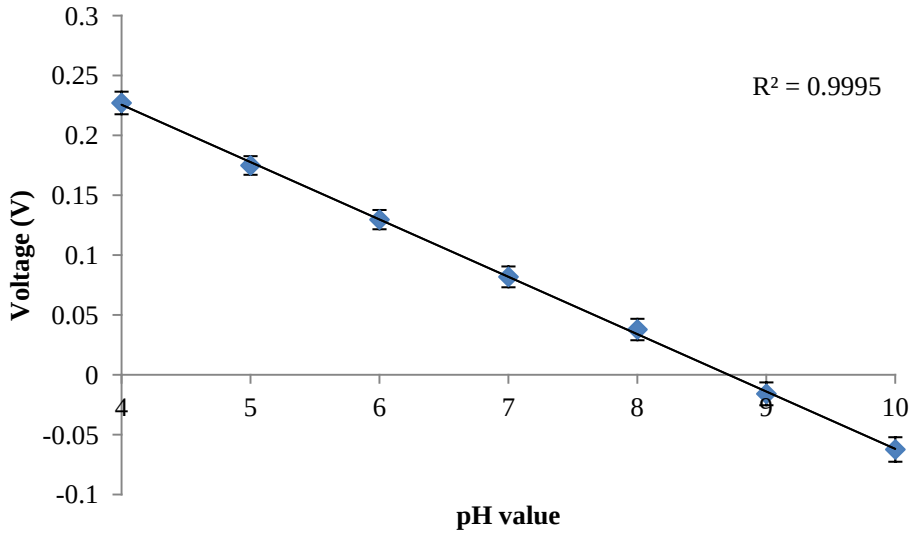

Figure 4.21 Potentiometric voltage response of PPYPTS membrane sensor to change in pH (n=7).

Figures 4.18 to 4.21 show the mean sensor voltage response with standard deviations across the different pH solutions. Each sensor type shows a change in voltage with variation of solution pH. The standard deviations show how consistent the voltage response of each sensor type is at each pH level. The ideal sensor will

produce a repeatable voltage at each pH level. If the mean of the standard deviations across the pH range is taken it gives a numerical value for assessing the repeatable voltage response across the pH levels. The Carbon membrane has the smallest mean of the standard deviation of 2.16±0.096mV. Both the electropolymerised conducting polymers had similar values of 11.03±1.61mV and 8.95±0.86mV for PPYCl and PPYPTS respectively. The carbon PEDOT electrode had the largest deviation across the sensors of 19.34±13.51mV. From this data it indicates that the carbon membrane sensor has the most consistent voltage response across the pH values.

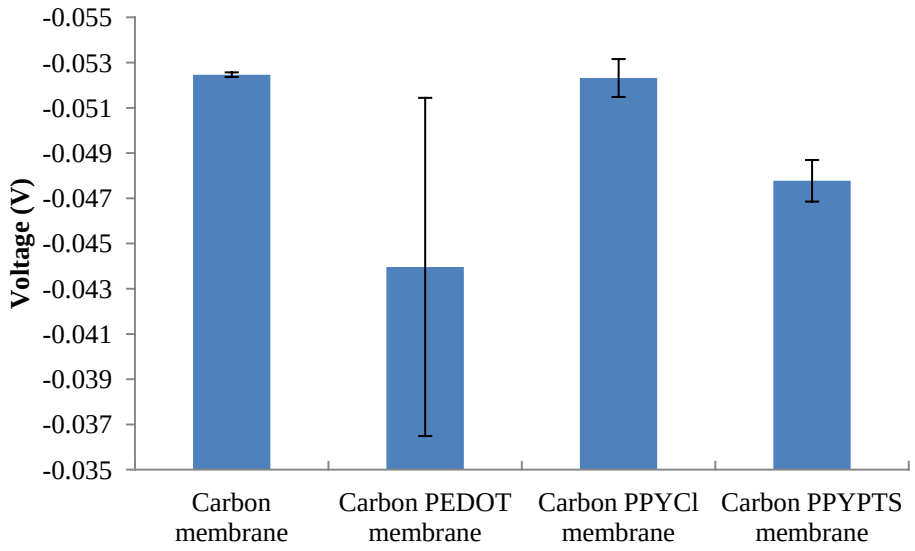

Figure 4.22 Voltage response per decade change in H+ ion concentration of sensors with different mid layer coatings (n=7). Error bars show standard deviation.

Figure 4.22 illustrates the response of the 4 different sensors tested. The Carbon and Carbon PPYCl sensors produced the largest voltage change of -52.46±0.102mV/decade change H^+ ion concentration and -52.32±0.84mV/decade change H^+ ion concentration respectively. The Carbon PPYPTS sensors have a slope of -47.77±0.92mV/decade change H^+ ion concentration. The carbon PEDOT sensor had the lowest voltage response of -43.96±7.47mV/decade change H^+ ion concentration. The most consistent sensor was the carbon and membrane with no mid layer. The most inconsistent sensor was the carbon PEDOT sensors which have a large standard deviation. These results show that each of the sensors tested produce a near Nernstian voltage response to change in pH of a solution. With the carbon

membrane sensor that has no mid layer giving the largest voltage response and also the most consistent voltage response at each pH level.

4.5.2 60 Day long life test

The original sensors from **Section 4.5.1** were retested after being stored in a dark environment at room temperature for a 60 day period. The method used was the same as the previous test for determining pH voltage response to decade change in H^+ concentration as detailed in **Section 3.3.4**.

The carbon membrane electrode produced the largest voltage change per decade of -52.42±0.14mV/decade change H^+ ion concentration. The electropolymerised conducting polymers had voltage responses of -49.18±0.31mV/decade change H^+ ion concentration and -48.45±1.18mV/decade H^+ ion concentration for PPYCl and PPYPTS respectively. The PEDOT membrane sensor has a voltage response of -38.62±8.61mV/decade change H^+ ion concentration.

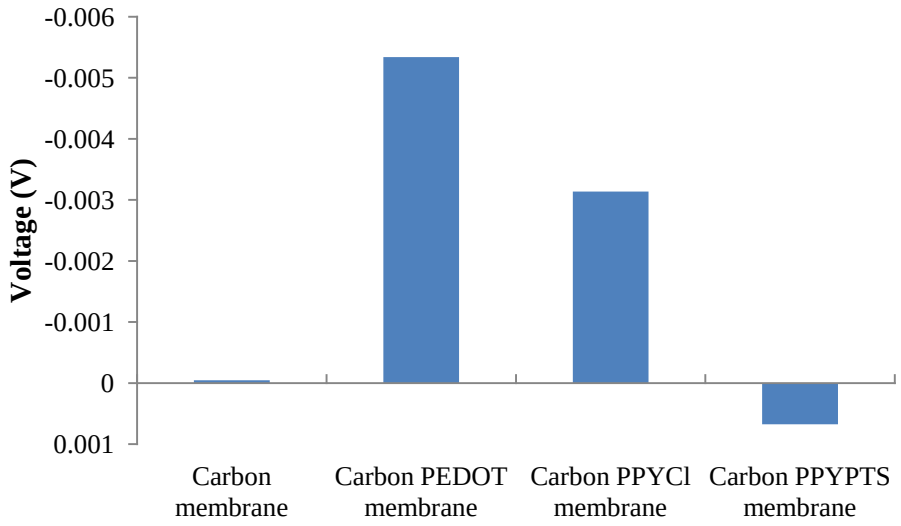

Figure 4.23 Change in voltage response per decade change in H^+ concentration after 60 day period. (n=7)

Figure 4.23 shows the change in voltage response per decade H^+ concentration after 60 days between the four sensors. The graph illustrates that the largest change between the two measurements was from the Carbon PEDOT membrane sensor this

changed by -5.34mV/decade change H^+ ion concentration over the 60 day period. The electropolymerised sensors performed differently with the PPYCl sensor having a larger change of -3.14mV/ decade change H^+ ion concentration compared to the PPYPTS which performance increased by 0.67mV/ decade change H^+ ion concentration over the 60 day period. The carbon membrane sensor produced the smallest change after 60 days storage of 0.046mV/ decade change H^+ ion concentration.

It should be noted that although the sensors voltage response slope changes by the values shown in **Figure 4.23** the potentials of the sensors change over time. After 60 days the carbon sensor potential reduced by an average of 28.2±1.5mV per pH level and the PEDOT by an average of 34.0±8.2mV per pH level. The electropolymerised sensors increased in voltage response by an average of 79.5±8.3mV and 38.6±3mV per pH level for PPYCl and PPYPTS respectively. The large standard deviations for the conducting polymer based sensors indicate that the reduction in potential is not uniform across the pH range. This could be due to the ion-selective membrane and conducting polymer properties changing after drying after initial immersion.

These results were unexpected as the conducting polymer sensors were expected to be the best performing and show stability in voltage response over time. The poor performance of the conducting polymers to the long life testing indicates that there is a problem in the sensors which affects their performance.

4.5.3 Sensor voltage settling

This section presents the results from the sensor voltage settling after initial immersion in a pH solution, the test is detailed in **Section 3.3.5**. The test involved each new sensor being immersed in a pH 4 solution to observe the voltage drift over a period of 1800 seconds (30 minutes). The initial drift will occur until the membrane and mid layer reach equilibrium with the solution. Once the sensors have achieved equilibrium with an initial solution they are said to be conditioned. A conditioned sensor achieves stability in a shorter time period than an unconditioned sensor. This test investigates which sensor is stable and conditioned in the shortest time period. **Figure 4.24** shows an example of sensor drift over the initial 30 minute period.

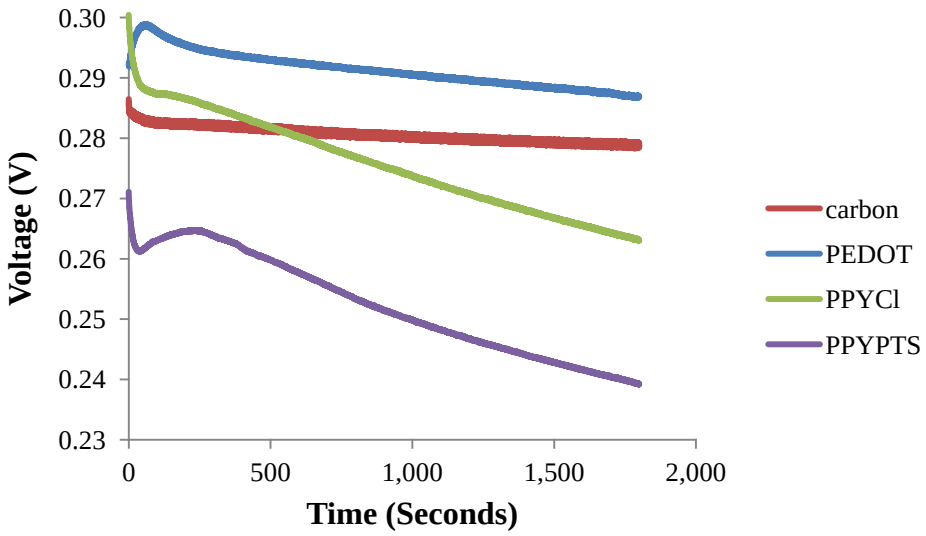

Figure 4.24 Figure showing initial sensor voltage drift over the first 1800 seconds of immersion against calomel reference electrode.

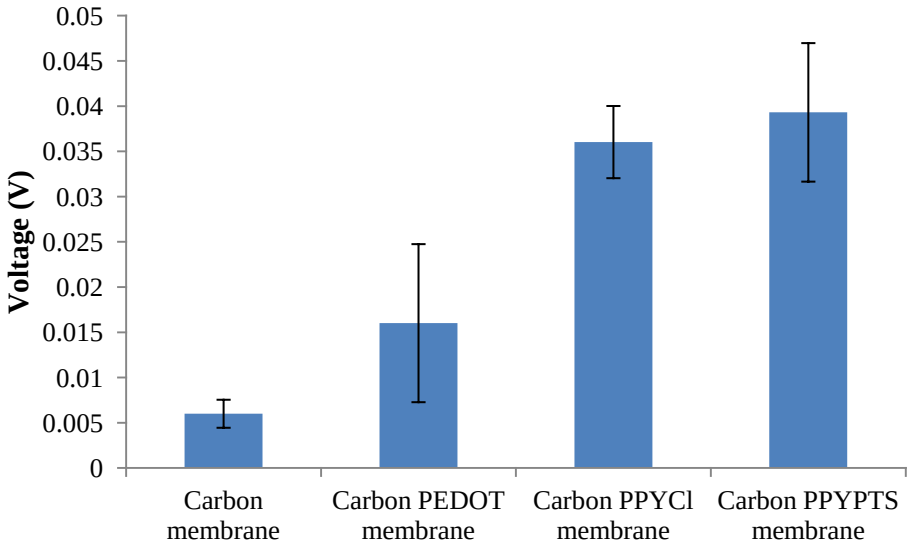

Figure 4.25 Voltage drift of the sensor in pH 4 solution after initial immersion to 30 minutes. (n=7)

Figure 4.25 shows the results for the initial sensor drift testing. The carbon showed the least amount of drift over the period of time studied the drift was 6±1.55mV for the 1800 second test period. The carbon PEDOT sensor had a drift of 16.01±8.73mV for the testing period. The electrodeposited conducting polymers were the worst

performing of four sensors tested. The Carbon PPYPTS had the largest drift of all the sensors of 39.31±7.65mV for the testing period. The carbon PPYCl sensor has a drift of 36.03±3.98mV over the testing period.

The drift was unexpectedly large for the conducting polymers sensors. This suggests that longer conditioning times are needed for the conducting polymer mid layers to reach equilibrium.

4.5.4 Selectivity

The selectivity of the sensors was determined using the separate solution method detailed in **Section 3.3.6**. The separate solution method first finds the voltage response to concentrations of the primary ion only which in this case is the H+ ion. Then the voltage response to the interfering ion is tested over a series of solutions containing only the interfering ion. The voltage responses to both the interfering and primary ion are extrapolated to 1M concentration to find the estimated voltage at this concentration. The selectivity coefficient is then calculated by **Equation 3.1** in **Section 3.3.6.** The higher the coefficient the more selective the electrode is to the interfering ion. Due to the interfering ion not giving Nernstian slopes the maximum activity level was used to determine the selectivity of the electrode as recommended in Bakker (Bakker et al., 2000). The selectivity coefficients shown are the maximal limiting values of selectivity.

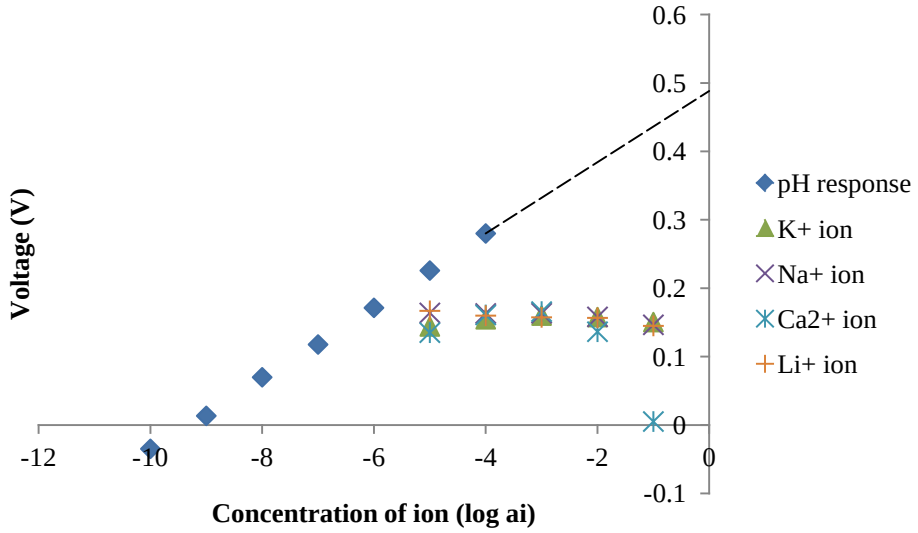

Figure 4.26 An example of performance of carbon membrane pH electrode using pH solutions and separate solutions of potential interfering ions. Shown is response to pH with dashed line extrapolated to 10^{0} M for calculation of selectivity measurement. The voltage response to each interfering ion was recorded over a concentration range 10^{-1}-10^{-5}M.

Figure 4.26 details the response of a carbon membrane pH electrode to a variety of interfering ion solutions of varying concentrations. The results of this show the almost flat response to the interfering ions across the different solution concentrations. All sensors tested produced similar responses to the one shown in **Figure 4.26**. The data from these tests is used to calculate the selectivity coefficient shown below in **Table 4.2**.

Sensor	K+	Na+	Ca2+	Li+
Carbon	-5.46±0.06	-5.38±0.05	-5.29±0.08	-5.39±0.04
PEDOT	-4.62±0.91	-4.72±0.89	-4.56±0.78	-4.78±0.90
PPYCl	-3.28±0.14	-3.30±0.21	-2.98±0.15	-3.28±0.09
PPYPTS	-3.85±0.16	-3.87±0.15	-3.45±0.14	-3.86±0.18

Table 4.2 Selectivity coefficients for full sensors for different ions. (n=7)

Table 4.2 shows the maximum selectivity coefficients of the four different sensors tested. The results show that the carbon membrane sensors are the most selective of all the interfering ions tested. The Carbon membrane PPYPTS is more selective than the other electropolymerised conducting polymer PPYCl. The results of the selectivity coefficient are further discussed in **Section 6.4.4**.

4.5.5 Sensor hysteresis

Sensor hysteresis is a test to investigate if the sensor voltage response is the same when immersed from pH4 to pH10 solution then from pH10 back down the pH range to pH4. This would determine if the sensor was accurate over a range of values of pH and if the sensor experienced any voltage change from cycling through pH solutions. The detailed method used for this test is described in **Section 3.3.7**. An ideal sensor would show identical voltage response so that an accurate pH can be calculated from the voltage.

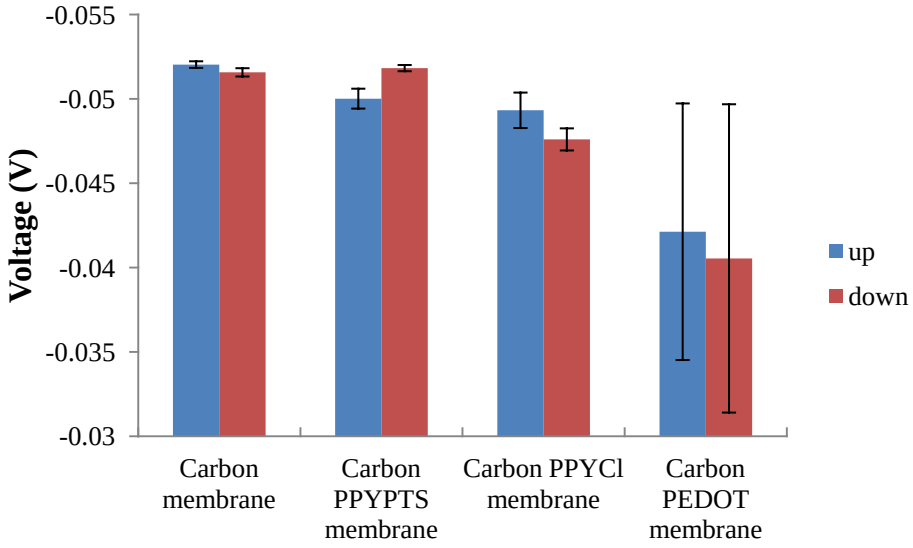

Figure 4.27 Hysteresis showing the difference in voltage response for pH per decade change in H^+ ion concentration going up and down pH range from 4-10 (n=7)

Figure 4.27 illustrates the voltage response per decade change in H^+ ion concentration from both the up and down cycle of the pH. All the sensors show a degree of hysteresis with the carbon showing the closest response between the up and the down slopes. The best performing pH sensor with the closest voltage response to pH cycling was the carbon membrane sensor it had a -0.46mV difference between the up and down slope. The carbon PPYCl sensor has a larger up slope the difference between the slopes is -1.73mV. The carbon PPYPTS sensor has a larger down slope which is the opposite of the PPYCl based sensors the difference between the two was +1.81mV. The carbon membrane and the electropolymerised sensors were constant in their voltage slope response. The Carbon PEDOT sensor had a difference in slopes of -1.58mV but had very high standard deviations due to the inconsistent membranes.

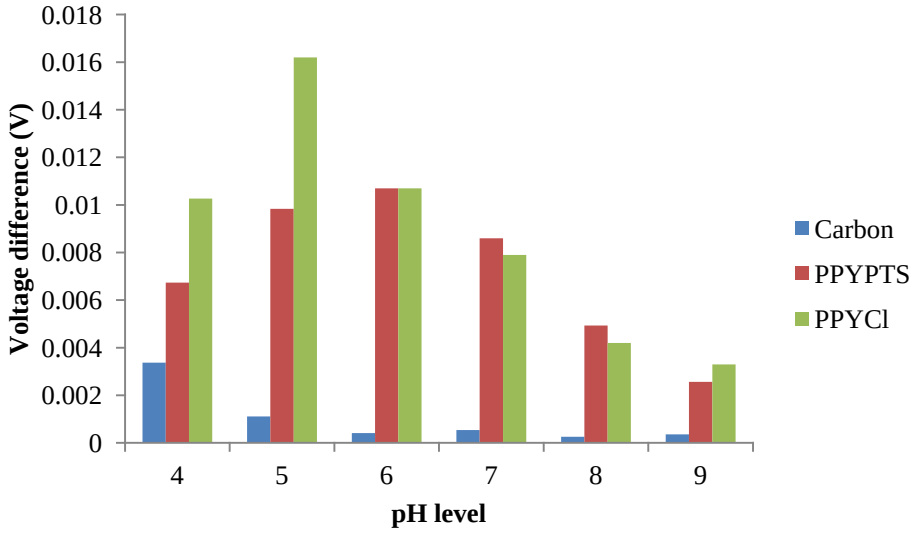

Figure 4.28 Showing recorded voltage difference between pH levels in pH hysteresis test. PEDOT not shown due to high standard deviation.

The voltage change per decade does give the full information of the sensor performance. If the voltage values are observed comparing the initially recorded values at the pH levels with the second recorded values it gives different voltage values as shown in **Figure 4.28**. This data shows large differences in recorded values between the initial pH measurement and second pH measurement for the electropolymerised conduction polymer based sensors. The PPYCl was the worst performing with a maximum difference of 16.2mV between the pH5 measurements. The PPYPTS showed the largest deviation of 10.7mV at pH 6. The carbon membrane was the best performing with a maximum difference of 3.4mV between the pH 4 measurements.

The results detailed show that the sensors based on conducting polymers would not be reliable for pH measurement due to the change in voltage response per decade. A constant voltage response is required to give accurate conversion to pH. It indicates that the conducting polymer based sensors have an issue with voltage drift which affects their performance this could be due to formation of a water layer.

4.5.6 Water layer testing

The conducting polymer based sensors showed inconsistent voltage response in the hysteresis testing which indicates a problem with the sensors. A potential problem could be the formation of a water layer between the membrane and conducting polymer as shown in **Figure 4.29**. The formation of a water layer can be due to poor membrane adhesion and it introduces new unwanted phase potential differences within the sensor that will affect the overall voltage response to the primary ion and degrade the sensor performance (Fibbioli et al., 2000).

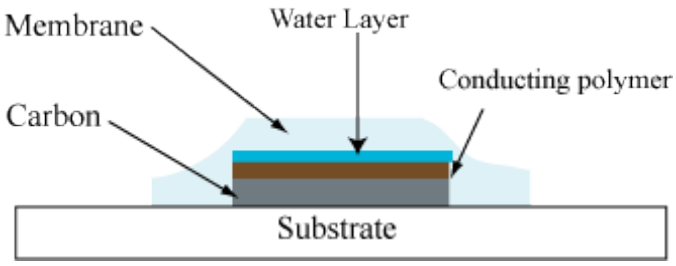

Figure 4.29 Cross section of conduction polymer sensor showing water layer formation.

To test for the formation of a water layer between the membrane and the other layers the sensors were immersed in a pH4 solution for 1 hour then immersed in pH10 for 1 hour then again in pH4 for 2 hours. If a liquid layer is formed a voltage drift will be observed when moving from one solution to another (Fibbioli et al., 2000). The method for this test is fully detailed in **Section 3.3.8**. Due to high inconsistency in the PEDOT membrane as shown in the previous sections the water layer tests were not included for this sensor type.

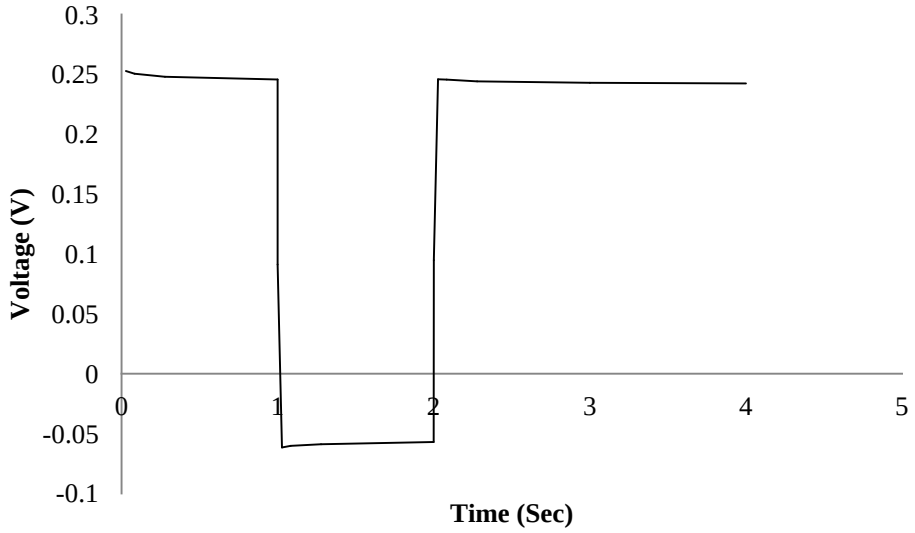

Figure 4.30 Carbon membrane sensor water layer test. Voltage response to immersion in pH 4 solution for 1 hour followed by pH 10 solution for 1 hour then pH4 solution for 2 hours.

Figure 4.30 illustrates the response of the carbon membrane sensor to water layer formation test. The voltage drift after the second immersion in the pH 4 solution is 3.23±0.41mV (n=3). The difference in potential from the final measurement in the first pH4 solution to the final measurement in the second pH 4 solution is 1.43±1.17mV (n=3). The carbon sensor has the least amount of voltage drift in all solutions. The lack of difference between measurements indicates the absence of any water layer.

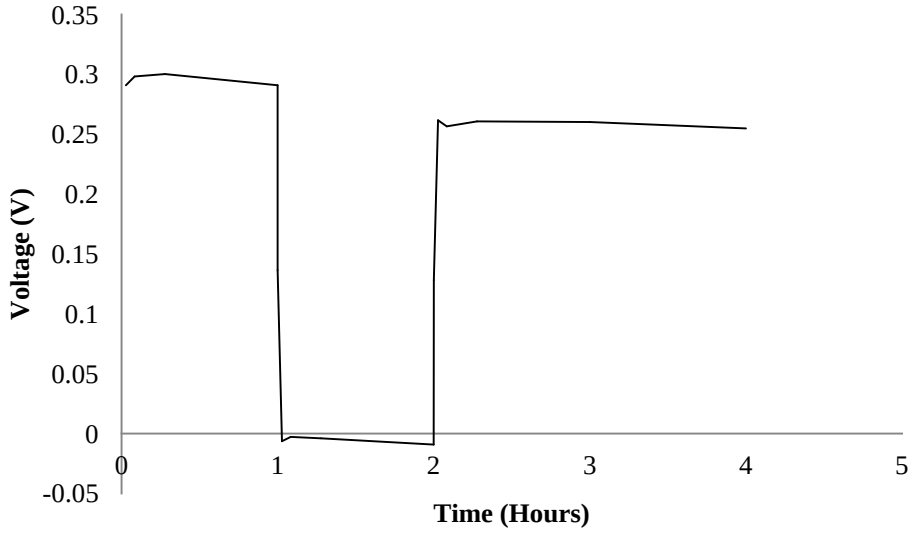

Figure 4.31 Carbon PPYCl membrane sensor water layer test. Voltage response to immersion in pH 4 solution for 1 hour followed by pH 10 solution for 1 hour then pH4 solution for 2 hours.

Figure 4.31 shows the voltage response of a carbon PPYCl sensor during water layer testing. The immersion in the second pH 4 solution produces a voltage drift of 10.4±7.75mV (n=3). The difference in potential from the final measurement in the first pH4 solution to the final measurement in the second pH 4 solution is 31.93±4.4mV (n=3).The PPYCl sensor in all pH solutions shows an initial drift towards more positive voltages after around 300 second the sensor drifts towards negative values. The drift is large which indicates that there is a formation of a water layer that interferes with voltage potential.

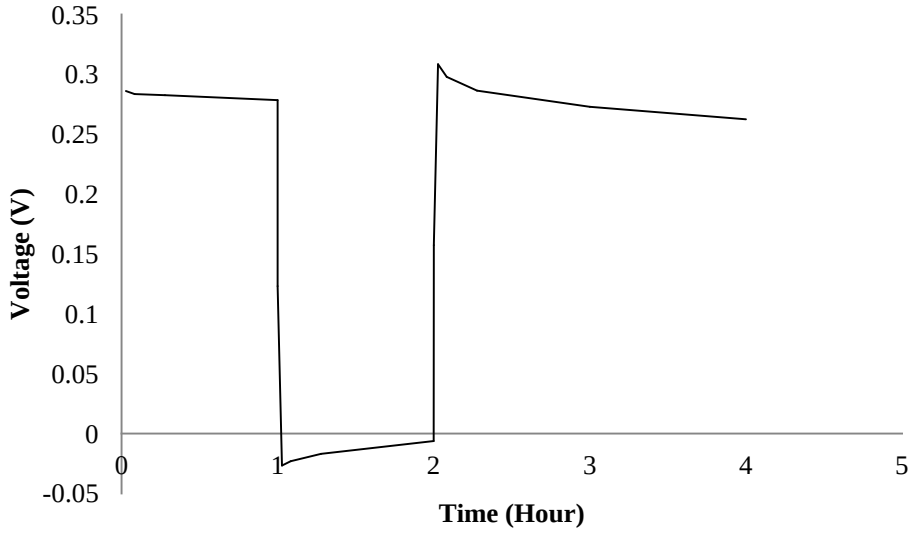

Figure 4.32 Carbon PPYPTS membrane sensor water layer test. Voltage response to immersion in pH 4 solution for 1 hour followed by pH 10 solution for 1 hour then pH4 solution for 2 hours.

Figure 4.32 illustrates the carbon PPYPTS water layer test. The PPYPTS was the worst performing of all the sensors tested when immersed for a second time in the pH 4 solution with an average voltage drift of 45.97±8.72mV (n=3). The difference in potential from the final measurement in the first pH4 solution to the final measurement in the second pH 4 solution is 16.17 ±0.93mV (n=3). The drift in the pH 10 solution is different from the PPYCl sensor as it drifts toward the positive voltages. The drift at the pH 4 solutions both show a drift toward negative voltages. The PPYPTS sensor shows the largest amount of drift in all solutions of all the sensors tested. This indicates that the sensor also has a formation of a water layer between the conducting polymer and the membrane as shown in **Figure 4.32**.

4.5.7 Full sensor testing summary

The full testing and characterisation of the 4 different solid state pH electrodes produced some unexpected results. The best performing sensor in all the tests was the carbon membrane sensor with no ion to electron mid layer. The poor performance of the screen printed PEDOT conducting polymer sensor could be attributed to the bubbles formed within the membrane as shown in **Section 4**. Both

the PPYCl and PPYPTS electropolymerised sensors suffered from the formation of a water layer between the membrane and conducting polymer which cause sensor voltage drift over longer term measurements which would lead to inaccurate pH measurements.

4.6 Carbon sensor

The carbon membrane sensor was found to be the best performing of all sensors tested. The next section specifically tests the physical properties of the carbon electrode with no membrane using Electrochemical Impedance Spectroscopy (EIS). The performance of the carbon membrane electrodes is also tested for heat stress, operating range and long term sensor voltage drift.

4.6.1 Electrochemical Impedance Spectroscopy

The carbon membrane sensor does not have any ion to electron transducer layer which is commonly referred to as a blocked interface which leads to unstable voltage potential of sensors as discussed in theory **Section 2.9.2**. One possible reason for the performance of the carbon electrode could be its double layer capacitance as if this is large it will reduce the voltage change as the double layer charges leading to a sensor with increased stability. Electrochemical impedance spectroscopy (EIS) was used to characterise the physical properties of the screen printed carbon electrode with no membrane to assess the charge transfer resistance and double layer capacitance of the electrode. The carbon electrode was run from 10kHz to 0.1Hz at 100mV amplitude in a 0.1M KCl solution. The method used for this investigation is detailed in **Section 3.3.12**. The frequency response of the electrodes was fitted to a circuit model shown in **Figure 4.41**. This is based on the Randles equivalent circuit discussed in **Section 2.13**. The circuit equivalent response will enable values to be found for electrode double layer capacitance and charge transfer resistance. From these values the exchange current density can be calculated which will give an indication of the polarisable nature of the electrode as discussed in **Section 2.6**.

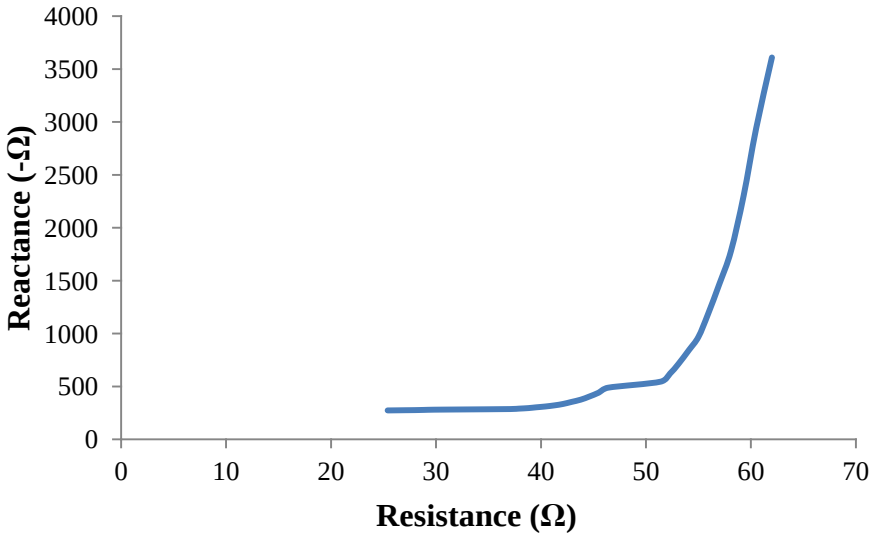

Figure 4.33 EIS complex impedance plot for printed carbon electrode showing frequency response from 1Hz-1kHz with a 100mV amplitude.

Figure 4.33 illustrates the complex impedance plot of the screen printed carbon electrode. The response shows that the screen printed carbon electrode has characteristics of a polarisable electrode due to the lack of semi circle complex impedance response as discussed in **Section 2.13**.

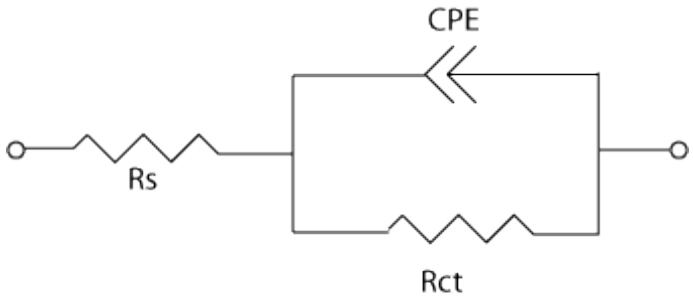

Figure 4.34 Modified Randles equivalent circuit model for carbon electrode complex impedance plot.

Figure 4.34 illustrates the equivalent circuit for the screen printed carbon electrode. The CPE is a constant phase element that has both properties of resistance and capacitance. This replaces the capacitor in Randles equivalent circuit as there is a constant phase response at lower frequencies. The constant phase response is due to

the surface roughness of the electrode. Rct is the charge transfer resistance and Rs is the solution resistance of the electrochemical cell, it is independent from the properties of the electrode. There is no complex impedance element as this has no influence in cells of high transfer resistance as discussed in **Section 2.13**.

The properties of the screen printed electrode were found by plotting the data from the EIS experiment into the equivalent circuit shown in **Figure 4.33**. The results from the EIS experiment show that the screen printed carbon electrode has a capacitance of 3.84±0.18µF at a constant phase of 0.957±0.003 (n=3). The constant phase indicates that the response of the CPE is almost all capacitive. The capacitance of the screen printed carbon electrode and how it affects the sensor performance is further discussed in **Section 6.6.4**.

The charge transfer resistance was $1.62x10^{6}\pm2.2x10^{5}\Omega$ which indicates a polarisable interface (n=3). This value has a large degree of uncertainty in the equivalent circuit model due to an estimated plot from the impedance data. This data cannot be accurately used to give a value of charge transfer resistance but the response of the electrodes shows that the electrode is polarisable in its response. As the charge transfer resistance is high the double layer capacitance is important as any current flow will charge the capacitor causing its potential to change. The solution resistance, Rs has a value of 267.5±5.54Ω. These results indicate that as expected the screen printed carbon electrode is a polarisable electrode. The results of the EIS experiments are further discussed in **Section 6.6.4**.

4.6.2 Sensor stress testing

To test the sensors in a heat stress environment the carbon membrane sensors were baked in an 80^{o}C oven and tested at various time points to determine if there is any change in the pH dependent voltage response slope performance characteristics. The full procedure is detailed in **Section 3.3.9**. Heat testing can also be used for accelerated lifetime stability testing so will give an indication of the products lifetime.

Cooking time	Voltage slope per decade H^+ concentration (mV)
Before	-55.3±0.3
15 hours	-53.7±0.18
30 hours	-52.9±0.16
150 hours	-50.7±0.51

Table 4.3 Sensor voltage response per decade of H^+ ion concentration after being stressed at 80^{o}C over various time points (n=5).

Table 4.3 details the results of the carbon electrode stress testing. The carbon membrane sensors show a reduction from a -55.3±0.3mV/decade H^+ ion concentration before the heat treatment to a -50.7±0.51mV/decade H^+ ion concentration slope after 150 hours baking time in the 80^{o}C oven.

Previous testing had shown that the voltage potential levels drop over the lifetime of the sensor, **Section 4.5.2**. The voltage potentials recorded at the various pH levels were subtracted to find the difference between the 0 hour and 150 hour tests. The largest changes were in pH4 and pH 10 values which fell 18.4mV and 16.1mV respectively. The pH values in between these values did not change by any greater than 6mV. This indicates that the range of the sensor may be affected by the heat treatment procedure.

The sensor heat stress testing shows that although the voltage response drops the sensor still displays a voltage response to changes in H^+ ion concentration. Due to the change in slope and voltage response the sensors will need to be calibrated before testing pH values to ensure accurate sensing values.

4.6.3 Sensor range

The sensors were tested to find the lower range for pH detection. Some dressings have low pH values outwith the sensor range and may lower the pH of the wound below the sensor operating range if using the sensor under a pH modifying dressing. This test immersed the sensors in pH solution from pH7 to pH2 to determine the voltage response; the method is fully detailed in **Section 3.3.10**.

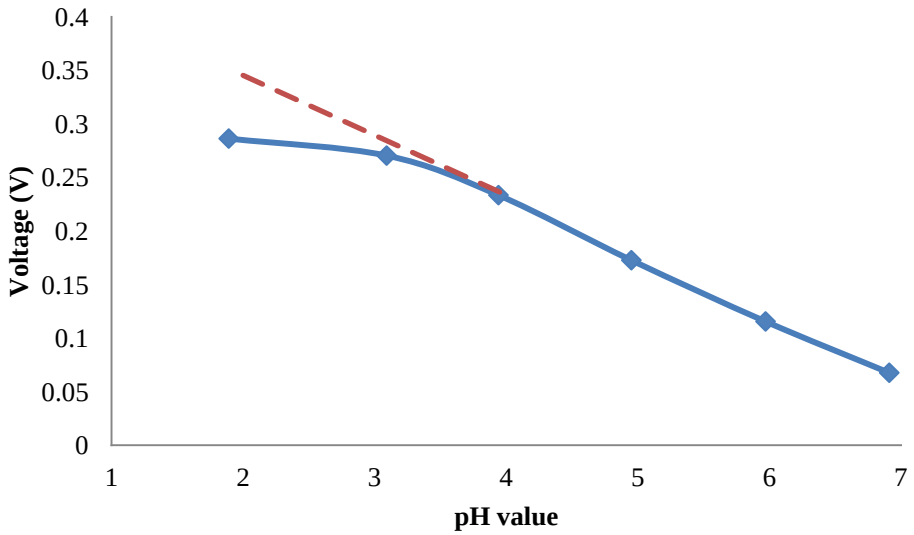

Figure 4.35 Voltage response of carbon membrane pH sensor at lower pH values to assess sensor range (n=4). The blue line is the measured voltage response at the pH levels. The red line is the continuation of the voltage response slope from pH 4 to pH7 to illustrate voltage response drop off at lower pH values.

Figure 4.35 shows the graph of the voltage response of the carbon membrane sensor from pH7 to pH2. The sensor responds from pH7 to pH4 with a slope of 55.9±0.41mV/decade H^+ ion concentration. The slope from pH4 to pH3 is -43.44±0.31mV/decade H^+ ion concentration. The slope from pH3 to pH2 is 13.25±1.1mV/ decade H^+ ion concentration. The ideal sensor would have the voltage response from pH4 to pH7 continued as illustrated by the red line in **Figure 4.35**. The range can be calculated as the point that the voltage response starts to deviate from the red line. The pH level at point of deviation from the voltage response slope

indicates the limit of accurate pH detection. For this sensor it falls at a pH value of around 3.5.

4.6.4 Sensor long term drift

The sensors were tested over a 12 hour period in a pH 7 solution to find the long term drift of the sensor in a pH solution. The full method is described in **Section 3.3.11**.

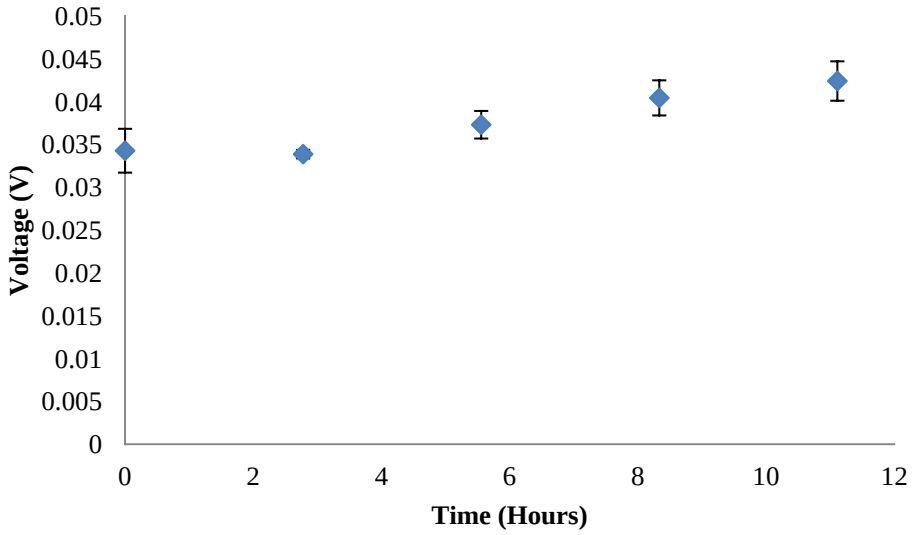

Figure 4.36 Long term drift voltage response of carbon membrane electrodes in a pH 7 solution for 12 hours (n=3)

Figure 4.36 shows the voltage drift of the carbon membrane sensors when immersed in a pH solution for 12 hours. The drift is -0.69±0.28mV per hour of test. This value indicates that the sensor would not be accurate over long time periods due to the change in voltage response. Further investigations would need to be conducted if the sensor was being used over long time periods.

4.7 Reference electrode

The aim of the reference electrode is to provide a stable half cell potential in a range of different solutions against which the voltage of the pH sensor can be measured. In this arrangement this means that the reference electrode must be stable across the range of pH values and concentration ranges of interfering ions. It is as important to the sensing electrode as without it no comparable results could be recorded. For the pH sensor system being investigated in this study the sensor has to be stable across the measurement range of pH4-pH10. The reference needs to be stable in the presence of interfering ions that would be commonly seen in its application such as K^+, Na^+ and Ca^+ ions. The reference electrode tested is a screen printed Ag/AgCl manufactured by Ohmedics.

4.7.1 Reference electrode response to pH

The potential of an Ag/AgCl electrode is determined by the chloride ion concentration in the solution as discussed in **Section 2.11**. To determine if this theory was correct with the Ag/AgCl reference electrode the potential was tested from pH4 to pH10 in a chloride adjusted pH solution to mimic the physiological chloride concentration. The reference electrode was tested against a glass calomel reference electrode. The method for this test is fully detailed in **Section 3.4.1**.

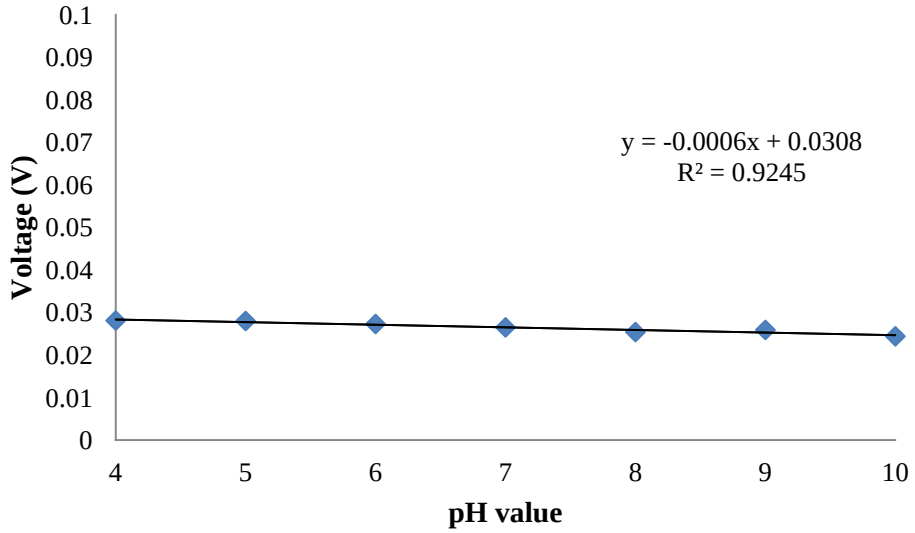

Figure 4.37 Voltage response of printed reference electrode in range of chloride adjusted pH solution.

Figure 4.37 shows the flat voltage response of a printed Ag/AgCl in chloride adjusted pH solutions from pH4 to pH10. The slope for the Ag/AgCl is 0.6mV/decade n=3 which demonstrates that it is not responsive to pH. The reference electrodes take around 30 seconds to stabilise in the chloride adjusted pH solutions.

4.7.2 Reference voltage response in chloride ion solutions

The Ag/AgCl reference electrode was tested for its voltage response to interfering ions. It is known that the chloride concentration will affect the potential of the Ag/AgCl electrode as discussed in **Section 2.11**. This test immerses the Ag/AgCl reference electrode in concentrations from 10^{-4}M to 10^{-0}M of Cl^- ions to find the voltage response. The full method is detailed in **Section 3.4.2**.

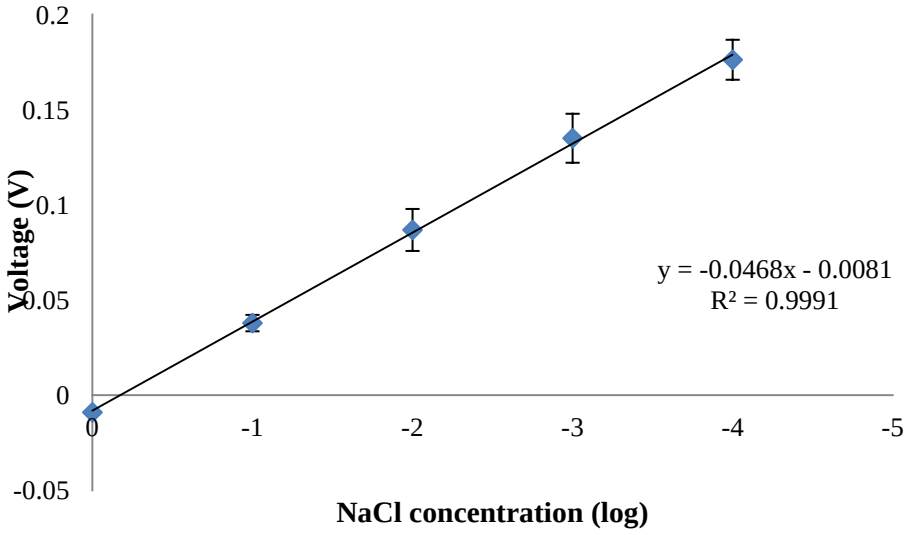

Figure 4.38 The voltage response of the Ag/AgCl reference electrode to 10^{-4}M to 10^{-0}M concentrations of NaCl salt (n=5).

Figure 4.38 details the voltage response of the reference against a calomel reference electrode when immersed in different concentrations of NaCl from 10^{0}M to 10^{-4}M. The response is a -46.8±2.6mV/decade response chloride ion concentration. The same test was also run in 10^{-4}M to 10^{-0}M concentrations of KCl salt and it produced a similar slope of -44.9±4.4mV/ decade response chloride ion concentration. In solutions where the Cl^- ion concentration varies the Ag/AgCl printed reference will not be suitable as the voltage potential will change and the reference will not provide a stable half cell. It would be possible to use a screen printed Ag/AgCl as a reference electrode in biological solutions as the Cl^- ion concentration is constant.

4.7.3 Reference electrode long term voltage drift

The Ag/AgCl reference electrodes were tested to find their voltage stability over a 12 hour time period in a chloride adjusted pH 7 solution. They were measured against a calomel electrode the detailed method can be found in **Section 3.4.2**.

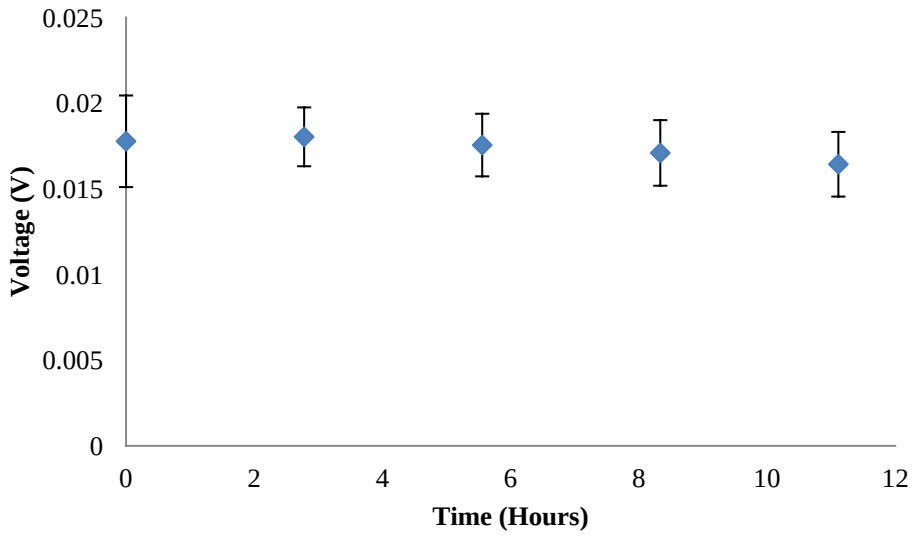

Figure 4.39 Voltage stability of screen printed Ag/AgCl electrodes in a chloride adjusted pH 7 solution for 12 hours (n=3).

Figure 4.39 illustrates that the printed Ag/AgCl reference has a stable voltage over a period of at least 12 hours. The voltage drift was small for all printed references with a 0.17±0.07mV/hour drift on the reference electrodes tested. The Ag/AgCl printed reference electrodes all have consistent response to the adjusted pH7 solution over time.

4.8 Hardware

A hand held battery operated measuring device was built to measure the pH and display the pH to the user. The design and construction of this is detailed fully in **Section 3.6**. The purpose of these tests was to ensure that the individual components of the designed measurement hardware function in the correct manner. The three main sections of the hardware were tested; these are the input amplifier, offset amplifier and the output from the microcontroller. The schematics of these circuit parts can be found in **Section 3.6.1**.

4.8.1 Input operational amplifier

The input operational amplifier function is to provide high input impedance and double the input signal voltage. This stage was tested by simulating the input voltage from the sensors with a voltage source that supplies a voltage between 350mV and -350mV. The full method can be found in **Section 3.8.1**.

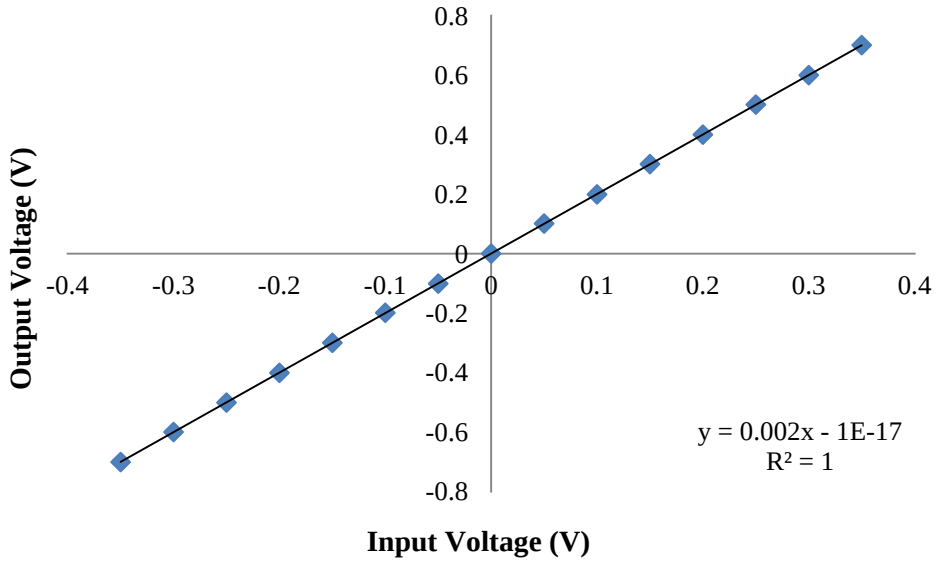

Figure 4.40 The voltage output from stage one of the operational amplifier.

Figure 4.40 details the output of the first stage of the operational amplifier. The results show a linear response across the input voltage range. The voltage slope of the line is 2mV per 1mV input. The slope is perfectly linear with a R^2 value of 1.

4.8.2 Offset operational amplifier

The purpose of the offset operational amplifier stage is to supply a positive voltage into the analogue to digital converter. The offset amplifier works by subtracting the input from the offset voltage of 0.963V. This stage was tested by supplying a voltage between 350mV and -350mV from a power supply to simulate the input from the sensors. The full method can be found in **Section 3.8.1**.

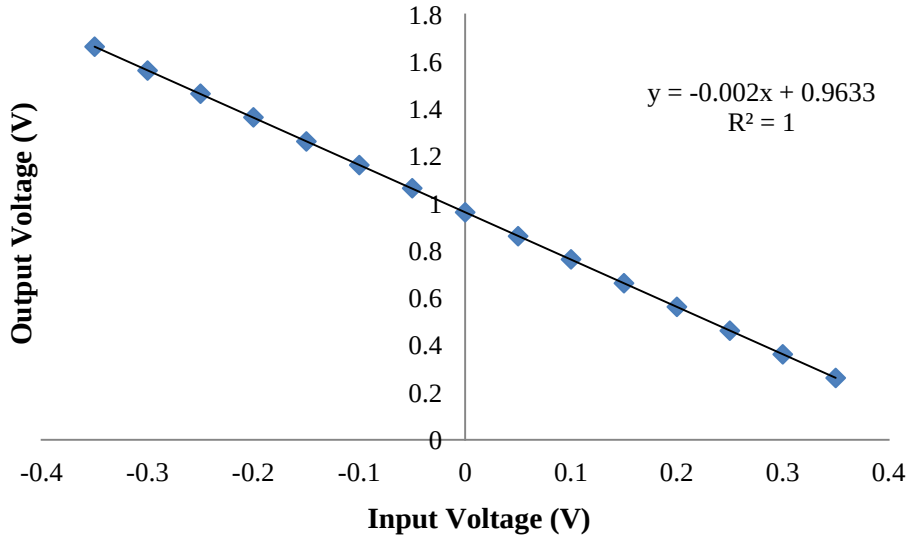

Figure 4.41 The voltage output from the second stage of the operational amplifier.

Figure 4.41 details the voltage response of the offset operational amplifier stage. The gain is zero from this stage as the voltage response slope is the same as the previous stage at 2mV per 1mV input. The offset maintains the linearity of the sensor with a R^2 value of 1. For an input of 350mV the output of the offset amplifier is 0.262V. For an input of -350mV the output from the offset amplifier is 1.664V.

4.8.3 ADC output

The input for the analogue to digital converter which is located within the microcontroller comes from the output of the offset amplifier. The output from the ADC is multiplied by the reference voltage to get the output voltage from the ADC. The Voltage out is displayed on the LCD screen where the output values are recorded from. This test measures the voltage difference between the voltage displayed on screen and the voltage input to the analogue to digital converter. The full method can be found in **Section 3.8.2**.

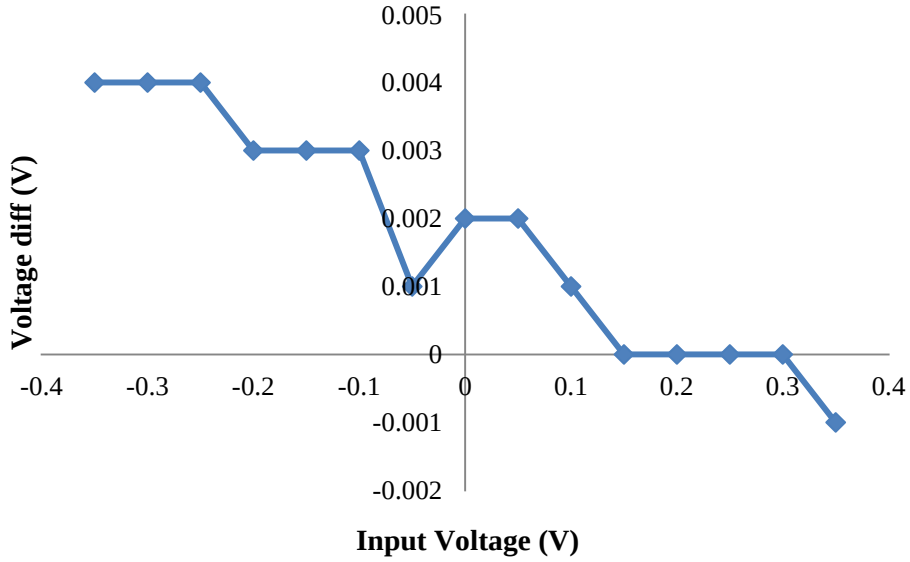

Figure 4.42 Difference between input voltage to ADC and output stage as displayed on screen.

Figure 4.42 illustrates the output from the ADC as shown on the meter LCD screen. The graph shows the difference between the input to the ADC and the voltage value shown on the LCD screen. The difference between the input voltage increases from -1mV difference for a 350mV input to a 4mV difference for a -350mV input. The overall circuit draws 40mA of current when in operation.

4.9 Sensor system combined performance testing

The sensor combined testing is designed to bring together all the elements in the previous sections of results to assess their combined performance. First the combined performance of the printed sensor couple was tested in a range of pH solutions. The second part of combined testing assesses the sensor system by calibrating the sensors then immersing the sensors in pH solutions to calculate the pH.

4.9.1 Sensor voltage response against screen printed Ag/AgCl reference electrode

The printed Ag/AgCl reference electrode and carbon membrane sensor was tested to find the pH dependent voltage response calibration slopes in a chloride adjusted pH

solution. The voltage for this was recorded on the Solartron 1286 electrochemical interface the full detailed method is given in **Section 3.10**.

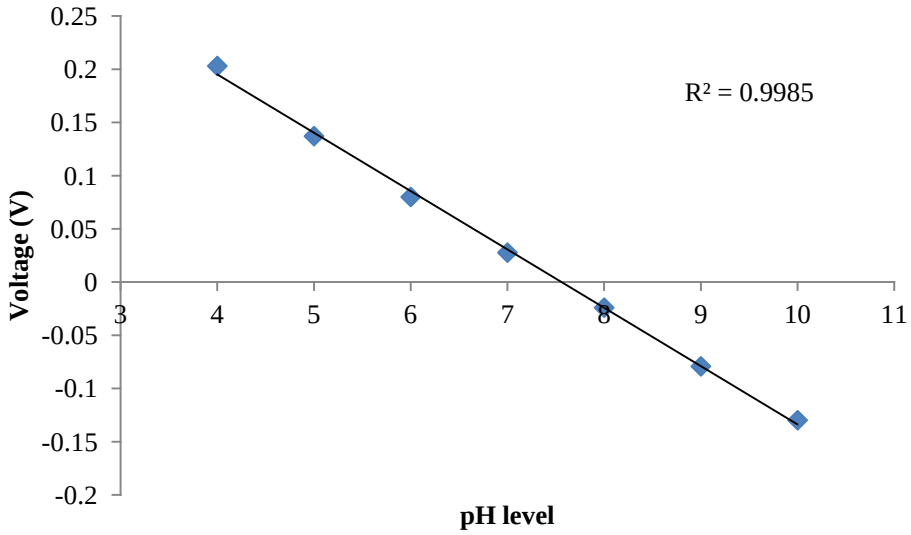

Figure 4.43 Carbon membrane electrode voltage response in range of chloride adjusted pH solutions from pH 4 - pH10 measured against screen printed Ag/AgCl reference electrode (n=5).

The result for this showed a voltage response of -54.83±0.16mV/ decade H^+ ion concentration. The standard deviations are all under 1mV and hence too small to be shown in **Figure 4.43**. The small standard deviations and good voltage response show that a screen printed reference and carbon membrane sensor can be used successfully to measure changes in pH.

4.9.2 Combined sensor system calibrated pH testing

Three different tests were conducted to assess the pH detection capabilities of the sensor. The sensor performance was tested against a screen printed Ag/AgCl electrode and a calomel glass electrode and the voltage potential were recorded using the Solartron 1286 electrochemical interface. It was tested against both the screen printed electrode and glass reference electrode to provide a comparison between different experimental setups. The different measurement setups are fully detailed in **Section 3.10**. The full method and formula for the pH calculation is detailed in **Section 3.9.3**. The carbon membrane pH electrode and screen printed Ag/AgCl

reference electrode was also tested with the designed battery operated measurement hardware to give a pH reading and testing the complete system accuracy.

For each of the tests the sensors were calibrated using a two point calibration method where the sensor couple was immersed in a pH 4 and pH 7 solution to get a voltage response per pH level for the sensor. This calibration enables the pH to be estimated from the voltage response of the sensor to new solutions. The formula for calculating the pH is shown in **Section 3.7.9**. The pH solutions used for this experiment are the chloride adjusted pH solution detailed in **Section 3.2.3**. The pH of the test solutions was measured by a glass pH meter.

pH Glass electrode (pH)	Sensor V ref (pH)	Sensor V ref printed (pH)	Device results (pH)
3.5	3.56±0.04	3.53±0.10	3.57±0.04
4.5	4.48±0.03	4.51±0.02	4.52±0.01
5.5	5.47±0.04	5.51±0.06	5.5±0.03
6.5	6.46±0.02	6.45±0.04	6.46±0.02
7.5	7.52±0.02	7.52±0.01	7.52±0.01

Table 4.4 pH levels of set solutions once calibrated using 2 point method with standard deviations. (n=3)

This test shows the calibrated pH response of the various sensor systems when immersed in the various chloride adjusted pH solutions shown on the left hand column of **Table 4.4**. These tests show the performance of the carbon membrane pH sensor against the different reference types and using the hardware that was designed for this experiment. **Table 4.4** shows the sensor operates effectively for both the printed and glass reference electrodes at each pH level. The results for the complete system testing show that the full system can measure and calculate the pH level of

the solutions accurately. The results show that the two point calibration is an effective way to calibrate the sensors for pH measurement.

Chapter 5 - Results wound dressings

5.1 Introduction

The pH of a wound influences many factors such as enzyme activity in tissue fluid and cell proliferation that contribute to the healing of the wound, these can be read about in detail in **Section 1.9**. Some modern wound dressings actively change the pH level of the wound to help control the healing properties. The pH effect of these dressings is not widely reported in the literature even though it plays an important role in the healing process (as discussed in **Section 1.11)**.

This chapter details the results from the second stage of experimentation when wound dressings are tested for their effect on pH. This section starts with commonly used wound dressings being tested for pH in a non buffered solution using a glass pH electrode. The testing then moves onto testing the performance of the components of the sensor system described in **Chapter 4** for their response to the pH of wound dressings and horse serum. This testing ensures that the designed pH sensor, reference and hardware can detect the pH of the wound dressings and horse serum successfully when compared to a glass pH electrode as it was unknown if their components may interfere with measurement. The final part of this chapter details the real time effect on pH that the wound dressings have when used in a wound bed model. Four different wound dressing types are tested first in Solution A which has no acid buffering characteristics. The experiments are then repeated using horse serum to mimic the buffering capabilities of wound fluid. These experiments will give an indication of the commonly used wound dressings acidic strength and the effect on the pH of a wound after application.

5.2 Wound dressing testing

The wound dressings tested for pH response were chosen as they are commonly used in clinical practice within the NHS in the UK. The dressings were chosen so that a broad range of dressing types was tested. All the dressings tested are in direct contact

with the wound and they are normally used in conjunction with a secondary dressing that covers the wound area. Three main dressing types were investigated:

- Hydrogels
- honey based dressings
- matrix metalloproteinase (MMP) modifiers

Hydrogels act to maintain a moist wound healing environment. Honey dressings are commonly used for their antibacterial and healing properties. MMP modifying dressings act to change the pH of a wound to reduce MMP enzyme proliferation which is known to delay wound healing. A summary of the wound dressings tested and their claimed key properties is detailed in **Table 5.1**. A detailed description of the dressings tested can be found in **Section 3.11.1**.

Dressing type	Dressing properties
Activon Tulle, Activon tube	Honey dressing (Manuka), antimicrobial, low pH due to acids naturally in honey, helps maintain moist wound
Aquacel	Hydrogel, maintains moist wound environment
Aquacel Ag	Hydrogel, maintains moist wound environment, contains silver ions which give antimicrobial properties
Cadesorb	MMP modifier uses acid to achieved this although acid used is not disclosed
Promogran	MMP modifier claims this is through cellulose, contains acetic acid
Promogran Prisma	MMP modifier claims this is through cellulose, contains silver ions which give antimicrobial properties, contains acetic acid
Tegaderm	MMP modifier through use of citric acid and metal ions

Table 5.1 Summary of key components of wound dressings tested.

5.2.1 Wound dressing pH

The aim of this experiment was to find the pH values of wound dressings when hydrated. The wound dressing were immersed in 20ml of Solution A and mixed then left for 20 minutes to ensure mixing of dressing constituents with measurement solution. The pH was then recorded of the solution containing the wound dressing. Solution A is an aqueous salt solution that mimics the physiological concentrations of salts in human serum (a detailed description can be found in **Section 3.2.2)**. The dressings were cut to 5cmx5cm squares and for the liquid dressings 2g were mixed into the Solution A. The measurements were made on a pH meter with a glass pH electrode 20 minutes after hydration. The full method for testing can be found in **Section 3.12**.

Dressing type	pH value (pH)
Activon tube	3.51±0.04
Activon Tulle	3.49±0.10
Aquacel	4.51±0.02
Aquacel Ag	4.59±0.03
Cadesorb	2.49±0.01
Promogran	2.30±0.03
Promogran Prisma	2.2±0.02
Tegaderm	3.25±0.01

Table 5.2 Measured pH after hydration of wound dressing in 20ml Solution A using glass electrode pH meter (n=3).

The results shown in **Table 5.2** illustrate that the pH of the dressings. The Activon Tulle dressing has similar pH for the tube and dressing of 3.51 and 3.49 respectively. The Activon Tulle dressing has the largest standard deviation of all the wound

dressings tested this could be due to different amount of honey on each dressing, this is further discussed in **Section 6.10.3**. Aquacel and Promogran dressings both have additional dressings with silver ions the pH of these is 4.59 and 2.2 respectively. The difference between the silver and non silver was 0.084 of a pH level for Aquacel with the non silver dressing being slightly more acidic. The difference between the Promogran dressings was 0.103 of a pH with the silver dressing being more acidic. The difference could be due to slightly different constituents in the different wound dressing types.

The pH of the tested dressings varies from a pH of 4.59 to a pH of 2.2. The pH of the honey and MMP modifying dressings was much lower than the recorded range of pH found in wounds which has been reported between 5.45-8.9 (Dissemond et al., 2003; Greener et al., 2005; Gethin, 2007). The lowest pH values recorded for Promogran and Cadesorb are particularly low as this is around the same acidity as lemon juice. Due to the pH of these dressings being very low they are outside the carbon membrane sensor range as discussed in **Section 4.6.3**. If testing the pH with these dressings the results may be inaccurate as the carbon membrane sensor only has a range to a pH of 3.5. The next section will investigate the response of the carbon membrane pH electrode to the wound dressings.

5.3 Disposable sensor system validation

5.3.1 Dressing pH testing with sensor system

This exact constituent of the wound dressings are unknown so the individual components of the sensor system were tested to validate their accuracy against the glass pH electrode measurement. Three different setups were used to measure the accuracy of each of the components designed in **Chapter 4**.

The screen printed carbon pH electrode was tested against a glass calomel reference electrode. The second setup replaced the glass reference with the screen printed Ag/AgCl reference electrode. The voltage was measured with the Solartron 1286 electrochemical interface for these two setups. This arrangement would enable the accuracy of the carbon membrane pH sensor to be measured against two different

reference electrodes. The first setup would test if the screen printed carbon pH electrode operation with the hydrated wound dressing solutions. The second would validate the use of a screen printed Ag/AgCl reference electrode by comparison to the result from the calomel glass reference electrode. The third setup tests the full designed system with screen printed carbon pH electrode, Ag/AgCl reference electrode and designed measurement hardware. These setups are further detailed in **Section 3.10**.

The wound dressing samples were cut into 5cmx5cm squares and for the liquid dressings (Cadesorb, Activon Tube) 2g were mixed into the Solution A and left to mix for 20 minutes before measurement the full method for this is detailed in **Section 3.12**. A two point calibration was performed on all sensors were the sensors were immersed in chloride adjusted pH 4 and pH 7 solution as discussed in **Section 3.9.2**. One sample of dressing solution was used with three different sensors. The Cadesorb and Promogran dressings were not tested for this experiment as they are too acidic for the range of the sensor at pH 2.49 and pH 2.3 respectively and would give inaccurate pH sensing results. The pH values were calculated using the formula in **Section 3.7.9**. The full system the pH reading was recorded from the LCD screen.

Dressing type	Meter pH (pH)	Sensor V ref Calomel (pH)	Sensor V ref printed (pH)	Device results (pH)
Aquacel	4.51	4.53±0.04	4.61±0.04	4.54±0.03
Aquacel Ag	4.56	4.53±0.04	4.54±0.08	4.57±0.03
Activon Tulle	3.60	3.67±0.01	3.66±0.05	3.66±0.02
Activon tube	3.55	3.59±0.05	3.66±0.03	3.58±0.02
Tegaderm	3.25	3.40±0.02	3.39±0.04	3.43±0.02

Table 5.3 Calculated dressing pH using carbon membrane pH sensors against calomel reference and screen printed Ag/AgCl reference electrode. The column "device results" details the pH response of the carbon membrane pH electrode

against the screen printed Ag/AgCl using the designed measurement hardware to record the pH value. (n=3)

Table 5.3 details the calculated pH from the various sensor and reference combinations. The sensor verses the calomel electrode has consistent performance similar to the pH meter reading for all dressing types bar the Tegaderm. The Tegaderm measured at a pH of 3.4 but it was measured at 3.25 on the pH meter. This is due to the Tegaderm being outside the measurement range of the pH electrode as detailed in **Section 5.2.1**.

The Screen printed pH sensor and screen printed reference electrode results are close to the pH meter reading. The largest difference between the meter reading and the sensor reading was for Tegaderm 0.143pH due to being outside the pH sensor range.

The combined system testing using both printed sensor and reference couple with pH measurements being taken on the battery operated designed measurement hardware. The results show that the Tegaderm was again the worst performing dressing with 0.18 pH difference between the glass electrode measured pH value and sensor system performance due to being outside the pH electrode measurement range. The other dressings all were within 0.07 of a pH of the measured value of pH meter.

For all sensor systems the Tegaderm pH measurement was the furthest from the glass electrode measurement with values measured with the carbon membrane pH sensor higher than the 3.25 pH measured with the glass pH electrode. This is due to the pH of the Tegaderm dressing being outwith the range of the carbon membrane pH sensor. For the other dressings tested, the pH values were close to those measured with the glass pH electrode. This indicates that the sensing system designed in C**hapter 4** can successfully measure the pH of hydrated wound dressings within the pH sensor range.

5.3.2 Horse serum testing with sensor system

All the previous pH testing of wound dressings was conducted using Solution A to hydrate the wound dressings. Solution A does not have any acidic buffering capacity and will not resist acidic change this is not realistic as wound fluid would buffer pH change through the amino acids of blood proteins as discussed in **Section 2.14.1**. To mimic the buffering capabilities of wound fluid horse serum was used as a substitute as is contains similar buffering capacity through proteins. On the final wound bed simulation pH testing this will enable the acidic strength of the acids to be observed through their influence on pH.

The purpose of this test was to assess the performance of the pH sensor when immersed in horse serum and a diluted horse serum mixture to ensure accurate measurement when compared against a glass pH electrode. Diluted horse serum was used to reduce the viscosity of the horse serum mixture the method is detailed in **Section 3.2.3**. The sensor was first calibrated by immersing in chloride adjusted pH 4 and pH7 solution as detailed in **Section 3.9.2**. The sensor was immersed in 20ml of horse serum solution where the voltage response was recorded using the 3 different measurement setups and the glass pH electrode. As in the wound dressing testing (**Section 5.3.1**) three different measurement setups were used to test the individual components of the disposable pH sensor, reference and measurement hardware. The first setup tests the screen printed carbon pH electrode against a glass calomel reference electrode. The second setup replaced the glass reference with the screen printed Ag/AgCl reference electrode. The voltage was measured with the Solartron 1286 electrochemical interface for these two setups. The third setup tests the full designed system; screen printed carbon pH electrode, Ag/AgCl reference electrode and designed measurement hardware. These setups are further detailed in **Section 3.10**. The pH value was then calculated by using the voltages recorded and the formula in **Section 3.7.9**. The full system the pH reading was recorded from the LCD screen.

	pH meter (pH)	Sensor V ref (pH)	Sensor V ref printed (pH)	Device results (pH)
Horse serum	7.88	8.01±0.04	7.92±0.02	7.98±0.03
Horse serum SolA 50/50	8.00	7.96±0.02	8.02±0.01	7.93±0.05

Table 5.4 Calculated pH values when carbon membrane pH sensor immersed in horse serum in 20ml solution measured against calomel reference and screen printed Ag/AgCl reference electrode. The column "device results" details the pH response of the carbon membrane pH electrode against the screen printed Ag/AgCl using the designed measurement hardware record the pH value. (n=3)

Table 5.4 details the results from the horse serum pH testing. The results show the pH found from the glass electrode pH meter has a difference of 0.12 of a pH between the horse serum and the horse serum Solution A mixture. The results from the tests show that the pH is near to the meter reading for all sensors tested. Overall the carbon membrane pH sensor was able to effectively measure pH in a horse serum mixture. This result indicates that the carbon membrane pH electrode with screen printed Ag/AgCl reference electrode is able to accurately measure the pH of human wound fluid.

5.4 Dressing simulation testing

This section details the wound dressing properties in a simulated wound bed model. The investigation is designed to show the change in pH once a wound dressing has been applied to a simulated wound bed as shown in **Figure 5.1**. The solutions used are a Solution A and a mixture of Solution A and horse serum. The horse serum was diluted so that a less viscous mixture could be tested. Both solutions were tested as the horse serum will have buffering capabilities through the amino acid chains in proteins in similar concentrations to human wound fluid as discussed in **Section 2.14.1** so the pH responses should differ. The response of the pH change should also let the acidic strength of the wound dressings be observed. The buffering capabilities of the horse serum will depend on the disassociation and concentration of the acid of

the wound dressings as discussed in **Section 2.14**. The dressings tested for both types of solution are the Activon Tulle, Aquacel, Tegaderm and Promogran more information on the dressing types can be found in **Section 3.11.2**. The Tegaderm and Promogran dressings were both shown to have pH values outside the range of the carbon membrane pH sensor as detailed in **Section 5.2.1**. They are used in this experiment as it is expected the buffering capabilities of the horse serum will prevent the pH dropping below the pH sensor range. The printed carbon membrane pH sensor and the screen printed Ag/AgCl reference electrode are used to measure the voltage response from which the pH is calculated. The sensors were given a two point calibration in chloride adjusted pH 4 and pH 7 solutions as described in **Section 3.9.2**. The voltage was recorded on a Solartron 1286 electrochemical interface. The full method can be found in **Section 3.13** and the formula for pH conversion in **Section 3.7.9**.

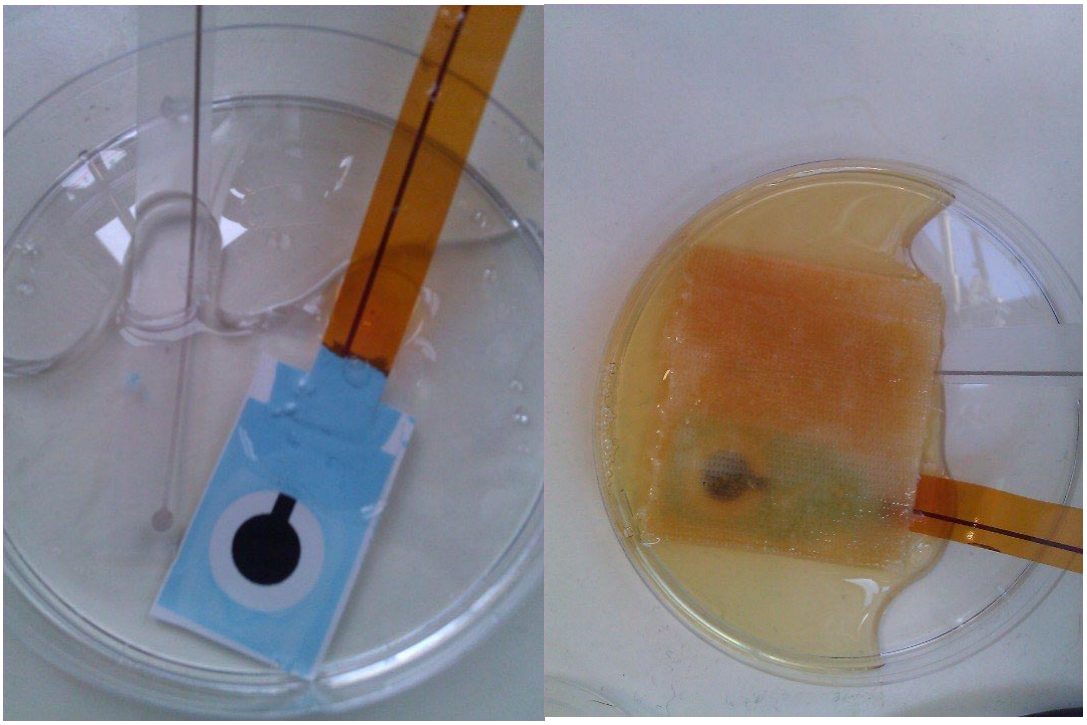

Figure 5.1 Carbon membrane pH sensor and Ag/AgCl reference before dressing application (Left) and Sensor couple after wound dressing application (Right).

5.5 Solution A testing

The tests in this section use 10ml of solution A to simulate the wound exudate. The full method can be found in **Section 3.13**. The 5cmx5cm wound dressing samples are applied after 120 seconds. The Solution A mixture does not contain any acid or buffering qualities, so it will enable the pH of the dressings to be recorded with no buffer resistance that it would experience in physiological solutions as explained in **Section 2.14**. The lack of buffering qualities will mean the pH will change even if the wound dressing acid concentration is low. The pH will depend on the acid disassociation in the solution.

5.5.1 Activon Tulle

The Activon Tulle dressing when fully immersed in 20ml of solution had a pH value of 3.49 this is described in **Section 5.2.1**. The Activon Tulle dressing was applied to the solution A after 120 seconds of testing. The Activon Tulle dressings have inconsistent amounts of honey across the dressing surface which means that different samples used may have different concentrations of honey this is detailed in **Section 6.10.3**.

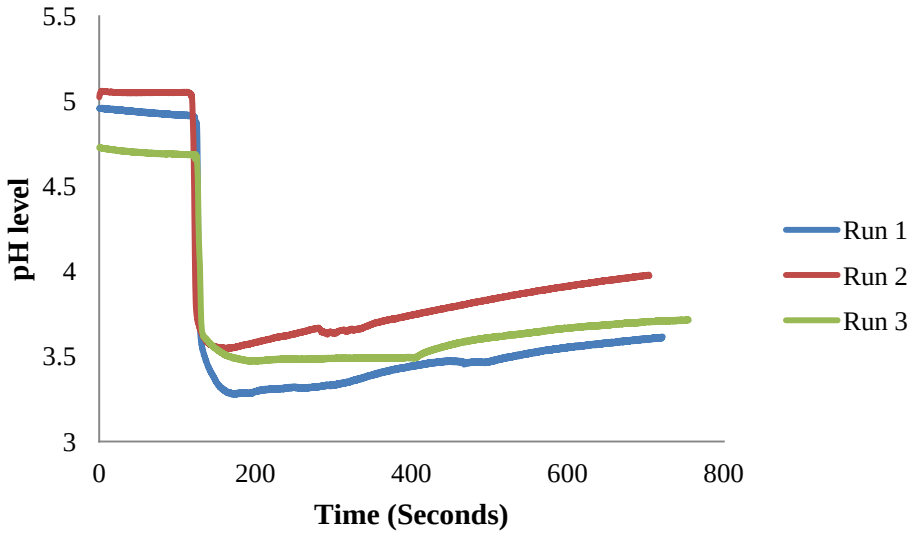

Figure 5.2 Activon Tulle in Solution A dressing added after 120 seconds.

The pH response to the application of the Activon Tulle dressing is illustrated in **Figure 5.2**. The application of the honey dressing causes a sharp change in the pH. The solution pH drifts up from an initial pH of 3.35, 3.55 and 3.54 for run 1 to 3 respectively at 150 seconds to pH values of 3.57, 3.94 and 3.68 for run 1 to 3 respectively at 650 seconds. The sensor does not fully stabilise after application of the Activon Tulle dressing within the measurement time period.

5.5.2 Aquacel

The Aquacel dressing when fully immersed in 20ml of solution had a pH value of 4.51 this is described in **Section 5.2.1**. The Aquacel dressing was applied to the solution A after 120 seconds of testing.

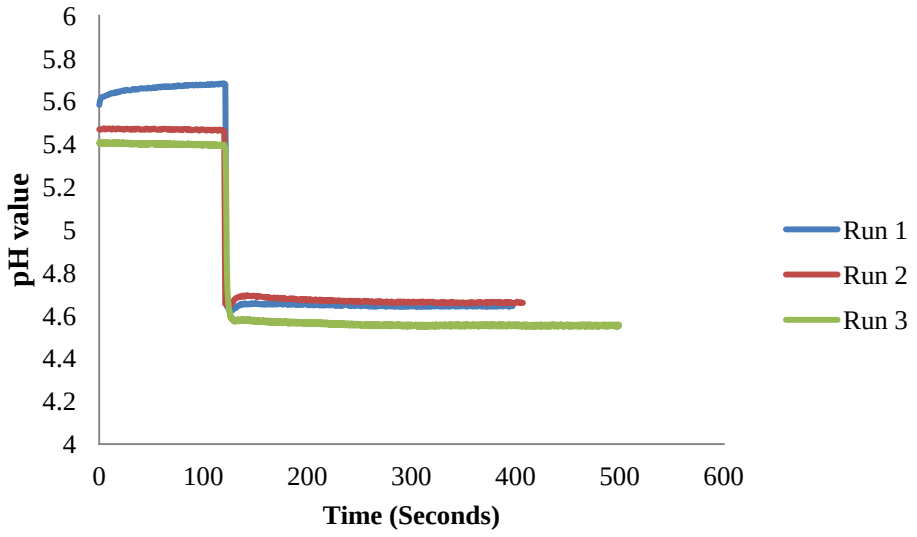

Figure 5.3 Aquacel in Solution A dressing added after 120 seconds.

Figure 5.3 illustrates the pH change in a 10ml solution after application of the Aquacel dressing. The Aquacel dressing produces a very sharp change in pH after application of the dressing. The pH value after the application of the Aquacel dressing at 390 sec is 4.65, 4.66 and 4.55 for run 1 to 3 respectively. The potential is stable once the dressing has been applied.

5.5.3 Tegaderm

The Tegaderm dressing when fully immersed in 20ml of solution had a pH value of 3.25 this is described in **Section 5.2.1**. The Tegaderm dressing was applied to the Solution A after 120 seconds of testing.

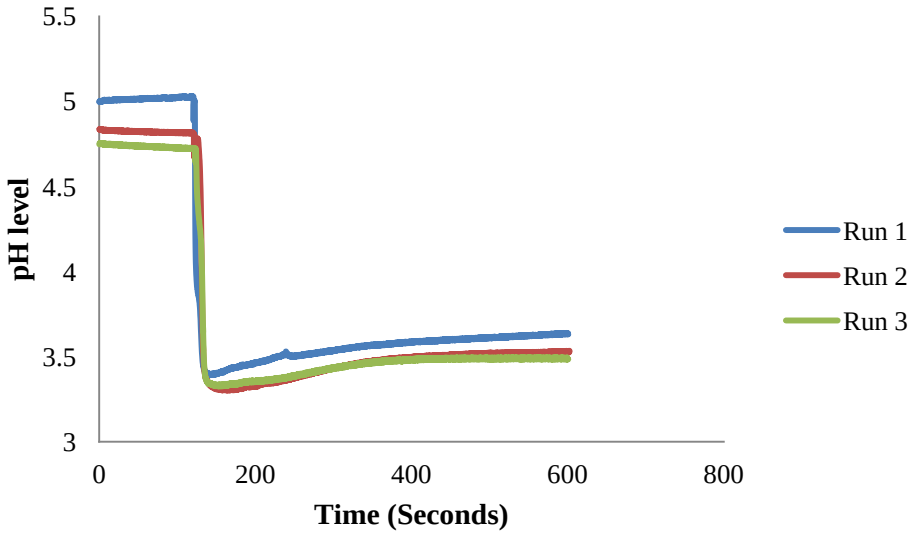

Figure 5.4 Tegaderm in Solution A dressing added after 120 seconds.

Figure 5.4 shows the pH response of Solution A after application of the Tegaderm dressing. At 150 seconds the pH of the three runs is 3.44, 3.31, 3.33 for run 1 to 3 respectively. This pH result will not be fully accurate as the pH level of the solution is below the range of the sensor. The pH changes over time until is stabilises at 3.61, 3.52 and 3.48 for run 1 to 3 respectively after 500 seconds. The Tegaderm produced pH values above the measured pH of hydrated Tegaderm in **Section 5.2.1** this is caused by the pH being below the carbon membrane pH sensor range.

5.5.4 Promogran

The Promogran dressing when fully immersed in 20ml of Solution A had a pH value of 2.3 this is described in **Section 5.2.1**. The Promogran dressing was applied to the Solution A after 120 seconds of testing.

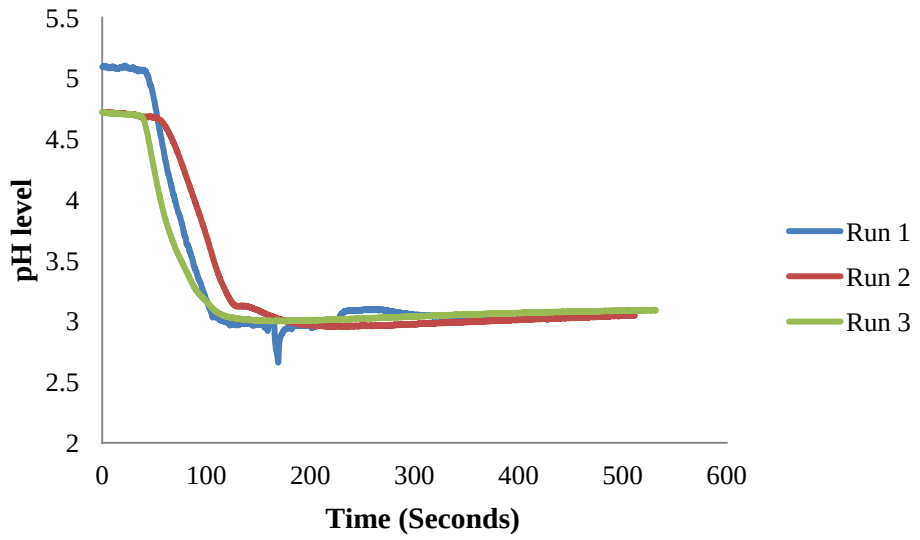

Figure 5.5 Promogran in Solution A dressing added after 30 seconds.

Figure 5.5 shows the pH change when the Promogran dressing is applied to the Solution A. The Promogran is more acidic than the performance range of the sensor so the final pH is limited by the performance of the sensor. The drop in pH is more gradual than the other dressing types shown. This could be due the dressing taking a longer time to absorb the liquid when placed on the wound sensor model. The pH value after the drop is 2.97, 3.09 and 3.00 for sensor 1 to 3 respectively. The Promogran produced pH values above the measured pH of hydrated Promogran in **Section 5.2.1** this is caused by the pH being below the carbon membrane pH sensor range.

5.5.5 Summary Solution A testing

All sensors displayed pH change when the dressing was applied. The Activon Tulle, Aquacel and Tegaderm showed an almost instantaneous pH drop which indicates fast absorption of the pH dressing into the solution A. The Promogran had a smaller gradient and took around 90 seconds to settle at a steady pH - this was caused by slower absorption with the wound dressing. Both the Tegaderm and Promogran dropped to pH levels out with the range of the sensor and hence the values recorded are not accurate once the pH drops below the lower limit of 3.5 for the pH electrode.

The results of the Solution A wound bed simulation are discussed in detail in **Section 6.10.3**.

5.6 Horse Serum

The same method was used as for the Solution A testing but the Solution A was replaced with a 50/50 mixture of horse serum and Solution A. The full method for this is found in **Section 3.13**. The horse serum and Solution A mix was used to produce a less viscous wound exudate for the testing of the dressings. The buffering capacity of horse serum is discussed in **Section 2.14.1**. The larger the acid salt disassociation the larger the pH drop when no buffer but when a buffer exists then the concentration and disassociation of acid on the wound dressings will influence the pH change this is discussed further in **Section 2.14**. The buffering capacity of horse serum will enable the different concentrations of acid in the wound dressings to be observed by the pH response.

5.6.1 Activon Tulle

The Activon Tulle dressing had a pH of 3.49 when immersed in a 20ml Solution A mixture this is described in **Section 5.2.1**. The dressing was added to the horse serum solution after 120 seconds.

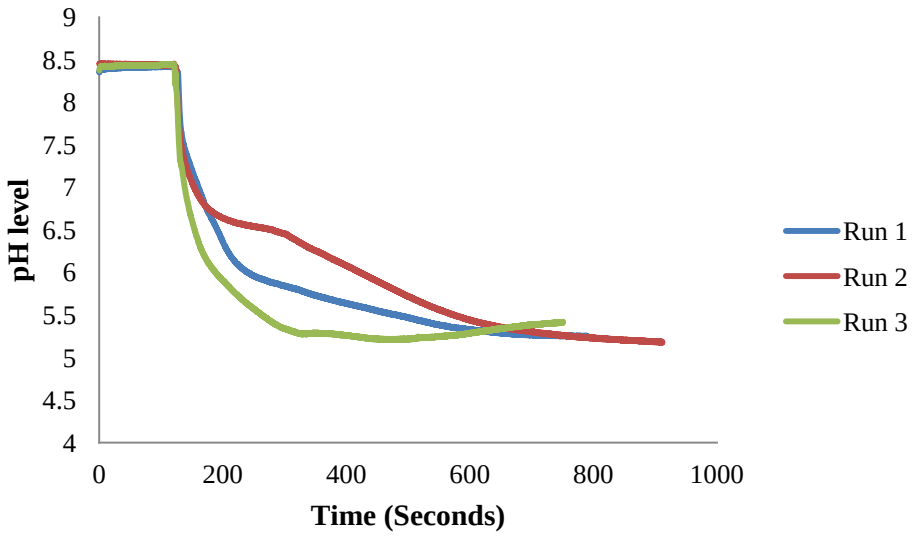

Figure 5.6 Activon honey dressing in 10ml horse serum/Solution A mixture (n=3).

Figure 5.6 shows the change in pH level when the Activon Tulle is applied after 120 seconds. The glass electrode pH meter readings of the horse serum mixture are 8.48, 8.41 and 8.41 respectively for runs 1 to 3. The initial pH reading for the printed sensor couple are 8.41, 8.45 and 8.43 after 60 seconds respectively for runs 1 to 3. Once the Dressing has been applied the drop is more gradual than with the Solution A alone. The pH stabilises at 700 seconds the readings are 5.27, 5.31 and 5.38 for runs 1 to 3 respectively. The mean pH change is 3.11 for the three sensors. The results of the change in pH are discussed in more detail in **Section 6.10.4**.

5.6.2 Aquacel

The Aquacel dressing when fully immersed in 20ml of Solution A had a pH value of 4.51 this is described in **Section 5.2.1**. The Aquacel dressing was applied to the horse serum mixture after 120 seconds of testing.

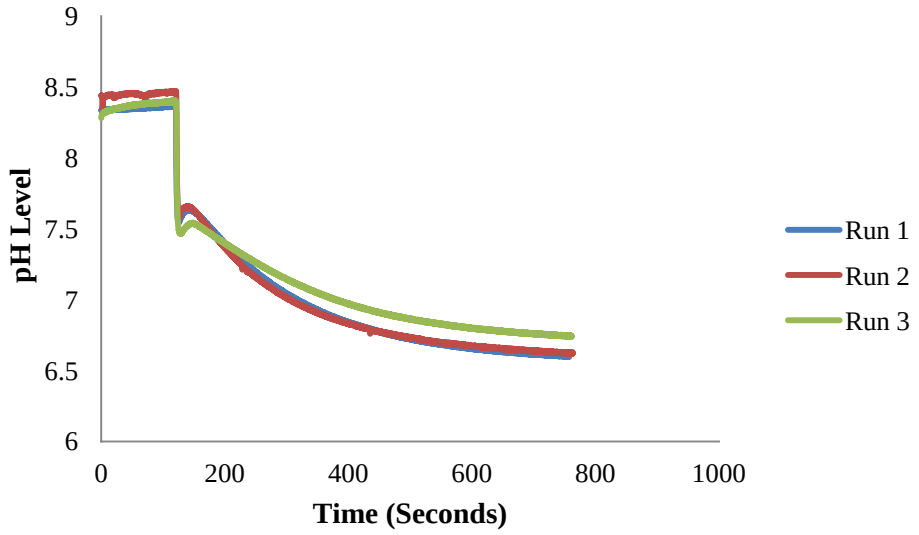

Figure 5.7 Aquacel in 10ml horse serum/ Solution A mixture (n=3).

Figure 5.7 shows the change in pH level when the Aquacel is applied after 120 seconds. The glass electrode pH meter readings of the horse serum mixture are 8.50, 8.50 and 8.38 respectively for runs 1 to 3. The initial pH reading for the printed sensor couple are 8.36, 8.44 and 8.38 after 60 seconds respectively for runs 1 to 3. After the application of the Aquacel dressing there is a sharp drop to 7.60, 7.64 and 7.48 respectively for runs 1 to 3. After this initial drop the pH gradually reduces until

it stabilises at pH 6.60, 6.62 and 6.74 for runs 1 to 3 respectively after 750 seconds. The average drop in pH is 1.74. The small reduction in pH with application of the dressing indicated that the concentration of acid is lower than the other dressings tested.

5.6.3 Tegaderm

The Tegaderm dressing when fully immersed in 20ml of Solution A had a pH value of 3.25 this is described in **Section 5.2.1**. The Tegaderm dressing was applied to the horse serum mixture after 120 seconds of testing.

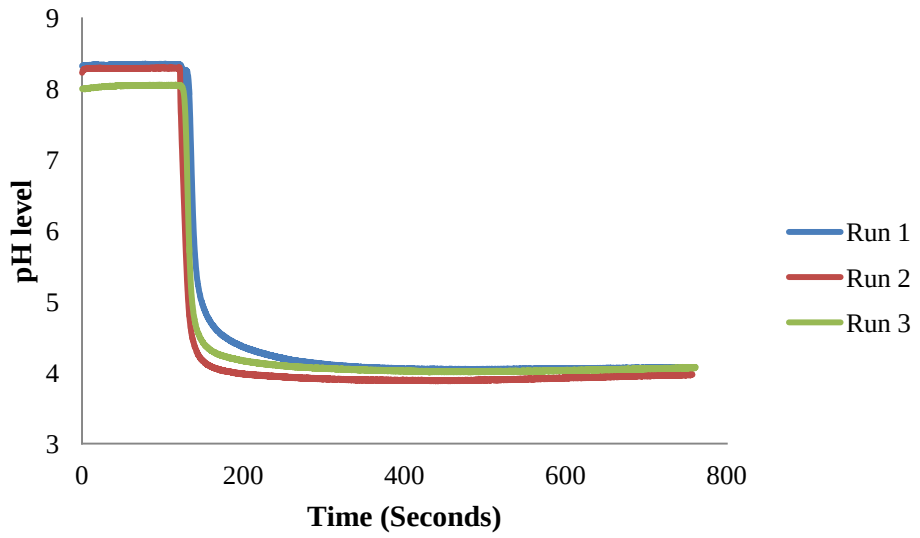

Figure 5.8 Tegaderm in 10ml horse serum/ Solution A mixture (n=3).

Figure 5.8 illustrates the change in pH level when the Tegaderm is applied after 120 seconds. The pH meter readings of the horse serum mixture are 8.42, 8.42 and 7.90 respectively for runs 1 to 3. There is a difference in the horse serum pH as this is due to a new batch of horse serum being used for run 3. The initial pH reading for the printed sensor couple are 8.33, 8.30 and 8.04 after 60 seconds respectively for runs 1 to 3. After the application of the dressing there is a sharp drop in pH and a fast stabilisation of pH. The pH once stabilised after dressing application is 4.18, 3.93 and 4.09 for runs 1 to 3 respectively after 250 seconds. The Tegaderm produces the fastest stabilisation of pH of all the dressing types tested. The average drop in pH after the dressing application is 4.15. The Tegaderm shows the largest drop in pH of

all sensors and the sharpest drop which indicates that the Tegaderm has the highest acid concentration of all the dressings tested.

5.6.4 Promogran

The Promogran dressing when fully immersed in 20ml of Solution A had a pH value of 2.3 this is described in **Section 5.2.1**. The Promogran dressing was applied to the horse serum mixture after 120 seconds of testing.

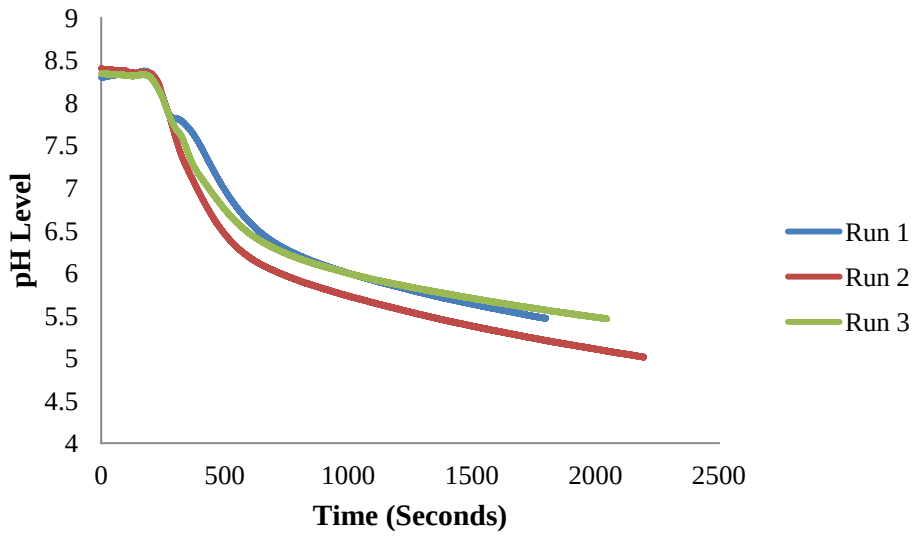

Figure 5.9 Promogran in 10ml horse serum/ Solution A mixture (n=3)**.**

Figure 5.9 illustrates the change in pH level when the Promogran is applied after 120 seconds. The pH meter readings of the horse serum mixture are 8.38, 8.40 and 8.40 respectively for runs 1 to 3. The initial pH reading for the printed sensor couple are 8.32, 8.38 and 8.33 respectively for runs 1 to 3 after 60 seconds. The Promogran does not settle as the pH continues to reduce over time. The Promogran is the only dressing tested with the horse serum mixture not to settle. After 1750 seconds the pH was 5.49, 5.24 and 5.58 respectively for runs 1 to 3. The average drop in pH after application of wound dressing is 2.91. The long settling time could be due to the absorption of the horse serum into the Promogran dressing. This would affect the concentration of acid in the solution if full absorption is not achieved.

5.6.5 Summary horse serum testing

The results with horse serum produced interesting results due to the buffering capacity of the horse serum mixture. The buffering capacity of the horse serum meant that all the pH values measured were within the pH sensor range. The Tegaderm produced the largest voltage drop which indicates that it has the strongest acid content in the wound dressing. The Activon Tulle honey dressing showed the second largest pH drop. The Aquacel shows the smallest pH drop that indicates that it has the lowest acid strength out of all the dressings tested. The Promogran although shown previously to have the lowest pH in Solution A did not produce the lowest pH when hydrated in horse serum this indicates that the acid concentration is less than the Tegaderm dressing. The Promogran gradual pH decline could relate to the time needed for full absorption to allow the full concentration of acid to be absorbed into the horse serum mixture. The Promogran and Activon Tulle show similar acid concentrations as they both reduce by similar pH values. The wound bed simulation testing is further discussed in **Section 6.10.4**.

Chapter 6 - Analysis and Discussion

The main aim of this study was to design a disposable pH sensor system that will measure and display the pH of wound fluid or wound dressing. To achieve this aim a pH sensor was designed, fabricated and characterised and its operation in a wound bed model was tested. This final chapter will discuss and analyse the results which are detailed in **Chapter 4 and Chapter 5**.

6.1 Formation of polypyrrole on screen printed electrodes

The initial experiments were made to test if polypyrrole conducting polymer would polymerise and adhere to a screen printed carbon electrodes. The conducting polymers are used as ion to electron transducers and are used in solid state electrodes to replace the liquid junction which should enable the sensors to provide a stable voltage response. This mechanism is further detailed in **Section 2.10.4**. The formation of conducting polymers on screen printed carbon electrodes has not been widely studied in the literature with only an investigation on the polymerisation of polypyrrole on different screen printed substrates (Li et al., 2005) and one reported use of polypyrrole formation in a screen printed hydrogen peroxide sensor (Li and Wang, 2007). If successful this technique would enable research on conducting polymers that used platinum wire and glassy carbon rods as electrodes to be transferred and applied to inexpensive disposable electrodes.

6.1.2 Conducting polymer and screen printed carbon surface images

The Scanning Electron Microscope (SEM) was used to obtain images of the surface structure of the deposited conducting polymers and surface of the screen printed carbon electrode. The optimum cyclic voltammetry triangular sweep of 0 to 3 volts with a 100mV/s scan rate was chosen from the literature as this had previously been shown to produce smooth coatings of polypyrrole (Segut et al., 2007). Cyclic voltammetry from 0 to 3 volts with a 100mV/s scan rate was used to coat the carbon electrodes with a number of cycles of 1, 3 or 5 cycles. The purpose of this was to determine the optimum layer of coating for application of an ion-selective

membrane. The ideal membrane coating should be smooth to ensure that the membrane could be coated evenly and without leaving air pockets that could fill with a water layer during measurement and affect the sensor performance.

The screen printed carbon electrode SEM (**Figure 4.2)** shows that it has a flake like structure these flakes are the particles of graphite that constitute the carbon ink. The rough surface structure means that the surface area of the carbon electrode is increased (Musa et al., 2011). A larger surface area should result in higher electrode double layer capacitance which can help improve the voltage stability of the carbon membrane sensor. A larger double layer capacitance will lead to less voltage drift as a larger charge will be needed to charge the double layer interface and change its voltage potential (Bobacka, 1999). This benefit is discussed further in **Section 2.6**.

The polypyrrole doped with Cl^- ions was chosen for these tests as it had previously displayed a stable structure and sensitivity to hydrogen ions when compared against other dopant ions by Michalska and Maksymiuk (2003). The structures of 1 and 3 cycles were the most uniform in appearance with spherical domes covering the surface of the carbon. The 5^{th} cycle showed growth of branch like structures growing from the surface of the polypyrrole. This is shown in **Figure 6.1**. The growth of these structures is similar to what is reported in the literature (Shiu et al., 1999). The rapid growth of structures from the conducting polymer could be due to lowering of polymerisation potential values as the polymer chains become longer (Cosiner and Karyakin, 2010). This lower polymerisation potential results in the monomer being oxidised before it reaches the surface of the electrode forming the branch like structures and increasing the growth of uneven structures. The growth of the branch like structures would make any electrode with more than three cycles deposition unsuitable for uniform coverage of the sensing membrane due to the uneven surface of the conducting polymer.

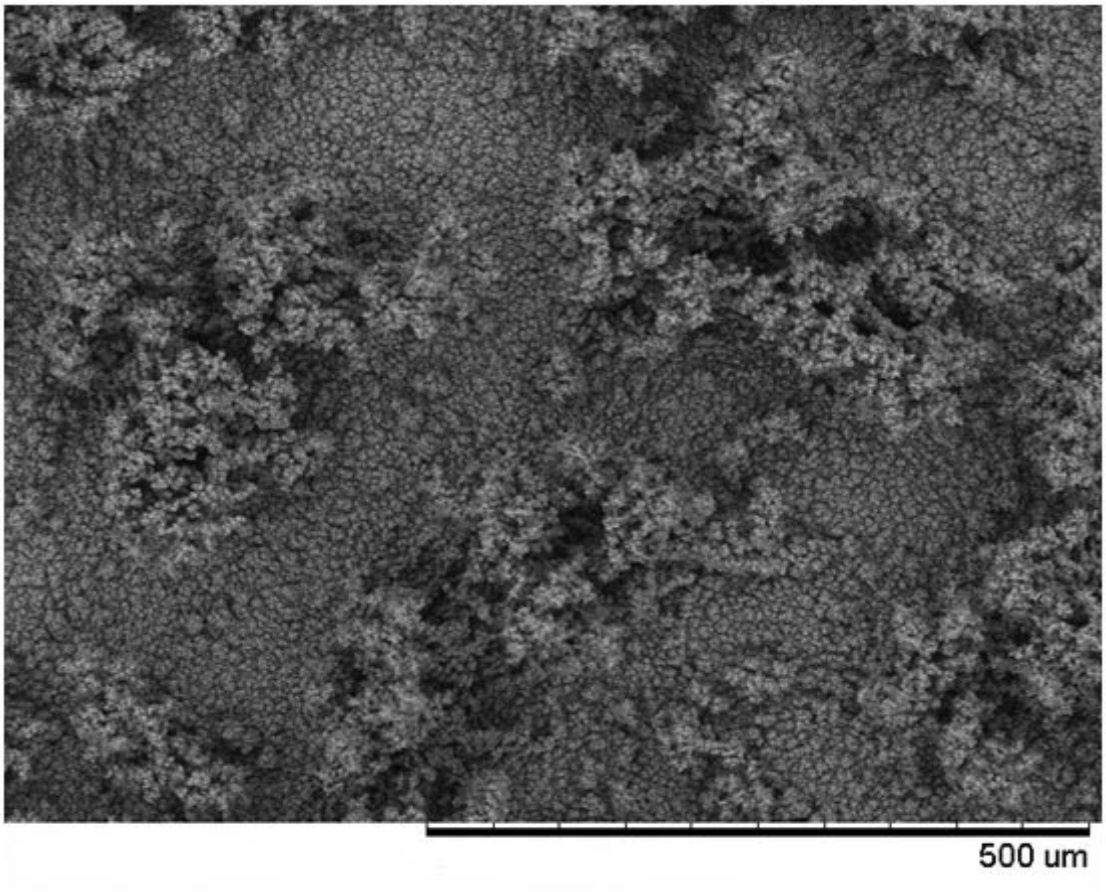

Figure 6.1 PPYCl showing uneven branch like growth at 200x magnification.

The PPY doped with PTS^- ions was chosen due to its performance in previously conducted research by Pandey and Singh (2008)as a pH sensing polymer and also to observe the effect of a larger dopant ion when compared to the Cl^- doped polymer. The structure formation is visually different from the deposits of the Cl^- doped conducting polymer. The surface appears more uniform that the PPYCl at the same number of cycles but due to the unusual chimney like growth any cycle after the third would be unsuitable for membrane coating due to the uneven surface as shown in **Figure 6.2**. Formation of similar chimney like structures has previously been reported, the reason for their formation was found to be a result of gas bubbles on the electrode surface which act as templates for the polymer to grow round during the polymerisation process. Different growth structure types were achieved depending on the polymerisation conditions and substrate material used (Qu et al., 2004). The 1 cycle and the 3 cycle depositions were the best choice to provide a smooth base surface for applying the ion-selective membrane.

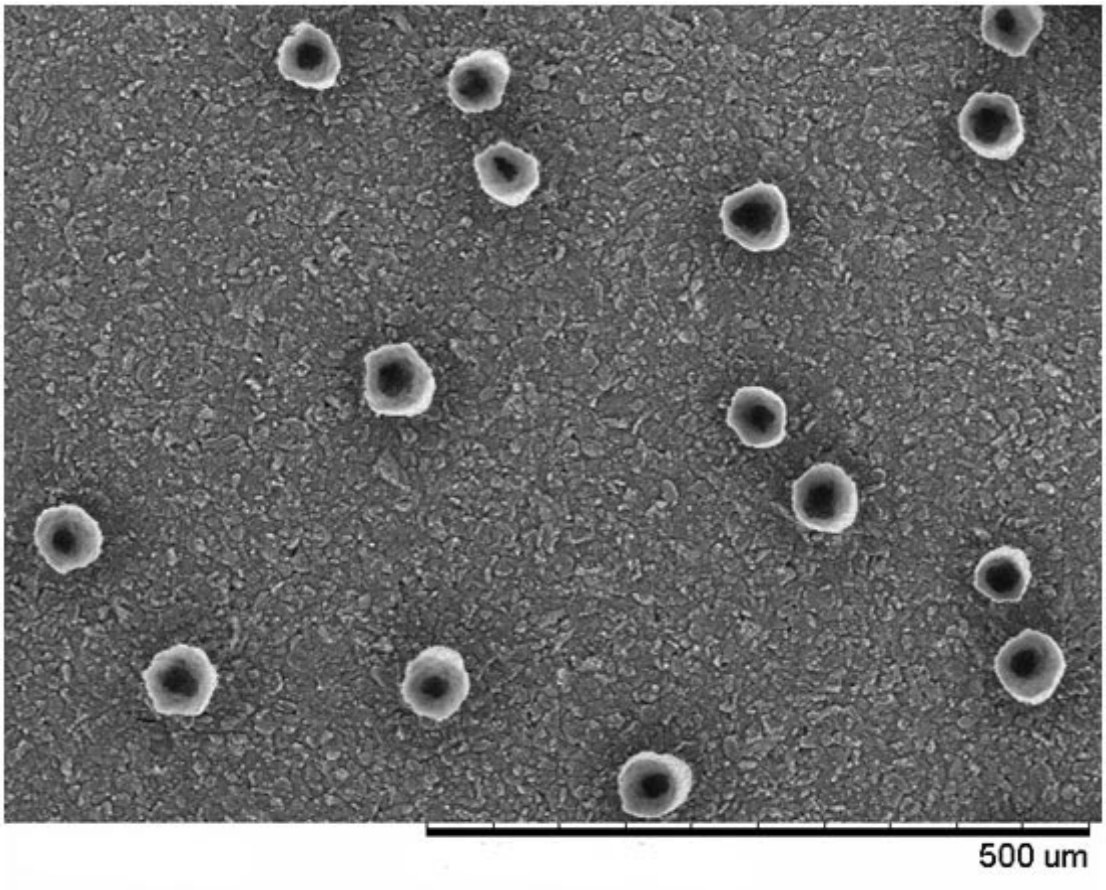

Figure 6.2 200x magnification of 5 cycle PPYPTS electrode showing unusual chimney type growth.

The 3 cycle deposits of both the PPYCl and PPYPTS were chosen to be used in the sensor experiments as they both had uniform coatings of the conducting polymer. These with the screen printed PEDOT polymer were used in the next stage of testing to assess their effect on the sensing ability of the Biodot deposited pH ion-selective membrane.

6.2 Ion-selective membrane

Before applying membranes to the conducting polymer sensors a repeatable method for depositing the ion-selective membrane was investigated. These initial experiments enabled the more complex sensors involving conducting polymers (screen printed PEDOT, electropolymerised PPYCl and electropolymerised PPYPTS) to be assessed with a consistent membrane deposition. The sensors

containing conducting polymers have been shown to provide better stability and sensing performance that coated wire electrodes; this is discussed in **Section 2.10**. The tests performed also provided information as to how the membrane thickness will affect the measurement of pH and initial settling time. The ion-selective membrane deposition and the influence of membrane thickness have not been widely discussed in the literature and this investigation gives information about an alternative deposition technique to the most commonly used manual drop-coating method.

6.2.1 Membrane deposition

The purpose of this section of testing was to find the optimum membrane coating method. The deposition method used was a Biodot Airjet system which enabled the membrane solution to be spray coated onto the substrate electrode (see **Section 3.1.4**). These tests were conducted using screen printed carbon electrodes only to find the most consistent method before being applied to conducting polymer based sensors. The initial tests found inconsistent membrane formation for hand-deposited drop coated membranes. The white light interferometer images of the sensor surface contours (**Figure 4.16**) further give evidence of the uneven membranes achieved through the drop coating method. The white light interferometer measurements showed differences of up to 0.06mm in membrane thickness across the surface of the membrane. These inconstancies would prevent a constant response for sensor voltage settling time due to different diffusion times through the membrane and this is needed to get reproducible results from the sensor (Bakker et al., 1997). The drop coating method would also not be suitable for mass manufacturing whereas the spray deposition technique has potential for mass manufacturing and producing uniform ion-selective membranes.

Membrane thickness

The sensor manufacturing using the Biodot machine resulted in different thicknesses of membrane deposition from 0.0384mm for the 75µl/cm membrane to 0.0092mm for the 12.5µl/cm membrane. Visually all the machine deposited membrane coatings covered the carbon electrode area completely apart from the 12.5µl/cm setting as it

did not seem to cover the whole sensor. This is reflected in the 12.5µl/cm sensors having the poorest results of all the sensors during the pH measurements. There is an inconsistency where the 100µl/cm has a thinner layer than the 75µl/cm deposit. When the sensors are deposited the spread of the membrane solution covers a larger area which could mean the deposit is spread thinner across the membrane in the 100µl/cm sensor. The white light interferometer results are quite similar to the micrometer measurements for the manually deposited hand, 75µl/cm and the 50µl/cm sensors this helps to validate the accuracy of the micrometer measurement technique. One of the advantages of the spray deposition technique is that it uses less membrane solution than the drop coating method for the 50µl/cm setting a total of 75µl of membrane solution was used compared to the drop coat deposit which uses 180µl. The membrane is the one of the most expensive parts of the solid state sensor so any reduction in the amount of solution needed will result in a lower cost sensor.

6.2.2 Membrane performance

Membrane deposition effect on voltage response

The voltage response is determined by the Nernst equation which is dependent on the ionophore ion recognition sites in the membrane surface and the activity of the primary ion in the solution this is described in detail in **Section 2.8.1**. The concentration of ionophore binding sites will be constant at the surface of the electrode which will result in the potential being determined by the concentration of primary ion in the solution as shown in **Equation 2.33 Section 2.8.1**. This should result in the voltage response not being affected by the different membrane thicknesses (Bobacka et al., 2008).

The hand deposited sensor showed inconsistencies in membrane deposition depth but this did not result in an inconstant voltage response to pH. This indicates that the voltage response is not affected by the different thicknesses of the membrane as the theory suggests. This result is in agreement with previous research into membrane thickness for Na^+ ion-selective membranes that demonstrates no change in voltage response with reduction in membrane thickness (Ceresa et al., 2001).

The sensor deposition method and thickness did not affect the overall response of the slope per decade significantly as shown in **Table 4.1 Section 4.3.2**. Only in the 2 thinnest deposits (25µl/cm and 12.5µl/cm) did the voltage response per decade pH start to drop off and standard deviation increase. The poorer response for these sensors is due to incomplete coverage of the carbon electrode which results in carbon being exposed and an inconsistent voltage response of the sensors. The standard deviation which shows the consistency of response helped to identify the 50µL/cm sensor as the most consistent across the pH ranges tested.

6.2.3 Initial immersion voltage settling

The initial voltage response time is important as the faster the sensors reach a stable voltage potential the sooner they are ready for measurement. The time taken to achieve a stable voltage potential is dependent on the diffusion of the primary ion into the ion-selective membrane (Bakker et al., 1997). If the membrane has not previously been immersed in a solution containing the primary ion then on first immersion the equilibrium potential value will take time to reach a stable value with ion diffusion through the ion-selective membrane. The limiting factors of the time to reach membrane equilibrium are the ion diffusion coefficient in the membrane and the diffusion distance or thickness of the ion-selective membrane (Morf et al., 2009). As the diffusion rate will be the same for all the membranes used during the experiments the limiting factor will be the membrane thickness. Once membrane equilibrium has been reached the effect of the ion diffusion is negligible and the sensor response is determined by the Nernst reaction described in **Section 2.8.1**.

The results found in **Section 4.3.3** show that the thicker the membrane deposits the larger the voltage drift and settling time. The only outlying result was the 100µl/cm which had the worst performance of all the sensors with a large drift of 7.58±0.96mV over a 30 minute measurement period. The best sensor was the 50µl/cm as this showed the lowest initial drift of 2.8±1.54mV over a 30 minute measurement period. The 25µl/cm and 12.5µl/cm have thinner membranes but due to their inconsistency relating to the incomplete coverage of the carbon surface they had inconsistent settling times. From the results it can be concluded that the thinner the complete membrane coverage the smaller the sensor initial drift which is in agreement with the

theory. In the literature almost all sensors are subjected to preconditioning where the membrane is immersed in a solution containing a concentration of primary ion to allow the ion to diffuse into the ion-selective membrane before testing so the initial drift times are not observed as the membrane is has already reached equilibrium. The effect of preconditioning is further discussed in **Section 6.4.3**. The thinner the membrane the faster the diffusion of ions through the membrane, this will lead to the equilibrium of ion concentrations being achieved faster and the sensor will stabilise quicker when immersed for the first time in a new solution. This due to the reduced time for ion transport (Bakker, 2011). This is an important factor in the design of a disposable sensor as if it is intended for a one time use device then the first immersion stabilisation time is important as it ideally needs to be as short as possible to enable fast measurement times.

6.3 Sensor manufacture

The manufacturing of the four sensor types (carbon only, screen printed PEDOT, electropolymerised PPYCl and electropolymerised PPYPTS) produced some unexpected problems. The Biodot machine spray deposition method was used to deposit the optimum 50µl/cm membrane deposit onto the four sensor types. The deposition technique uses an air pressurised air spray to deposit a set amount of membrane solution. The deposition method produced consistent membranes on the carbon only (**Figure 4.18**) and electropolymerised sensors (**Figure 4.23**).

The PEDOT electrode was not coated effectively using this method as bubbles were formed on the electrode surface as shown in **Figure 6.3**. These bubbles formed on all the PEDOT sensors produced. The PEDOT conducting polymer is said to have regions of hydrophilic and hydrophobic properties (Mathiyarasu et al., 2008)(Veder et al., 2011). The PSS dopant ions are responsible for the hydrophilic regions and the PEDOT conducting polymer chains cause the hydrophobic region (Xia and Ouyang, 2011). The difference in surface properties of PEDOT could affect the settling of the spray deposited membrane. Once the membrane dries the bubbles that form during membrane application appear to form holes in the membrane direct to the screen printed layer. Many electrodes were produced using the Biodot all of which formed

bubbles in the membrane. The formation of the bubbles in the ion-selective membrane will result in large membrane inconsistencies between PEDOT sensors.

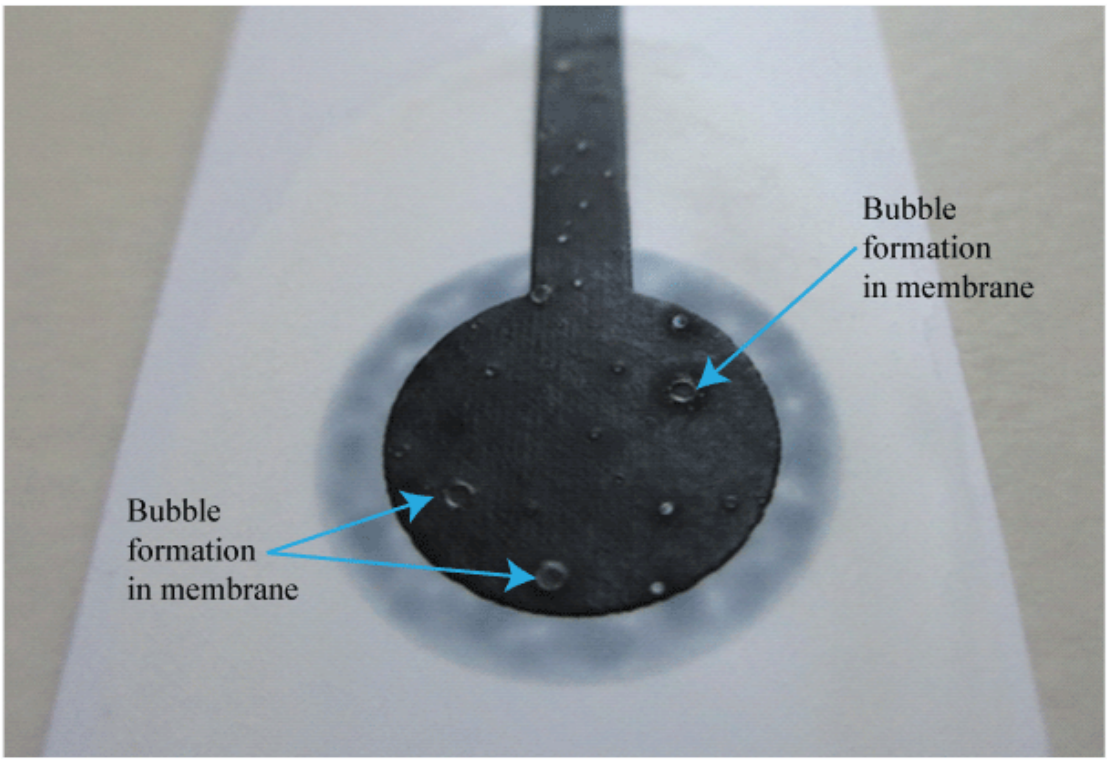

Figure 6.3 Surface of PEDOT electrode after application of Biodot machine deposited ion-selective membrane showing bubble formation in membrane.

6.4 Full sensor testing

6.4.1 Voltage response

The results of the Voltage response graphs show that all four sensors have a linear voltage response to the change in pH. The voltage response should be determined solely by the ion-selective membrane as discussed in **Section 2.8.1** (Bakker et al., 2004). Any vast difference in voltage level between sensors coated with the same membrane solution suggests other issues with the sensor performance as factors other than the membrane are determining potential (Lindner and Gyurcsányi, 2008). Within the literature there are many reports of a change in voltage response with a change in the mid layer of the electrode (Musa et al., 2011)(Han et al., 2003a).

Changes in voltage response values could indicate additional reactions taking place within the sensor to determine the overall potential.

The carbon membrane electrode was the best performing sensor the largest voltage response of 52.46±0.1mV/per decade change in H^+ ion. The carbon sensor also had the smallest standard deviation between sensors this indicates that the carbon membrane sensors were the most consistent of all the four sensor types tested. The voltage response of the sensor should only be determined by the ion-selective membrane, hence, it was expected that there would not be much variation in voltage response between the sensor types. The electropolymerised sensors had similar standard deviations but the response of the PPYPTS was 4.55mV per decade change in H^+ concentration less than the PPYCl electrode of 52.32±0.84mV/decade change H^+ ion concentration. This difference in voltage response to change in pH indicates that there is another process which is affecting the response of the electropolymerised sensors. It could be related to the water layer formation discussed in S**ection 6.5**. The PEDOT was the worst performing sensor with the lowest voltage response to pH change and a high standard deviation value. The poor performance of this sensor is due to the bubbles formed in the membrane during manufacture which results in inconsistent membranes.

Sensor type (paper)	Response slope
Printed carbon experimental best performing sensor tested	52.46±0.1mV/decade
Liquid junction using same membrane formation (Schulthess et al., 1981)	57.8±0.1mV/decade
Solid state carbon nanotube pH sensor with PMMA ion-selective membrane (Crespo, Gugsa, et al., 2009)	58.8±0.4mV/decade
Solid state polypyrrole Cl- doped ion-selective PVC membrane pH sensor (Han et al., 2003a)	54.8±2.3mV/decade
Screen printed carbon pH sensor with PVC ion-selective membrane (Musa et al., 2011)	51.7mV/decade

Table 6.1 Slope response comparison with literature for different sensor types.

The sensors all had a response below the ideal theoretical Nernstian value of 59.16mV/decade change in H^+ ions at 25^{o}C (Bockris and Reddy, 2000). **Table 6.1** details the response of similar sensors taken from the literature against the best performing carbon membrane sensor. The original paper that the membrane formulation was taken from reported a response of 57.8±0.1mV/decade change in H^+ ion concentration (Schulthess et al., 1981). This voltage response was 5.34mV/decade change H^+ ion concentration larger than for the best performing screen printed electrode (Carbon membrane). A direct comparison between these is difficult to make due to the different measurement arrangement of use in a liquid junction electrode similar to the standard glass electrode with the glass membrane replaced by the ionophore based membrane. Other factors such as slight differences in membrane formulation could result in this reduced response for the screen printed sensors. The carbon membrane sensor was below the ideal Nernst response value, further experimentation of the ion-selective membrane composition could provide a greater voltage per decade response. The sensor developed by Musa is similar to the carbon membrane sensor as it was screen printed with a drop coated membrane the

sensors having similar voltage response. It is difficult to compare the reported values in the literature due to different ion-selective membrane components and experimental arrangements so they can only be used as a reference for the voltage response range to expect. Many papers in the literature focus on getting a Nernst voltage response to the primary ion but this is not the only important factor as the sensor needs to display a consistent voltage response. The screen printed sensors with spray deposited ion-selective membranes have a standard deviation of 0.1mV which indicates that the manufacturing technique produces consistent sensors.

6.4.2 Sensor repeated use long life testing

The long life sensor investigation retests the original sensors after 60 days of storage in a dry dark environment at room temperature. The aim of the test is to assess if there is any change in voltage response performance over a 60 day time period while the sensor is in storage. This type of test is not reported often in literature but it is important that a sensor can still operate effectively after being in storage. The carbon membrane sensor had the smallest change in voltage response to pH of only 0.046mV/ decade change H^+ ion concentration which implies that it is the most stable of the four sensors tested. This could be due to the simplicity of the sensor manufacturing technique. Another factor could be the bonding of the membrane to the carbon as this would achieve a good seal to prevent a liquid layer forming which would disrupt the performance of the sensor this is further discussed in **Section 6.5**. Within the literature the membrane plasticiser has been shown to improve the lifetime of the sensor with DOS plasticiser giving the membrane a 5 month lifetime (Delosaaradaperez, 2003). Other research for screen printed chloride selective electrodes found that carbon membrane electrodes reduced in response over a two month period due to organic compounds in the carbon ink (Zielinska et al., 2002). The stability of the carbon membrane electrode indicates that it will have a lifetime of at least 60 days; further testing will have to be conducted to find the full lifespan of the sensor. The PPYCl and PEDOT had reduced voltage response to change in pH after 60 days where as the PPYPTS voltage response increased slightly. The conducting polymer based sensors did not perform well in these experiments showing a drop of up to 5.34mV/decade change H^+ ion concentration over the 60 day

period for the PEDOT based sensor. The change in performance with could be due to a number of factors such as water layer formation between the conducting polymer and membrane (Marco et al., 2008) or spontaneous charging/discharging of conducting polymer which could lead to change in voltage potential (Dumanska, 2002). Water layer formation if further discussed in **Section 6.5**.

6.4.3 Full sensor initial immersion voltage settling

The test for sensor settling immersed a new unconditioned electrode into pH 4 buffer solution and the time for the sensor to reach a stable voltage was then measured. This is achieved when the membrane is in equilibrium with the solution and is driven by membrane diffusion times (Bakker et al., 1997). The aim of this test was to assess the initial voltage drift from first immersion over a 30 minute time period. The drift occurs while the membrane and conduction polymers equilibrate through diffusion of ions from the solution. The initial sensor drift is an important factor in sensor design as the ideal sensor would not need preconditioning and would settle within seconds of initial immersion. As discussed earlier in the same experiments for the membrane assessment (**Section 6.1.2**) it is of practical importance that the sensor has short settling equilibrium times. This factor is not widely studied in the literature as most papers state only the preconditioned values of the sensor performance. A long preconditioning time would cause practical problems in the use of the sensor. Within the literature some sensors require up to 48 hours of preconditioning to achieve stable potentials (Musa et al., 2011)(Crespo, Gugsa, et al., 2009). To get around the problem of preconditioning times storage in a humid storage box was proposed (Chen and Chou, 2009), however, this may cause further complications in sensor degradation which would have a negative effect on the sensitivity of the electrode. Other possible solutions could be investigated to see the effects of different preconditioning techniques to improve the stability time for the end user of the device.

The carbon electrode was the best performing with an initial drift of 6mV for the 30 minute test period. After 30 seconds immersion the sensor settled to within 4mV of the potential at the 30 minute mark. All the conducting polymer based sensors had large voltage drifts across the first 30 minutes in the range 16.01mV-39.3mV. This

indicates that the conducting polymer needs time to equilibrate when initially immersed in a solution as oxidation or reduction of the conducting polymer chains can still occur with integration of the H^+ cations into the conducting polymer (Michalska and Maksymiuk, 2005). This is described in **Section 2.10.3**. The large drifts could also be caused by a reaction with the liquid since, if a water layer forms, this will produce a change in the voltage response. The voltage drift in the experiments for conducting polymers was greater than that reported elsewhere for similar screen printed sensors (Gyurcsányi et al., 2004) where a drift of 5.8mV was reported over the first 30 minutes. This highlights that the problem could be linked to water layer formation as further discussed in **Section 6.5**. After immersion in the initial solution the electrodes stabilise quickly on the next immersion. The first immersion will always take the longest to stabilise due to the diffusion and integrations of cations from the solution into the membrane and conducting polymer. Once the membrane has been equilibrated with primary ions the response of the sensor is determined by the surface concentration of ionophore ion complex and activity of the measurement solution. This is discussed in more depth in **Section 2.8.1**. Thinner membranes help with producing faster equilibrium times due to shorter diffusion times as discussed in **Section 6.1.2.** The thin membrane the basic screen printed carbon electrode produces the fastest initial stabilisation times for the sensors.

6.4.4 Selectivity

The selectivity is important as it determines the limit of operation of the sensor to the primary ion when interfering ions are present. The sensors intended use is for measuring wound fluid pH. The molar content of potential interfering ions in wound fluid has been reported as being in a similar range as blood with ion concentrations being Na^+ 140mM, Cl^- 119mM, K^+ 5mM, Ca^{2+} 1mM (Martini, 2006). The absolute molar concentration range of salts within wound in unknown as it will change with evaporation and absorption in dressings. This change in concentration of salts in wound fluid should not be a problem if the sensor has high enough selectivity to the interfering ions. The ions that could affect the performance of the sensor are the cations K^+, Na^+ and Ca^{2+} that are found in physiological solutions. These tests found

the selectivity coefficients of the four sensor types to the highest concentrations of interfering ions. Lithium ions were also tested although they are not present in physiological solutions they have a smaller ion size than the other ions that were tested and are therefore more challenging to the membrane.

The selectivity coefficients are proposed by the IUPAC as a method of assessing the selectivity of an ion-selective membrane (Buck and Lindneri, 1994). The selectivity coefficient gives a numerical value of the selectivity of an ion-selective membrane. The formula used to calculate the selectivity coefficient is given in **Equation 6.1**, it is derived from the Nikolski-Eisenmann equation given in **Equation 2.36 Section 2.8.2**.

$$\log K_{I,J} = \frac{(E_j - E_I)z_i F}{2.303RT} + \left(1 - \frac{z_I}{z_j}\right) lga_I \qquad \textbf{Equation 6.1}$$

Where $\log K_{I,J}$ is the selectivity coefficient, E_j the interfering ion voltage potential at 1 Molar activity, E_I the primary ion activity at 1Molar activity and z_I and z_j the charge of the primary and interfering ion respectively.

The separate solution method was used to find the selectivity coefficient using **Equation 6.1**. The results (**Section 4.5.4**) show that the carbon membrane sensor was the most selective with the highest selectivity coefficients across all interfering ions. The selectivity is decided by the membrane so the difference in results between the carbon membrane sensor and the three conducting polymer based sensors suggests that there is another factor affecting their selectivity such as formation of water layer or the interfering ion reacting with the conducting polymer.

The ion-selective membrane formula was taken from a paper that used the same membrane formulation in a liquid junction electrode to replace the glass membrane (Schulthess et al., 1981). **Table 6.2** details the reported selectivity coefficients of this ion-selective membrane used in a liquid junction type electrode. Also reported is the selectivity measurement for a glass pH electrode. The selectivity is lower for all the screen printed electrodes tested this could be down to a number of factors: different

method of membrane operation, slight changes in membrane component ratios due to some of the ingredients such as ionophore being used in such small quantities accurate measurement becomes difficult.

Sensor type	Selectivity Na+	Selectivity K+	Selectivity Ca2+
Printed carbon experimental best performing sensor	-5.38	-5.46	-5.29
Liquid junction using same membrane formation (Schulthess et al., 1981)	-10.4	-9.8	-11.1
Glass ph electrode (Galster, 1991)	-15	n/a	n/a

Table 6.2 Selectivity coefficients of other membrane based sensors from literature the larger the value the better the selectivity.

The selectivity should be solely determined by the composition of the ion-selective membrane and change from sensor to sensor would suggest that there are other factors that determining the electrode potentials (Bakker et al., 2004). The conducting polymers had lower selectivity than the carbon membrane sensor with the water layer described in **Section 6.5** a possible reason for the lower selectivity values. Various solid state pH sensor papers detail the selectivity coefficients but it is difficult to do a direct comparison.

Due to the flat voltage response to interfering ion concentrations of all pH sensor types tested only the maximum activity selectivity values could be reported. The maximum voltage response across the concentration range of interfering ion solution for each ion type (K^+, Na^+, Ca^{2+} and Li^+) was used to calculate the selectivity coefficient due to the absence of a Nernst response to the interfering ions tested. The flat voltage response to the interfering ion means that only the maximum selectivity values can be calculated from these results (Bakker et al., 2000). Bakker states that

the maximum selectivity may be lower than the actual selectivity of the pH sensors using this method. This introduces some uncertainty into the results as the International Union of Pure and Applied Chemistry (IUPAC) ion-selective electrode guidelines do not recommend using these interference tests for interfering ions that do not show Nernstian response to the interfering ion (Buck and Lindneri, 1994). These selectivity tests are designed for use in liquid junction electrodes so they may be unsuitable for solid state electrodes that display flat voltage responses to interfering ions.

The original IUPAC document recommends that for electrodes that do not show a Nernst response to the interfering ion that the interference be assessed using a fixed interference method which uses similar levels of interfering ions that the electrode may encounter during use. The carbon membrane electrode was tested for voltage response to pH with solutions that included physiological levels of salts (**See Section 3.3.4**). The response to a solution with the salts and without is shown in **Figure 6.4**.

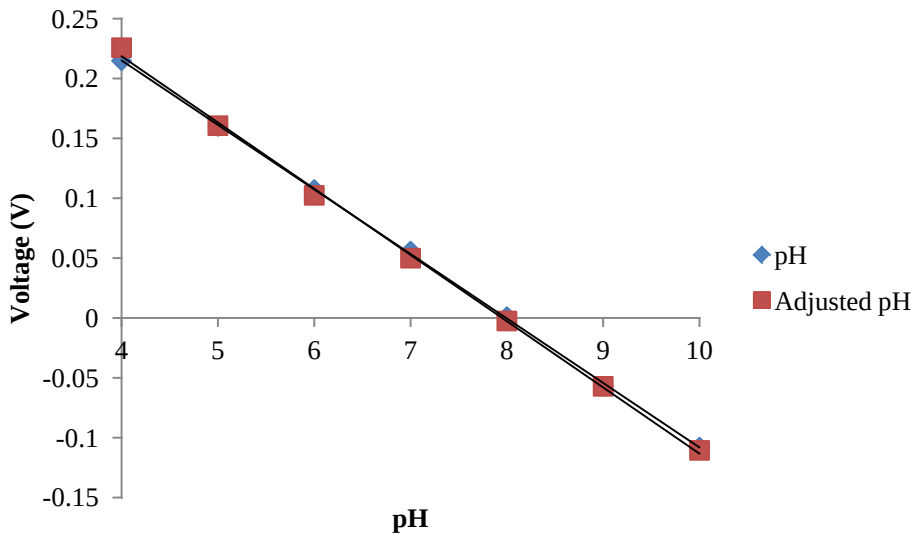

Figure 6.4 Voltage response of screen printed carbon membrane sensor to pH solutions (blue) and pH response to solutions containing Solution A levels of ionic salts.

Figure 6.4 illustrates that when the pH solution is adjusted with physiological salt levels it produces a similar sensing response to the pH solution without adjusted salt

levels. It is important that the sensor could perform effectively when in contact with ions found in significant concentrations in wound fluid. This demonstrates that although the selectivity coefficients calculated using Bakker et al (2000) recommendations are lower than expected, the response to physiological salt levels of interfering ions within a solution does not affect the performance of the sensor.

6.4.5 Sensor hysteresis

The four different sensors were tested to show any change in voltage potential at each pH level when immersed in consecutive pH solutions from pH 4 to pH 10 then from pH 10 to pH 4 as reported in **Section 4.5.5**. The sensors would be expected to show no change in voltage at each pH level tested. The carbon membrane had similar voltage performance at each pH level tested and was the best performing sensor. The PEDOT electrode suffered from very high standard deviations which would relate to the inconsistent membrane application. The conducting polymer based sensors showed consistent performance when the slope per decade was calculated but there was an issue with repeatable voltage values. The conducting polymers experienced large changes in potential between the voltage recorded on the first and second cycle. This indicates that there is an issue with the conducting polymer sensors as the change in potential would make these sensors very unreliable for measuring pH. The change in potential could be caused by a water layer between the conducting polymer and membrane that changes content with successive measurements and produces different measurements (Lindner and Gyurcsányi, 2008).

6.5 Water layer testing

The previous tests indicated poor performance of the conducting polymer based sensors. This test would investigate if the problem was due to formation of a water layer which is a common problem in solid state sensors (Marco et al., 2008). The test immerses a sensor in a pH4 solution for 1 hour then immersed it in pH 10 for 1 hour then again in pH 4 for 2 hours. If a liquid layer is formed a voltage drift will be observed when moving from one solution to another. The carbon membrane sensor and the two electropolymerised polypyrrole sensors were tested for water layers. The

PEDOT based sensor was not tested due to inconsistent membranes and poor performance in previous tests.

6.5.1 Carbon sensor

The results showed that the carbon membrane sensors preformed well showing a voltage drift of only 3.23±0.41mV (n=3) over the two hour period in the second immersion in the pH 4 solution. The voltage potential was only 1.43±1.17mV (n=3) different between the last final measurement in the first pH 4 solution to the final measurement in the second pH 4. These results show little drift between the solutions and show that the carbon membrane electrode did not show any evidence of a water layer between the carbon contact and the ion-selective membrane. It is well documented in the literature that membrane adhesion plays a large role in preventing water layer formation and providing long time stable sensors (Fibbioli et al., 2000). Different methods of improving membrane adhesion have been used such as increasing surface roughness (Musa et al., 2011), Adhesive layers (Cha et al., 1991) and the use of hydrophobic mid layers (Lindfors, 1999).

The stable response from the carbon electrode could be due to the THF solvent used in the membrane solution partially dissolving the carbon ink. The membrane dissolving the carbon ink results in a good seal between the layers once the solvent has evaporated and the membrane has set. This will help increase stability as it will reduce the likelihood of formation of a water layer. The mixing of the carbon contact and the membrane could cause a transition layer with mixing of membrane and carbon contact. This could act to increase the surface area of the sensor conducting contact which would again increase stability due to larger double layer capacitance. A larger double layer capacitance would mean the sensor could take more charge before the voltage level starts to drift this is discussed in more detail in **Section 6.6.4**.

When the membrane is applied to the screen printed electrode there is evidence that the ink is dissolved as it is possible to easily disturb the carbon conducting contact by touching it with a pipette tip. The carbon graphite particles are suspended in a polymer blend for screen printed inks that will form and set on a printed substrate (Wang et al., 1998). The polymer for graphite suspension is dissolved in a solvent to

enable the printing process. The constituents of the ink are a trade secret to the company so it is difficult to know the exact formulation of the carbon ink but the information from the carbon ink MSDS sheet shows that the solvent used for the carbon ink is Isophorone. By looking at the Hansen solubility parameters (Hansen, 2000) the Isophorone and the THF solvents can be compared for solubility factor. They can be viewed in **Table 6.3**.

Solvent	Total Hildebrand parameter	dispersion component	polar component	hydrogen bonding component
THF	19.4	16.8	5.7	8.0
Isophorone	19.9	16.6	8.2	7.4

Table 6.3 Hansen solubility properties of THF and Isophorone solvents.

Table 6.3 shows the Hansen solubility parameters this gives a measure of the solubility parameters. The data shows that the two solvents are very close in parameters and should be able to dissolve the same materials. When the THF in the membrane solution is deposited onto the screen printed carbon it will act to dissolve the binding polymer of the carbon ink and lead to a better adhesion between the two sensor layers. This could be a key advantage of the screen printed sensor as it allows almost complete integration between the different material phases of the ion conducting membrane and the electron conducting carbon contact. Platinum wires or carbon rods that the majority of the solid contact research is conducted on in the literature would not experience the same effect as the membrane would sit on the surface without any integration with a greater possibility of water layer formation.

6.5.2 Electropolymerised polypyrrole based sensors

The conducting polymers based PPYCl and PPYPTS sensors both showed large drifts and changes in voltage potentials from the first pH 4 measurement to the second pH 4 measurement. The drift in the second immersion over the two hour time period for PPYCl and PPYPTS sensors was 10.4±7.75mV (n=3) and 45.97±8.72mV (n=3) respectively. The PPYCl based sensor showed a smaller drift than the PPYPTS

sensor however the overall change in voltage potential between the final pH 4 of the first immersion measurement and final pH 4 of the second was 31.93±4.4mV (n=3) compared to the PPYPTS value of 16.17 ±0.93mV (n=3). These values show very poor voltage stability and voltage potential consistency between the pH 4 solutions. This poor performance indicates the formation of a water layer. The formation of a water layer may also explain why the sensor takes more time to achieve stable voltage potential due to the liquid layer forming and changing depending on what solution it is immersed in.

The formation of a water layer has been attributed to a number of factors within the literature. Sutter, Lindner, et al (2004) relates the formation of water layers to entrapment of excess salts from the polymerisation solution within the polymer during electropolymerisation. In another paper Sutter, Radu, et al (2004) demonstrated that a hydrophobic layer and better membrane adhesion prevents liquid accumulation. It has been reported that the using highly plasticised PVC membranes can lead to creation of a liquid layer due to its permeability to water molecules (Fibbioli et al., 2002). To negate against formation of a water layer PMMA membranes have been used as they have diffusion around 1000 times slower than PVC based membranes (Lai et al., 2007)(Heng et al., 2004). Electrochemically formed polypyrrole is insoluble in common organic solvents due to its strong inter chain bonding (Ju et al., 2002). As the polypyrrole polymer is not soluble in THF the membrane will sit on top of the conducting polymer. If there are any areas between the membrane and conducting polymer/conducting contact then this will fill with liquid that diffuses through the membrane.

In conventional liquid junction electrodes any flow of liquid through the membrane will not greatly affect the voltage potential due to the high ionic content of the inner ionic solution which is normally a saturated ionic solution as discussed in **Section 2.9**. Liquid diffusing through the membrane can cause a problem in solid state sensors due to the fact that there is not a strong ionic solution so any liquid flowing through will have a large effect on the membrane potential. A liquid layer will create a second voltage variable interface that can cause unwanted voltage drift and lead to inaccurate measurements of the solution (Fibbioli et al., 2000). There will be a

further third voltage variable due to the interaction of the solution with the conducting polymer or conducting contact which will lead to further voltage instability. The new variable voltage interfaces are shown in **Figure 6.5 and Equation 6.2**.

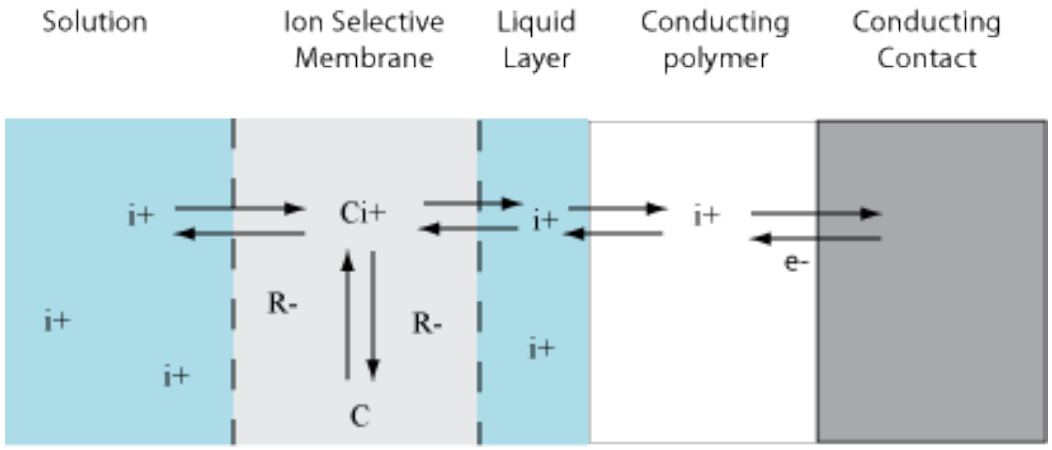

Figure 6.5 Showing conducting polymer phases with formation of a water layer between ion-selective membrane and conducting polymer.

$$E = E_{Solution/Membrane} + E_{Membrane} + E_{Membrane/Solution} + E_{Solution/Polypyrrole}$$

Equation 6.2

Equation 6.2 details the potential determining phases of the sensor electrode. As discussed previously (**Section 2.9**) the ideal sensor will have stable voltage potentials in all phase but the interface of interest $E_{Solution/Membrane}$ which would vary dependent on solution concentration that the electrode was immersed in. When a water layer forms all the interfaces will change potential bar the $E_{Membrane}$ which will remain constant. The effects of the formation of a water layer have been modelled by Morf et al (2000) and Fibbioli et al (2000). They model the membrane performance with a water layer that changes ionic content depending on the ionic content of the solution that the sensor is immersed in; this in turn alters the potential of the unwanted phases.

The water layer formation means that the conducting polymer sensors would not be suitable for use due to their unstable voltage potentials that will change dependening on the formation and ionic content of a water layer. For this reason the carbon membrane sensor was chosen for further investigation and use within the wound dressing testing experiments.

6.6 Carbon membrane sensor testing

The carbon membrane sensor was the only sensor that operated effectively in all the tests. It showed promising attributes that would make it suitable for a one time use pH sensor. To further investigate the operation of the carbon membrane further tests were conducted; to find the sensor pH range, how it responded to heat stress and EIS to find the properties of the screen printed carbon electrode.

6.6.1 Sensor range

The results presented in **Section 4.6.3** show that the sensor responds well in a linear manner from pH 7 to pH 4. It starts to drop off between pH 4 to pH 3 this indicates that the sensor is only accurate to a pH of 3.5 as it is at this point the response deviates from the linear voltage slope. The sensor was found to have a lower pH sensitivity range than the original membrane recipe, which had a lower linear detection limit of pH 4.5 when used as a traditional liquid junction electrode (Schulthess et al., 1981**).** This could be due to the different measurement arrangement (solid state versus liquid junction electrodes) or slight differences in the ion-selective membrane components. The range of the sensor meets the initial requirements of having a linear response between pH 4 to pH 10. One of the limitations of these sensors is that some of the pH modifying wound dressings are much more acidic than expected with pH values as low as 2.2 (as detailed in **Section 5.2.1)**. The pH buffering capability of physiological solutions was shown in further testing to prevent the pH dropping below the range of the sensor when pH modifying dressings were placed in physiological solutions. The sensor design will be suitable as the wound fluid will have a pH buffer to prevent the pH dropping below the range of the sensor, this is discussed further in **Section 6.10.4**.

6.6.2 Heat stress testing

This test was conducted to assess if the performance of the sensor would be affected by heating the sensors in an 80^{o}C oven. The 80^{o}C oven was needed to cure the additional isolation paste used to ensure that no unwanted part of the electrode is exposed to the solution when fully immersing the sensor in a solution as shown in **Figure 6.6**.

Figure 6.6 Fully isolated sensor to allow full emersion in solution.

The results show that the voltage response reduces in proportion to the time that the sensor is subjected to 80^{o}C. The sensors still respond in a linear manner but the voltage response per decade change in hydrogen ion concentration of the sensors drops with time spent in the oven. The biggest change in potentials over the 150 hours came in the extreme pH that was tested with the voltage potentials falling by 18.4mV for pH 4 and 16.1mV for pH 10. The drop off in potential may be due to the dehydration and further release of THF solvent from the membranes during the cooking process. The drying out of the membrane after its initial use could lead to some salts remaining in the ion-selective membrane; which when immersed in a new solution change the potential of the membrane. Future designs of a fully immersible

sensor could avoid the membrane heating as it could be applied last in the manufacturing process.

6.6.3 Long term voltage drift during pH measurement

This test was performed to assess how the sensor performed in a pH 7 solution over a 12 hour period. The test investigated the voltage potential change over the time of the experiment. This is one of the disadvantages of having no mid layer to act as a link between the electronic and ionic conducting phases as charge from the electronic measuring equipment or electrical noise will be able to build at the interface between the carbon and membrane which can cause voltage drift as discussed in **Section 2.9**. The sensor shows a drift of 0.69mV/per hour, this is greater than the values reported in the literature (Bobacka, 1999; Lai et al., 2007; Musa et al., 2011). The sensors were not preconditioned before the test unlike the other papers reported values. It was decided not to perform any preconditioning on the electrodes as it would not be practical to precondition all electrodes for up to 2 days before each test in a clinical environment. Other reports where preconditioning had not been used showed initial drifts of 2mV/hour over the first 9 hours before stabilising at much smaller drift of 0.03mV/hour (Gyurcsányi et al., 2004). It is difficult to compare the sensors in the literature due to different sensor types, experimental setups and different lengths of sensor preconditioning.

The long term drift may be influenced by the input bias current of the measurement hardware as detailed in **Section 2.12**. Over short periods of time this would not be an issue due to only small charges flowing, so the sensor would not charge significantly. The measurement hardware (Solartron 1286A) used for this experiment has an input operational amplifier bias current as smaller than 1nA. The 1nA listed in the data sheet will be the worst case scenario as this is a large value and would lead to large voltage drifts being observed in the potentiometric pH measurements. The bias current will act to charge the interface like a capacitor between the carbon contact and membrane which will result in a constant voltage drift in the sensor. If measurement hardware with smaller bias current was used the drift may have been reduced. This design consideration was taken into account when designing the measurement hardware as discussed in **Section 3.6**. Although the current induced by

the measurement hardware will change the voltage potential of the electrode this may not be the only factor that influences the current drift. It is possible that electrical noise in the surrounding environment may act on the sensor due to it not being shielded (Bobacka et al., 2008). The effect of this it unknown and would need to be investigated further to gain further knowledge of its influence. Other factors that could lead to voltage drift over long time periods are leaching of membrane components into the solution such as ionophore, ionic salts and plasticiser.

As a single use sensor the voltage drift should not be an issue as the sensors are calibrated before every measurement, for example it could be used to measure wound pH during wound dressing change. The issue would be if the sensor was in continuous use over a period of time for example being integrated into a wound dressing bandage. This is a possible future application of the sensor and until the long term voltage drift and changes in potential are studied further the sensor in its current form may not be suitable for this long term measurement application inside a wound dressing.

6.6.4 Electrochemical Impedance Spectroscopy

Electrochemical Impedance Spectroscopy (EIS) analysis was performed on the screen printed carbon electrode so that double layer capacitance and exchange current density values could be found. The values found help the understanding of the properties of the screen printed carbon and how they relate to the operation of the membrane coated electrode as detailed in **Section 2.13**. Using the EIS technique the complex impedance response of the carbon screen printed electrode was found. Electrical parameter values for resistance and capacitance were then found by modelling the response with the best fit Randles equivalent circuit. The values found using this equivalent circuit, over an average of 3 electrode measurements, were a double layer capacitance of 3.84±0.18µF and a charge transfer resistance of $1.62x10^{6}\pm2.2x10^{5}\Omega$.

Equation 2.23 from **Section 2.6** can be rearranged to give a calculated value for exchange current density, i_o as shown in **Equation 6.3**.

$$i_o = \frac{RT}{R_{CT}F} \qquad \textbf{Equation 6.3}$$

Where R_{CT} is the differential charge transfer resistance, R is the general gas constant, T is the temperature in Kelvin and F is the Faraday constant. Using the charge transfer resistance calculated in the EIS experiment a value of exchange current density can be calculated if a semi circle response is found as shown in **Figure 6.7**. A non polarisable electrode would display a semi circle; if the Rct value gets larger the semi circle increased in size. The carbon electrode displayed polar qualities; there is large uncertainty in the Rct value due to a semi circle response not being observed at the frequency ranges tested. All that can be proven from this data on the exchange current density is that the screen printed electrode has low exchange currents and is polarisable which is expected due to no redox couples present on the electrode or in solution.

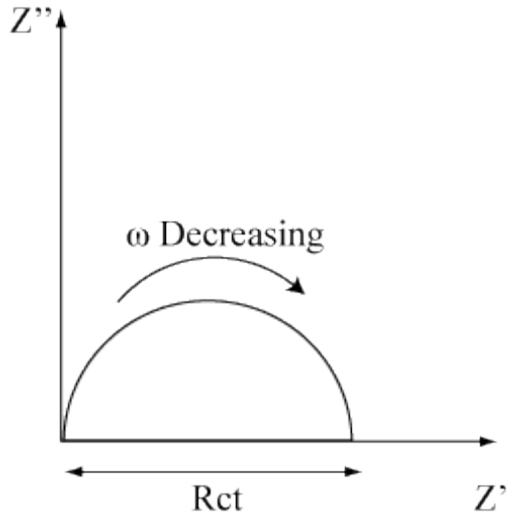

Figure 6.7 Complex plot of non-polarisable electrode showing how Rct value is found.

Bockris and Reddy (2000) states that the exchange current density is important for design of electronic measurement hardware as if the current passed by the measuring

device is higher than the exchange current density then the interface will begin to charge resulting in voltage drift. As expected due to the lack of a redox couple at the interface between the carbon electrode and solution the interface has a small current exchange density which results in an easily polarisable interface. In the traditional liquid junction electrode that uses an Ag/AgCl electrode as the redox contact the exchange current density is high which enables a larger current to be passed through the interface without changing the potential of the electrode. As the carbon membrane does not have this the design of the hardware needs to be carefully chosen so that any current passed will be smaller than the exchange current density and prevent any voltage drift, this is further discussed in **Section 6.8.1**.

When there is no redox active couple the double layer capacitance replaces the redox capacitance found in conducting polymers. The double layer capacitance is small and hence the electrode will be more susceptible to charging and voltage drift (Bobacka, 1999). The double layer capacitance, C_{dl} is directly related to the size of the electrode surface area as shown in **Equation 6.4**. The charge density, σ is measured in μC/cm^2.

$$\frac{d\sigma}{dV} = C_{dl} \qquad \textbf{Equation 6.4}$$

If this is reduced in size the capacitance, C will be smaller and the voltage, V will have a larger change in potential with current flow as shown in **Equation 6.5**.

$$dV = \frac{dq}{C} \qquad \textbf{Equation 6.5}$$

This will prevent these electrodes being reduced in size significantly as if the surface area is small the capacitance is small and the electrode will change voltage at a faster rate. The size of the exchange current will also reduce as it is dependent on the area of the electrode multiplied by the exchange current density, i_o. The electrodes used in this test has a surface area of 0.636 cm^2 these sensors are quite large and an ideal sensor would be able to measure the pH of the wound fluid with as small a volume of

liquid as possible to immerse both the sensor and reference electrodes. Further investigations would be needed to find the smallest sized sensor that could operate effectively without being affected by voltage drift for one time measurement of pH. For longer time measurements the size of the sensor and overall capacitance could cause problems if the sensor is to be integrated into a wound dressing or placed in the wound environment for long periods of time for continuous pH measurement. To increase capacitance carbon nanotubes could be used in the screen printed ink as this has been shown to increase double layer capacitance (Wang and Musameh, 2004; Lai et al., 2007; Crespo, Macho, et al., 2009). Pre treatment of carbon electrodes and modification of ink constituents has been shown to alter the double layer characteristics of a screen printed electrode (Biniak, 1995; Wang et al., 1998). Set voltage pre conditioning treatments have been shown to increase the double layer capacitance of the electrodes (Cui et al., 2001). These methods could potentially be used to increase the double layer capacitance, and hence improve sensor stability.

The values presented for double layer capacitance are for the bare screen printed electrode. When the ion-selective membrane is coated onto the electrode the surface properties will likely change due to the dissolving of the screen printed ink by the membrane solution. The dissolving and mixing layer of the screen printed carbon ink (S**ection 6.5.1**) may act to increase the area of contact at the electrode surface with the ion-selective membrane. This would need to be investigated further but it may help increase the stability of the electrode by creating a large surface area in contact with the ion-selective membrane.

6.7 Reference electrode

The screen printed Ag/AgCl reference electrode was found to provide a stable voltage half cell when immersed in a range of chloride adjusted pH solutions from pH 4 to pH 10. This was expected as the potential is dependent on the chloride level of the solution (Janz and Ives, 1968). The voltage stability across the range of pH levels at which the pH sensor will operate shows the Ag/AgCl electrodes suitability for use as the stable half cell for measuring the voltage of the pH sensor against. The potential of the Ag/AgCl electrode, $E_{Ag/AgCl}$ is given by **Equation 6.6.**

$$E_{Ag/AgCl} = E^0_{Ag/AgCl} - \frac{RT}{F} \ln a_{Cl^-}$$ **Equation 6.6**

Where $E^0_{Ag/AgCl}$ is the standard potential of the electrode, $\frac{RT}{F}$ the Nernst term and a_{Cl^-} the activity of the chloride ions. This relationship was shown when the silver chloride electrode was immersed in a series of different solutions of different Cl^- concentrations. With an average voltage response of -46.8±2.6mV/decade response chloride ion concentration it is below the Nernstian response that the equation predicts however it does show a linear response. The reduction in response could be down to impurities or formulation of the Ag/AgCl ink used for the screen printed electrodes.

The long term voltage drift of the Ag/AgCl reference electrode was tested to investigate the stability over a 12 hour time period. The drift was found to be 0.17mV/hour this drift could be accounted to the evaporation of the measurement solution which would result in a more concentrated Cl^- in the solution. Further research would have to be conducted if the reference electrode was to be used with the pH sensor from continuous pH measurement over long time periods.

The Ag/AgCl reference electrode are commonly used as reference electrodes in devices that measure the properties of blood such as a blood glucose sensor as the chloride level in blood the concentration of chloride ions is within a small range 100-108 mmol/L. It has been reported that wound fluid has also been reported in this range (White, 2002). A possible problem of using a silver chloride reference electrode in wound fluid measurements is that the concentration of salt may change with evaporation or absorption with wound dressings. The chloride concentration of wounds would have to be studied to ensure that it is within a small enough range, so that it would not affect the potential of the reference electrode and hence the accuracy of the full sensor system. If there is an issue with different chloride levels in wound fluid then a more complex solution to reference electrode would have to be investigated.

6.8 Hardware testing

The hardware testing tested the three main components of the measurement hardware input op amp offset operational amplifier and analogue to digital converter (ADC). All of these components play a vital role in the measurement of voltage potential of the sensor system.

The current when in operation is 40mA with further optimisation this could be lowered to ensure longer battery life for the sensor. At the current level a Duracell Procell 9 volt battery would last for around 14 hours in continuous use. The prototype measurement hardware circuitry is on a breadboard which does not make optimal use of the space available and could be made smaller if produced on a printed circuit board in further design iterations.

6.8.1 Input operational amplifiers

The operational amplifier testing shows that the input operational amplifier stages are accurate as they provide a large input impedance and linear gain. The offset stage performs the function it was designed for by offsetting the voltage to ensure that only positive voltages reach the input of the ADC. The most vital part of the hardware with regards to influence on the sensor is the input operational amplifier. This plays a major role in ensuring the initial voltage measurement is accurate as discussed in **Section 2.12**. The OPA137 operational amplifier was chosen due to its high input impedance and low bias current. It has a maximum bias current of 100pA and an input impedance of $10^{12}\Omega$.

The input impedance needs to be as large as possible so that any current flow does not go across the input operational amplifier impedance as this would mean voltage values being measured are inaccurate this is discussed further in **Section 2.12**. One of the advantages of using a polymeric membrane is that the electrical resistance is much lower than a glass electrode. The carbon membrane coupled with the screen printed electrode had a resistance of 0.5MΩ where as glass pH electrodes can have resistances of up to 100MΩ (Galster, 1991). This reduction enables smaller input impedances to be used without affecting the measurement performance. With an

impedance of 0.5MΩ for a voltage measurement error of 0.1% the input resistance needs to be at least 50MΩ as the resistances are in parallel. This lower value means that the input impedance does not have to be as high as is needed in glass based electrodes.

The characteristic that is most important to overall stability of the carbon membrane sensor is the operational amplifiers input bias current. The operational amplifier bias current has to pass through the sensing system to ground, this is described in **Section 2.12**. It is vital that the bias current be as small as possible; this has previously been discussed as being an issue with the Solartron 1286 electrochemical interface measuring device causing long term voltage drift in **Section 6.6.3**. The effect of the input bias current is not mentioned in the sensor literature but it is important to consider when using solid state sensors. The carbon membrane sensor has an interface between the membrane and screen printed carbon which was shown in the EIS experiments to be a polar interface as it has a low exchange current density. Any operational amplifier input bias current has to flow into this interface and due to its polar nature will charge like a capacitor if the current is larger than the exchange current density. For this reason the bias current must be as small as possible. If the input bias current is large it can also cause an unwanted voltage into the input terminal of the operational amplifier this is due to the large impedance of the sensor system.

From the EIS results the transfer resistance is large but there is a large element of uncertainty as a full response could not be plotted so this shows that the electrode is a polar electrode but the extent of which is unknown using this experimental technique. The most polar electrodes have an exchange current density of 10^{-12}A/cm^2 (Bockris and Reddy, 2000). If this value is taken as a worst case scenario then the bias current or any induced currents would have to be smaller than 1pA to not cause any charging of the double layer. As the operational amplifier used in the hardware has a 100pA maximum bias current it would charge the double layer and over a long time lead to voltage drift depending on the capacitance of the double layer between the carbon and ion-selective membrane. Chronopotentiometry is an analysis technique that subjects the sensor to a small current flow to assess the voltage

stability of the electrode; it has been used to assess solid state sensors (Bobacka, 1999; Crespo et al., 2008). This technique is similar to the effect that the sensors will experience if the input bias current is large and could be used to assess the stability of sensors in further testing.

6.8.2 ADC output

The ADC is the part of the digital meter that converts the analogue signal from the output of the operational amplifier stage into a digital value so that the calculations for pH level can be made and displayed on the screen. The test took the measured input and compared it to the digital voltage output of the sensor. The results show that the output becomes slightly offset due the input voltage reference not being absolutely fixed which leads to a multiplication error of the ADC when converting the analogue signal to digital signal. The error gets larger as the voltage rises due to the multiplication faction to find the voltage of Vref/4096. This can be improved with a more accurate voltage reference in future hardware designs.

6.9 Combined sensor and reference testing

The combined testing of all the elements of the pH sensor system (pH sensor, reference electrode and measurement hardware) assessed if the sensor system functioned as expected.

First the carbon membrane was tested with the screen printed Ag/AgCl reference. The results show that using the combined electrode and reference system a linear response to pH can be found, as shown in **Section 4.9.2**. The voltage response of -54.83±0.16mV/ decade H^+ ion concentration was close to the values of voltage response found in previous testing. It should be noted that this system will only give accurate results if the chloride ion concentration is consistent across the range of measurement solutions. Any variation on chloride levels between the different solutions and the potential of the reference electrode will change and this will result in an inaccurate voltage reading for the sensor, this is further discussed in **Section 6.7**.

The second part of the combined testing used a 2 point calibration method to assess the accuracy of calculated pH measurements. It also used 3 different measurement arrangements using the carbon membrane pH sensor to test how accurate the whole system was at detecting the pH level of a solution (**Section 3.10**). Both the arrangements with glass and printed reference electrodes used the Solartron 1286 electrochemical interface to measure voltage the voltage measurements produced calculated pH levels within ±0.06 of a pH level of those recorded with a glass pH electrode as shown in **Table 4.4**. The pH equation was calculated using the voltages recorded during calibration and the voltage recorded in the pH solutions the equations for this calculation can be found in **Section 3.7.9**.

The testing of the full system pH sensor, reference electrode and battery operated measurement hardware gave pH measurement in a fully portable system. Once calibrated the battery operated hardware calculates the pH from the measured voltage potential of the sensing cell and converts the voltage into a pH value that is displayed on the screen. The full hand held system produced results within ±0.07 a pH level of those recorded with a glass pH electrode. This shows that the full designed system works effectively at detecting pH levels in solutions.

The slight differences in measurement may be due to temperature variations which have an influence on the pH of a solution. It is influenced by the Nernst equation which is temperature dependant due to the RT/zF term. If the temperature changes significantly then the sensor will need to compensate. An acid is also influenced by temperature, T due to the acid disassociation, pK_a as shown in **Equation 6.7**.

$$\frac{dpK_a}{dT} = \frac{0.9 - pK_a}{T} \qquad \textbf{Equation 6.7}$$

The temperature of wound fluid being tested should be within a tight enough range to not effect the measurement significantly although it may play a role if the calibration solutions are different temperatures to the wound fluid. A future improvement to the pH sensor would be the addition of a temperature sensor.

6.10 Wound dressing testing

The purpose of these experiments was to further test the pH sensor and use it to assess the pH of some of the most commonly use dressings that are known to modify pH in the wound.

6.10.1 Wound dressing pH testing

The wound dressings were immersed in 20ml of Solution A to simulate the salt content of wound fluid. Once immersed the dressings were left for 20 minutes so that the solution could fully absorb and mix with the dressing to ensure full immersion. This is an important stage as the different dressing types absorbed moisture at different rates, and to ensure that the pH is accurate the dressing contents need to be fully dissolved into the Solution A.

The lowering of wound pH levels has many implications in the healing process this is further discussed in **Section 1.10**. Of the dressings tested the Promogran, Cadesorb and Tegaderm specifically state that they modify the activity of the MMPs. The low pH of the MMP modifying dressings suggests that this is the main mechanism of reducing the MMP activity which delays healing in chronic wounds (Schultz et al., 2005). The reduction of pH has been shown in an in vitro model to reduce the proliferation of the MMPs (Greener et al., 2005). The pH of these dressings is similar to lemon juice as this has a pH level between 2-3. This low pH value may produce discomfort when applied to the wound. Natural honey also showed a low pH of 3.5, this low pH will help to lower the pH of the wound which combined with the natural antibiotic qualities will help the wound heal faster. The naturally low pH of these dressings could also act to reduce MMP levels in the same manner as the MMP specific modifying dressings. The pH values recorded in the Solution A indicate the pH of the wound dressings are but they do not give any information as to the concentration of the specific acid. The concentration of the specific acid in the dressings is important due to the acid buffering qualities of physiological solutions.

6.10.2 Sensor validation with wound dressings

The purpose of these tests was to ensure that the designed sensor system could accurately detect the pH of the wound dressings. The different reference electrodes (Screen printed Ag/AgCl and glass calomel electrode) were used to assess the performance of the system. This stage of testing was needed as the components that the wound dressings are composed of are mostly unknown due to the manufacturers protecting their wound dressing formulations. The response across all the dressings tested showed the dressings did not interfere with the sensing and reference electrodes as they recorded pH values close to that measured with the glass electrodes. The only results that were problematic was the Tegaderm dressing measurements as the pH of this dressing, at pH 3.25, was out-with the sensor pH range of detection (as discussed **Section 6.6.1**) which resulted in incorrect pH values being calculated. This inaccurate result was expected as the linear sensing range of the carbon membrane sensor is only down to a pH level of 3.5. The results from this testing demonstrate that the disposable sensor system can measure the pH of wound dressings successfully.

Due to the use of Ag/AgCl reference electrode the Aquacel and Promogran silver dressings were tested to see if the Ag^+ ions would interfere with the potential of the electrode. The theory states that the Ag^+ ion concentration needs to be far higher than the Cl^- concentration to have an effect on the potential (Janz and Ives, 1968). This had to be tested as the concentration of silver ions in the dressing was unknown. The silver ions within the dressings did not affect the measured potential and are able to be tested using a Ag/AgCl reference electrode as the background concentration of chloride is the overriding reaction that determines the potential of the electrode.

The same testing arrangement was used to test if the sensors could detect the pH accurately of a horse serum solution. The horse serum solution has similar ion and proteins types and concentrations that are found in human wound fluid. The pH levels detected were all close to those found using the glass pH electrode. This shows that the various sensor setups including the disposable sensor couple and the battery operated measurement hardware were able to measure the pH of a biological solution successfully. Both the testing of the wound dressing for pH and the horse serum were

shown to accurately detect the pH of the various solutions. This validated the sensors for use in the wound bed model experiments to provide accurate pH values.

6.10.3 Wound dressing simulation Solution A

A wound bed simulation experiment as described in **Section 3.13** was used to test the influence on pH once a wound dressing has been applied to a wound bed model in real time. This test used Solution A which does not have any buffering capacity to resist pH change and horse serum which has similar buffering concentrations as human wound fluid through albumin, globulin and bicarbonate ions. The proteins buffer the serum through reactions with its amino acid chains this is further discussed in **Section 2.14.1**. The pre testing calibration/validation was important as the volume of liquid (10ml) was insufficient to get a reading with the glass pH electrode. For this reason the pre sensor testing was needed to ensure that the pH of the wound dressings could be measured accurately using the carbon membrane and Ag/AgCl electrodes.

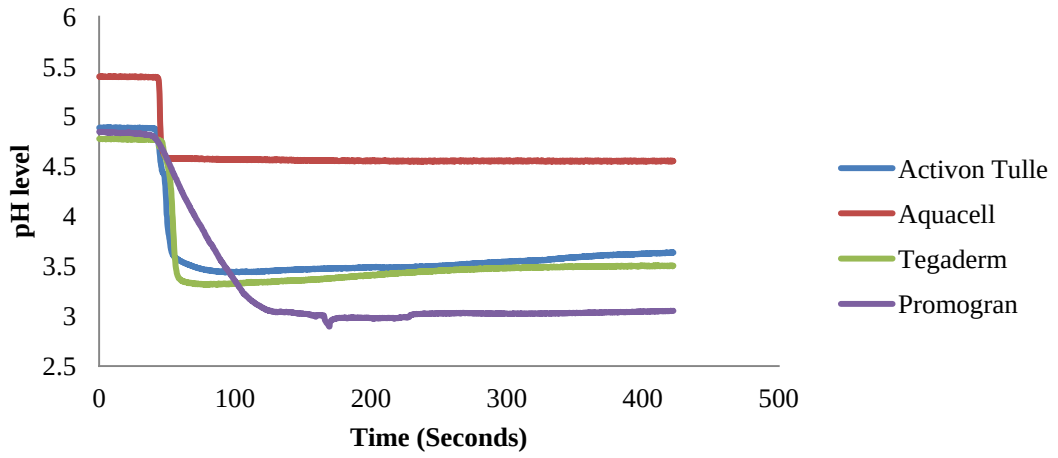

Figure 6.8 Average pH response after application of wound dressing at 40 second point.

Figure 6.8 shows the average pH response over a 700 second measurement after application of the wound dressings to the Solution A wound bed model. The Aquacel shows different starting pH this is due to the Solution A having no buffering capability so the pH can easily change. This same problem is observed in the

individual results with varying pH start levels before application of the wound dressing.

The results for the Solution A testing showed sharp falls in pH for all the dressings tested bar the Promogran which took around 20 seconds to fully drop to a settled level. The slower pH drop of the Promogran will be due to the absorbance of the material used in the Promogran dressing which took longer to absorb and integrate with the Solution A and hence delayed the mixing for the pH change. The Activon Tulle dressing does not settle fully at a stable pH in the 1800 second time period measured. This could be due to the inconsistent coating of the honey in the dressing which results in a concentrated coating of honey on the sensor until it dissolves into the Solution A mixture, a picture of the honey dressing is shown in **Figure 6.9**.

Figure 6.9 Thick inconsistent coating of honey on the wound dressing.

The sharp drop in all the tests in Solution A was expected due to no buffering capacity in the Solution A mixture to resist the acidic contents of the dressings. The final values for the Tegaderm and Promogran were not accurate due to the pH being

out-with the pH range (less than 3.5pH) of the sensor. The results show that all the dressings have an instant effect on the pH after they are placed onto the Solution A wound bed model. The values of pH were similar to those recorded for wound dressings in earlier testing (**Section 5.2.1**).

6.10.4 Wound dressing simulation Horse serum

The same experiment was conducted as before with the Solution A being replaced by a horse serum solution. The results show that the buffering capacity of horse serum plays a role it the pH response of the wound. The buffering capacity of the amino acid chains of the albumin and globulin proteins within the horse serum act to give a more realistic response to change in pH in a wound bed model this is discussed in detail in **Section 2.14.1**.

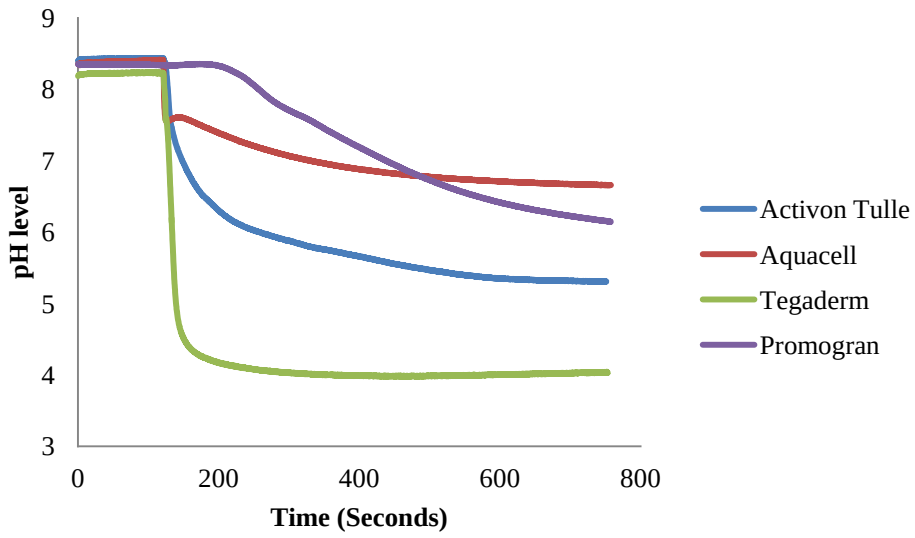

Figure 6.10 Average pH response in horse serum wound bed model after application of dressing after 120 seconds.

The Promogran dressings in horse serum were run for over 2000 seconds and the pH of the solution had not fully stabilised in this time which was by far longer than any other dressing type. When Promogram was run in Solution A it appeared to stabilise this, however, may of been a false result due to the range of the sensor being saturated so any further reduction in pH would not have been observed. In the initial experiments into the pH of the dressings it was found that Promogran was the most

acidic of all tested (pH 2.3). These results suggest that the Promogran dressing has a slow release/mixing of pH modifying ingredients when in contact with the pH buffering horse serum solution.

The Activon Tulle and Aquacel both experianced a fast drop in pH once the dressings were applied (**Figure 6.10**) then as the horse serum mixture fully mixes with the dressing a more gradual drop until the pH stabilises after around 600 seconds for both dressings. The Tegaderm dressing although not the lowest pH tested in Solution A showed the largest drop in horse serum. The sharp drop can be explained by the acid strength and the dressing surface which is a mesh that the active components are coated around this would result in faster dissolving/mixing of the active components on contact with the horse serum. The surface of the Tegaderm dressing is shown in **Section 3.11.5 Figure 3.22**.

Dressing	pH in Solution A	pH in horse serum	difference	pH change horse serum
Activon Tulle	3.49	5.32	1.83	3.11
Aquacel	4.51	7.57	3.06	1.74
Tegaderm	3.24	4.07	0.83	4.15
Promogran	2.30	5.44	3.14	2.91

Table 6.4 Summary of pH change after application of wound dressing.

The results show that the buffering capacity of horse serum plays a role it the pH response influenced by the wound dressings. The buffering capacity of the proteins within the horse serum act to give a more realistic response to change in pH in a wound bed model. The buffering capability of the horse serum prevents the pH change dependent on the concentration of the acid used in the experiments. From the data shown in **Table 6.4** it gives the recorded pH of the Solution A experiments using a glass electrode and the final pH of the horse serum dressing testing. The calculation for concentration of acid added to the solution is shown in **Equation 6.8**.

$$dn = \beta V_0 dpH \qquad \textbf{Equation 6.8}$$

This equation enables the strength of acid, dn in the dressing to be assessed for change in pH value as the volume of buffer solution (horse serum), V_0 and buffer capacity, β is constant for all the tests conducted. Although the buffer capacity is unknown it will be constant in all of the experiments conducted. The two constants in **Equation 6.8** simplify the equation so that the change in pH is a direct measure of the strength of acid in each wound dressing type.

The Aquacel dressing is the weakest out of all tested it also has the highest pH out of all tested in Solution A. The acidic concentration is very low as the pH in horse serum is at the extremity of the buffering capacity of the albumin proteins and carbolic acid buffers in the horse serum which have an estimated range from approximately pH 7.75 – pH 5.37. From this data the Aquacel will not have much influence on the pH of a wound the dressing is meant to hydrate the wound and does not make any claim of modifying properties other than moisture in the wound (Convatec, 2011). The Aquacel dressing is composed of a hydrofiber that turns into a gel on contact with liquid. This fast absorption of liquid can be seen in the Aquacel response with a fast pH drop off after initial application of the wound dressing.

The other dressings are interesting as they produce a larger change in pH and hence will have a larger influence on the wound healing properties. The pH response of Promogran dressing shows that it is the slowest of all dressings to alter pH after initial immersion in the wound bed model. These results suggest that the Promogran dressing has a slow release/mixing of pH modifying ingredients when in contact with the pH buffering horse serum solution. The Promogran was the most acidic in Solution A with a pH of 2.30; it produced a change of pH of 2.91 in the horse serum to settle on a final value of 5.44. Promogran uses acetic acid to lower the pH of a wound it has been documented that there is 0.05M of acetic acid within the dressing (Cullen et al., 2002). When applied to a wound the dressing will change the pH to a level that has previously been shown to have an influence on MMP levels (Greener et al., 2005).

The Activon Tulle produced the second highest change in pH when used in the horse serum wound bed model. The overall change in horse serum pH was 3.11 after the application of the dressing. The honey naturally includes a number of acidic components with gluconic acid having the largest concentration. Each honey has different amounts and types of acid depending on honey type and concentration (Kwakman and Zaat, 2012). It has been reported that the acidity of honey is the main factor in its antibacterial properties (Stefan and Bogdanov, 1997). The dressing samples are covered in the honey the thick coating of honey on the fabric gause; this will result in larger molar values of the acids in the honey which will account for the large change in pH in the horse serum solution. This coating also is responsible for the fast initial drop in pH with the honey being able to mix easily with the horse serum solution.

The Tegaderm showed the largest change in pH of 4.15 and also was the closest to the pH value in Solution A. The Tegaderm dressing experienced a sharp drop that can be explained by the acid strength and the dressing type. The dressing surface is a mesh that the active components are coated around; this results in faster dissolving of the active components on contact with the horse serum which can be observed with the fast drop in pH after dressing application. The data sheet for the Tegaderm states that it uses citric acid to lower pH although it does not state the concentration (3M, 2011). The large change in pH indicates that the Tegaderm dressing has the strongest acid concentration out of all the dressings tested. When applied to a wound the Tegaderm dressing will produce the largest drop in pH and this will help the dressing achieve its stated aim of reducing the MMP activity level within the wound (Greener et al., 2005).

6.11 Conclusion and future work

6.11.1 Conclusion

The aim of this work was to find an easy to produce disposable sensor for measuring the pH of sampled wound fluid. Four different sensor types (Screen printed carbon, screen printed PEDOT, electropolymerised PPYCl and electropolymerised PPYPTS) were tested with the aim of replacing the conventional glass liquid junction pH electrodes that are the only current method of measuring wound pH.

The investigation into membrane application found that the thinner deposited membranes produced more consistent membrane coverage and had the additional benefit of using less membrane material which results in less expensive sensors. Although the membrane investigation did not produce any improvement in voltage response to pH change that already reported in literature, the significant finding was first immersion settling time. The shorter settling times obtained with thinner machine deposited membranes enables shorter times for accurate first pH measurement.

The full sensor testing found that the sensor with the best performance was the carbon membrane sensor. The PEDOT sensor formed bubbles in the membrane during manufacture which led to inconsistent sensors. The two electropolymerised conducting polymer based sensors had poor voltage stability due to formation of water layer between conducting polymer and ion-selective membrane.

The carbon sensor was found to have good sensing characteristics. The main factor for the performance was attributed to the partial dissolving of the screen printed carbon layer during membrane deposition. This enabled good sensor adhesion between the membrane and conducting contact which prevented formation of an unwanted water layer. The measurement hardware designed as part of the project plays an important role in ensuring no voltage drift occurs. The hardware has a low input bias current meaning the sensor will be suitable for point of care measurements of pH. The dependence on double layer capacitance may result in the sensor

experiencing voltage drift if the sensor is used over long time periods or the sensor size is reduced.

In initial testing the wound dressing pH of many of the dressings were shown to have very low pH values. The testing in horse serum showed how the pH may change in a wound once the wound dressing have been applied. It was observed that when adding the wound dressings, that the buffering qualities of the horse serum lessen the pH change of the acidic wound dressings. The results of this investigation highlight the important role that pH modifying dressings can play within the wound healing environment. These results have never been reported in other literature as the system developed in this thesis is the first system capable of monitoring the dressing pH in real time. The low values of pH in the results may somewhat surprise the clinical community. Further testing of wound dressings on real wounds will help to achieve a better understanding of how the pH changes within a wound and how wound dressings influence this.

The investigation found a potential solution for the introduction of a disposable pH sensor using a potentiometric sensor produced using screen printing and a machine deposited ion-selective membrane. The sensor system operation in physiological solutions enabled the influence of wound dressings on pH of the solution to be observed. The pH is still not a fully understood part of the wound healing process but it plays a key role in many of the different elements of wound healing. With further development the device could be used to gain a further understanding of the role of pH and the optimum conditions for wound healing.

6.11.2 Future work

Suggestions for future work are:

- Investigation into how size of sensor affects its stability as reduced capacitance should result in sensor that has voltage drift
- Further study into membrane adhesion and its effect on double layer capacitance of the electrode
- Optimise the initial voltage settling drift of the sensors to find the fastest method of stabilization
- Toxicology study of sensor
- Investigation into hardware and how the input bias current may cause voltage drift
- Study of Cl^- content in wound fluid to assess if the chloride ion levels are within a small enough range to ensure stable operation of screen printed reference electrode.
- Produce PCB of hardware and miniaturise the instrumentation
- Test sensor system with wound fluid samples
- Development of a sensor that can be used in wound dressing for continuous pH monitoring within the wound possibly integrated in band.
- Titration experiments on wound dressings to determine the acid content of the wound dressings

The future work will enable a better understanding of the sensor properties and help to further optimise design. This will help to produce reliable sensors that can detect the pH of a wound easily and accurately.

References

3M, 2011. Tegaderm Matrix [WWW Document]. 3M.co.uk. URL http://solutions.3m.co.uk/wps/portal/3M/en_GB/HealthCare/Home/ProdInfo/SkinWoundCare/WoundManagement/TegadermMatrix/

Abbott, 2011. ISTAT Cartridge and Test Information Sheets pH.

Adhirajan, N., Shanmugasundaram, N., Shanmuganathan, S., Babu, M., 2009. Functionally modified gelatin microspheres impregnated collagen scaffold as novel wound dressing to attenuate the proteases and bacterial growth. European journal of pharmaceutical sciences : official journal of the European Federation for Pharmaceutical Sciences 36, 235–45.

AdvancisMedical, 2011. Activon Medical Honey [WWW Document]. medicalhoney.com. URL http://medicalhoney.com/

Aizawa, H., Ohkubo, K., Katsumata, T., Komuro, S., 2007. Multi-channel optical pH sensor using organic dye, in: International Conference on Control, Automation and Systems. pp. 2365–2368.

Ammann, D., Pretsch, E., Simon, W., Lindner, E., Bezegh, A., Pungor, E., 1985. Lipophilic salts as membrane additives and their influence on the properties of macro- and micro-electrodes based on neutral carriers. Analytica Chimica Acta 171, 119–129.

Anker, P., Ammann, D., Simon, W., 1983. Blood pH measurement with a solvent polymeric membrane electrode in comparison with a glass electrode. Microchimica Acta 79, 237–242.

Bakker, E., 2011. Membrane response model for ion-selective electrodes operated by controlled-potential thin-layer coulometry. Analytical chemistry 83, 486–93.

Bakker, E., Buhlmann, P., Pretsch, E., 1997. Carrier-based ion-selective electrodes and bulk optodes. 1. General characteristics. Chemical Reviews 97, 3083–3132.

Bakker, E., Bühlmann, P., Pretsch, E., 2004. The phase-boundary potential model. Talanta 63, 3–20.

Bakker, E., Pretsch, E., Buhlmann, P., 2000. Selectivity of potentiometric ion sensors. Analytical Chemistry 72, 1127–1133.

Bakker, E., Xu, A., Pretsch, E., 1994. Optimum composition of neutral carrier based pH electrodes. Science 295, 253–262.

Bard, A.J., Faulkner, L.R., 2001. Electrochemical Methods, 2nd Editio. ed. John Wiley & Sons.

Barrett, K., Ganong, W., 2010. Ganong's review of medical physiology, 23rd ed. McGraw-Hill.

Bickers, D.R., Lim, H.W., Margolis, D., Weinstock, M. a, Goodman, C., Faulkner, E., Gould, C., Gemmen, E., Dall, T., 2006. The burden of skin diseases: 2004 a joint project of the American Academy of Dermatology Association and the Society for Investigative Dermatology. Journal of the American Academy of Dermatology 55, 490–500.

Biniak, S., 1995. The electrochemical behaviour of carbon fibre electrodes in various electrolytes. Double-layer capacitance. Carbon 33, 1255–1263.

Bobacka, J., 1999. Potential stability of all-solid-state ion-selective electrodes using conducting polymers as ion-to-electron transducers. Analytical chemistry 71, 4932–4937.

Bobacka, J., 2006. Conducting Polymer-Based Solid-State Ion-Selective Electrodes. Electroanalysis 18, 7–18.

Bobacka, J., Ivaska, A., Lewenstam, A., 2008. Potentiometric ion sensors. Chemical Reviews 108, 329–351.

Bockris, J., Reddy, A., 2000. Modern Electrochemisrty, 2nd editio. ed. Kluwer Academic.

Brem, H., Tomic-canic, M., 2007. Cellular and molecular basis of wound healing in diabetes 117, 1219–1222.

British Pharmacopoeia Addendum, 1995. British Pharmacopoeia, Sodium chloride and calcium chloride solution. HMSO, London.

Buck, R.P., Lindneri, E.R.N., 1994. COMMISSION ON ELECTROANALYTICAL CHEMISTRY * RECOMENDATIONS FOR NOMENCLATURE OF ION-SELECTIVE ELECTRODES ion-selective electrodes (IUPAC 66, 2527–2536.

Buhlmann, P., Pretsch, E., Bakker, E., 1998. Carrier-based ion-selective electrodes and bulk optodes. 2. Ionophores for potentiometric and optical sensors. Chemical Reviews 98, 1593–1687.

Cattrall, R.W., Freiser, H., 1971. Coated Wire Ion Selective Electrodes. Analytical Chemistry 43, 1905–&.

Ceresa, A., Sokalski, T., Pretsch, E., 2001. Influence of key parameters on the lower detection limit and response function of solvent polymeric membrane ion-selective electrodes. Journal of Electroanalytical Chemistry 501, 70–76.

Cha, G.S., Liu, D., Meyerhoff, M.E., Cantor, H.C., Midgley, a R., Goldberg, H.D., Brown, R.B., 1991. Electrochemical performance, biocompatibility, and adhesion of new polymer matrices for solid-state ion sensors. Analytical chemistry 63, 1666–72.

Chen, C.C., Chou, J.C., 2009. All-Solid-State Conductive Polymer Miniaturized Reference Electrode. Japanese Journal of Applied Physics 48, 111501.

Convatec, 2011. Aquacel [WWW Document]. Convatec.com. URL http://www.convatec.co.uk/engb/cvtuk-aqcdrwsbuk/cvt-portallev1/0/detail/0/1028/2057/aquacel-dressing.html

Cosiner, S., Karyakin, A., 2010. Electropolymerization. Wiley-VCH, Germany.

Crespo, G. a, Gugsa, D., Macho, S., Rius, F.X., 2009. Solid-contact pH-selective electrode using multi-walled carbon nanotubes. Analytical and bioanalytical chemistry 395, 2371–6.

Crespo, G. a, Macho, S., Rius, F.X., 2008. Ion-selective electrodes using carbon nanotubes as ion-to-electron transducers. Analytical chemistry 80, 1316–22.

Crespo, G.A., Macho, S., Bobacka, J., Rius, F.X., 2009. Transduction Mechanism of Carbon Nanotubes in Solid-Contact Ion-Selective Electrodes. Analytical Chemistry 81, 676–681.

Cui, G., Yoo, J.H., Lee, J.S., Yoo, J., Uhm, J.H., Cha, G.S., Nam, H., 2001. Effect of pre-treatment on the surface and electrochemical properties of screen-printed carbon paste electrodes. The Analyst 126, 1399–1403.

Cullen, B., Smith, R., Mcculloch, E., Silcock, D., Morrison, L., 2002. Original research articles Mechanism of action of PROMOGRAN , a protease modulating matrix , for the treatment of diabetic foot ulcers. Wound Repair and Regeneration 16–25.

Delosaaradaperez, M., 2003. Influence of different plasticizers on the response of chemical sensors based on polymeric membranes for nitrate ion determination. Sensors and Actuators B: Chemical 89, 262–268.

Diegelmann, R., Evans, M., 2004. Wound healing: an overview of acute, fibrotic and delayed healing. Front Biosci 283–289.

Dissemond, J., Witthoff, M., Brauns, T.C., Haberer, D., Goos, M., 2003. pH values in chronic wounds. Evaluation during modern wound therapy. Hautarzt 54, 959–965.

Dissemond, J., Witthoff, M., Grabbe, S., 2004. Investigations on pH-values in milieus of chronic wounds during modern wound therapy The lowering of pH

values in chronic wounds by the application of CADESORB ™, in: World Congress.

Doblhofer, K., 1992. The non-metallic character of solvated conducting polymers. Journal of Electroanalytical Chemistry 331, 1015–1027.

Dumanska, J., 2001. Studies on spontaneous charging/discharging processes of polypyrrole in aqueous electrolyte solutions. Electroanalysis 13, 567–573.

Dumanska, J., 2002. Charge trapping in bilayers of conducting polymers under open circuit conditions: a protection of conducting polymer films from spontaneous charging/discharging. Corrosion science 44, 1681–1693.

Ehlers, C., Ivens, U.I., Møller, M.L., Senderovitz, T., Serup, J., 2001. Comparison of two pH meters used for skin surface pH measurement: the pH meter "pH900" from Courage & Khazaka versus the pH meter "1140" from Mettler Toledo. Skin research and technology : official journal of International Society for Bioengineering and the Skin (ISBS) [and] International Society for Digital Imaging of Skin (ISDIS) [and] International Society for Skin Imaging (ISSI) 7, 84–9.

Eming, S., Smola, H., Hartmann, B., Malchau, G., Wegner, R., Krieg, T., Smola-Hess, S., 2008. The inhibition of matrix metalloproteinase activity in chronic wounds by a polyacrylate superabsorber. Biomaterials 29, 2932–40.

Fibbioli, M., Bandyopadhyay, K., Liu, S.-G., Echegoyen, L., Enger, O., Diederich, F., Gingery, D., Bühlmann, P., Persson, H., Suter, U.W., Pretsch, E., 2002. Redox-Active Self-Assembled Monolayers for Solid-Contact Polymeric Membrane Ion-Selective Electrodes. Chemistry of Materials 14, 1721–1729.

Fibbioli, M., Morf, W.E., Badertscher, M., de Rooij, N.F., Pretsch, E., 2000. Potential Drifts of Solid-Contacted Ion-Selective Electrodes Due to Zero-Current Ion Fluxes Through the Sensor Membrane. Electroanalysis 12, 1286–1292.

Frost, Sullivan, 2003. European Advanced Wound. Frost&Sullivan Management Market.

Galster, H., 1991. pH Measurement, 1st Editio. ed. VCH Publishers, New York.

Gethin, G., 2007. The significance of surface pH in chronic wounds. Wounds A Compendium Of Clinical Research And Practice 3, 52–55.

Gethin, G., Cowman, S., 2005. Case series of use of Manuka honey in leg ulceration. International wound journal 2, 10–5.

Gethin, G.T., Cowman, S., Conroy, R.M., 2008. The impact of Manuka honey dressings on the surface pH of chronic wounds. Int Wound J 5, 185–194.

Gilbert, D.L., 1960. Buffering of Blood Plasma. The Yale Journal of Biology and Medicine 32, 378.

Gill, E., Arshak, K., Arshak, A., Korostynska, O., 2007. Mixed metal oxide films as pH sensing materials. Microsystem Technologies 14, 499–507.

Grant, S.A., Glass, R.S., 1997. A sol – gel based fiber optic sensor for local blood pH measurements. Sensors And Actuators 45, 35 – 42.

Greener, B., Hughes, A.A., Bannister, N.P., Douglass, J., 2005. Proteases and pH in chronic wounds. J Wound Care 14, 59–61.

Gyurcsányi, R.E., Rangisetty, N., Clifton, S., Pendley, B.D., Lindner, E., 2004. Microfabricated ISEs: critical comparison of inherently conducting polymer and hydrogel based inner contacts. Talanta 63, 89–99.

Hammond, P.A., Ali, D., Cumming, D.R.S., 2002. A Single-Chip pH Sensor Fabricated by a Conventional CMOS Process T3B4 T3B4. Sensors And Actuators 840–841.

Han, W.-S., Chung, K.-C., Kim, M.-H., Ko, H.-B., Lee, Y.-H., Hong, T.-K., 2004. A hydrogen ion-selective poly(aniline) solid contact electrode based on

dibenzylpyrenemethylamine ionophore for highly acidic solutions. Analytical sciences : the international journal of the Japan Society for Analytical Chemistry 20, 1419–22.

Han, W.-S., Yoo, S.-J., Kim, S.-H., Hong, T.-K., Chung, K.-C., 2003a. Behavior of a polypyrrole solid contact pH-selective electrode based on tertiary amine ionophores containing different alkyl chain lengths between nitrogen and a phenyl group. Analytical sciences : the international journal of the Japan Society for Analytical Chemistry 19, 357–60.

Han, W.S., Yoo, S.J., Kim, S.H., Hong, T.K., Chung, K.C., 2003b. Behavior of a polypyrrole solid contact pH-selective electrode based on tertiary amine ionophores containing different alkyl chain lengths between nitrogen and a phenyl group. Analytical Sciences 19, 357–360.

Hansen, C., 2000. Hansen solubility parameters : a user's handbook. CRC Press.

Heng, L.Y., Toth, K., Hall, E. a H., 2004. Ion-transport and diffusion coefficients of non-plasticised methacrylic-acrylic ion-selective membranes. Talanta 63, 73–87.

Henry, M.C.W., Moss, R.L., 2005. Primary versus delayed wound closure in complicated appendicitis: an international systematic review and meta-analysis. Pediatric surgery international 21, 625–30.

Hidalgo, E., Domínguez, C., 1998. Study of cytotoxicity mechanisms of silver nitrate in human dermal fibroblasts. Toxicology letters 98, 169–79.

Hunt, T.K., Hopt, H.W., 1997. Wound healing and wound infection - What surgeons and anesthesiologists can do. Surgical Clinics of North America 77, 587–&.

Inzelt, G., 2008. Conducting Polymers. Springer, Berlin, London.

James, T.J., Hughes, M. a, Cherry, G.W., Taylor, R.P., 2000. Simple biochemical markers to assess chronic wounds. Wound repair and regeneration : official

publication of the Wound Healing Society [and] the European Tissue Repair Society 8, 264–9.

Janz, G.J., Ives, D.J.G., 1968. SILVER, SILVER CHLORIDE ELECTRODES. Annals of the New York Academy of Sciences 148, 210–221.

Johnson, R.D., Bachas, L.G., 2003. Ionophore-based ion-selective potentiometric and optical sensors. Analytical and bioanalytical chemistry 376, 328–41.

Jones, R.D., Neuman, M.R., Sanders, G., Cross, F.S., 1982. Miniature Antimony pH Electrodes for Measuring Gastroesophageal Reflux. The Annals of Thoracic Surgery 33, 491–495.

Ju, E., Sik, K., Macdiarmid, A.G., 2002. High molecular weight soluble polypyrrole. Synthetic Metals 125, 267–272.

Kaehaeri, V., 1997. Matrix metalloproteinases in skin. Experimental Dermatology 199–214.

Kainulainen, V., Wang, H., Schick, C., Bernfield, M., 1998. Syndecans, heparan sulfate proteoglycans, maintain the proteolytic balance of acute wound fluids. The Journal of biological chemistry 273, 11563–9.

Kaufman, T., Eichenlaub, E.H., Angel, M.F., Levin, M., Futrell, J.W., 1985. Topical acidification promotes healing of experimental deep partial thickness skin burns: a randomized double-blind preliminary study. Burns including thermal injury 12, 84–90.

Kim, I.T., Lee, S.W., Elsenbaumer, R.L., 2004. New conducting poly(1-alkyl-3,4-dimethyl-2,5-pyrrolylene) (alkyl: butyl, hexyl): synthesis, characterization and properties. Synthetic Metals 141, 301–306.

Koncki, R., Mascini, M., 1997. Screen-printed ruthenium dioxide electrodes for pH measurements. Analytica Chimica Acta 2670.

Konopka, A., Sokalski, T., Lewenstam, A., Maj-Żurawska, M., 2006. The Influence of the Conditioning Procedure on Potentiometric Characteristics of Solid Contact Calcium-Selective Electrodes in Nanomolar Concentration Solutions. Electroanalysis 18, 2232–2242.

Korostynska, O., Arshak, K., Gill, E., Arshak, A., 2008. Review paper: Materials and techniques for in vivo pH monitoring. Ieee Sensors Journal 8, 20–28.

Kuruoğlu, D., Canel, E., Memon, S., Yilmaz, M., Kiliç, E., 2003. Hydrogen ion-selective poly(vinyl chloride) membrane electrode based on a calix[4]arene. Analytical sciences : the international journal of the Japan Society for Analytical Chemistry 19, 217–21.

Kwakman, P.H.S., Zaat, S. a J., 2012. Antibacterial components of honey. IUBMB life 64, 48–55.

Lai, C.-Z., Fierke, M. a, Stein, A., Bühlmann, P., 2007. Ion-selective electrodes with three-dimensionally ordered macroporous carbon as the solid contact. Analytical chemistry 79, 4621–6.

Lai, C.-Z., Joyer, M.M., Fierke, M. a, Petkovich, N.D., Stein, A., Bühlmann, P., 2009. Subnanomolar Detection Limit Application of Ion-Selective Electrodes with Three-Dimensionally Ordered Macroporous (3DOM) Carbon Solid Contacts. Journal of solid state electrochemistry : current research and development in science and technology 13, 123–128.

Lakard, B., 2004. Miniaturized pH biosensors based on electrochemically modified electrodes with biocompatible polymers. Biosensors and Bioelectronics 19, 595–606.

Lakard, B., Segut, O., Lakard, S., Herlem, G., Gharbi, T., 2007. Potentiometric miniaturized pH sensors based on polypyrrole films. Sensors and Actuators B-Chemical 122, 101–108.

Laursen, L., 2011. Optical Fiber Watches Wounds [WWW Document]. IEEE Spectrum. URL http://spectrum.ieee.org/biomedical/diagnostics/optical-fiber-watches-wounds

Lengheden, A., Jansson, L., 1995. pH effects on experimental wound healing of human fibroblasts in vitro. European Journal of Oral Sciences 103, 148–155.

Leung, Mok, Yu, 2001. Use of distilled white vinegar dressing supplemental to oral antibiotics in the management of Pseudomonas aeruginosa exit site infection in continuous ambulatory peritoneal dialysis patients. Hong Kong Journal of Nephrology 3, 38–40.

Leveen, H.H., Falk, G., Borek, B., Diaz, C., Lynfield, Y., Wynkoop, B.J., Mabunda, G.A., 1973. Chemical Acidification of Wounds - Adjuvant to Healing and Unfavorable Action of Alkalinity and Ammonia. Annals of Surgery 178, 745–753.

Li, C.M., Sun, C.Q., Chen, W., Pan, L., 2005. Electrochemical thin film deposition of polypyrrole on different substrates. Surface and Coatings Technology 198, 474–477.

Li, G., Wang, Y., 2007. A hydrogen peroxide sensor prepared by electropolymerization of pyrrole based on screen-printed carbon paste electrodes. Sensors 239–250.

Li, J.P., Peng, T.Z., Fang, C., 2002. Screen-printable sol-gel ceramic carbon composite pH sensor with a receptor zeolite. Analytica Chimica Acta 455, 53–60.

Lin, J., 2000. Recent development and applications of optical and fiber-optic pH sensors. TrAC Trends in Analytical Chemistry 19, 541–552.

Lindfors, T., 1999. Characterization of a single-piece all-solid-state lithium-selective electrode based on soluble conducting polyaniline. Analytica Chimica Acta 385, 163–173.

Lindner, E., Cosofret, V., Buck, R., 1995. Electroanalytical and biocompatibility studies on microfabricated array sensors. Electroanalysis 7, 964.

Lindner, E., Gyurcsányi, R.E., 2008. Quality control criteria for solid-contact, solvent polymeric membrane ion-selective electrodes. Journal of Solid State Electrochemistry 13, 51–68.

Liu, Y., Kalén, A., Risto, O., Wahlström, O., 2002. Fibroblast proliferation due to exposure to a platelet concentrate in vitro is pH dependent. Wound repair and regeneration : official publication of the Wound Healing Society [and] the European Tissue Repair Society 10, 336–40.

Lobmann, R., Ambrosch, A., Schultz, G., Waldmann, K., Schiweck, S., Lehnert, H., 2002. Expression of matrix-metalloproteinases and their inhibitors in the wounds of diabetic and non-diabetic patients. Diabetologia 45, 1011–1016.

Lutov, V.M., Mikhelson, K.N., 1994. A new pH sensor with a PVC membrane : analytical evaluation and mechanistic aspects. Sensors And Actuators 19, 400–403.

MacDonald, R., 1987. Impedance Spectroscopy. John Wiley & Sons.

Maksymiuk, K., 2006. Chemical Reactivity of Polypyrrole and Its Relevance to Polypyrrole Based Electrochemical Sensors. Electroanalysis 18, 1537–1551.

Marco, R.D., Veder, J., Clarke, G., Nelson, A., 2008. Evidence of a water layer in solid-contact polymeric ion sensors. Physical Chemistry 10, 73–76.

Marquesdeoliveira, I., Plaroca, M., Escriche, L., Casabo, J., Zine, N., Bausells, J., Teixidor, F., Crespo, E., Errachid, a, Samitier, J., 2006. Novel all-solid-state copper(II) microelectrode based on a dithiomacrocycle as a neutral carrier. Electrochimica Acta 51, 5070–5074.

Martini, F., 2006. Anatomy & Physiology, 7th Editio. ed. Pearson.

Marxer, S.M., Schoenfisch, M.H., 2005. Sol-gel derived potentiometric pH sensors. Analytical chemistry 77, 848–53.

Masalles, C., Borrós, S., Viñas, C., Teixidor, F., 2002. Simple PVC-PPy electrode for pH measurement and titrations. Analytical and bioanalytical chemistry 372, 513–8.

Mathiyarasu, J., Senthilkumar, S., Phani, K.L.N., Yegnaraman, V., 2008. PEDOT-Au nanocomposite film for electrochemical sensing. Materials Letters 62, 571–573.

McColl, D., Cartlidge, B., Connolly, P., 2007. Real-time monitoring of moisture levels in wound dressings in vitro: an experimental study. International journal of surgery (London, England) 5, 316–22.

McGraw-Hill, 2002. McGraw-Hill encyclopedia of science & technology, 9th ed. New York : McGraw-Hill .

MedlinePlus, 2011a. Pressure ulcer [WWW Document]. MedlinePlus. URL www.nlm.nih.gov/medlineplus/ency/article/007071.htm

MedlinePlus, 2011b. Burns [WWW Document]. MedlinePlus. URL http://www.nlm.nih.gov/medlineplus/burns.html

Menke, N.B., Ward, K.R., Witten, T.M., Bonchev, D.G., Diegelmann, R.F., 2007. Impaired wound healing. Clinics in dermatology 25, 19–25.

Mercier, R.C., Stumpo, C., Rybak, M.J., 2002. Effect of growth phase and pH on the in vitro activity of a new glycopeptide, oritavancin (LY333328), against Staphylococcus aureus and Enterococcus faecium. Journal of Antimicrobial Chemotherapy 50, 19–24.

Michalska, A., 2000. Potentiometric selectivity of p-doped polymer films. Analytica chimica acta 406, 159–169.

Michalska, A., Maksymiuk, K., 2003. Counter-Ion Influence on Polypyrrole Potentiometric pH Sensitivity. Microchimica Acta 143, 163–175.

Michalska, A., Maksymiuk, K., 2005. The influence of spontaneous charging/discharging of conducting polymer ion-to-electron transducer on potentiometric responses of all-solid-state calcium-selective electrodes. Journal of Electroanalytical Chemistry 576, 339–352.

Michalska, A., Skompska, M., Mieczkowski, J., Zagórska, M., Maksymiuk, K., 2006. Tailoring Solution Cast Poly(3,4-dioctyloxythiophene) Transducers for Potentiometric All-Solid-State Ion-Selective Electrodes. Electroanalysis 18, 763–771.

Milgrew, M.J., Cumming, D.R.S., 2008. Matching the transconductance characteristics of CMOS ISFET arrays by removing trapped charge. Electron Devices, IEEE Transactions on 55, 1074–1079.

Momma, T., Yamamoto, M., Komaba, S., Osaka, T., 1996. Analysis of the long-term potential stability of an all-solid-state potassium-selective electrode with electroactive polypyrrole film. Journal of Electroanalytical Chemistry 407, 91–96.

Morf, W.E., Badertscher, M., Zwickl, T., Reichmuth, P., de Rooij, N.F., Pretsch, E., 2000. Calculated Effects of Membrane Transport on the Long-Term Response Behavior of Polymeric Membrane Ion-Selective Electrodes. The Journal of Physical Chemistry B 104, 8201–8209.

Morf, W.E., Pretsch, E., de Rooij, N.F., 2009. Memory Effects of Ion-Selective Electrodes: Theory and Computer Simulation of the Time-Dependent Potential Response to Multiple Sample Changes. Journal of electroanalytical chemistry (Lausanne, Switzerland) 633, 137–145.

Mousavi, Z., Bobacka, J., Lewenstam, A., Ivaska, A., 2009. Poly(3,4-ethylenedioxythiophene) (PEDOT) doped with carbon nanotubes as ion-to-

electron transducer in polymer membrane-based potassium ion-selective electrodes. Journal of Electroanalytical Chemistry 633, 246–252.

Muller, M., Trocme, C., Lardy, B., Morel, F., Halimi, S., Benhamou, P.Y., 2008. Matrix metalloproteinases and diabetic foot ulcers: the ratio of MMP-1 to TIMP-1 is a predictor of wound healing. Diabetic medicine : a journal of the British Diabetic Association 25, 419–26.

Musa, A.E., del Campo, F.J., Abramova, N., Alonso-Lomillo, M.A., Domínguez-Renedo, O., Arcos-Martínez, M.J., Brivio, M., Snakenborg, D., Geschke, O., Kutter, J.P., 2011. Disposable Miniaturized Screen-Printed pH and Reference Electrodes for Potentiometric Systems. Electroanalysis 23, 115–121.

Mustoe, T., 2004. Understanding chronic wounds: a unifying hypothesis on their pathogenesis and implications for therapy. American journal of surgery 187, 65S–70S.

Myers, R.J., 2009. One-Hundred Years of pH. Journal of Chemical Education 87, 30–32.

NHS Authority Business Services, N., 2012. National Wound Management Charts [WWW Document]. NHSBSA. URL http://www.nhsbsa.nhs.uk/PrescriptionServices/Documents/PPDPrescribingAnalysisCharts/Wound_Management_National_Jan_2012.pdf

Nagase, H., Woessner, J.F., 1999. Matrix metalloproteinases. The Journal of biological chemistry 274, 21491–4.

Nelson, D., Lehninger, A., 2008. Lehninger principles of biochemistry, 5th Editio. ed. New York.

Oesch, U., Brzozka, Z., Xu, A., Rusterholz, B., Suter, G., Viet, P.H., Welti, D., Ammann, D., Pretsch, E., Simon, W., 1986. Design of neutral hydrogen ion carriers for solvent polymeric membrane electrodes of selected pH range. Analytical Chemistry 58, 2285–2289.

O'Toole, E. a, 2001. Extracellular matrix and keratinocyte migration. Clinical and experimental dermatology 26, 525–30.

Paciorek, R., Zurawska, M.M.-, 2005. Miniature planar chloride electrodes. Sensors and Actuators B: Chemical 108, 840–844.

Pandey, P., Singh, G., 2008. Dopants dependent ion sensitivity of polypyrrole-modified electrode: Case of pH sensing. Journal of Applied Polymer Science 107, 2594–2599.

Pandey, P.C., Singh, G., Srivastava, P.K., 2002. Electrochemical Synthesis of Tetraphenylborate Doped Polypyrrole and Its Applications in Designing a Novel Zinc and Potassium Ion Sensor. Methods 427–432.

Pasche, S., Angeloni, S., Ischer, R., Liley, M., Luprano, J., Voirin, G., 2008. Wearable Biosensors for Monitoring Wound Healing. Advances in Science and Technology 57, 80–87.

Pei, Q., Qian, R., 1991. Protonation and deprotonation of polypyrrole chain in aqueous solutions. Synthetic Metals 45, 35–48.

Peng, L.B., Heng, L.Y., Hasbullah, S. a., Ahmad, M., 2007. A solid-state pH transducer fabricated from a self-plasticized methacrylic-acrylic membrane for potentiometric acetylcholine chloride biosensor. Journal of Analytical Chemistry 62, 884–888.

Percival, S.L., Bowler, P.G., Dolman, J., 2007. Antimicrobial activity of silver-containing dressings on wound microorganisms using an in vitro biofilm model. International wound journal 4, 186–91.

Piao, M., Yoon, J., Shim, Y., Korea, S., 2003. Characterization of All Solid State Hydrogen Ion Selective Electrode Based on PVC-SR Hybrid Membranes. Microscope 192–201.

Pipelzadeh, M.H., Naylor, I.L., 1998. The in vitro enhancement of rat myofibroblast contractility by alterations to the pH of the physiological solution. European journal of pharmacology 357, 257–9.

Pourciel-Gouzy, M., Assiesouleille, S., Mazenq, L., Launay, J., Templeboyer, P., 2008. pH-ChemFET-based analysis devices for the bacterial activity monitoring. Sensors and Actuators B: Chemical 134, 339–344.

Prager, M.D., Baxter, C.R., Hartline, B., 1994. Proteolytic activity in burn wound exudates and comparison of fibrin degradation products and protease inhibitors in exudates and sera. The Journal of burn care & rehabilitation 15, 130–136.

Qu, L., Shi, G., Yuan, J., Han, G., Chen, F., 2004. Preparation of polypyrrole microstructures by direct electrochemical oxidation of pyrrole in an aqueous solution of camphorsulfonic acid. Journal of Electroanalytical Chemistry 561, 149–156.

Reiber, 1995. Diabeties in America, 2nd editio. ed. DIANE Publishing.

Reiss, M.J., Han, Y.P., Garcia, E., Goldberg, M., Yu, H., Garner, W.L., 2010. Matrix metalloproteinase-9 delays wound healing in a murine wound model. Surgery 147, 295–302.

Renedo, O.D., Alonso-Lomillo, M. a, Martínez, M.J.A., 2007. Recent developments in the field of screen-printed electrodes and their related applications. Talanta 73, 202–19.

Romanelli, M., Gaggio, G., Coluccia, M., Rizzello, F., Piaggesi, A., 2002. Technological advances in wound bed measurements. Wounds-a Compendium of Clinical Research and Practice 14, 58–66.

Sabouraud, G., Sadki, S., Brodie, N., 2000. The mechanisms of pyrrole electropolymerization. Chemical Society Reviews 29, 283–293.

Samsonova, E.N., Lutov, V.M., Mikhelson, K.N., 2008. Solid-contact ionophore-based electrode for determination of pH in acidic media. Journal of Solid State Electrochemistry 13, 69–75.

Schmid-Wendtner, M.-H., Korting, H.C., 2006. The pH of the skin surface and its impact on the barrier function. Skin Pharmacology and Physiology 19, 296–302.

Schneider, L.A., Korber, A., Grabbe, S., Dissemond, J., 2007. Influence of pH on wound-healing: a new perspective for wound-therapy? Archives of dermatological research 298, 413–20.

Schreml, S., Szeimies, R.M., Karrer, S., Heinlin, J., Landthaler, M., Babilas, P., 2010. The impact of the pH value on skin integrity and cutaneous wound healing. Journal of the European Academy of Dermatology and Venereology 24, 373–378.

Schulthess, P., Shijo, Y., Pham, H., Pretsch, E., Ammann, D., Simon, W., 1981. A hydrogen ion-selective liquid-membrane electrode based on tri-n-dodecylamine as neutral carrier. Analytica Chimica Acta 131, 111–116.

Schultz, G., Mozingo, D., Romanelli, M., Claxton, K., 2005. Wound healing and TIME; new concepts and scientific applications. Wound Repair and Regeneration 13, S1–S11.

Segut, O., Lakard, B., Herlem, G., Rauch, J.Y., Jeannot, J.C., Robert, L., Fahys, B., 2007. Development of miniaturized pH biosensors based on electrosynthesized polymer films. Analytica Chimica Acta 597, 313–321.

Shai, A., 2005. Wound healing and ulcers of the skin : diagnosis and therapy : the practical approach. Springer, Berlin ; New York.

Sharpe, J.R., Harris, K.L., Jubin, K., Bainbridge, N.J., Jordan, N.R., 2009. The effect of pH in modulating skin cell behaviour. British Journal of Dermatology 161, 671–673.

Shi, J., Alves, N.M., Mano, J.F., 2006. Drug release of pH/temperature-responsive calcium alginate/poly(N-isopropylacrylamide) semi-IPN beads. Macromolecular bioscience 6, 358–63.

Shiu, K.K., Song, F.Y., Lau, K.W., 1999. Effects of polymer thickness on the potentiometric pH responses of polypyrrole modified glassy carbon electrodes. Journal of Electroanalytical Chemistry 476, 109–117.

Shriver, D.F; Atkins, P.W., 1999. Inorganic Chemistry, 3rd editio. ed. Oxford: Oxford University Press.

Smith&Nephew, 2011. Cadesorb [WWW Document]. smith-nephew.com. URL http://global.smith-nephew.com/master/CADESORB_27561.htm

Snyder, R.J., 2005. Treatment of nonhealing ulcers with allografts. Clinics in dermatology 23, 388–95.

Stefan, B., Bogdanov, S., 1997. Nature and Origin of the Antibacterial Substances in Honey. LWT - Food Science and Technology 30, 748–753.

Subramaniam, K., Pech, C.M., Stacey, M.C., Wallace, H.J., 2008. Induction of MMP-1, MMP-3 and TIMP-1 in normal dermal fibroblasts by chronic venous leg ulcer wound fluid*. International wound journal 5, 79–86.

Sutter, J., Lindner, E., Gyurcsányi, R.E., Pretsch, E., 2004. A polypyrrole-based solid-contact Pb(2+)-selective PVC-membrane electrode with a nanomolar detection limit. Analytical and bioanalytical chemistry 380, 7–14.

Sutter, J., Radu, A., Peper, S., Bakker, E., Pretsch, E., 2004. Solid-contact polymeric membrane electrodes with detection limits in the subnanomolar range. Analytica Chimica Acta 523, 53–59.

Systagenix, 2011. Systagenix Promogran [WWW Document]. systagenix.com. URL http://www.systagenix.com/our-products/lets-promote

Sánchez, S., Pumera, M., Cabruja, E., Fàbregas, E., 2007. Carbon nanotube/polysulfone composite screen-printed electrochemical enzyme biosensors. The Analyst 132, 142–7.

Thomas, S., 2000. Alginate dressings in surgery and wound management--Part 1. Journal of wound care 9, 56–60.

Thomas, S., Loveless, P., 1997. A comparative study of the properties of twelve hydrocolloid dressings. World Wide Wounds 1–14.

Trengove, N.J., Stacey, M.C., Macauley, S., Bennett, N., Gibson, J., Burslem, F., Murphy, G., Schultz, G., 1999. Analysis of the acute and chronic wound environments: the role of proteases and their inhibitors. Wound Repair and Regeneration 7, 442–452.

Tymecki, L., Glab, S., Koncki, R., 2006. Miniaturized, Planar Ion-selective Electrodes Fabricated by Means of Thick-film Technology. Sensors 6, 390–396.

Ulrich, D., Noah, E.-M., Von Heimburg, D., Pallua, N., 2003. TIMP-1, MMP-2, MMP-9, and PIIINP as serum markers for skin fibrosis in patients following severe burn trauma. Plastic and Reconstructive Surgery 111, 1423–1431.

Veder, J.-P., De Marco, R., Clarke, G., Jiang, S.P., Prince, K., Pretsch, E., Bakker, E., 2011. Water uptake in the hydrophilic poly(3,4-ethylenedioxythiophene):poly(styrene sulfonate) solid-contact of all-solid-state polymeric ion-selective electrodes. The Analyst 136, 3252–8.

Vork, F., 1988. Application and characterization of polypyrrole-modified electrodes with incorporated catalyst particles.

Vázquez, M., Danielsson, P., Bobacka, J., Lewenstam, A., Ivaska, A., 2004. as ion-to-electron transducers in all-solid-state ion-selective electrodes. Materials Research 97, 182–189.

Wang, J., Musameh, M., 2004. Carbon nanotube screen-printed electrochemical sensors. The Analyst 129, 1–2.

Wang, J., Tian, B., Nascimento, V.B., Angnes, L., 1998. Performance of screen-printed carbon electrodes fabricated from different carbon inks. Electrochimica acta 43, 3459–3465.

White, R., 2002. Trends in Wound Care. Quay Books.

White, R., 2006. Modern exudate management : a review of wound treatments [WWW Document]. Worldwide Wounds. URL www.worldwidewounds.com/2006/september/white/modern-exudate-mgt.html

Xia, Y., Ouyang, J., 2011. PEDOT:PSS films with significantly enhanced conductivities induced by preferential solvation with cosolvents and their application in polymer photovoltaic cells. Journal of Materials Chemistry 21, 4927.

Xu, H., Yang, X., Wang, Y., Zheng, J., Luo, Z., Li, G., 2010. Disposable blood potassium sensors based on screen-printed thick film electrodes. Measurement Science and Technology 21, 055802.

Yáñez-Sedeño, P., Pingarrón, J.M., Riu, J., Rius, F.X., 2010. Electrochemical sensing based on carbon nanotubes. TrAC Trends in Analytical Chemistry 29, 939–953.

Zielinska, R., Mulik, E., Michalska, A., 2002. All-solid-state planar miniature ion-selective chloride electrode. Analytica chimica 451, 243–249.

Appendix A

Full Program

This section details the main program used for the designed hardware to show voltage and pH reading.

MAIN.C

```
#include <hidef.h> /* for EnableInterrupts macro */

#include <stdio.h>

#include "derivative.h" /* include peripheral declarations */



  float voltagefinal;

  float adjadcnumber;

     char *outstring[5];

       char bit[4];

       int number;

int control=0;

float volph4;

float volph7;

float savevoltage;

  float slope;

float intercept;
```

```
float pH;


    void InitKBI() {
// Enables KBI as interrupt
KBISC=0x00;   // comment
KBIES=0x80;   //
KBIPE=0x80;   //
KBISC=0x07;   //
}


 void delaymain(void){
  long int count;
  count =1000;
  while (count > 0){
  count--;}
  }


    void charconvert(int number1){                // compares the result and converts to
string for ascii sending
          switch (number1){
case 0:
```

```
    outstring[number]="0";
    break;
case 1:
    outstring[number]="1";
    break;
case 2:
    outstring[number]="2";
    break;
case 3:
    outstring[number]="3";
    break;
case 4:
    outstring[number]="4";
    break;
case 5:
    outstring[number]="5";
    break;
case 6:
    outstring[number]="6";
    break;
case 7:
```

```
    outstring[number]="7";
    break;
case 8:
    outstring[number]="8";
    break;
case 9:
    outstring[number]="9";
    break;
          }
     }


void ADCread(){
int high;
  int low;
  long int fullnumber;
APCTL1=0x02; /*disables the input pin for other use*/
ADCCFG= 0x04;
ADCSC2=0x00;  /*sets conversion to 12bit using internal clock sets low power conversion mode as dont need max speed  */
ADCSC1=0x01;
   while  (ADCSC1_COCO==0){}        //wait for conversion before reading result
```

```
  high=ADCRH;

  low=ADCRL;

    fullnumber = (long int)high << 8 | low;          /* normalise the high result by adding the two values high and low by sifting bits*/

adjadcnumber= (float) fullnumber;

}


void voltage(){

    voltagefinal=adjadcnumber*0.00058203;    //this number is 2.383/4096 to give the output of the sensor

            savevoltage=voltagefinal;


   // this converts the float number for transmission to LCD

 bit[0]=(int) voltagefinal;                  //gets most significant bit

 number =0;   // sets position counter for data saving as a string

       charconvert(bit[0]);

       outstring[1]=".";

    voltagefinal = (voltagefinal * 10)-bit[0]*10;    //shifts numbers by 1 and saves next sig bit

    bit[1]=(int) voltagefinal;

    number=2;

    charconvert(bit[1]);                     //sends int for ascii conversion
```

```
        voltagefinal = (voltagefinal * 10)-bit[1]*10;
       bit[2]=(int) voltagefinal;
       number=3;
       charconvert(bit[2]);
       voltagefinal = (voltagefinal * 10)-bit[2]*10;
       bit[3]=(int) voltagefinal;
        number=4;
        charconvert(bit[3]);

    PTDD=0x80;    //address set location 0
LCDSend();
    LCDPrint(outstring[0],1);
    LCDPrint(outstring[1],1);
    LCDPrint(outstring[2],1);
    LCDPrint(outstring[3],1);
    LCDPrint(outstring[4],1);
    LCDPrint("V",1);
}

void pHlevel(){
  slope= (volph7-volph4)/3;
```

```
 intercept= volph4-(slope*4);
 pH = (savevoltage-intercept)/slope;


 // this converts the float number for transmission to LCD module for pH to 2 decimal places
 bit[0]=(int) pH;                    //gets most signifcant bit
 number =0;   // sets position counter for data saving as a string
       charconvert(bit[0]);
       outstring[1]=".";
      pH = (pH * 10)-bit[0]*10;    //shifts numbers by 1 and saves next sig bit
      bit[1]=(int) pH;
      number=2;
      charconvert(bit[1]);                    //sends int for ascii conversion
       pH = (pH * 10)-bit[1]*10;
      bit[2]=(int) pH;
      number=3;
      charconvert(bit[2]);
  //sends to lcd
  PTDD=0xC0;
LCDSend();
    LCDPrint(outstring[0],1);
```

```
    LCDPrint(outstring[1],1);
    LCDPrint(outstring[2],1);
    LCDPrint(outstring[3],1);
    LCDPrint(" pH ",4);
}

void main(void) {
  int run=1;
  EnableInterrupts; /* enable interrupts */
  ICSC1=0x06;   // sets controle register for clock setting
 ICSC2=0xC0;
  SOPT1 = 0x40;  // disables COP reset
  InitKBI();
  delaymain();
  LCDInit();
  // runs this forever once program starts
  while (run=1){
    delaymain();  // stops refresh being too fast
    ADCread();
     voltage();
     delaymain();
```

```
      switch (control){
     case 0   :
      PTDD=0xC0;    //address set row 2
LCDSend();
  LCDPrint("Voltage ",8);
    break;

      case 1:
      PTDD=0xC0;    //address set row 2
LCDSend();
  LCDPrint("Cal pH4 ",8);
   break;

  case 2:
      PTDD=0xC0;    //address set row 2
LCDSend();
  LCDPrint("Cal pH7 ",8);
    break;

        case 5:
```

```
        case 4:
        case 3:                // displays both the pH and the voltage for 3 button pushes
 pHlevel();
   break;


   case 6:  // resets to zero after 6th button push
     control=0;
      break;


     default  :
     //  LCDClear();
     PTDD=0xC0;    //address set location 0
LCDSend();
  LCDPrint("ERROR   ",8);     //on row 2
  control=0;
    }
  }


  for(;;) {
   __RESET_WATCHDOG(); /* feeds the dog */
  } /* loop forever */
```

```
  /* please make sure that you never leave main */
}

////////////////////////////////////////////////////////////////////////////////
// KBI_ISR
// -------------------------------------------------------------------------------
// Reads interupt then increments counter
// Debounces switch
// Acknowledges KBF
////////////////////////////////////////////////////////////////////////////////
interrupt VectorNumber_Vkeyboard void KBI_ISR(void){
byte d,b;

  //capture which pin was pushed
  //mode = (byte)(KBI_VAL);
  //debounce button
  for (d=0xff;d>0;d--){
   for (b=0x80;b>0;b--){}
  }

    control++;
```

```
   switch (control){
     case 2 :
     volph4=savevoltage;

     case 3 :
     volph7=savevoltage;

     default : ;
    }

  //clear KBF
  KBISC_KBACK = 1;
}
```

LCD.C

```
#include "derivative.h" /* include peripheral declarations */
#include "lcd.h"
 char howmany;
 char *nextchar;
```

```
void delay(void){
int count;
count =50;
while (count > 0){
count--;}
}

 void LCDSend(void) {
 lcdE = 1;
 delay();
 lcdE = 0;
}

 void LCDClear(void) {
 lcdRS = 0;
  lcdPort = 0x01;
   LCDSend();
 }

 void LCDPrintNext(void) {
```

```
      while (howmany-- > 0) {
    lcdRS = 1;
      lcdPort = (*nextchar);
      LCDSend();
    nextchar++;
   }
      lcdRS=0; // resets rs bit so adrees can be changed elsewhere in prog easily
 }
 /* Display a string with a specific length */
 void LCDPrint(char *where, int length) {                  //char *where, int length
    if (length > 0) {
      howmany = length;
      nextchar = where;
      LCDPrintNext();
    }
 }


void LCDInit(void){
lcdEDD =  1;                /* LCD Enable pin as output          */
    lcdE =    0;              /* LCD Enable pin is clear           */
    lcdRSDD = 1;              /* Data/Instruction pin as output    */
```

```
    lcdRS =   0;                /* Data/Instruction is clear          */

    lcdRWDD=1;

    lcdRW = 0;


        LCDSUPPLY_VSUPPLY0 = 1;

        LCDSUPPLY_VSUPPLY1 = 1;

        LCDRVC_RVEN = 0;

        LCDC1_FCDEN = 1;


PTDDD=0xFF;

PTDD=0x03;          //clear

LCDSend();

PTDD=0x3C;    //function set

LCDSend();

PTDD=0x06; //enterymode set

LCDSend();

PTDD=0x0C; //turn on

LCDSend();

}
```